Subcellular localisation of α3-GABA$_A$ receptors: a role for phosphorylation

Harriet Elizabeth Warwick Oliver

A thesis submitted to University College London for the degree of Doctor of Philosophy

October 2021

Department of Neuroscience, Physiology & Pharmacology

University College London

Gower Street

London

WC1E 6BT

Declaration

I, Harriet Oliver, confirm that the work presented in this thesis is my own. Where information has been derived from other sources, I confirm that this has been indicated in the thesis.

Abstract

GABA$_A$ receptors are the primary mediators of inhibitory neurotransmission in the brain. In contrast to most αβγ-GABA$_A$ receptor synaptic-subtypes, α3 subunit-containing receptors localise in both synaptic and extrasynaptic locations, where they mediate phasic and tonic inhibition respectively. Of particular note is the synaptic localisation of α3-GABA$_A$ receptors in the thalamic reticular nucleus, a brain region linked to absence epilepsy; and the extrasynaptic localisation of α3-GABA$_A$ receptors in the basolateral amygdala, a region involved in the expression of anxiety and fear disorders.

To date, our understanding of the molecular mechanisms that control the subcellular localisation of the α3-GABA$_A$ receptor remains limited, including its interactions with the synaptic scaffold protein gephyrin, which tethers GABA$_A$ receptors at inhibitory synapses. In this study, we investigated the role that phosphorylation, a common post-translational modification that affects receptor trafficking, plays in the regulation of α3-GABA$_A$ receptor subcellular localisation. Phospho-null (phenyl)alanine and phospho-mimetic aspartate mutations were used to manipulate the phosphorylation states of three key residues – T400, T401 and Y402 – in the gephyrin binding domain of α3. Electrophysiological interrogation of these phospho-mutants in HEK-293 cells and cultured hippocampal neurons revealed alterations in receptor GABA sensitivity and kinetics, consistent with changes in subcellular localisation, when phosphorylation was mimicked at Y402. Further investigation using structured illumination microscopy demonstrated a reduction in the proportion of inhibitory synapses containing α3^{Y402D}-GABA$_A$ receptors, but these receptors were more concentrated in those synapses where they were retained. This concentration appears to be mediated through gephyrin-independent mechanisms, as co-localisation between α3^{Y402D}-GABA$_A$ receptors and gephyrin was reduced compared to phospho-null and wildtype receptors.

These data indicate that phosphorylation of Y402 affects the subcellular localisation of α3-GABA$_A$ receptors. This study provides a basis for further investigation of the role

phosphorylation plays in receptor localisation in distinct brain regions, and how this may be manipulated for therapeutic benefit.

Acknowledgements

There are many people without whom this PhD would not have been completed. First, many thanks to Prof. Trevor Smart for his unwavering support and enthusiasm over the last three years. Thanks also to all the members of the Smart lab, past and present, for making it such an open, friendly and enjoyable place to work. Thanks to Phil for helping whenever my rig misbehaved – inevitably during a particularly important experiment! A special thanks goes to Damian, for providing a limitless supply of feedback and guidance.

I would also like to thank my parents for their unending love and support, as well as for providing such a wonderful environment to escape to when London life became too much. To Lauren for always making me laugh, even while being the nuisance that little sisters are supposed to be. To Archie and Floyd, for making home so much fun whenever I visited. To Mick, Anne, Mark and Mel, for being the best second family I could hope for.

Thank you to my friends, in London and beyond, who were always there to remind me of life outside of my PhD. Thanks also to Val and Lindsey, for being with me to celebrate and commiserate through the highs and lows of PhD life.

Finally, the biggest thank you of all goes to Chris for his constant encouragement, unrelenting support and for believing in me when I didn't believe in myself (and his cooking is alright too).

Impact Statement

The subcellular cell surface localisation of $GABA_A$ receptors dictates the physiological functions that they perform in the brain. Receptors that are localised at synapses mediate rapid, transient phasic inhibition in response to transiently high (millimolar) GABA concentrations to regulate point-to-point communication between neurons. In contrast, extrasynaptic $GABA_A$ receptors mediate continuous, low-amplitude tonic inhibition to control not only basal levels of action potential firing, but also the input-output gain of individual neurons, and this is achieved at nanomolar to micromolar levels of ambient GABA.

The α3-$GABA_A$ receptor has not received as much attention as other isoforms of this receptor. It exhibits some unique characteristics: it is one of the few $GABA_A$ receptor subtypes to localise to both synaptic and extrasynaptic positions in different brain regions, for example. How the subcellular localisation of the α3-$GABA_A$ receptor is controlled remains a largely unexplored area of research. By using a multidisciplinary approach coupled with recombinant $GABA_A$ receptors and native and variant $GABA_A$ receptors expressed in cultured neurons, this study has investigated the roles that new phosphorylation sites play in this process. As a consequence, this study provides a new and important contribution to this area by expanding our understanding of the molecular mechanisms involved in regulating the subcellular localisation of the α3-$GABA_A$ receptor isoform.

The distinct cell surface localisation patterns of the α3-$GABA_A$ receptor in specific regions of the adult brain indicates its contribution to GABAergic inhibition across an array of behavioural and cognitive states. This study has uncovered a new series of residues in the α3 subunit intracellular domain that may form the basis of phosphorylation consensus sites for serine/threonine and tyrosine kinases. The phosphorylation status of one residue, tyrosine 402, was critical for several functional features (e.g., kinetics) of α3-$GABA_A$ receptors, and significantly for regulating their clustering at inhibitory synapses in, unusually for $GABA_A$ receptors, a likely gephyrin-independent manner. Thus, phosphorylation-dependent cell signalling could have a significant impact on the localisation and physiological role of α3-$GABA_A$ receptors.

Of interest is the receptor's synaptic localisation in the thalamic reticular nucleus, a brain region associated with absence epilepsy. Indeed, the α3-GABA$_A$ receptor is the only GABA$_A$ receptor subtype to be expressed in this brain region. Also worthy of note is the receptor's extrasynaptic localisation in the basolateral amygdala, an area associated with anxiety and fear disorders. Given the pathological disease states associated with these brain regions, in which α3-GABA$_A$ receptors demonstrate differential expression patterns, this study provides insight into how the phosphorylation status of these receptors affects both their physiology and trafficking, which will impact on any future therapeutic role.

Contents

9

List of Tables and Figures

List of Abbreviations

3D	Three dimensions
4-PIOL	5-(4-piperidyl)-3-isoxazolol
ANOVA	Analysis of variance
AP2	Clathrin adaptor protein 2
bAP	Backpropagating action potential
BDZ	Benzodiazepine
BIG2	Brefeldin A-inhibited GDP/GTP exchange factor 2
BLA	Basolateral amygdala
BSA	Bovine serum albumin
CA1 - CA3	*Cornu ammonis* (CA) regions 1-3 of the hippocampus
CaMKII	Ca^{2+}/calmodulin-dependent kinase II
cDNA	Complementary deoxyribonucleic acid
CER	Conditioned emotional response
CMV	Cytomegalovirus
CNS	Central nervous system
Co-IP	Co-immunoprecipitation
CRC	Concentration-response curve
CT	Corticothalamic
CV	Coefficient of variation
DBI	Diazepam binding inhibitor
DHEAS	Dehydroepiandrosterone sulfate
DMEM	Dulbecco's modified Eagle's medium
DNA	Deoxyribonucleic acid
DS2	Delta selective compound 2
EC_{50}	Half-maximal effective concentration
ECD	Extracellular domain
EDTA	Ethylene-diamine-tetra-acetic acid
eGFP	Enhanced green fluorescent protein
EGTA	Ethylene glycol-bis(β-aminoethyl ether)-N,N,N',N'-tetraacetic acid
EPSC	Excitatory postsynaptic current

ERK	Extracellular signal-regulated kinase
FCS	Foetal calf serum
GABA	γ-aminobutyric acid
GABA$_A$, GABA$_B$	Type A/B GABA receptor
GABARAP	GABA$_A$ receptor-associated protein
GARHL	GABA$_A$ receptor regulatory LHPFL protein
GAT	GABA transporter
GEF	Guanine exchange factor
GODZ	Golgi-specific DHHC zinc finger protein
HAP1	Huntingtin-associated protein 1
HBBS	Hank's balanced salt solution
HBS	HEPES-buffered saline
HEK	Human embryonic kidney
HEPES	4-(2-hydroxyethyl)-1-piperazineethanesulfonic acid
HRP	Horseradish peroxidase
ICD	Intracellular loop domain
IPSC	Inhibitory postsynaptic current
kb	Kilobase
kDa	Kilodalton
LB	Lysogeny broth
LC	Locus coeruleus
LHFPL	Lipoma HMGIC fusion partner-like 3 and 4
MEM	Minimal essential medium
MIE	Major immediate-early
mIPSC	Miniature inhibitory postsynaptic current
mRNA	Messenger ribonucleic acid
NGS	Normal goat serum
NL2	Neuroligin-2
NMDA	*N*-methyl-*D*-aspartate
nRT	Thalamic reticular nucleus
NSF	N-ethylmaleimide-sensitive factor

PBS	Phosphate-buffered saline
PCR	Polymerase chain reaction
PI3-K	Phosphoinositide 3-kinase
PKA	Cyclic-AMP dependent protein kinase / Protein kinase A
PKC	Phospholipid-dependent protein kinase C
PKG	cGMP-dependent protein kinase / Protein kinase G
PMSF	Phenylmethylsulfonyl fluoride
PTX	Picrotoxin
PVDF	Polyvinylidene fluoride
RNA	Ribonucleic acid
RT	Reticulothalamic
SDS-PAGE	Sodium dodecyl sulphate–polyacrylamide gel electrophoresis
SEM	Standard error of the mean
shRNA	Short hairpin ribonucleic acid
SIM	Structured illumination microscopy
sIPSC	Spontaneous inhibitory postsynaptic current
SOC	Super optimal broth with catabolite repression
SWD	Spike-wave discharges
TC	Thalamocortical
THDOC	Allo-tetrahydro-deoxy-corticosterone / $3\alpha,21$-dihydroxy-5α-pregnan-20-one
THIP	Tetrahydroisothiazolo-[5,4-c]pyridin-3-ol
TM1-4	Transmembrane domains 1-4
TTX	Tetrodotoxin
VIAAT	Vesicular inhibitory amino acid transporter
$\gamma2S$, $\gamma2L$	Short (S) and long (L) isoforms of the $\gamma2$ subunit

Chapter 1: Introduction

1.1. The GABA$_A$ receptor

The main inhibitory neurotransmitter of the mature central nervous system (CNS), γ-aminobutyric acid (GABA), plays a key role in the regulation of neuronal excitability. GABA is the endogenous ligand of two different classes of receptor: the ionotropic type-A (GABA$_A$) receptors and the metabotropic type-B (GABA$_B$) receptors (Kuriyama et al., 1993). GABA$_A$ receptors (GABA$_A$Rs) are heteropentameric ligand-gated anion channels (Fritschy & Panzanelli, 2014) which, upon activation by the binding of GABA, become permeable to Cl$^-$ and, to a lesser extent, HCO$_3^-$ ions. The resulting influx of anions into to the target neuron causes both membrane hyperpolarisation and an increase in the membrane conductance (known as "shunting" inhibition) which reduces neuronal excitability (Hübner & Holthoff, 2013).

Multiple different types of subunit co-assemble to produce GABA$_A$Rs with diverse physiological functions and kinetic properties (Sigel & Steinmann, 2012). It is therefore unsurprising that aberrant GABAergic signalling has been linked to a myriad of neurodegenerative disorders, including epilepsy, anxiety disorders, depression, schizophrenia, autism spectrum disorder and Alzheimer's disease (Fritschy & Brünig, 2003; Gonzalez-Burgos et al., 2010; Brickley & Mody, 2012; Nuss, 2015; Robertson et al., 2016; Kim & Yoon, 2017). The numerous different types of GABA$_A$R present a wide variety of pharmacological drug targets for the potential treatment of such disorders; these receptors have thus been the subject of rigorous scientific investigation for many decades and will likely remain so for many more to come.

1.1.1. Subunit & receptor structure & expression

The pentameric GABA$_A$R is assembled from a pool of nineteen possible subunits, encoded by multiple isoforms of eight different gene families to give: α1-6, β1-3, γ1-3, δ, ε, θ, π and ρ1-3 (Olsen & Seighart, 2009). A large extracellular amino (NH$_2$)-terminal domain (ECD), four membrane-spanning helices (TM1-TM4), a large intracellular loop domain (ICD) between TM3 and TM4 and a small extracellular

carboxy (COOH)-terminus form the structure of each subunit (Lorenz-Guertin & Jacob, 2018) (see Fig. 1.1A).

The ECD is formed mostly of orthogonal inner and outer β-sheets and contains binding sites for the natural agonist GABA and allosteric modulators such as benzodiazepines (BDZs) (Miller & Aricescu, 2014), although this canonical site is only present in α1-3, α5 and γ subunit-containing receptors (Fig. 1.1B). The channel pore is lined by the TM2 α-helix of each subunit in the pentamer (Miller & Aricescu, 2014). The ICD between TM3 and TM4 is large, comprising ~10% of the mass of an individual subunit, and is where the highest variability is found between subunits (Moss & Smart, 2001). The ICD is the site of numerous protein-protein interactions required for receptor trafficking and clustering (Luscher et al., 2011) including those with the scaffold protein gephyrin (Tretter et al., 2012), and contains many consensus sites for post-translational modifications, such as those mediated by serine/threonine and tyrosine protein kinases (Moss & Smart, 1996). It is thus a key structure for regulating the localisation and function of GABA$_A$Rs.
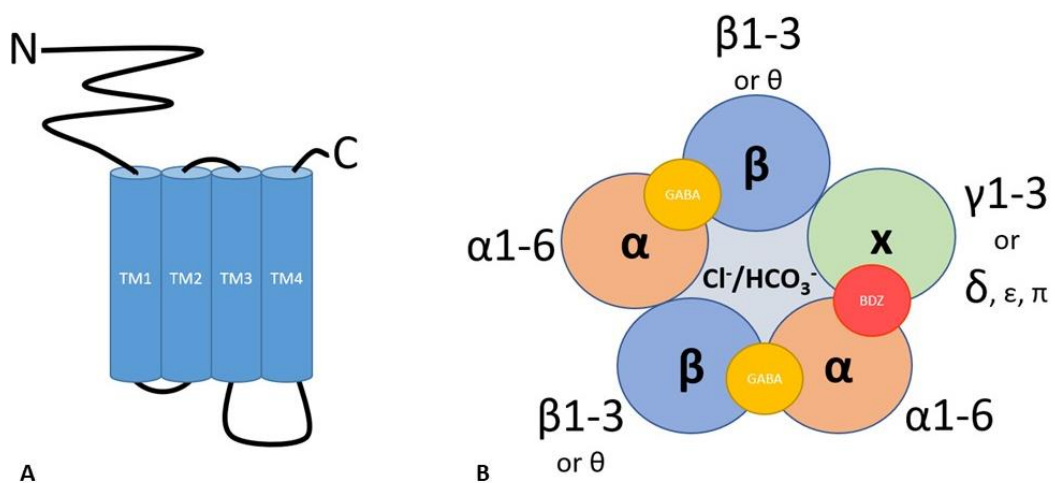
FIGURE 1.1. Generalised GABA$_A$R structure. (**A**) Schematic of the topology of a single subunit. All subunits share this structure, including an extracellular N-terminal domain, four transmembrane domains (TM1-4) and a C-terminal tail. (**B**) Subunit arrangement of the pentamer as viewed from the extracellular surface. The different possible subunits at each position, as well as the interfacial locations for the GABA and benzodiazepine binding sites, are indicated. Note, the BDZ binding site is only present when x is the γ subunit.

As GABA$_A$Rs are ligand-gated, they become permeable to anions upon activation via the binding of an agonist, the canonical example being GABA. However, spontaneous

activation of specific GABA$_A$R subtypes has also been identified (Sexton et al., 2021). Each pentameric receptor possesses two GABA binding sites, located at the β+/α– subunit interfaces of the extracellular domain (Sigel et al., 1992; Amin & Weiss, 1993) (see Fig. 1.1B). The binding of GABA at these sites induces a series of conformational changes in the receptor, which result in the opening of a gate approximately midway in the α-TM2 helix. When the receptor is in its resting state, this gate blocks the passage of ions through the pore (Masiulis et al., 2019). Once open, Cl$^-$ and HCO$_3^-$ anions are able to flow through the pore along their electrochemical gradients. In the mature CNS, this results in hyperpolarisation and neuronal inhibition. During early brain development, however, immature neurons have a high intracellular Cl$^-$ concentration. Under such conditions, the flow of Cl$^-$ ions along their electrochemical gradient results in depolarisation, action potential generation and neuronal excitation (Ben-Ari, 2002). As the brain develops, the Cl$^-$ gradient reverses and GABA$_A$Rs begin to mediate the inhibitory transmission which is their principal function in the mature CNS.

GABA$_A$Rs appear to follow certain rules of assembly: the majority of receptors found *in vivo* are pentamers formed of two α, two β and one other x subunit (Fig. 1.1B) in the counter-clockwise arrangement of xβαβα when viewed from the extracellular space (Baumann et al., 2002). Typically, in synaptic receptors x is a γ subunit isoform (Moss & Smart, 2001; Farrant & Nusser, 2005), while in extrasynaptic receptors x is the δ subunit (Farrant & Nusser, 2005; Mangan et al., 2005; Brickley & Mody, 2012). π and ε may replace γ or δ in the pentamer for cells in which they are expressed, while θ is thought to replace a β subunit (Sieghart & Sperk, 2002) and may have evolved from the β subunit family (Simon et al., 2004). These are by no means hard assembly rules, however: no GABA$_A$R subunit isoform has yet been identified that exists exclusively synaptically (Farrant & Nusser, 2005). Furthermore, receptors consisting of only α and β subunits (without the usual accompanying x subunit) have been observed in hippocampal neurons (Mortensen & Smart, 2006), demonstrating that GABA$_A$Rs do not always contain three different types of subunit. The subunits ρ1-3 provide a further exception. These are expressed as both homo- and hetero-oligomers, with properties distinct from those of the typical αβx GABA$_A$R (Sieghart & Sperk, 2002).

In addition to the numerous different subunit types capable of forming the GABA$_A$R, further diversity is imparted by RNA editing (Daniel & Öhman, 2009) and alternative splicing. For example, short and long splice variants exist for the γ2 subunit (γ2S and γ2L respectively), with an extra eight amino acids in the ICD of γ2L (Whiting et al., 1990). While these numerous subunits offer the potential for vast numbers of different pentameric receptor isoforms, relatively few combinations occur *in vivo*, depending on which subunits are co-expressed within a cell and perhaps upon underling assembly rules (Möhler, 2006; Olsen & Sieghart, 2009).

Two general receptor populations emerge from the physiological assembly of subunits: those localised at synapses and those that exist extrasynaptically (Farrant & Nusser, 2005). The subunits α1-3, β and γ typically comprise postsynaptic receptors, while extrasynaptic receptors are generally formed from the subunits α4/6, β and δ. α5βγ receptors are predominantly extrasynaptic, but can also localise synaptically, with both types of localisation observed in the hippocampus (Brünig et al., 2002; Serwanski et al., 2006; Magnin et al., 2018). α3βγ receptors have also been found in both post- and extrasynaptic locations. However, in contrast to α5-GABA$_A$Rs, the α3-GABA$_A$R populations appear mostly distinct from one another depending on the brain region: postsynaptic α3-GABA$_A$Rs are present in the thalamic reticular nucleus (Studer et al., 2006; Liu et al., 2007) and reelin-positive cells in the medial entorhinal cortex (Berggaard et al., 2018), while extrasynaptic α3-GABA$_A$Rs have been observed in the basolateral amygdala (Marowsky et al., 2012) and the inferior olivary nucleus (Devor et al., 2001).

On a broader level, the prevalence and expression patterns of individual subunits in the adult rat brain have been examined using immunostaining, *in situ* hybridisation and affinity column-based immunoprecipitation techniques. These experiments have demonstrated that different subunits exhibit distinct expression patterns across different areas of the brain (Wisden et al., 1992; Pirker et al., 2000), which change as the brain develops (Laurie et al., 1992). Some subunits – α1, β1-3 and γ2 in particular – are widely expressed throughout the CNS; indeed, α1β2γ2 receptors are thought to be the most abundant (~35%) of all the GABA$_A$R isoforms in the adult rat brain (Fritschy & Mohler, 1995; Pirker et al., 2000). The expression of other subunits is more

restricted: α6 is expressed exclusively in cerebellar granule cells and the cochlear nucleus, for example (Pirker et al., 2000), while the expression of ρ1-3 is mostly restricted to the retina (Sieghart & Sperk, 2002). Many subunits are also expressed outside of the CNS, in peripheral tissues (Bowery & Smart, 2006): a recent study identified the expression of multiple different GABA$_A$R subunits in the mouse bladder, heart, kidney, liver, lung, and stomach (Everington et al., 2018), while others have been found in several types of immune cell (Alam et al., 2006; Bjurstöm et al., 2008). Of all the receptor subunits, π is the only one that lacks any expression in neural tissue; it has, however, been identified in the uterus and other peripheral tissues (Hedblom & Kirkness, 1997). Finally, it has been observed that two isoforms of the same subunit can exist within the same receptor – α1α3β2/3γ2 receptors, for instance (Duggan & Stephenson, 1991; McKernan et al., 1991; Fritschy et al., 1992).

1.1.2. GABA$_A$ receptors: trafficking

Synthesis and assembly of GABA$_A$Rs occurs within the endoplasmic reticulum, following which they are transported to the Golgi apparatus (Jacob et al., 2008). Once inside the Golgi stack, the receptors are bound by GABA$_A$R associated protein (GABARAP) and N-ethylmaleimide-sensitive factor (NSF) complexes, which enable their trafficking to the plasma membrane (Leil et al., 2004). Transport to the plasma membrane is regulated by a number of proteins, such as: the palmitoyltransferase GODZ (Golgi-specific DHHC zinc finger protein), which palmitoylates γ2 subunits (Keller et al., 2004); BIG2 (brefeldin A-inhibited GDP/GTP exchange factor 2), an ADP ribosylation factor (Arf) guanine nucleotide exchange factor (GEF) that promotes vesicular budding and transport from the Golgi (Charych et al., 2004); and SNAP23-syntaxin 1A/B-VAMP2 complexes, which are necessary for the insertion of GABA$_A$R-containing vesicles into the plasma membrane (Gu et al., 2016). Many of these proteins interact with the receptors via the intracellular domains of specific subunits.

Within the plasma membrane, receptors may be clustered at synaptic or extrasynaptic sites, or exist as diffuse populations. All receptor subtypes are initially inserted into the membrane at extrasynaptic sites, from which, depending on subunit composition,

they may laterally diffuse to postsynaptic locations (Thomas et al., 2005; Bogdanov et al., 2006; Jacob et al., 2008). Such lateral diffusion through the membrane facilitates the continual exchange between these distinct receptor populations (Fig. 1.2). Receptors are maintained at the synapse by interaction with a variety of postsynaptic receptor-associated scaffold proteins, mostly via the large intracellular loops of individual subunits (Luscher et al., 2011). These scaffold proteins recruit specific signalling pathway components to synapses and bind to both cytoskeletal elements and receptors, creating between them a physical link that anchors the receptors in place. As such, they are critical to the correct organisation of functional synapses and the postsynaptic density (Fritschy et al., 2008). Synaptic inhibition is further regulated by endocytosis of neuronal GABA$_A$Rs, which occurs mainly via a clathrin-mediated dynamin-dependent mechanism that is facilitated by the clathrin adaptor protein 2 (AP2) complex (Kittler et al., 2000; Kittler et al., 2005). Internalised receptors are either recycled back to the neuronal plasma membrane – a process dependent on the interaction of the β1-3 subunits with huntingtin-associated protein 1 (HAP1) (Kittler et al., 2004) – or targeted for lysosomal degradation.
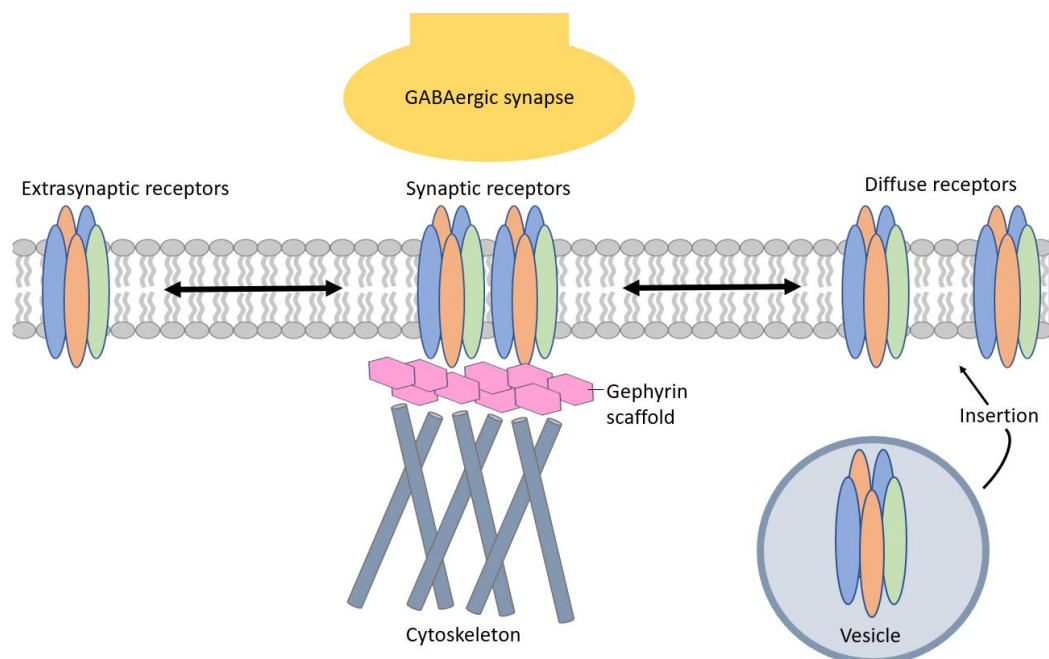
FIGURE 1.2. Lateral diffusion of GABA$_A$Rs at GABAergic inhibitory synapses. Following initial insertion into the plasma membrane at extrasynaptic sites, receptors may move by lateral diffusion (represented by the black two-headed arrows) to postsynaptic locations. Scaffold proteins, such as gephyrin, transiently retain receptors at the synapse by forming physical links between the receptors and cytoskeletal elements. Lateral diffusion enables receptors from diffuse, extrasynaptic and synaptic

populations to be continually exchanged, contributing to the dynamic nature of the synapse and replenishment of receptors.

The principal scaffolding protein gephyrin plays a key role in the recruitment and anchoring of GABA$_A$Rs at GABAergic synapses (Tyagarajan & Fritschy, 2014). Several studies, for example, have identified a loss of postsynaptic clustering of α2- and γ2-containing GABA$_A$Rs when gephyrin expression is reduced by mRNA knockdown or gene knockout experiments (Essrich et al., 1998; Kneussel et al., 1999; Jacob et al., 2005), while others have reported a loss of α3 and β2/3 subunits in the spinal cord neurons of gephyrin knockout mice (Kneussel et al., 2001). For many years, it was unknown as to whether this gephyrin-mediated synaptic clustering occurred via a direct interaction with gephyrin, until Tretter et al. (2008) demonstrated that a hydrophobic motif within the ICD of the α2 subunit bound directly to gephyrin. Indeed, the authors demonstrated that α2-containing GABA$_A$Rs actually require gephyrin binding in order to localise at the inhibitory synapses of hippocampal neurons (Tretter et al., 2008). Motifs responsible for gephyrin binding have since been reported in the α1, α3 and α5 subunits (Mukherjee et al., 2011; Tretter et al., 2011; Brady & Jacob, 2015), as well as the β2 and β3 subunits (Kowalczyk et al., 2013). To further cement the importance of gephyrin as an inhibitory synapse scaffold protein, Jacob et al. (2005) found that surface clusters of GABA$_A$Rs were three times more mobile than those in control neurons when formed in the absence of gephyrin, suggesting that gephyrin promotes the trapping of receptors at synapses.

However, gephyrin-independent clustering mechanisms clearly also exist in vivo: the clustering of α1 and α5 subunits, for instance, is unaffected in gephyrin knockout mice (Kneussel et al., 2001), while cell surface labelling experiments have indicated that gephyrin does not contribute to the insertion or stabilisation of α2- and γ2-GABA$_A$Rs in the plasma membrane of hippocampal inhibitory synapses (Lévi et al., 2004). Additionally, as α4, α5, and α6 subunit-containing GABA$_A$Rs are preferentially located extrasynaptically, other clustering proteins are likely to mediate their localisation. For example, the actin-binding protein radixin specifically localises α5-GABA$_A$Rs at extrasynaptic sites (Loebrich et al., 2006). Interestingly, the subcellular localisation of gephyrin itself requires the presence of specific GABA$_A$R subtypes. For example,

deletion of the genes encoding the subunits α1, α2, α3 and γ2 causes a loss of synaptic gephyrin clusters, instead resulting in non-synaptic dendritic gephyrin aggregates (Schweizer, 2003; Kralic et al., 2006; Studer et al., 2006; Panzanelli et al., 2011).

There are many other proteins that play important roles in the subcellular localisation of GABA$_A$Rs. These include: collybistin, a GEF that induces the submembrane clustering of gephyrin (Kins et al., 2000); neuroligin-2 (NL2), a cell adhesion molecule that binds to gephyrin and functions as a specific activator of collybistin (Poulopoulos et al., 2009); and members of the GABA$_A$R regulatory lipoma HMGIC fusion partner-like 3 and 4 (LHFPL; overall, GARLH) family, which form a complex with NL2 and the γ2 subunit in order to promote synaptic clustering of receptors (Yamasaki et al., 2017).

The subunit composition of a GABA$_A$R is integral to its subcellular localisation, for it is the subunits themselves that mediate interactions with intracellular proteins. As previously mentioned, receptors containing the δ subunit – generally along with α4/6 subunits – localise extrasynaptically, while those containing the γ subunit, and typically also α1-3 subunits, cluster at postsynaptic sites (Farrant & Nusser, 2005). It has been shown that both the ICD and TM4 of the γ2 subunit play critical roles in the synaptic localisation of GABA$_A$Rs (Alldred et al., 2005); indeed, a γ2 gene knockout almost entirely eliminated postsynaptic receptor clustering (Essrich et al., 1998). Using a molecularly engineered GABAergic synapse model that allowed them to control the exact subunit composition of the GABA$_A$Rs being studied, Wu et al. (2012) found that the same δ-γ2 chimeric subunit was being differentially targeted to synaptic or extrasynaptic sites, depending on whether it was co-assembled with the α2 or α6 subunit respectively. These studies demonstrate a direct role for individual subunits in the subcellular targeting of GABA$_A$Rs. However, despite this knowledge, much remains to be elucidated about the mechanisms that target these subunits to precise locations (e.g., dendrites, soma, axon initial segment) within a cell.

1.1.3. GABA$_A$ receptors: biophysical properties

In addition to subcellular localisation, the biophysical properties of GABA$_A$Rs – including the binding of agonist to the receptor, and receptor gating – are largely

determined by receptor subunit composition. Parameters such as receptor EC_{50} (the concentration of a ligand required to elicit a half-maximal response), activation rate (how quickly current is generated upon agonist exposure), desensitisation rate (how the current reduces in the continued presence of agonist) and deactivation rate (current decline following agonist removal) are key to measuring such properties (Farrant & Nusser, 2005).

The sensitivity of a receptor to its endogenous agonist – of which the EC_{50} is a principal measure – is a reflection of both the affinity of the receptor for its ligand and the efficacy of the ligand (how effectively it induces receptor opening) (Colquhoun, 1998). As a general rule, extrasynaptic $GABA_ARs$ have a much higher apparent GABA affinity, and hence lower EC_{50}, compared to synaptic receptors (Mody, 2001). Synaptic receptors mediate phasic inhibition: fast, short-lasting inhibition generated when postsynaptic $GABA_ARs$ respond to high concentrations (>1 mM) of GABA released into the synaptic cleft, following the activation of presynaptic interneurons (Farrant & Nusser, 2005). In contrast, tonic inhibition is a persistent inhibitory current mediated by extrasynaptic $GABA_ARs$ which are activated by ambient GABA in the extracellular space (Mody, 2001; Brickley & Mody, 2012). Thus, extrasynaptic receptors are exposed to much lower levels of GABA than their synaptic counterparts, necessitating their higher GABA affinity.

The GABA potency of distinct receptor subtypes varies depending on the subunit composition, with the type of α subunit present being a key determinant. Although there is variation across studies, there is a general consensus that α6 subunits exhibit the highest, and α3 subunits the lowest, GABA potency (Böhme et al., 2004; Picton & Fisher, 2007), although it has also been suggested that the lowest potency is conferred by α2 (Mortensen et al., 2011). The β subunit identity further affects receptor sensitivity, with β3 being suggested to confer the most, and β1 the least, sensitivity of the three β isoforms (Mortensen et al., 2011). The presence of either a γ or δ subunit is also a significant factor for determining GABA potency: the EC_{50} of α4β3δ is five times lower than that of α4β3γ2 receptors (Brown et al., 2002), consistent with the detection of low GABA concentrations by extrasynaptic δ-containing receptors. Furthermore, GABA acts as only a partial agonist for α4β3δ, as opposed to a full

agonist for α4β3γ2 receptors (Brown et al., 2002), demonstrating that extrasynaptic δ-containing receptors are high affinity, but low efficacy, receptors. Such receptors are more amenable to potentiation by endogenous modulators such as neurosteroids (Bianchi & Macdonald, 2003).

In addition to sensitivity, subunit composition also strongly influences the rates of activation, desensitisation and deactivation of GABA$_A$Rs. Several studies have employed rapid applications of saturating GABA concentrations to show that the type of α subunit present in αβγ2 receptors affects the receptor activation rate, with those containing α2 activating twice as fast as those containing α1 (Lavoie et al., 1997; McClellan & Twyman, 1999). As always, the presence of a γ versus a δ subunit is significant: the activation rate of α1β3γ2 receptors is five-fold greater than that of α1β3δ receptors, but the deactivation rate of the γ-containing receptors is much slower (Haas & Macdonald, 1999). The α subunit isoform affects deactivation for both αβγ and αβδ receptors: the deactivation rate of α1β1γ2 receptors is five-fold greater than that of α2β1γ2 receptors (McClellan & Twyman, 1999), while α1β3δ receptor deactivation is four-fold faster than that of α6β3δ receptors (Bianchi et al., 2002).

Desensitisation provides a mechanism for preventing excessive receptor activation. The exact physiological roles of desensitisation are still under debate but are likely to include a reduction in the ability of postsynaptic receptors to repeatedly respond to high-frequency neurotransmitter release (Papke et al., 2011), the initiation of inhibitory synaptic plasticity (Field et al., 2021) and the modulation of extrasynaptic receptors that are subjected to tonic activation by low ambient GABA concentrations (Bright et al., 2011). Consistent with their roles mediating phasic and tonic currents respectively, αβγ receptors desensitise more quickly and extensively than αβδ receptors (Haas & Macdonald, 1999; Bianchi et al., 2002). This is again influenced by the α subunit: α1βγ receptors desensitise faster than α5βγ (Caraiscos et al, 2004) and α6βγ receptors (Tia et al., 1996), while α1βδ receptors desensitise more slowly than α6βδ receptors (Bianchi et al., 2002). The importance of subunit composition for determining the biophysical properties of GABA$_A$Rs, and the downstream effects these may have on inhibition, are thus remarkably clear.

1.1.4. Phosphorylation of GABA_A receptors

Phosphorylation is one of the most common, and perhaps the most important, of the post-translational modifications that can be made to a protein. It is a reversible mechanism by which a phosphoryl (PO_3^-) group is added to specific amino acid residues – most commonly serine, threonine and tyrosine – via the action of a protein kinase binding to specific consensus sites (Ardito et al., 2017). Phosphorylation provides a key mechanism for the regulation of GABA_ARs, influencing numerous processes including receptor trafficking, cell surface expression, channel function and sensitivity to pharmacological agents (Nakamura et al., 2015). A selection of known GABA_AR phosphorylation sites and their effects are summarised in Table 1.1.

As has been previously mentioned, the ICD between TM3 and TM4 is the region of greatest heterogeneity between different receptor subunits. This region contains numerous consensus sequences for phosphorylation by both serine/threonine and tyrosine protein kinases (Moss & Smart, 1996). Phosphorylation of the ICD has been most extensively characterised for the β and γ2 subunits, for which multiple kinases that target sites in this domain have been identified (see review by Nakamura et al., 2015). Some sites are kinase-specific while others interact with several kinases.

A notable example is a conserved serine residue found in all three β subunits (S409 in β1 and β3; S410 in β2) that is capable of being phosphorylated by four different kinases: cyclic-AMP dependent protein kinase (PKA), phospholipid-dependent protein kinase C (PKC), protein kinase G (PKG) and Ca^{2+}/calmodulin-dependent protein kinase II (CaMKII) (Moss et al., 1992a; McDonald & Moss, 1994; McDonald & Moss, 1997). Interestingly, the action of the same kinase – PKA – at these sites in β1 and in β3 has opposing effects: PKA activity reduces the GABA-evoked currents of α1β1γ2 receptors (Moss et al., 1992b) but potentiates the currents of α1β3γ2 receptors (McDonald et al., 1998). This is due to the presence of a second phosphorylation site, S408, in β3, which enables two adjacent PO_3^- groups to be added to the subunit (McDonald et al., 1998). Substitution of S408 in β3 with alanine – a mutation that blocks phosphorylation – converted the effect of PKA from potentiation of GABA-evoked currents to inhibition of the currents, as occurs with the β1 subunit. Similarly,

introduction of a second phosphorylation site into β1, adjacent to S409, converted the effect of PKA into inducing current potentiation (McDonald et al., 1998). These differential effects on GABA-evoked currents between β1 and β3 arise due to differences in receptor trafficking: phosphorylation of the β subunit inhibits the binding of the AP2 complex (Kittler et al., 2005). As β3 can be phosphorylated more extensively than β1, it experiences a greater reduction in AP2 binding. This ultimately results in a reduction in receptor internalisation, and hence increased surface expression, of β3 receptors (Kittler et al., 2005). Furthermore, phosphorylation at either S408 or S409 on β3 enhances the neurosteroid-mediated potentiation of GABA-evoked currents (Adams et al., 2015).

Other phosphorylation sites within the intracellular loops of the β subunits have been identified and investigated. In addition to S409, β1 contains S384, which is phosphorylated by CaMKII (McDonald & Moss, 1994). An equivalent phosphorylation site, S383, exists on β3 and is also phosphorylated by CaMKII, resulting in potentiation of GABA-evoked currents (Houston & Smart, 2006; Houston et al., 2007). Phosphorylation of S410 on β2 by PKC downregulates GABA-evoked currents (Kellenberger et al., 1992). Two additional sites, Y372 and Y379, have also been located on β2 and are phosphorylated by the proto-oncogene tyrosine-protein kinase Src (c-Src) (Vetiska et al., 2007). In the presence of insulin, these phosphorylated residues may be bound by phosphoinositide 3-kinase (PI3-K), resulting in the upregulation of receptor surface expression and enhanced GABA$_A$R-mediated miniature inhibitory postsynaptic currents (mIPSCs) (Vetiska et al., 2007). Various other phosphorylation sites across the β subunit family have been identified by mass spectrometry and include T227 and Y230 on β1, Y215 and T439 on β2 and T282 and S406 on β3 (Kang et al., 2011). The effects of phosphorylation at these sites have yet to be investigated.

Numerous phosphorylation sites also exist within the ICD of the γ2 subunit. Phosphorylation of the residue S327 by PKC causes a reduction in GABA-evoked currents (Kellenberger et al., 1992), as does phosphorylation of S343 – a residue that exists only in the eight amino acid longer γ2L splice variant – by PKC and CaMKII (Moss et al., 1992a; Krishek et al., 1994). c-Src phosphorylates Y365 and Y367 on γ2S and its

homologous residues, Y373 and Y375, on γ2L, resulting in enhancement of GABA-evoked currents (Moss et al., 1995). Interestingly, mutating these tyrosine residues in the γ2 subunit abolishes the potentiation of GABA-evoked currents seen when S383 on β3 is phosphorylated (Houston et al., 2007), illustrating the complexity of regulation that can be imparted by this post-translational modification. Further γ2 phosphorylation sites include S348 and T350, which are targets of CaMKII (McDonald & Moss, 1994).

In contrast to the β and γ2 subunits, only one α subunit phosphorylation site has been definitively identified and investigated: residue S443 of α4, which is located within the intracellular loop and targeted by PKC (Abramian et al., 2010). Phosphorylation of S443 increases the stability of the α4 subunit within the endoplasmic reticulum, which subsequently increases the rate of receptor insertion into the plasma membrane (Abramian et al., 2010). Neurosteroids potentiate this process by enhancing PKC phosphorylation of S443. This further increases membrane insertion of α4-GABA$_A$Rs and consequentially increases the efficacy of tonic inhibition (Abramian et al., 2014). Moreover, S443 phosphorylation prevents current rundown (Abramian et al., 2010) and so further enhances the tonic activity mediated by these receptors.

While the effects of only one α subunit phosphorylation site have been investigated, novel and putative phosphorylation sites have been identified across the α subunit family (Bell-Horner et al., 2006; Munton et al., 2007; Ballif et al., 2008; Huttlin et al., 2010; Mukherjee et al., 2011). There are reports of kinase activity increasing the phosphorylation levels of α subunits: Churn et al. (2004), for example, found that CaMKII activation directly increases the phosphorylation level of the α1 subunit, although they did not identify the specific residues involved. Of the potential α subunit phosphorylation sites identified, the most notable is the putative phosphorylation site T375 on α1, as investigated by Mukherjee et al. (2011). This study found that mutation of T375 to the negatively charged amino acid aspartate (D), which mimics phosphorylation, diminished the binding affinity between α1 and the scaffold protein gephyrin. This consequently led to reductions in both postsynaptic α1-GABA$_A$R clusters and the amplitude of mIPSCs (Mukherjee et al., 2011), suggesting that the phosphorylation state of a GABA$_A$R can modulate the binding efficacy of gephyrin. This

is supported by a study by Kowalczyk et al. (2013), who investigated the gephyrin binding affinity of various peptides containing the β2 subunit gephyrin-binding motif; the peptide that bound most strongly to gephyrin contained the critical phosphorylation site S410.

TABLE 1.1. Non-exhaustive list of phosphorylation sites within GABA$_A$R subunits. Serine, threonine and tyrosine residues that serve as phosphorylation sites are detailed, along with the kinases that phosphorylate them and any known effects of their phosphorylation. Unknown effects and kinases are indicated by a dash.

GABA$_A$R subunit	Residues	Physiological effect	Kinases	References
α4	S443	Increases expression	PKC	Abramian et al. (2010)
β1	T227, Y230	-	-	Kang et al. (2011)
	S384	-	CaMKII	McDonald & Moss (1994)
	S409	Reduces currents	PKA, PKC, PKG, CaMKII	Moss et al. (1992a); Moss et al. (1992b); McDonald & Moss (1994); McDonald & Moss (1997)
β2	Y215, T439	-	-	Kang et al. (2011)
	Y372, Y379	Increases expression	PI3-K	Vetiska et al. (2007)
	S410	Reduces currents	PKA, PKC, PKG, CaMKII	Kellenberger et al. (1992); McDonald & Moss (1997)
β3	T282, S406	-	-	Kang et al. (2011)
	S383	Increases currents	CaMKII	Houston & Smart (2006); Houston et al. (2007)
	S408, S409	Phosphorylation of both sites increases currents. Phosphorylation of either site enhances neurosteroid-mediated current potentiation	PKA, PKC, PKG, CaMKII	McDonald et al. (1998); Kittler et al. (2005); Adams et al. (2015)
γ2S	S327	Reduces currents	PKC	Kellenberger et al. (1992)
	S348, T350	-	CaMKII	McDonald & Moss (1994)
	Y365, Y367	Enhances currents	c-Src	Moss et al. (1995)
γ2L	S343	Reduces currents	PKC, CaMKII	Moss et al. (1992a); Krishek et al. (1994)

1.2.   GABA$_A$ receptor activation & function

GABA is the main fast inhibitory neurotransmitter of the mature CNS, along with glycine in the hind brain and spinal cord (Bowery & Smart, 2006). Inhibition is mediated through distinct GABA$_A$R populations, distinguished by their subunit composition and subcellular localisation. Generally, postsynaptic and extrasynaptic GABA$_A$Rs mediate two functionally distinct types of inhibitory transmission: phasic inhibition and tonic inhibition, respectively. Phasic, or transient, inhibition is fast, high-amplitude, short-lasting inhibition generated when postsynaptic GABA$_A$Rs respond to high concentrations of GABA released into the synaptic cleft, following the activation of presynaptic interneurons. Postsynaptic receptors can thus typically be characterised by having low sensitivity to GABA, due to their exposure to such high (millimolar) levels of the agonist. In contrast, tonic inhibition is a continuous inhibitory current mediated by extrasynaptic GABA$_A$Rs, which have a much higher sensitivity to GABA (nanomolar – micromolar). As such, they are activated by the ambient GABA in the extracellular space (Farrant & Nusser, 2005; Brickley & Mody, 2012). GABA$_A$Rs constantly regulate these two different types of inhibition to maintain control of neuronal excitability within the brain.

1.2.1.   Phasic inhibition

Phasic inhibition consists of fast, transient inhibitory postsynaptic currents (IPSCs) and regulates point-to-point communication between neurons (Fig. 1.3A). It occurs when an action potential at a presynaptic nerve terminal stimulates the influx of Ca^{2+} ions and subsequent fusion of synaptic vesicles with the presynaptic membrane, resulting in the release of thousands of GABA molecules into the synaptic cleft. This generates a maximal GABA concentration within the cleft likely exceeding 1 mM, which activates GABA$_A$Rs clustered on the postsynaptic membrane and causes rapid Cl$^-$ flux (Farrant & Nusser, 2005).

The minimal time for which the postsynaptic receptors are exposed to GABA is a key feature of phasic receptor activation, resulting in the transient IPSCs that define phasic inhibition. There are several suggested time constants of synaptic GABA clearance,

which vary depending on the study: experiments using allosteric modulators to slow down the binding of GABA to its receptors suggest that GABA remains in the cleft for approximately 100 μs (Mozrzymas et al., 2003), while others that use low-affinity competitive antagonists suggest a slightly more conservative estimate of <500 μs (Overstreet et al., 2002; Scimemi & Beato, 2009). Regardless, GABA clearance is fast and this is because, following exocytosis, GABA diffuses rapidly away from its site of release (Overstreet et al., 2002). Most GABA is subsequently taken up, via GABA transporters (GATs), into neurons and glial cells (Scimemi, 2014); however, following diffusion, GABA may also activate perisynaptic receptors, receptors in other postsynaptic clusters adjacent to the same axon terminal, more distant extrasynaptic receptors or receptors at neighbouring synapses (Farrant & Nusser, 2005).

Fast, transient inhibitory neurotransmission is necessary to regulate the level and flow of excitatory information through the CNS, in order to prevent the development of pathological network activity. Synaptic GABAergic inhibition is primarily mediated through interneurons, which form feedforward and feedback inhibitory circuits, depending on local and afferent activity or neuromodulation (Ferrante et al., 2009). Feedforward inhibition occurs when excitatory pyramidal cells excite inhibitory interneurons, which subsequently inhibit downstream excitatory principal neurons (Stafstrom & Rho, 2017). In contrast, feedback inhibition occurs when principal cells synapse onto interneurons that project directly back onto, and inhibit, the principal cells that excited them (Stafstrom & Rho, 2017). In the hippocampus, different types of interneuron synapse onto discrete principal cell domains: basket cells form synapses onto pyramidal somata and dendrites, for example, while chandelier cells synapse onto axons (Klausberger & Somogyi, 2008). The location of a given synapse influences how the phasic inhibition it mediates subsequently affects neuronal activity, such as in cases of coincidence detection. For example, Pouille & Scanziani (2001) demonstrated that the effects of feedforward inhibition mediated by interneurons in the rat hippocampus differ depending on whether the interneurons synapse onto the soma or the dendrites of pyramidal cells. When an interneuron synapses onto the soma of a pyramidal cell, only a very short temporal window (< 2 ms) is available within which excitatory inputs can be summated to reach the

threshold for action potential generation (coincidence detection). However, this window is broader for cells in which interneurons instead synapse onto the dendrites of pyramidal cells, thus allowing excitatory inputs to be summed over a longer timeframe (Pouille & Scanziani, 2001). This illustrates the diverse effects that phasic inhibition can have on neuronal activity throughout the brain.
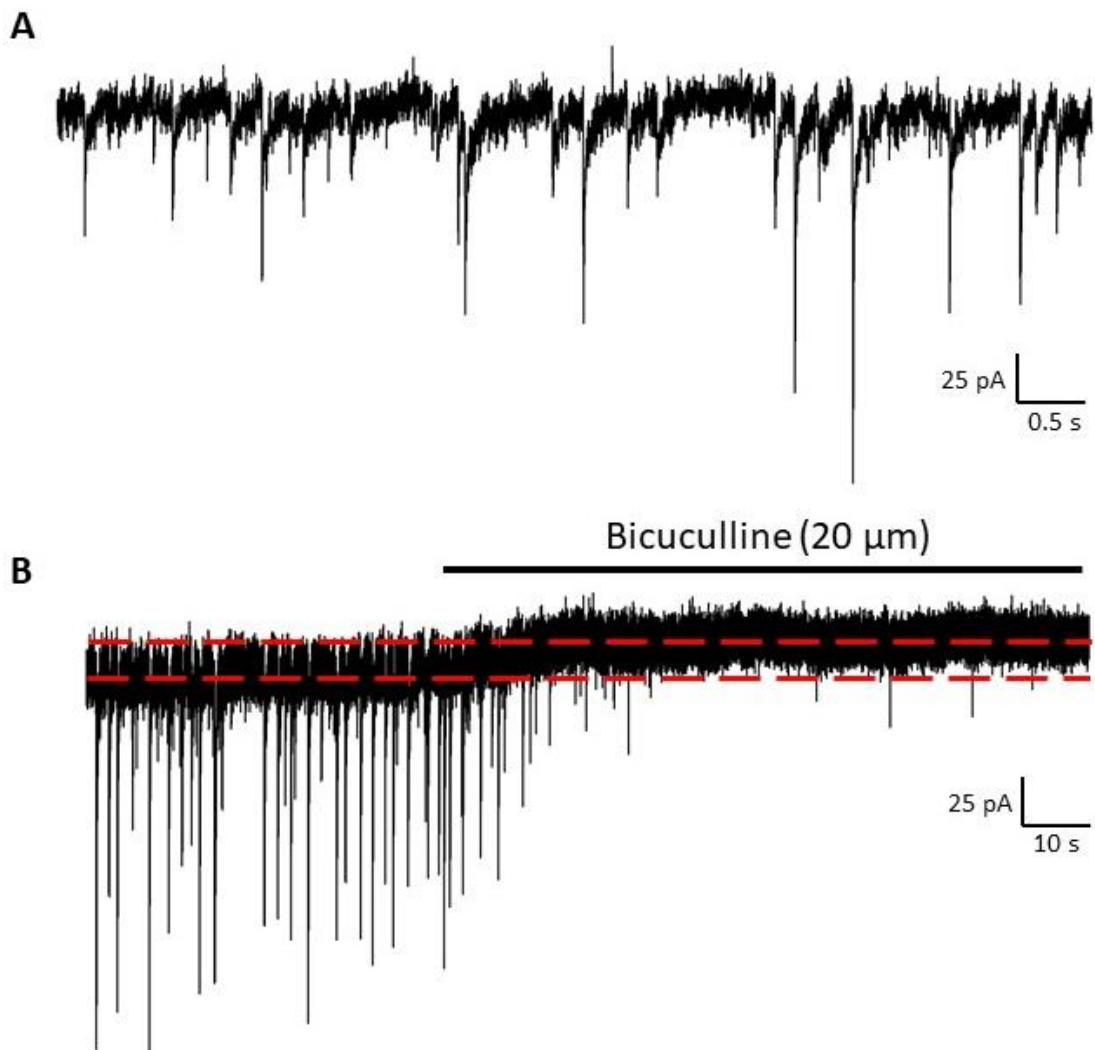
FIGURE 1.3. Phasic and tonic inhibition in hippocampal neurons in cell culture. **(A)** Phasic inhibition comprises synaptic GABA$_A$R activity and consists of transient, rapid IPSCS, which result from GABA release from presynaptic terminals. **(B)** The competitive antagonist bicuculline (20 μM) reveals tonic inhibition, mediated by extrasynaptic GABA$_A$Rs, by reducing the holding current, as indicated by the dashed red lines.

A critically important role of phasic inhibition is its ability to synchronise neuronal networks. Theta and gamma frequency network oscillations in the hippocampus, for example, are thought to be involved in the processing of sensory inputs and memory processes, and to coordinate communication between different brain regions (Lisman & Jensen, 2013). The generation and maintenance of these network oscillations is achieved by the synchronisation of the activity of pyramidal cell populations that receive inhibitory inputs from cortical and hippocampal basket cells (Cobb et al., 1995; Somogyi & Klausberger, 2005). The interneurons involved in such networks are mutually interconnected by gap junctions, disruption of which has been shown to slow theta oscillations and impair short-term spatial memory in mice (Allen et al., 2011), further demonstrating the importance of phasic inhibition in regulating networks of neuronal activity.

1.2.2. Tonic inhibition

In contrast to the short, sharp IPSCs that characterise phasic inhibition, tonic inhibition is defined by a continuous, low-amplitude, hyperpolarising current that is capable of controlling action potential firing (Fig. 1.3B). It does this by causing a persistent increase in the current conductance of a cell, which diminishes the voltage changes induced by a given excitatory input; and by narrowing the temporal window available for signal integration of excitatory inputs – this "shunting" inhibition reduces the likelihood of action potential generation (Farrant & Nusser, 2005).

Various sources exist for ambient GABA that is found in extracellular spaces and activates extrasynaptic GABA$_A$Rs. The most prominent of these is synaptic spillover from action potential-dependent vesicular GABA release, which has been demonstrated in the hippocampus (Glykys & Mody, 2007) and the thalamus (Bright et al., 2007). Other sources of extracellular GABA include release from astrocytes through the Bestrophin-1 channel (Lee et al., 2010; Yoon et al., 2011), reversal of GABA transporters (Gaspary et al., 1998; Richerson & Wu, 2003) and non-vesicular release (Song et al., 2013).

Like phasic inhibition, tonic inhibition is involved in the regulation of many processes throughout the CNS, including network oscillations. For example, Mann & Mody (2010), reported that an N-methyl-D-aspartate (NMDA) receptor-mediated increase in gamma oscillation frequency in the CA3 region of the mouse hippocampus was counteracted by the tonic conductance of δ-containing GABA$_A$Rs, thus maintaining a balance between excitation and inhibition. Furthermore, an increase in tonic activity has been shown to change the firing mode of CA3 hippocampal interneurons to one that supports synchronised oscillations in brain networks (Pavlov et al., 2014).

Tonic inhibition has been shown to modulate the gain (slope) of neuronal input-output curves, which affects, for instance, the processing of rate-coding information (Mitchell & Silver, 2003). Conversely, tonic conductance can also modulate neuronal offset (threshold) independently of gain. This has been demonstrated in hippocampal pyramidal cells and appears to be dependent upon the outward rectification of tonic receptors (Pavlov et al., 2009). There are examples of tonic inhibition regulating cognitive function: pharmacological inhibition or genetic deletion of extrasynaptic α5-containing GABA$_A$Rs improves spatial learning and memory (Collinson et al, 2002; Dawson et al., 2006). It is possible that tonic activity affects cognition through the regulation of long-term potentiation (Cheng et al, 2006). A role for tonic inhibition in development is also likely: dendritic backpropagating action potentials (bAPs) are regulated by tonic GABAergic inhibition in adolescent, but not in preadolescent, CA1 pyramidal neurons (Groen et al., 2014), while in postnatal animals, the tonic currents of cerebellar granule cells develop over time (Brickley et al., 1996). Tonic inhibition is thought to suppress motor behaviour as a default state in animals in order to conserve energy (Benjamin et al., 2010). Finally, tonic conductance provides an important mechanism of neuronal plasticity. The aforementioned study by Groen et al. (2014), for example, found that the induction threshold for spike timing-dependent plasticity in adolescent pyramidal neurons was altered by changes in tonic inhibition, while Saliba et al. (2012) reported that CaMKII-dependent phosphorylation of the β3 subunit residue S383 increased membrane insertion of, and subsequently enhanced tonic currents mediated by, α4β3δ receptors. Tonic inhibition is thus a critical player in the regulation of neuronal excitability in the brain.

1.3.   GABA$_A$ receptor pharmacology

Mirroring the diversity displayed by different GABA$_A$R subtypes, there exists many ligands, both endogenous and pharmacological, that are capable of interacting with, and influencing the activity of, these receptors. These ligands range from agonists to antagonists to allosteric modulators, each with their own distinct functions (Olsen & Sieghart, 2009). Endogenous ligands exist to regulate the activity of the receptors under physiological conditions; researchers use experimental drugs to interrogate receptor properties and functions; and therapeutic drugs are used to target receptors that are involved in certain disease states, with epilepsy being a notable example (see review by Palma et al., 2017). The following sections discuss a number of these ligands and their effects on GABA$_A$Rs.

1.3.1. Receptor agonists

The drive to understand the nature of inhibitory GABAergic neurotransmission, and the potential therapeutic targets it presents, was the catalyst for the development of a spectrum of different GABA agonists. The two most well-known orthosteric agonists of GABA$_A$Rs are the mushroom-derived psychoactive agent musicmol and THIP (also known as gaboxadol), which was developed from muscimol (Krogsgaard-Larsen et al., 2004).

Muscimol is a full agonist, and THIP a partial agonist, of the (typically synaptic) αβγ receptors (Mortensen et al., 2010). However, both compounds act as super-agonists at extrasynaptic αβδ receptors, eliciting peak currents 120% (muscimol) and 220% (THIP) the size of those generated with saturating GABA concentrations (Mortensen et al., 2010). Agonists such as these have been used in studies to interrogate the properties of GABA$_A$Rs (e.g., Stórustovu & Ebert, 2006; Mortensen et al., 2010). Muscimol and THIP act across a broad spectrum of receptor subtypes; multiple partial agonists with a range of affinities and efficacies for receptors with different subunit compositions have therefore been developed, in order to more specifically probe the properties of individual receptor subtypes. 4-PIOL (5-(4-piperidyl)-3-isoxazolol), for instance, is a low-affinity, weak partial agonist of GABA$_A$Rs (Mortensen et al., 2002). A

study by Patel et al. (2016) used 4-PIOL to identify a hitherto unknown population of low-affinity γ2 subunit-containing GABA$_A$Rs in the thalamus which, upon a rise in GABA levels, were able to contribute to tonic inhibition. Agonists are thus indispensable for the continued expansion of our knowledge of these receptors.

The therapeutic importance of GABA$_A$R agonists is also evident: THIP has been trialled as a potential treatment for insomnia (Roth et al., 2010), while muscimol has been shown to prevent neocortical seizures in rats and non-human primates (Ludvig et al., 2009), to highlight only a couple of examples.

1.3.2. Receptor antagonists

In addition to agonists, the functionality and therapeutic potential of GABA$_A$Rs is also investigated using receptor antagonists. Among the most commonly used of these is bicuculline, which acts as both a competitive antagonist at the GABA binding site (Andrews & Johnston, 1979; Johnston, 2013; Masiulis et al., 2019) and as a negative allosteric modulator of GABA$_A$R gating (Ueno et al., 1997). Using single channel experiments, bicuculline has been shown to reduce both the opening frequency and the channel open times of GABA$_A$Rs, thus reducing GABA-activated membrane conductance (Macdonald et al., 1989). Functionally, bicuculline is often used to investigate tonic currents in neuronal recordings: addition of bicuculline abolishes both the IPSCs produced by phasic transmission and the tonic current, as evidenced by a change in the holding current (see Fig. 1.3B). In a more therapeutic context, bicuculline has also been used to screen for potential anti-epileptic drugs, due to its pro-convulsant activity (e.g., Colombi et al., 2013; Eickhoff et al., 2014).

Similar to bicuculline is gabazine (SR-95531), which acts as a competitive antagonist at the GABA binding site (Johnston, 2013) and also shows negative allosteric properties, although to a lesser extent than bicuculline (Ueno et al., 1997). Functionally, gabazine is often used to investigate spontaneous receptor activity, as at low concentrations it selectively abolishes IPSCs without affecting spontaneous tonic currents (McCartney et al., 2007).

Another commonly used GABA$_A$R antagonist is picrotoxin (PTX): a non-competitive antagonist that binds within the channel pore of the receptor (Masiulis et al., 2019). Despite its binding site location, studies using single-channel recordings and IPSC analyses have suggested that PTX does not directly block the open ion channel pore, but instead acts by stabilising an agonist-bound closed (or potentially desensitised) receptor state (Smart & Constanti, 1986; Newland & Cull-Candy, 1992; Korshoej et al., 2010). This has been more recently corroborated with cryo-electron microscopy, which demonstrated that binding of PTX to the channel pore induces conformational changes that are consistent with allosteric antagonism, rather than blockade of the pore itself (Masiulis et al., 2019).

The identification of single point mutations that confer PTX-insensitivity to GABA$_A$Rs (Ffrench-Constant et al., 1993; Zhang et al., 1994; Xu et al., 1995; Ueno et al., 2000; Sedelnikova et al., 2006) has facilitated a range of functional studies. For example, Sun et al. (2018) used gene editing to introduce PTX-insensitivity into the δ subunit in mice, which enabled the researchers to pharmacologically isolate extrasynaptic δ-containing receptors. They found that, despite their extrasynaptic localisation, these typically tonically-activated receptors significantly contributed towards phasic inhibition in dentate granule and thalamocortical neurons (Sun et al., 2018). This illustrates the importance of antagonists in elucidating the functional properties of GABA$_A$Rs. With regards to therapeutic applications, PTX is a pro-convulsant and so, as with bicuculline, has been used to investigate epileptic disease states (Cho et al., 2018) and screen for putative anti-epileptic drugs (Kalitin et al., 2018).

1.3.3. Allosteric modulators

Many endogenous neurosteroids are potent modulators of neuronal excitability, primarily acting via the enhancement of GABA$_A$R activity. They are synthesised in the central and peripheral nervous system from cholesterol and sex and stress steroidal precursors (Baulieu, 1997) and can be structurally classified into different groups. Most are positive allosteric modulators of GABA$_A$Rs, including the pregnane neurosteroids, which are the most commonly studied of the neurosteroids and include

allopregnanolone and THDOC (allotetrahydrodeoxycorticosterone), and the androstane neurosteroids, which include etiocholanone and androstanediol. There are also sulfated neurosteroids which, in contrast to the majority of neurosteroids, are negative allosteric modulators of $GABA_A$Rs, and include pregnenolone sulfate and dehydroepiandrosterone sulfate (DHEAS) (Reddy, 2010).

Enhancement of GABA responses occurs when neurosteroids bind to a site within the transmembrane domains of the α subunit, at the β(+)/α(−) interface (Hosie et al., 2006, Laverty et al., 2017). Potentiation at this site is critically dependent on a key glutamine residue that is conserved across the α subunits and has been identified as Q241 and Q246 in α1 and α4 respectively (Hosie et al., 2006; Hosie et al., 2007; Hosie et al., 2009; Laverty et al., 2017). The binding of neurosteroids potentiates GABA-evoked currents at the single channel level by increasing both the open frequency and open duration of the ion channel (Twyman & Macdonald, 1992). Furthermore, the binding of neurosteroids at this site, when present in high (>10 µM) concentrations and in the absence of GABA, can result in the direct activation of the receptor (Majewska et al., 1986; Callachan et al., 1987; Hosie et al., 2006; Chen et al., 2019).

While neurosteroids modulate most $GABA_A$R subtypes, a greater degree of potentiation is seen in δ-subunit containing receptors (Belelli et al., 2002; Pillai et al., 2004). This is because GABA is only a partial agonist at δ-$GABA_A$Rs, so neurosteroid binding increases GABA efficacy (Brown et al., 2002). Furthermore, δ-$GABA_A$Rs have a higher GABA affinity, and desensitise to a lesser extent in the continued presence of GABA, compared to other receptor subtypes (Haas & Macdonald, 1999; Bianchi et al., 2002; Brown et al., 2002). Therefore, even in the presence of saturating GABA concentrations, neurosteroids are able to enhance the currents generated by δ-containing receptors. As such, they tend to have a greater modulatory effect on tonic inhibition, which, as has been previously mentioned, is the primary type of inhibition mediated by these receptors.

In addition to directly modulating $GABA_A$R activity, a distinct interplay exists between neurosteroid activity and phosphorylation-dependent receptor regulation. For example, Abramian et al. (2014) demonstrated that the PKC-dependent phosphorylation of S443 of the α4 subunit is potentiated by neurosteroids, resulting

in the increased insertion of α4 subunit-containing GABA$_A$Rs into the plasma membrane and the subsequent enhancement of tonic inhibition. THDOC has been shown to increase phosphorylation of the adjacent β3 subunit residues S408 and S409; in turn, phosphorylation at these residues increases THDOC-mediated potentiation of GABA-evoked currents (Adams et al., 2015), suggesting that reciprocal pathways exist for the mutual regulation of GABA$_A$Rs by neurosteroids and phosphorylation. Furthermore, although independent of phosphorylation, short-term neurosteroid treatment has been shown to enhance the insertion of δ-containing receptors into the membrane (Shen et al., 2005), again elevating the level of tonic conductance mediated by these receptors and further illustrating the significance of neurosteroid-mediated regulation of GABA$_A$Rs.

There exists a myriad of drugs that act as allosteric modulators of GABA$_A$Rs and are used to treat a range of conditions (Korpi et al., 2002). The majority of these drugs – the benzodiazepines (BDZs), the barbiturates, ethanol and general anaesthetics being the most well-known – are positive allosteric modulators that potentiate inhibitory GABA-evoked currents. BDZs – perhaps the most famous of all the GABA$_A$R-targeting drugs – were for many years used in a variety of therapeutic contexts, including as anti-epileptics, hypnotics and anxiolytics. However, due to the associated risks of developing physical and psychological tolerance and dependence, the use of BDZs is now limited to a much narrower range of conditions (Olsen, 2018).

The actions of BDZs, which enhance GABA-evoked currents by increasing the frequency of single channel openings (Rogers et al., 1994), are critically dependent on the subunit composition of the receptor. Potentiation only occurs for receptors containing the γ subunit (Günther et al., 1995; McKernan et al., 1995) due to the location of the canonical BDZ binding site at the α(+)/γ(-) interface (Sigel & Luscher, 2011). The α subunit identity is similarly crucial, with α4 and α6 – the α subunit isoforms most commonly associated with the mediation of tonic currents – showing no potentiation (Wieland et al., 1992; Wafford et al., 1996). The presence of a key histidine residue – identified as H101 in α1 and conserved across α2, α3 and α5 – is essential for the potentiating actions of BDZs (Wieland et al., 1992). This histidine is replaced by an arginine residue in the α4 and α6 subunits; indeed, substituting H101

for an arginine in α1 abolishes BDZ-mediated potentiation of GABA-evoked currents (Rudolph et al., 1999). However, it should be noted that α subunits are dispensable for some actions of BDZs (Wongsamitkul et al., 2017).

As with GABA$_A$R agonists and antagonists, allosteric modulators are important tools for probing receptor functionality. As illustrated by the lack of BDZ-mediated potentiation at δ subunit-containing receptors, few pharmacological tools exist for modulating these receptors, although a possible candidate is the delta selective compound 2 (DS2). The maximal GABA-evoked currents of δ-GABA$_A$Rs are potentiated by DS2, with its potency increased by the presence of the α4 and α6 subunits (Wafford et al., 2009; Jensen et al., 2013; Lee et al., 2016). As the first identified positive allosteric modulator that is selective for α4/6βδ receptors, DS2 has the potential for use as a novel tool for the investigation of extrasynaptic δ-GABA$_A$Rs.

1.4.   α3 subunit-containing GABA$_A$ receptors

The subunit composition of the GABA$_A$R determines its kinetic and pharmacological properties, as well as its subcellular localisation. The α subunit plays a key role in determining several of these features, as already discussed. While in-depth studies have been made of most of the GABA$_A$R α subunits, relatively little is known about α3. The following sections will provide a detailed discussion on α3 subunit-containing GABA$_A$ receptors (α3-GABA$_A$Rs): their expression patterns, functions in the brain and relevance to certain disease states.

1.4.1.   The expression patterns and physiological functions of α3-GABA$_A$Rs

The α3-GABA$_A$Rs represent 10-15% of all GABA$_A$Rs in the adult rat brain (McKernan & Whiting, 1996) and are most commonly of the α3β2/3γ2 subtypes (Fritschy & Mohler, 1995). *In situ* hybridisation and immunohistochemical studies have identified the expression of the α3 subunit in numerous regions of the rodent brain (Fig. 1.4A), including the hippocampus, thalamus, amygdala and olfactory bulb (Pirker et al., 2000; Hörtnagl et al., 2013). However, compared to the more ubiquitous distribution of, for

example, the α1 subunit, α3 expression is relatively confined, occurring primarily at inhibitory synapses of the thalamic reticular nucleus (nRT; Fig. 1.4C) (Studer et al., 2006; Liu et al., 2007) and reelin-positive cells in the medial entorhinal cortex (Berggaard et al., 2018). α3 is also expressed extrasynaptically in the basolateral amygdala (BLA; Fig. 1.4B) (Marowsky et al., 2012) and the inferior olivary nucleus (Devor et al., 2001).

The subcellular localisation of the α3-GABA$_A$R affects the physiological function it performs. For example, in the nRT, the synaptically-localised α3-GABA$_A$Rs mediate phasic inhibition (Studer et al., 2006; Schofield & Huguenard, 2007). In contrast, in the BLA, the extrasynaptically-localised α3-GABA$_A$Rs mediate tonic inhibition (Marowsky et al., 2012). It is therefore likely that, depending on its localisation, the α3-GABA$_A$R performs diverse roles in different areas of the brain and contributes to GABAergic inhibition across an array of behavioural and cognitive states.
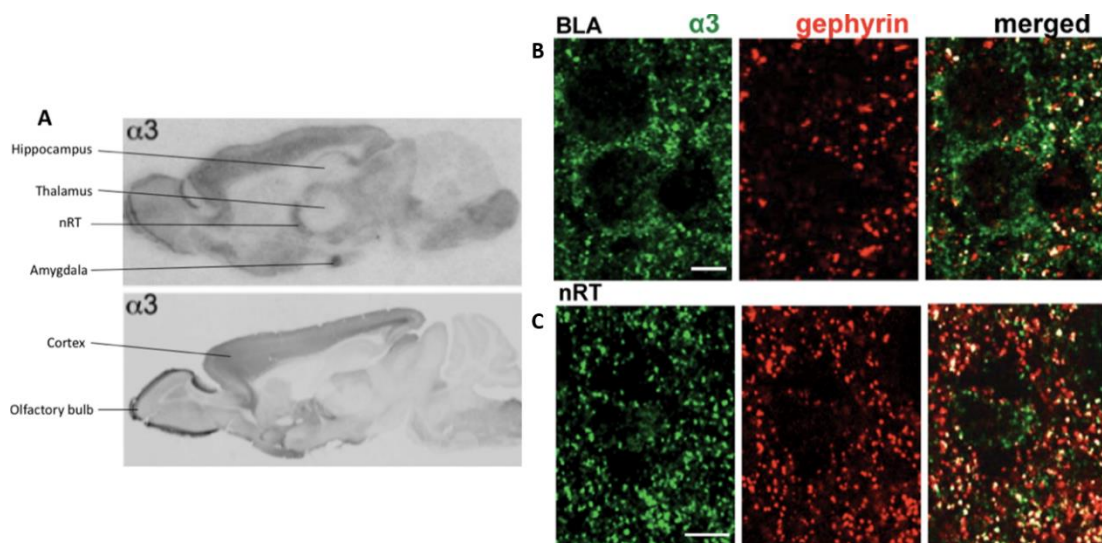
FIGURE 1.4. Expression of the GABA$_A$R α3 subunit in the brain. **(A)** Distribution of α3-GABA$_A$R mRNA and protein shown by *in situ* hybridisation (top) and immunohistochemistry (bottom) in sagittal sections of the mouse brain. **(B)** α3-GABA$_A$R labelling (green) in the mouse BLA only partially co-localises with the postsynaptic marker gephyrin (red), as shown by the poor co-localisation in white, suggesting that α3-GABA$_A$Rs are preferentially localised at extrasynaptic sites in this region. **(C)** α3-GABA$_A$R labelling in the mouse nRT (green) co-localises well with gephyrin (red), as shown by the co-localisation in white, suggesting α3-GABA$_A$Rs are preferentially localised synaptically in this region. Scale bar, 5 μm. Adapted from Hörtnagl et al. (2013) **(A)** and Marowsky et al. (2012) **(B)** and **(C)**.

α3 is one of the most widely expressed α subunits in the embryonic and neonatal rat brain (Laurie et al., 1992; Wisden et al., 1992), indicating an important role for the subunit early in neurodevelopment. These high expression levels begin to decline 10-12 days postpartum as α3 is replaced with α1, the dominant GABA$_A$R subunit in the adult brain (Pirker et al., 2000). The decrease in α3 expression levels is associated with editing of *Gabra3* (the gene that encodes the α3 subunit) mRNA, resulting in the replacement of an isoleucine (I) with a methionine (M) at residue 342 (Ohlson et al., 2007). I/M editing during brain development has been shown to be inversely related to α3 protein abundance (Daniel et al., 2011); indeed, the rate of *Gabra3* mRNA editing rapidly increases from birth, reaching maximal levels 7 days postpartum (Rula et al., 2008). In the adult brain, approximately 90% of the α3 subunits are of the edited methionine form, although lower levels of editing occur in the hippocampus (Rula et al., 2008). Methionine substitution in the α1 subunit, at the residue corresponding to the α3 I/M site, caused similarly reduced surface expression of α1, suggesting that I/M editing of *Gabra3* mRNA is involved in the regulation of α3-GABA$_A$R trafficking and so may facilitate the observed developmental switch in subunit composition (Daniel et al., 2011). Rula et al. (2008) reported that non-edited α3(I)-GABA$_A$Rs activated faster and deactivated more slowly than their edited α3(M)-GABA$_A$R counterparts, which indicates that the high levels of the non-edited α3(I) subunit observed during early brain development, when the action of GABA is depolarising, may facilitate the strong excitatory responses necessary for healthy synapse formation. Hence, α3-GABA$_A$Rs likely play a critical role in early development, while their targeted expression in specific regions of the adult brain indicate their involvement in multiple cognitive processes.

The α3-GABA$_A$R has distinct kinetic properties, with kinetic parameters generally appearing to be slower than those of receptors containing other α subunits. Picton & Fisher (2007) used rapid application recordings from excised macropatches to investigate the activation, deactivation, desensitisation and recovery kinetics for each of the six α subunit isoforms. Along with α5 subunit-containing receptors, α3-GABA$_A$Rs were found to have one of the slowest decay rates of all GABA$_A$R subtypes (Picton & Fisher, 2007). Indeed, a recent study used a HEK-293 cell-neuron co-culture expression

system – which enabled the recording of IPSCs mediated by a pure population of GABA$_A$Rs with a defined stoichiometry – to demonstrate that the decay time constant of α3β3γ2 receptors is significantly slower than that of their α1β3γ2 counterparts (Syed et al., 2020). α3-GABA$_A$Rs also have one of the slowest deactivation rates, comparable only to α6 subunit-containing receptors, and display the slowest rates of desensitisation and activation of all the α subunits (Picton & Fisher, 2007). Interestingly, along with α4- and α5-containing receptors, α3-GABA$_A$Rs recover rapidly from desensitisation (i.e., they remain desensitised for a shorter time period) (Picton & Fisher, 2007). This rapid rate of recovery, combined with their slow entry into the desensitised state, suggests that α3-GABA$_A$Rs are able to maintain their maximal current amplitude, even with rapid firing input (Picton & Fisher, 2007).

Due to the vital importance of GABAergic inhibition in maintaining normal levels of excitation in the CNS, different GABA$_A$R isoforms are implicated in a variety of disease states. This is certainly the case for α3 subunit-containing GABA$_A$Rs. The role that α3-GABA$_A$Rs may play in the regulation of anxiety and stress disorders is well-documented (Atack et al., 2005; Dias et al., 2005; Morris et al., 2006; Fischer et al., 2011), if controversial, and will be discussed in more detail in the following section. Similarly, α3-GABA$_A$Rs have been strongly implicated in several epileptic seizure types (Loup et al., 2006; Liu et al., 2007; Christian et al., 2013; Niturad et al., 2017); again, these will be discussed later. There is emerging evidence that the dysregulated activity of non-neuronal α3-GABA$_A$Rs may have proinflammatory effects and contribute to the development of pathologies such as cancer (Gumireddy et al., 2016; Liu et al., 2016; Long et al., 2017) and colon inflammation (Seifi et al., 2018). Furthermore, a close association between the impaired expression and function of α3-GABA$_A$Rs and the expression of toxic amyloid β-oligomers was recently identified in the locus coeruleus (LC) of Alzheimer's patients, indicating the potential of these receptors to dysregulate LC activity (Kelly et al., 2020). As such, the correct functioning of α3 subunit containing-GABA$_A$Rs is critical for the maintenance of a healthy physiological state.

1.4.2. A role for α3-GABA$_A$Rs in the regulation of anxiety

Over the last couple of decades, emerging evidence has indicated a role for both α2 and α3 subunit containing-GABA$_A$Rs in the mediation of anxiolysis, with the suggestion that these receptors may provide therapeutic targets for the treatment of anxiety and fear disorders. However, the relative contributions of each receptor subtype to the mediation of anxiolysis is controversial, with different studies suggesting primary roles for α2- and α3-GABA$_A$Rs respectively.

The first study to posit a role for α3-GABA$_A$Rs in anxiety was conducted by Atack et al. (2005) and reported that a negative allosteric modulator, α3IA, which is selective for GABA$_A$Rs containing the α3 subunit, is anxiogenic in rats subjected to the elevated plus maze. Another study later that same year identified TP003, a functionally selective positive allosteric modulator of the α3-GABA$_A$R that acts via the BDZ binding site. TP003 produced a robust anxiolytic-like effect in both rodent and non-human primate behavioural models of anxiety (Dias et al., 2005). Furthermore, TP003 retained its efficacy in α2(H101R) mice – mice containing a point mutation that renders α2-GABA$_A$Rs insensitive to BDZs – in a stress-induced hyperthermia model, suggesting that the anxiolytic effects of BDZs are produced by the potentiation of α3-containing, and not α2-containing, receptors (Dias et al., 2005). L-838417, a drug with positive allosteric properties at α2-, α3 and α5-containing receptors, elicited anxiolytic effects in α2(H101R) mice in the conditioned emotional response (CER) test, again indicating that α3-GABA$_A$Rs contribute to anxiolysis (Morris et al., 2006). In 2011, Fischer et al. reported that TP003 had anxiolytic properties when tested on monkeys, without causing the sedative, ataxic and hyperphagic responses commonly elicited by BDZs. They concluded that α3-GABA$_A$Rs are fundamental to the mediation of the anxiolytic and motor effects of BDZ-type drugs (Fischer et al., 2011).

The amygdala, and in particular the BLA, has been shown to play an important role in associative fear conditioning, which is vital for an animal's survival by ensuring adaptive behavioural responses to aversive stimuli (Krabbe et al., 2018). The BLA plays a key role in regulating anxiety, with excitation reported to increase, and inhibition decrease, anxiety-like behaviour (Sajdyk & Shekhar, 1997). Accumulating evidence

suggests that the aberrant functioning and remodelling of these fear learning circuits is involved in the development and expression of psychiatric conditions, including anxiety disorders (Lüthi & Lüscher, 2014). In 2012, a study by Marowsky et al. identified a population of extrasynaptically localised $\alpha3$-GABA$_A$Rs in the BLA that mediate the majority of tonic inhibition in BLA principal neurons. The extrasynaptic localisation of these receptors in a region of the brain so important for the regulation of fear and anxiety suggests $\alpha3$-GABA$_A$Rs play an important role in mediating these emotions. Marowsky and colleagues further reported that TP003 both increases tonic currents and dampens excitability in wildtype BLA principal cells, but not in principal cells in which the $\alpha3$ subunit has been knocked out ($\alpha3$KO), again adding to the evidence that $\alpha3$-GABA$_A$Rs are involved in anxiety.

However, the apparent functional selectivity of TP003 for $\alpha3$ subunit-containing receptors has been called into question over recent years. Christian et al. (2015) could not replicate the strong functional selectivity for $\alpha3$-GABA$_A$Rs initially reported by Dias et al. (2005). de Lucas et al. (2015) found that TP003 potentiated GABA responses through $\alpha3$- and $\alpha5$-containing receptors almost equally (43% and 41% relative to diazepam respectively). TP003 also caused considerable potentiation at $\alpha1$- and $\alpha2$-containing receptors (21% and 19% respectively). In 2018, Neumann et al. reported TP003 to be completely non-selective, with efficacy at $\alpha1$-, $\alpha2$ and $\alpha5$-containing receptors comparable to that at $\alpha3$-containing receptors. These investigations all indicate that TP003 is not functionally selective for $\alpha3$-GABA$_A$Rs., which compromises the results of studies using TP003 as a tool to demonstrate the anxiolytic properties of these receptors.

Furthermore, there is evidence to suggest that $\alpha2$ subunit-containing GABA$_A$Rs are in fact the primary mediators of anxiolysis. Low et al. (2000) concluded that anxiolysis is mediated through $\alpha2$-GABA$_A$Rs because the anxiolytic effects of diazepam were absent in $\alpha2$(H101R) mice but present in $\alpha3$(H126R) mice. Yee et al. (2005) reported that both anxiety-related behaviour in the elevated plus maze test, and the anxiolytic actions of diazepam, were unaffected in $\alpha3$KO mice. In contrast, $\alpha2$KO mice displayed increased risk assessment to novelty and enhanced behavioural aversion (Koester et al., 2013), indicating that $\alpha2$-GABA$_A$Rs are key to regulating anxiety-related responses.

Neumann et al. (2018) found that triple point-mutated mice with α2-only BDZ-sensitive receptors displayed significantly reduced anxiety in the elevated plus maze test compared to wildtype animals, while triple point-mutated mice with α3-only BDZ-sensitive receptors did not. Together, these data strongly support a substantial role for α2-GABA$_A$Rs in regulating anxiety-related behaviours.

The picture is therefore mixed on whether α2- or α3-containing receptors contribute more significantly to anxiety. Taking all the evidence together, it is likely that α2-GABA$_A$Rs are the primary mediators of anxiolysis – certainly, they appear to have a larger effect than α3-GABA$_A$Rs do. However, there is too much evidence implicating α3-GABA$_A$Rs in anxiety-related processes for these receptors not to perform at least an auxiliary role in the regulation of such behaviours. Additionally, the extrasynaptic α3-containing receptors that generate tonic currents in the BLA, identified by Marowsky et al. (2012), further implicate α3-GABA$_A$Rs in anxiety, given their localisation in a brain region so key to the processing of fear-related emotions.

1.4.3. α3-GABA$_A$Rs, the thalamic reticular nucleus and absence epilepsy

The thalamic reticular nucleus (nRT) is a layer of GABAergic neurons surrounding the lateral and anterior aspects of the dorsal thalamus. Thalamocortical (TC) and corticothalamic (CT) axons, which connect the thalamus and the cortex, pass through and innervate the nRT with collateral projections. This provides excitatory input into the nRT, which in turn provides synaptic inhibition onto TC neurons. The resulting hyperpolarisation deinactivates low threshold T-type calcium channels, causing TC rebound bursting and the subsequent re-excitation of reticulothalamic (RT) neurons to create a reciprocal synaptic loop (von Krosigk et al., 1993; Pinault, 2004) (see Fig. 1.5).

The reciprocal synaptic connectivity that exists between excitatory TC relay neurons and inhibitory RT neurons is critically required for the maintenance of normal thalamic oscillations. The feedforward and feedback connections that exist between the cortex and thalamus strengthen these intrinsic thalamic oscillations into larger networks of thalamocortical activity (Huguenard & McCormick, 2007). Synchronisation of the

electrical activity of the groups of neurons involved in this circuit creates spindle oscillations, such as the 7-14 Hz spindles that occur during sleep (von Krosigk et al., 1993; McCormick & Bal, 1997). Hypersynchronisation of these networks results in pathological 3 Hz spike-wave discharges (SWD) that are the hallmark of generalised absence epilepsy (Terlau et al., 2020).

α3 is the only GABA$_A$R α subunit for which expression has been detected in the mature nRT, where it is synaptically localised (Pirker et al., 2000; Studer et al., 2006; Liu et al., 2007; Hörtnagl et al., 2013). Using a genetic rat model of absence epilepsy, Liu et al. (2007) observed a specific loss of α3 subunit immunoreactivity from the inhibitory synapses of the nRT, suggesting a requirement for α3-GABA$_A$Rs in the maintenance of normal thalamic oscillations. More recently, Niturad et al. (2017) identified six rare loss-of-function variants in the *GABRA3* gene in patients presenting with a variety of epileptic seizure types, including absence epilepsy, intellectual disability and neurodevelopmental delay, and in some cases, dysmorphic features.

Interestingly, α3KO mice do not show spontaneous seizures, as may be expected; instead, they display increased nRT-mediated inhibition and a reduced susceptibility to seizures induced by pharmacological agents (Schofield et al., 2009). It has been suggested that this is due to a compensatory mechanism that increases the expression of a modified α subunit in the knockout animals, although these alternative α subunits have not yet been identified (Schofield et al., 2009). However, Christian et al. (2013) reported an increase in
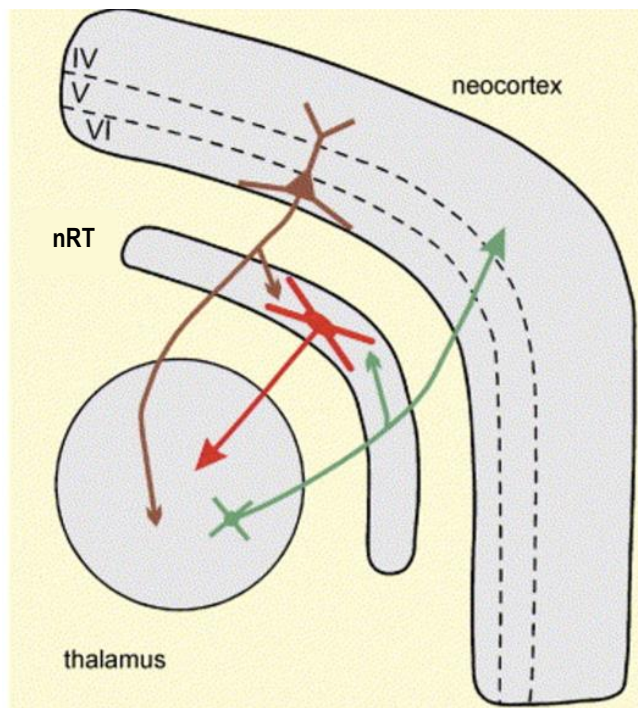
FIGURE 1.5. Simplified schema of the three principal neurons that comprise the excitatory corticothalamic (brown neuron), excitatory thalamocortical (green neuron) and inhibitory reticulothalamic (red neuron) systems. Neurons and structures are not to scale. Adapted from Pinault (2004).

SWD, a characteristic of absence seizures, in a mouse model in which the BDZ binding site of the α3 subunit had been mutated. It is therefore possible that the impaired function of the α3 subunit of GABA$_A$Rs may lead to epileptic seizures, which are undetected in α3KO animals due to a compensatory mechanism or other adaptive processes.

It has been suggested that α3-GABA$_A$Rs in the nRT are potentiated by "endozepines" (endogenous, BDZ-mimicking molecules) such as diazepam binding inhibitor (DBI), which are likely released by astrocytes and may be instrumental in the development of therapies against absence seizures (Christian et al., 2013; Christian & Huguenard, 2013). Hence, exploring the synaptic localisation of α3-GABA$_A$Rs in the nRT, and their subsequent role in maintaining normal thalamocortical oscillations, is of significant therapeutic value.

1.5. Summary and project aims

While the α3-GABA$_A$R accounts for 10-15% of all GABA$_A$Rs in the adult rat brain (McKernan & Whiting, 1996) and is expressed in various nuclei across the CNS (Pirker et al., 2000; Hörtnagl et al., 2013), it remains relatively understudied. Inhibition mediated by these receptors is clearly important for normal brain function, as evidenced by the aberrant phenotypes displayed when α3-GABA$_A$R expression is altered (Loup et al., 2006; Liu et al., 2007), or when the *Gabra3* gene is mutated (Christian et al., 2013; Christian & Huguenard, 2013; Niturad et al., 2017) or knocked out (Sturder et al., 2006; Schofield et al., 2009). In particular, α3-GABA$_A$Rs may provide a therapeutic target for mediating anxiolysis (Atack et al., 2005; Dias et al., 2005; Morris et al., 2006; Fischer et al., 2011; Marowsky et al., 2012) and treatment of absence seizures (Liu et al., 2007; Christian et al., 2013; Christian & Huguenard, 2013; Niturad et al., 2017). Finally, compared to receptors containing other α subunit isoforms, the α3-GABA$_A$R is unusual in having distinct subcellular localisation patterns in different brain areas – the most noteworthy being its synaptic localisation in the nRT (Pirker et al., 2000; Sturder et al., 2006; Liu et al., 2007; Hörtnagl et al., 2013) and its extrasynaptic localisation in the BLA (Marowsky et al., 2012) – that allow it to

perform distinct roles in phasic and tonic inhibition respectively. This in turn may be important for the way in which α3-GABA$_A$R-mediated inhibition modulates information processing in these different brain areas.

With this in mind, the overall aim of this project was to investigate the molecular mechanism(s) that control the differential subcellular localisation of α3-GABA$_A$Rs in distinct brain regions. To achieve this, the aim was broken down into the following sections.

1.5.1. *Putative phosphorylation sites on the α3 subunit*

Phosphorylation is a common post-translational modification that regulates a number of important processes, including receptor trafficking (Nakamura et al., 2015). Several putative phosphorylation sites have been identified within the α3 subunit (Huttlin et al., 2010; Maric et al., 2014) that have never been investigated for the potential roles they may play in receptor regulation. The first aim, therefore, was to investigate these putative phosphorylation sites by creating phospho-null and phospho-mimetic mutants of these residues and assessing their effects on receptor GABA sensitivity and cell surface expression via their expression in HEK-293 cells. Following the results of these experiments, selected residues were further studied in hippocampal neurons in cell culture in order to assess their effects on inhibitory synaptic transmission.

1.5.2. *α3-GABA$_A$R subcellular localisation*

Several of the residues investigated in the first aim have been identified as playing a critical role in mediating the binding between the α3 subunit of the GABA$_A$R and gephyrin (Maric et al., 2014). Gephyrin is a scaffold protein that tethers GABA$_A$Rs at inhibitory synapses (Tyagarajan & Fritschy, 2014); affecting this interaction may consequently affect the subcellular localisation of the α3-GABA$_A$R. Therefore, the second aim was to use structured illumination microscopy to investigate whether the phospho-mutants in the first aim influenced both the subcellular localisation of the α3-GABA$_A$R, as well as its co-localisation with gephyrin. The effects of the mutations

on gephyrin binding were then further investigated using co-immunoprecipitation experiments.

1.5.3. *The physiological functions of the α3-GABA$_A$R*

Relatively little is known about the α3-GABA$_A$R or the physiological role(s) it performs. The final aim, therefore, was to elucidate the functions performed by the α3-GABA$_A$R in the brain. This was attempted by creating a picrotoxin-insensitive mutant of the α3 subunit to enable isolation of sIPSCs mediated specifically through α3-GABA$_A$Rs in hippocampal neurons in cell culture. Additionally, short hairpin RNAs were used in an attempt to knockdown endogenous α3 subunit expression.

1.5.4. *Summary of thesis aims*

1. To investigate the potential effects of putative phosphorylation sites within the α3 subunit on α3-GABA$_A$R agonist sensitivity, cell surface expression and sIPSC kinetics (chapter 3).

2. To investigate the effects of phosphorylation at one of these sites on the subcellular localisation of the α3-GABA$_A$R (chapter 4).

3. To investigate the effects of phosphorylation at one of these sites on the interaction between the α3-GABA$_A$R and the scaffold protein gephyrin (chapter 4).

4. To examine some of the physiological functions the α3-GABA$_A$R may perform in the brain (chapter 5).

Chapter 2: Materials & Methods

2.1. Site-directed mutagenesis

Site-specific mutations were introduced into the murine *Gabra3* gene, cloned into the pRK5 vector, using the Q5 High-Fidelity DNA Polymerase (New England BioLabs; NEB) according to the manufacturer's instructions. Custom-made forward and reverse primers (Merck), designed using the NEBaseChanger tool (NEB), for all mutant subunits are detailed in Table 2.1. The polymerase chain reaction (PCR) amplification conditions were: 10 s denaturation at 98°C, 30 s annealing (at 50-72°C depending on the primers used) and finally a 3 minute extension at 72°C for 30 cycles.

PCR products were labelled with GelRed (Biotium) and run on a 0.8% agarose gel at 100 V for 45 minutes alongside a 1 kb ladder, which was used as a molecular weight calibration to identify the appropriately sized DNA band for the α3 subunit. Bands were visualised under UV light, extracted and purified using the Monarch® DNA gel extraction kit (NEB), according to the manufacturer's instructions. Briefly, this involved dissolving the extracted band, spinning through a column to harvest the DNA from the solution and eluting the purified DNA. The DNA was then heated to 70°C for 5 minutes to open up any secondary structures. The DNA was then ligated: 16 μl of the purified DNA was added to 2 μl of T4 ligase buffer (NEB) and 1 μl of T4 polynucleotide kinase (NEB). This was incubated at 37°C for 30 minutes, before the addition of 1 μl of T4 ligase (NEB). The reaction was further incubated at room temperature for 2 h, after which the ligase was inactivated by heating the solution to 65°C for 20 minutes.

The ligation product was used to transform 5-alpha competent *E. Coli* cells (NEB). 5-alpha cells were allowed to thaw on ice. 12.5 μl of thawed cells were added to 5 μl of the ligation product and mixed by gentle flicking of the tube. The mixture was incubated on ice for 30 minutes, before being heat-shocked at 42°C for 30 s and re-incubated on ice for a further 5 minutes. 220 μl of super optimal broth with catabolite repression (SOC) medium was added to the cells and the bacteria were incubated at 37°C with gentle shaking for 1 h. The *E. coli* cells were plated onto ampicillin-selective agar plates, pre-warmed to 37°C, and incubated overnight at 37°C. Individual colonies

were picked from the dishes and allowed to grow overnight in lysogeny broth (LB) + ampicillin (1:1000).

TABLE 2.1. Primer nucleotide sequences used for the mutagenesis of the α3 subunit of the GABA$_A$R are shown along with their respective annealing temperatures (Tm, °C). All sequences are indicated in the 5' to 3' direction. All mutations are point mutations, with the exception of the myc tag insertion, which was inserted between residues 33 and 34 of the mature α3 subunit protein.

Subunit	Forward primer	Reverse primer	Tm (°C)
myc-α3	AGCGAAGAAGATCTGCGACA AGAACCTGGGGACTTTGTGAA ACAAG	AATCAGTTTCTGTTCTCTTGAT TCCCCTTGGCTAGTGGTTCCA GGG	72
α3^{S426A}	CAGTGCTTCTGCAACTCCAAC	GGAGCAGCAGCAGACTTG	62
α3^{S427A}	TGCTTCTTCAGCTCCAACAGC G	CTGGGAGCAGCAGCAGAC	66
α3^{S433A}	AGCGATTGCTGCACCCAAGGC	GTTGGAGTTGAAGAAGCACT GG	67
α3^{T400A}	CATAGTGGGTGCCACCTATCC	TTGAAGGTGGTGTTTTTCTTT G	62
α3^{T401A}	AGTGGGTACCGCCTATCCTAT	ATGTTGAAGGTGGTGTTTTTC	62
α3^{Y402A}	GGTACCACCGCTCCTATCAAT CTG	ACTATGTTGAAGGTGGTG	59
α3^{Y402F}	GGTACCACCTTTCCTATCAATC	CACTATGTTGAAGGTGGTG	61
α3^{T400D}	CATAGTGGGTGACACCTATCC TATC	TTGAAGGTGGTGTTTTTC	58
α3^{T401D}	AGTGGGTACCGACTATCCTAT CAATC	ATGTTGAAGGTGGTGTTTTTC	62
α3^{Y402D}	GGGTACCACCGATCCTATCAA TC	ACTATGTTGAAGGTGGTG	59
α3^{T313F}	CTTTGGTGTCTTCACTGTTCTC AC	ACTGTGCGGGCAGGGACA	67
α3^{V309C}	TGCCCGCACATGCTTTGGTGT C	GGGACAGATTCTCTATTAAG	57
α3^{V309S}	TGCCCGCACATCCTTTGGTGT C	GGGACAGATTCTCTATTAAG	57

DNA was extracted from the bacteria using the Monarch® plasmid miniprep kit (NEB) according to the manufacturer's instructions. The extracted DNA was fully sequenced (Source Bioscience) with the SP6 forward primer and a custom-made reverse primer P5 (5'-GACAAACCACAACTAGAATGCAG-3'). Upon confirmation of the presence of the desired point mutation, the corresponding bacterial colonies were grown further and

the DNA extracted using the HiSpeed plasmid maxi kit (Qiagen). The subunit DNA was then re-sequenced, to confirm the presence of the mutation of interest and the absence of any unintended mutations.

2.2. HEK cell culture & electrophysiology

2.2.1. HEK cell culture & expression of recombinant GABA$_A$ receptors

Human embryonic kidney (HEK)-293 cells were grown in Dulbecco's modified Eagle's medium (DMEM) with 10% (v/v) fetal calf serum (FCS), 100 units/ml penicillin-G, 100 µg/ml streptomycin and 2 mM glutamine in 5% CO_2 at 37°C (Wooltorton et al., 1997). At 70% confluency, the cells were washed in Hank's balanced salt solution (HBBS) and dissociated with 0.05% (w/v) trypsin-EDTA. Trypsin was neutralised with the addition of DMEM-based growth medium, following which the cells were centrifuged at 1000 *x g* and resuspended in fresh growth medium. Cells were plated onto poly-L-lysine-coated glass coverslips and transfected 1 h later with equimolar ratios of murine cDNAs encoding wildtype GABA$_A$R-α3, point-mutated GABA$_A$R-α3, wildtype GABA$_A$R-β3 and wildtype GABA$_A$R-γ2L receptor subunits, as well as enhanced green fluorescent protein (eGFP). A calcium phosphate protocol was followed for cell transfection: a solution containing 4 µg of cDNA, 24 µl of 2x HBS (50 mM HEPES, 280 mM NaCl, 2.8 mM Na_2HPO_4) and 20 µl of 340 mM $CaCl_2$ was pipetted dropwise onto each coverslip. Electrophysiological recordings were performed on the cells 22-30 h post-transfection.

2.2.2. Voltage-clamp electrophysiology for HEK-293 cells

Voltage-clamp electrophysiology was used to record whole-cell GABA-activated currents from transfected HEK-293 cells. Whole cell currents were recorded at room temperature with an Axopatch 200B amplifier (Axon Instruments), digitised with a Digidata 1322A (Axon Instruments), acquired using Clampex 10.2 and analysed with Clampfit 10.2 (Molecular Devices). Recordings were sampled at 10 kHz and filtered at 5 kHz using a 4-pole Bessel filter.

Fire-polished patch electrodes pulled to a resistance of 3-4 MΩ using thin-walled borosilicate glass pipettes (World Precision Instruments, TW150-4) were filled with an internal solution containing (mM): NaCl (1), KCl (140), EGTA (11), HEPES (10), CaCl$_2$ (1) and K$_2$-ATP (2); pH adjusted to 7.2 with 1 M NaOH. Osmolarity of the internal solution was 300 ± 10 mOsm/L. Cells were constantly superfused with a Krebs solution containing (mM): NaCl (140), KCl (4.7), MgCl$_2$ (1.2), CaCl$_2$ (2.5), glucose (11) and HEPES (5); pH adjusted to 7.4 with 1 M NaOH. The flow rate was approximately 2-5 ml per minute, with a bath volume of approximately 1 ml. Cells were voltage-clamped at -20 mV, using compensation for series resistance (R$_s$) of >70%. Drug solutions (e.g., GABA) were diluted in Krebs solution and rapidly applied to cells using a Y-tube fast drug application system, with an approximate solution exchange rate of 100-200 μs (Mortensen & Smart, 2006).

2.2.3. Acquisition & fitting of concentration-response curves

GABA-evoked currents were generated from GABA$_A$R-expressing HEK-293 cells by the addition of a range of GABA concentrations applied in a random order. In all recordings, 300 μM GABA was applied at regular intervals to the cells to monitor for run-up or run-down of GABA responses. The R$_s$ was repeatedly measured between GABA applications; an R$_s$ change of >20% led to the termination of the experiment. The peak amplitudes of the currents were measured relative to the baseline holding current of the cell prior to GABA application. GABA-evoked responses induced by all GABA concentrations were normalised to the peak amplitude of the current generated by the maximal GABA concentration (10 mM). Once plotted, these data were curve fitted using the Hill equation (equation 1), to generate GABA concentration-response curves (CRCs). During curve fitting, the minimum value was constrained to >0.

Equation 1:

$$I = Imax\left[\frac{[GABA]^n}{[GABA]^n + EC_{50}{}^n}\right]$$

Where I represents the current, Imax the maximum GABA current, [GABA] the GABA concentration, EC_{50} the GABA concentration that elicits a half-maximal response, and n is the Hill coefficient.

2.2.4. Calculation of maximum current density

Maximum current density, an indirect measure of receptor cell surface expression, was calculated by normalising the maximum current, generated following a 10 mM GABA application, to the cell capacitance (C_m). C_m was calculated using equation 2 and is expressed in picofarads (pF).

Equation 2:

$$C_m = \frac{\tau_{rec} \; x \; (R_s \; + \; R_{in})}{(R_s \; x \; R_{in}) \; x \; 1000}$$

Where τ_{rec} represents the recording tau, R_s represents the series resistance and R_{in} represents the input resistance.

2.2.5. Calculation of desensitisation & deactivation kinetics

Voltage-clamp recordings of $GABA_A$R-expressing HEK-293 cells exposed to saturating (10 mM) GABA concentrations were selected and a two-term exponential fitted to the GABA current decay phase, allowing the estimation of both the fast and slow phases of desensitisation. A weighted tau (τ_w) was calculated from these estimates using equation 3.

Equation 3:

$$\tau_w = \frac{(A1 \; x \; \tau1) + (A2 \; x \; \tau2)}{A1 + A2}$$

Where A1 and A2 represent the amplitudes of the fast and slow components, and $\tau1$ and $\tau2$ represent the time constants of the fast and slow components.

Deactivation kinetics were calculated using the same equation, by fitting the two-term exponential to the deactivation phase of the current.

2.3. Primary hippocampal culture & electrophysiology

2.3.1. Hippocampal cell culture & transfection

The brain of an E18 Sprague-Dawley rat embryo was removed, the hippocampus isolated and the cells dissociated in 0.1% (v/v) trypsin for 10 minutes in 5% CO_2 at 37°C. The cells were washed three times in Hank's balanced saline solution with Ca^{2+}/Mg^{2+} (HBSS++). The cells were then moved into 2 ml of plating media (minimal essential medium (MEM) supplemented with 2 mM L-glutamine, 100 units/ml penicillin-G, 100 µg/ml streptomycin, 5% (v/v) FCS, 5% (v/v) horse serum and 20 mM glucose) and triturated with fire-polished glass pipettes. 0.25 ml of the neuron-containing plating media was plated onto individual poly-L-ornithine-coated 18 mm coverslips, which was replaced after 2 h with 1 ml maintenance media (Neurobasal medium, B27 serum-free supplement, GlutaMAX-I supplement, 100 units/ml penicillin-G, 100 µg/ml streptomycin and 20 mM glucose). Neurons were maintained for 12 – 16 days in 5% CO_2 at 37°C prior to use.

Neurons were transfected 7 days post-culture, with equimolar ratios of selected cDNAs, following either an Effectene or calcium phosphate-based protocol. For transfection using Effectene, a solution containing 0.8 µg cDNA, 6.4 µl enhancer and 100 µl buffer per coverslip was mixed and left to stand for 3-4 minutes. 10 µl Effectene was then added to the solution, which was again mixed and left for 10 minutes, before the addition of 600 µl maintenance media. Following washing with HBSS(++), the transfection solution was added to the neurons and left for 2 h. The neurons were again washed with HBSS(++) and then maintained in maintenance media.

For transfection with calcium phosphate, a solution containing 60 µl of 2x HBS (274 mM NaCl, 10 mM KCl, 1.4 mM Na_2HPO_4, 15 mM D-glucose, 42 mM HEPES), 2.5 µl of 2.5 M $CaCl_2$ and 4 µg of cDNA was made up to 120 µl with TE buffer. The solution was incubated at room temperature for 30 minutes, with frequent mixing. Neurons were washed with HBSS(++) and their media replaced with neurobasal-A containing 2 mM

kynurenic acid. 60 µl of the transfection solution was pipetted dropwise onto each coverslip. The neurons were incubated in 5% CO_2 at 37°C for 30 minutes, before being washed in HBSS(++) and maintained in maintenance media. Electrophysiological recordings were performed 5-9 days post-neuronal transfection; immunocytochemistry was performed 7 days post-transfection.

2.3.2. Voltage-clamp electrophysiology for neurons

Fire-polished thin-walled borosilicate patch electrodes (World Precision Instruments, TW150-4) were pulled to a resistance of 3-4 MΩ and were filled with an internal solution containing (mM): CsCl (140), NaCl (2), HEPES (10), EGTA (5), $MgCl_2$ (2), $CaCl_2$ (0.5), Na_2ATP (2), Na_2GTP (2) and QX-314 (2); pH adjusted to 7.2 with 1 M CsOH. Osmolarity was 300 ± 10 mOsm/L. Neurons were constantly superfused, at an approximate rate of 2-5 ml/min, with a Krebs solution containing (mM): NaCl (140), KCl (4.7), $MgCl_2$ (1.2), $CaCl_2$ (2.5), glucose (11), HEPES (5) and kynurenic acid (2); pH adjusted to 7.4 with 1 M NaOH. Kynurenic acid was added to block excitatory postsynaptic currents (EPSCs). Drugs (20 µM bicuculline; 50 µM picrotoxin) were solubilized in Krebs solution and bath-applied to the cells. Neurons were voltage-clamped at -60 mV, using compensation for R_s of >70%. Current recordings were low-pass filtered with a cut-off frequency of 5 kHz with a 4-pole Bessel filter.

2.3.3. sIPSC analysis

Spontaneous inhibitory postsynaptic current (sIPSC) recordings obtained from voltage-clamp electrophysiology of hippocampal neurons in cell culture were analysed using two programmes:

(1) WinEDR V3.9.0 (Strathclyde Electrophysiology Software), which was used to detect and select true sIPSCs, as opposed to baseline current fluctuations. Settings used for event detection were: threshold amplitude, 4-6 pA; threshold time, 0.7 ms; baseline tracking time, 2 ms; dead time, 8 ms; rising edge window, 1 ms. Once all the sIPSC

events from a single neuron were detected, the frequency and mean amplitude of the sIPSCs were calculated.

(2) WinWCP V5.5.2 (Strathclyde Electrophysiology Software), which was used to select 'clean' sIPSCs. A 'clean' sIPSC is one that does not contain contaminating events, such as another sIPSC appearing in the decay phase of the first event. A minimum of 50 clean events were required to perform reliable kinetic analyses. From the clean events, the mean rise time, mean decay tau and the weighted decay tau were calculated.

2.4.   Immunocytochemistry

Neurons were washed twice in ice-cold phosphate-buffered saline (PBS) before being fixed in 4% paraformaldehyde (PFA) in PBS with 4% sucrose. The cells were again washed twice in ice-cold PBS, following which the surface proteins were blocked in 10% normal goat serum (NGS) in PBS for 20 minutes. The cells were washed twice in ice-cold PBS and the surface α3 subunit-containing proteins were labelled with rabbit anti-myc antibody (ab32, Abcam) at a 1:700 dilution in 3% NGS for 1 h at room temperature. The cells were washed three times in PBS with 1% bovine serum albumin (BSA) and permeabilised for 5 minutes in 0.1% Triton-X100. After washing of the Triton, intracellular proteins were blocked in 10% NGS in PBS for 20 minutes, and the cells were washed three times in PBS with 1% BSA. The intracellular proteins gephyrin and VIAAT were then labelled with mouse anti-gephyrin (147111, Synaptic Systems; 1:200) and guinea pig anti-VIAAT (AGP129, Alomone; 1:500), both in 3% NGS for 1 h at room temperature. The cells were washed three times for 5 minutes each in PBS with 1% BSA. All neurons were incubated with the secondary antibodies goat anti-rabbit IgG H&L Alexa Fluor® 555 (A21424, ThermoFisher); goat anti-mouse IgG H&L Alexa Fluor® 488 (A11001, ThermoFisher); and goat anti-guinea pig IgG H&L Alexa Fluor® 647 (A21450, ThermoFisher) at a dilution of 1:500 in 3% NGS for 1 h at room temperature. The cells were washed four times for 5 minutes each in PBS with 1% BSA before being mounted onto glass coverslips using ProLong gold antifade mountant (ThermoFisher Scientific). Coverslips were allowed to set overnight prior to imaging.

2.5.   Structured illumination microscopy (SIM)

2.5.1. SIM imaging

SIM was performed on a Zeiss ELYRA PS.1 super-resolution microscope. Images were acquired at room temperature with a 63x, 1.4 NA oil objective lens using HF Halogen-Free immersion oil (SPI Supplies), a pco.edge sCMOS camera and ZEN Black software (v.11.0.2.190; Zeiss). Samples were excited using 488 nm, 561 nm and 642 nm laser lines. Images were acquired with 100 nm grating at three angles with five rotations per angle, to give a total of 15 images per z-section. Fluorophores were excited with 10% of maximum laser intensity and 100 ms exposure time. Images were processed in ZEN Black using the default settings in the SIM reconstruction module. Drift corrections between the channels were performed with respect to 200 nm TetraSpeck fluorescent microspheres (Invitrogen).

2.5.2. Image analysis

Images were analysed using the open-source ImageJ distribution package FIJI (v1.53c). Object segmentation, distance measurements and co-localisation analyses were performed in three dimensions (3D) using the procedures implemented in the ImageJ-based DiAna plugin, described extensively by Gilles et al. (2017).

Spot segmentation

Objects in digital images are identified through the process of segmentation. In spot segmentation, objects are detected by centring the 3D intensity radial distribution on the local maximum fluorescence intensity of each object. The process is described in Gilles et al. (2017), but in brief: DiAna computes the local maxima in the digital image, following which a threshold (defined by the user; in this study, the parameters suggested for use by Gilles and colleagues were implemented – see below) is applied to select local maxima belonging to objects. Then, for each local maximum, the 3D radial distribution of voxel intensities is computed, which allows a border intensity threshold to be estimated for each object. Following this, an algorithm is used to examine the voxels surrounding the local maximum. The voxels are sequentially

included in the object if they meet the following criteria: (1) their florescence intensity is above the border threshold; (2) their fluorescence intensity is lower than the voxel that was previously added to the object; and (3) their neighbours would also be added to the object (Gilles et al., 2017).

Segmentation was performed with the following parameters, as suggested by Gilles and colleagues: for maxima detection, the radius in xy-axis = 4, in z-axis = 3, noise parameter = 0; the threshold for maxima selection = 5000; the parameters for Gaussian fit and threshold calculation were radius maximum = 10 and S.D. value = 1.5.

3D measurements, distance measurements and co-localisation analysis

Following segmentation, 3D measurements (volume and mean grey value) and distance measurements were calculated. The distance measurements performed in DiAna utilise Euclidean distance computation. Centre-to-centre, centre-to-edge and edge-to-edge distances between objects are computed (Gilles et al., 2017). These precise 3D measurements enable effective co-localisation analyses.

Co-localisation was determined by the detection of overlapping or touching objects in different channels (e.g., the overlap of a gephyrin-segmented object with a VIAAT-segmented object). Again, the process is described by Gilles et al. (2017), but in brief: to compute voxel co-localisation, the corresponding labelled images of the objects are analysed. In the first image, object 1 is labelled with the value 1. In the second image, object 2 is labelled with the value 2. The two images are then summed. The voxels with the value 3 will correspond to the co-localised voxels between the two images.

2.6. Co-immunoprecipitation & immunoblotting

HEK-293 cells at 70% confluency were plated on 6 cm dishes and transfected with either myc-GABA$_A$R-α3, myc-GABA$_A$R-α3^{Y402F} or myc-GABA$_A$R-α3^{Y402D} along with equimolar amounts of GABA$_A$R-β3, GABA$_A$R-γ2L and where necessary, GFP-gephyrin, and allowed to grow for 48 h. Cells were washed twice in ice-cold PBS and lysed in 600 μl lysis buffer containing: 50 mM HEPES pH 7.5, 0.5% (v/v) triton, 0.1% (v/v) NP40, 150 mM NaCl, 1 mM EDTA, and a protease inhibitor cocktail of 1 mM phenylmethylsulfonyl

fluoride (PMSF; Sigma), 10 µM chymostatin (Sigma), 10 µM leupeptin (Sigma), 1 µM pepstatin (Sigma) and 100 µM antipain (Sigma). Lysed cells were collected and passaged 15 times through a 26G needle, before being incubated on an end-over rotator for 1 h at 4°C. Lysates were then centrifuged at 16,000 x g for 30 minutes to pellet the membrane. The subsequent supernatants were incubated with 12 µl of GFP-Trap Agarose bead slurry (ChromoTek) on an end-over rotator for 2 h at 4°C. The beads were washed three times in lysis buffer and eluted in 6x SDS-PAGE sample buffer.

SDS-PAGE electrophoresis, using NuPAGE 4-12% Bis-Tris gels (Invitrogen) and NuPAGE MES SDS running buffer (Invitrogen), was performed on the resulting eluates, along with 15 µl of the inputs, at 175 V for 50 minutes. Samples were transferred onto polyvinylidene fluoride (PVDF) membranes in Tris/Glycine Electroblotting buffer (Geneflow) and blocked in 5% (w/v) skimmed milk in tris-buffered saline with 0.1% Tween-20 (TBST). The membranes were probed with mouse anti-myc (ab32, Abcam; 1:500) followed by goat anti-mouse horseradish peroxidase (HRP; 610-103-121, Rockland; 1:10,000), each for 1 h at room temperature. The membranes were developed and imaged under chemiluminescence using an ImageQuant LAS 4000 (Cytiva). Blots were stripped for re-probing via incubation with mild stripping buffer (15 g glycine, 1 g SDS, 10 ml Tween-20; pH adjusted to 2.2 and volume brought up to 1 L with ultrapure water) for 10 minutes. Membranes were washed twice in PBS for 10 minutes, twice in TBST for 5 minutes and re-blocked in 5% (w/v) skimmed milk. Membranes were re-probed with rabbit anti-GFP (ab290, Abcam; 1:1000) followed by goat anti-rabbit HRP (605-403-B69, Rockland, 1:10,000), each for 1 h at room temperature. The membranes were again developed and imaged using the ImageQuant LAS 4000.

The intensity of each signal on the blots was quantified using FIJI (v1.53c). The intensity of the myc co-immunoprecipitation (co-IP) signal for each condition was normalised to that of the equivalent GFP co-IP signal (e.g., $\alpha3^{Y402F}$ myc co-IP signal intensity divided by $\alpha3^{Y402F}$ GFP co-IP signal intensity). The resulting myc:GFP ratio of each experimental sample was then normalised back to the myc:GFP ratio of the wildtype pulldown.

2.7. shRNA knockdown

Short hairpin RNAs (shRNAs) that selectively target sequences in both rat and mouse *Gabra3* were used to knockdown α3 protein expression. HEK-293 cells were plated onto poly-L-lysine-coated glass coverslips and transiently transfected with equimolar ratios of GABA$_A$R-α3, GABA$_A$R-β3, GABA$_A$R-γ2L, eGFP and one of each of the following shRNAs: A, B, C or a combination of A+B+C (Horizon Discovery); and D, E, F, or a combination of D+E+F (Merck; see Table 2.2. for shRNA sequences). Control cells were transfected with a scrambled, non-targeting shRNA (5'-TCTCGCTTGGGCGAGAGTAAG-3'). Electrophysiological recordings were performed on the cells 22-30 h post-transfection.

TABLE 2.2. shRNA sequences that selectively target sequences in both rat and mouse *Gabra3* and were used to knockdown α3 subunit expression. All sequences are indicated in the 5' to 3' direction.

shRNA	Sequence	Clone ID	Company
A	TTATCTGTACTATCGTCAG	V2LMM_187607	Horizon Discovery
B	TGGAGTTGAAGAAGCACTG	V3LMM_487807	Horizon Discovery
C	ATTCTCCTGTACTAGACCG	V2LMM_71580	Horizon Discovery
D	CCGGTACCTAAAGTGGCAT ACGCGACTCGAGTCGCGTA TGCCACTTTAGGTATTTTT	NM_008067.x-1202s1c1	Merck
E	CCGGGCCGTCTGTTATGCC TTTGTACTCGAGTACAAAG GCATAACAGACGGCTTTTG	NM_000808.2-1266s1c1	Merck
F	CCGGCCAGACCTACTTGCC ATGTATCTCGAGATACATG GCAAGTAGGTCTGGTTTTTG	NM_000808.2-1079s1c1	Merck

2.8.   Data analysis

All data were obtained from at least three different cell preparations or neuronal cultures. GraphPad Prism version 9.2.0 was used to conduct statistical analyses and for graphical presentation of the data. Data are expressed as the mean ± standard error of the mean (SEM). Data were tested for normal distribution using the D'Agostino-Pearson test. If normally distributed, the data were tested for significance using unpaired t tests and ordinary one-way ANOVA tests with Tukey's multiple comparisons tests as indicated. Non-Gaussian distributed data were tested for significance using Welch's t tests and Kruskal-Wallis tests with Dunn's multiple comparisons tests as indicated. Significance was determined by a p value of < 0 .05 and indicated by *. p values of < 0.01, < 0.001 and < 0.0001 are represented by **, *** and **** respectively.

Chapter 3: putative phosphorylation sites on the α3 subunit of the GABA$_A$ receptor

3.1. Introduction

The potency of GABA reflects its ability to activate GABA$_A$Rs and mediate inhibitory neurotransmission. There is evidence that the GABA potency for α3 subunit-containing GABA$_A$Rs is low; that is, a relatively high GABA concentration is needed to activate these receptors. Verdoorn (1994) found the EC$_{50}$ of α3β2γ2 receptors to be six times higher than that of α1β2γ2 receptors (103 μM and 17.4 μM respectively). Similarly, Gingrich et al. (1995) reported the EC$_{50}$ of α3β2γ2S receptors to be 75 μM, compared to the 7 μM EC$_{50}$ of α1β2γ2S receptors: a difference of nearly eleven-fold. Mortensen et al. (2011) also reported the EC$_{50}$ of α3 subunit-containing receptors to be six-fold greater than that of α1 subunit-containing receptors, albeit with lower absolute values (12.5 μM and 2.1 μM respectively).

However, evidence of α3-GABA$_A$Rs exhibiting high GABA potency also exists: Keramidas & Harrison (2010) estimated the GABA equilibrium dissociation constant at α3β3γ2 channels to be ~2.6 μM, compared with ~19 μM for α1β2γ2 channels, indicating that GABA binds with a higher affinity to α3β3γ2 receptors. There are thus contradictory reports on the affinity of α3-GABA$_A$Rs for GABA. As previously discussed, GABA$_A$Rs mediating tonic currents typically have a high GABA affinity, as they sense and respond to the ambient GABA concentration, often low nanomolar. In contrast, those mediating phasic inhibition have a low GABA affinity, as they respond to the high concentration of GABA released from the presynaptic terminal into the synaptic cleft, generally in the millimolar range. Given all of these studies were performed in mammalian cells, these inconsistencies in the published literature may reflect differential post-translational modifications on the recombinant α3-GABA$_A$Rs studied by these groups.

The ICDs of the GABA$_A$R subunits α1-3 and α5 show striking primary sequence similarity and almost fully align, with the exception of an extra ten amino acid insert in the ICD of α3 that is not present in the other three subunits (Fig. 3.1, pink arrow). In 2010, Huttlin et al. performed a screen of nine different mouse tissues, including

the brain, in which phospho-peptides were enriched and analysed using mass spectrometry. The screen identified three residues – S426, T427 and S433 – within this additional ICD region of the α3 subunit as putative phosphorylation sites. Numerous protein-protein interactions, required for the trafficking and clustering of GABA$_A$Rs, occur via the ICD (Luscher et al., 2011). Additionally, numerous consensus sequences for phosphorylation by both serine/threonine and tyrosine protein kinases exist in the ICD (Moss & Smart, 1996). Phosphorylation of residues in the ICD of α subunits is known to play an important role in regulating dynamic processes, including receptor accumulation at inhibitory synapses (Abramian et al., 2010; Mukherjee et al., 2011), modulation by endogenously occurring neurosteroids (Abramian et al., 2014; Adams et al., 2015) and the binding of allosteric modulators such as benzodiazepines (Churn et al., 2004) (see section 1.1.4). Therefore, it is plausible that phosphorylation of one or more of these residues affects the apparent affinity of α3-GABA$_A$Rs for GABA and potentially the localisation and function of α3 subunit-containing receptors.

In a further example of the importance of the ICD in the regulation of GABA$_A$R localisation and function, the binding sites for the principal scaffold protein gephyrin, which plays a key role in the recruitment and anchoring of GABA$_A$Rs at GABAergic synapses, have been identified within the ICDs of the α1-3 and α5 subunits (Tretter et al., 2008; Mukherjee et al., 2011; Tretter et al., 2011; Brady & Jacob, 2015) (see Fig. 3.1).

The gephyrin binding site on the α3 subunit has been identified as the motif 395-FNIVGTTYPI-404 (Tretter et al., 2011). In 2014, Maric et al. used a combination of chemical, biophysical and structural investigations to identify three residues within this α3 gephyrin binding motif – T400, T401 and Y402 – as being of major importance in mediating the binding of the subunit to gephyrin, due to the thermodynamic interactions of their side chains with gephyrin (see Fig. 3.2). Y402, a residue conserved across the α1, α2 and α3 subunits, was highlighted as being particularly critical to this process as its side chain engages in key hydrophobic interactions with gephyrin (Maric et al., 2014).
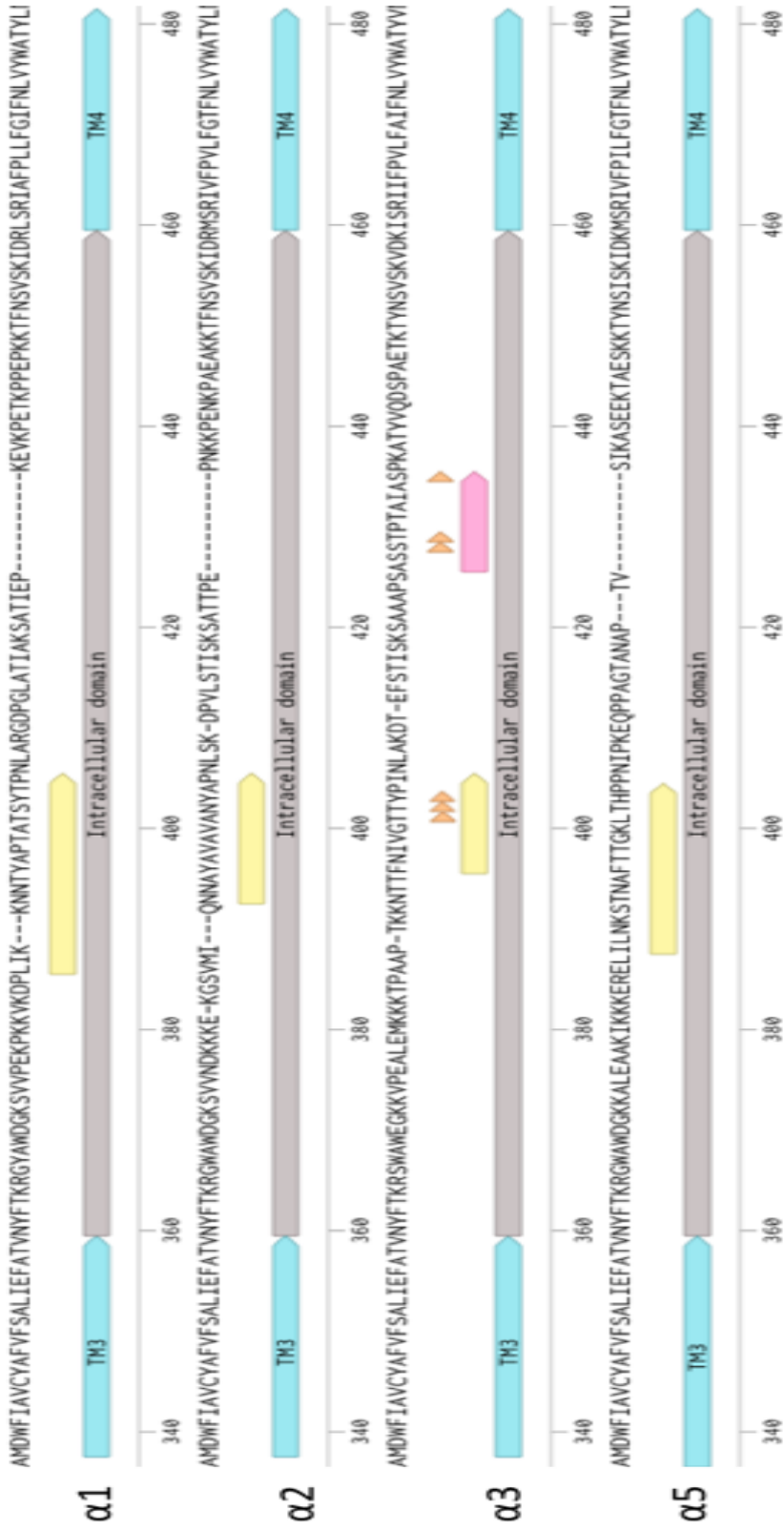
FIGURE 3.1. Alignment of the intracellular domains of GABA$_A$R subunits α1-3 and α5. The α3-specific ICD insert region is indicated by the pink arrow. The gephyrin binding domain of each subunit is indicated by the yellow arrow. The putative phosphorylation sites in both the α3-specific ICD region and the α3 gephyrin binding domain are indicated by the orange arrows heads.

67

Despite each mediating gephyrin binding through unique binding motifs, the different α subunits all engage in robust and specific direct interactions with gephyrin, indicating that these interactions may be regulated through subunit-specific post-translational modifications. In their 2014 study, Maric and colleagues suggest that functional investigations of the phosphorylation states of the residues T400, T401 and Y402 of the α3 subunit are likely to reveal an important role for the regulation of gephyrin binding via post-translational modifications. Indeed, the corresponding residue of T400 in the α1 subunit has already been identified as a putative phosphorylation site (Bell-Horner et al., 2006; Mukherjee et al., 2011), which may play an important role in the extracellular signal-regulated kinase (ERK)-induced regulation of GABAergic inhibition (Bell-Horner et al., 2006) and regulating the accumulation of α1-GABA$_A$Rs at inhibitory synapses (Mukherjee et al., 2011). Furthermore, the corresponding residues T401 in α1 (Munton et al., 2007), and Y402 in both the α1 and α2 subunits (Ballif et al., 2008), have already been shown to be phosphorylated *in vivo*, although the effects of phosphorylation of these residues are yet to be investigated.

To investigate the potential effects of phosphorylation at these residues (S426, T427 and S433 within the α3-specific insert and T400, T401 and Y402 within the gephyrin binding site), phospho-null, and in the case of the gephyrin binding site residues, phospho-null and phospho-mimetic mutants were created by substituting the native S and Y residues with either alanine (for S) or phenylalanine (in the case of Y402) and for both with aspartate, respectively. These mutated α3 cDNA constructs were transfected into HEK-293 cells, along with constructs expressing β3 and γ2L, and investigated using whole-cell voltage-clamp electrophysiology. Following these initial investigations, several of the mutants were expressed in hippocampal neurons in cell culture and subjected to further electrophysiological investigations in order to assess their impact on sIPSC kinetics.
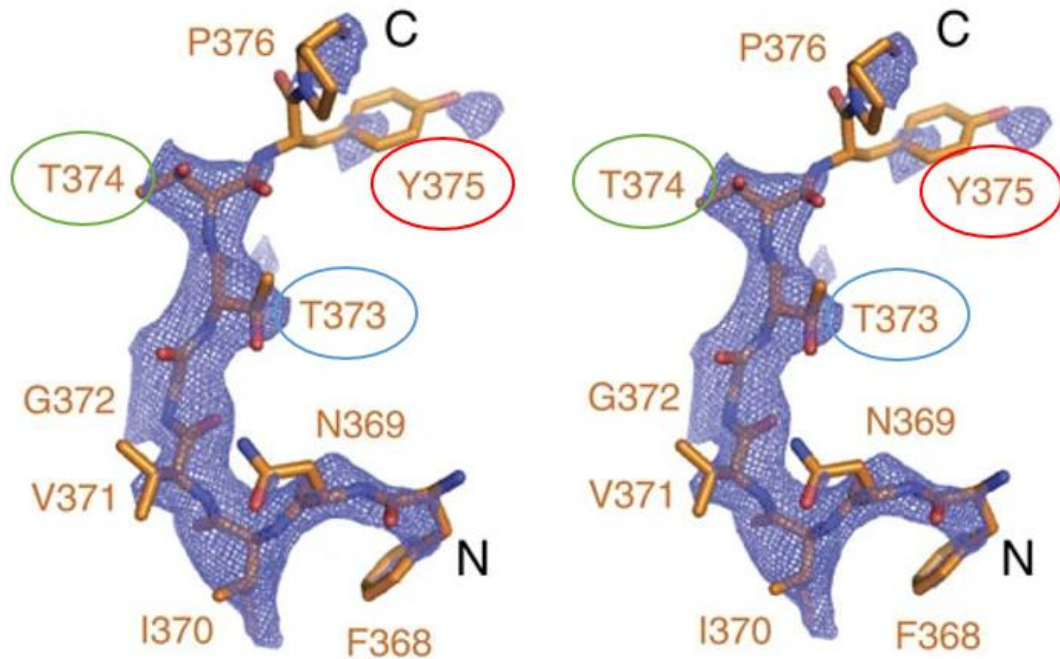
FIGURE 3.2. Electron density map of the GABA$_A$R α3 peptide (stereo representation) used in the structural interrogations of the α3 gephyrin binding site by Maric and colleagues. The residues of interest are numbered differently here due to the exclusion of the 27 residue signal peptide. These residues are circled: T373 = T400 (blue), T374 = T401 (green) and Y375 = Y402 (red). C indicates the C terminus; N indicates the N terminus. Adapted from Maric et al. (2014).

3.2. Results

3.2.1. *Preventing phosphorylation of putative sites within the α3-specific insert in the ICD does not affect receptor GABA sensitivity or cell surface expression*

To assess whether preventing phosphorylation at S426, T427 or S433 affected the GABA sensitivity of the α3-GABA$_A$R, phospho-null mutants of each residue were created by substituting the native residues with alanine – which cannot be phosphorylated – to give α3^{S426A}, α3^{T427A} and α3^{S433A}. These constructs were transfected into HEK-293 cells, along with equimolar ratios of constructs expressing β3, γ2L and eGFP, which was required for the identification of transfected cells. Whole-cell voltage-clamp electrophysiology was performed on transfected cells. Peak current responses of the wildtype (α3β3γ2L) and mutant (α3^{S426A}β3γ2L, α3^{T427A}β3γ2L, α3^{S433A}β3γ2L) receptors were measured in response to 4 s applications of eleven different GABA concentrations: 0.1 μM, 0.3 μM, 1 μM, 3 μM, 10 μM, 30 μM, 100 μM, 300 μM, 1 mM, 3 mM and 10 mM. These different GABA concentrations were applied

to the cells in a random order, with normalising 300 µM applications interspersed throughout. GABA concentration-response data were collected for each cell and curve fitted with the Hill equation (Equation 1, section 2.2.3) to generate concentration-response curves (CRC) for each receptor. Maximum current density, an indirect measure of receptor cell surface expression, was calculated by normalising the maximum current, generated following a 10 mM GABA application, to the cell membrane capacitance (see section 2.2.4).
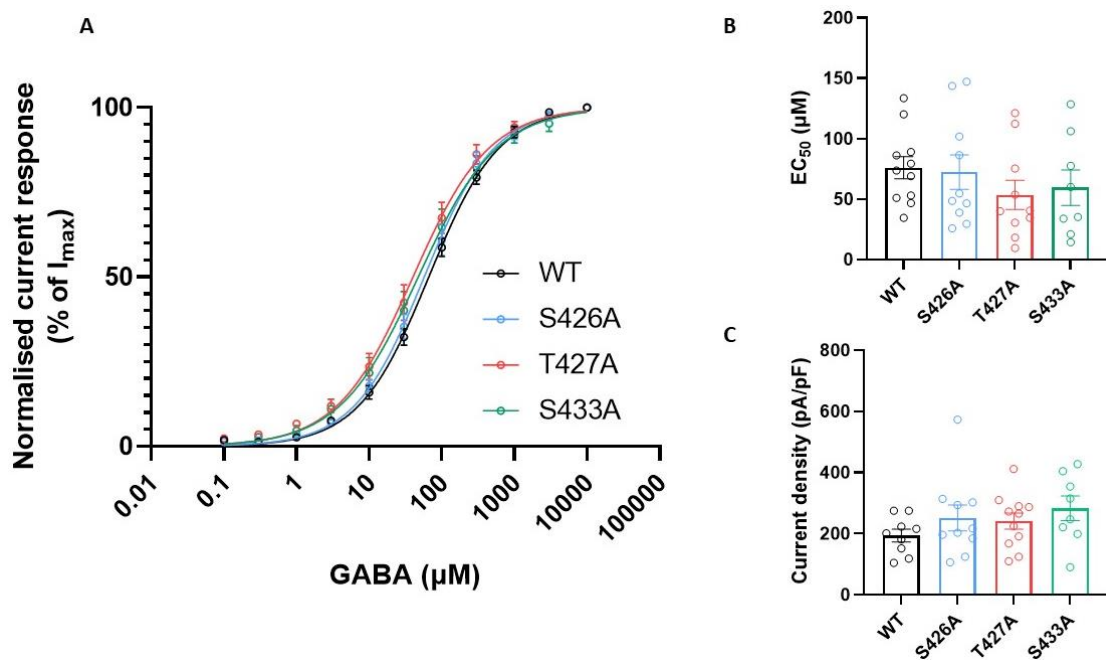
FIGURE 3.3. Alanine substitutions of the putative phosphorylation sites S426, T427 and S433 in the ICD of the α3 subunit of the GABA$_A$R do not affect receptor GABA sensitivity. **(A)** GABA CRC fitted to all data points of wildtype α3β3γ2L receptors (n=9; n_H=0.896; black) or α3^{S426A}β3γ2L (n=10; n_H=0.899; blue), α3^{T427A}β3γ2L (n=10; n_H= 0.827; red) and α3^{S433A}β3γ2L (n=8; n_H=0.801; green) receptors. **(B)** The mean GABA EC$_{50}$ value for wildtype α3β3γ2L (64.8 ± 6.4 µM; n=9) was not significantly different to that of the α3^{S426A}β3γ2L (72.4 ± 14.3 µM; n=10), α3^{T427A}β3γ2L (53.7 ± 11.9 µM; n=10) or α3^{S433A}β3γ2L receptors (59.6 ± 14.7 µM; n=8; one-way ANOVA test). The EC$_{50}$ values represent the means of those derived from curves fitted for each cell. **(C)** Maximum current density values did not differ significantly between the wildtype α3β3γ2L (193.8 ± 20.5 pA/pF; n=9) and the α3^{S426A}β3γ2L (251.4 ± 42.2 pA/pF; n=10), α3^{T427A}β3γ2L (241.2 ± 26.8 pA/pF; n=10) or α3^{S433A}β3γ2L receptors (282.4 ± 40.4 pA/pF; n=8; Kruskal-Wallis test). Circles, bars and error bars represent individual cells, population means and the standard error of the means (SEMs) respectively.

None of the phospho-null mutant receptors had a statistically significant effect on the GABA CRC compared to that elicited by the wildtype receptor (Fig. 3.3A). This is

reflected in the EC_{50} values of the mutant receptors, none of which differed significantly from the EC_{50} of the wildtype receptor (Fig. 3.3B). The current density values, which serve as an indirect measure of receptor cell surface expression, of the phospho-null receptors similarly showed no significant difference compared to wildtype (Fig. 3.3C). With the assumption that these residues are basally phosphorylated in the wildtype cells, these data indicate that preventing phosphorylation at these residues in the α3-specific region of the ICD has little impact on receptor activation or cell surface expression. Given these results, no further investigations into these residues were conducted.

3.2.2. Phosphorylation of residues in the gephyrin binding domain of the α3 subunit has differential effects on receptor GABA sensitivity and cell surface expression

To investigate the effects of preventing or mimicking phosphorylation at the residues T400, T401 and Y402 in the gephyrin binding site of the α3-GABA$_A$R, phospho-null and phospho-mimetic mutants of these residues were created. This was achieved by substituting the native threonine residues with alanine to give $α3^{T400A}$ and $α3^{T401A}$. Tyrosine was substituted with phenylalanine, with which it shares greater structural similarity than alanine, to give $α3^{Y402F}$. Similarly, the phospho-mimetic mutants were created by substituting the native residues with aspartate to give $α3^{T400D}$, $α3^{T401D}$ and $α3^{Y402D}$ to reproduce the negative charge associated with phosphorylation.

As with the previous set of experiments, wildtype α3, the phospho-null and phospho-mimetic mutant α3 subunits were expressed in HEK-293 cells, along with equimolar ratios of β3, γ2L and eGFP. Whole-cell voltage-clamp electrophysiology was performed on the transfected cells. Peak current responses of the wildtype (α3β3γ2L) and mutant ($α3^{T400A}$β3γ2L, $α3^{T400D}$β3γ2L, $α3^{T401A}$β3γ2L, $α3^{T401D}$β3γ2L, $α3^{Y402F}$β3γ2L, $α3^{Y402D}$β3γ2L) receptors were measured in response to 4 s applications of the various GABA concentrations detailed in section 3.2.1 (see Figs. 3.4D, 3.5D, 3.6D for representative membrane currents). As before, the Hill equation was used to analyse these data (Equation 1, section 2.3.3) and generate CRCs for each receptor.

The first residue to be investigated was T400. The CRCs for both the $\alpha3^{T400A}\beta3\gamma2L$ receptors and $\alpha3^{T400D}\beta3\gamma2L$ receptors displayed a leftward shift compared with the wildtype $\alpha3\beta3\gamma2L$ receptors (Fig. 3.4A). This is reflected in the GABA EC_{50} concentrations for the two mutant receptors, both of which were significantly lower than that of the wildtype receptor (Fig. 3.4B). These results indicate that both the alanine and the aspartate mutations increase the sensitivity of the receptor for GABA. As discussed in section 1.1.4, phosphorylation of $GABA_A R$ subunits plays an important role in the regulation of a variety of dynamic processes. A phosphorylated subunit is therefore likely to behave differently to a non-phosphorylated subunit; as such, different effects are expected when comparing a phospho-null mutation with a phospho-mimetic mutation. These results could therefore indicate that mutating residue T400 of the $\alpha3$ subunit has allosteric effects on the receptor that are unrelated to phosphorylation.

Interestingly, the current density of the $\alpha3^{T400D}\beta3\gamma2L$ receptor was higher than that of the wildtype receptor (Fig. 3.4C). A possible, albeit not the only, explanation of this result is that an alteration in receptor trafficking occurs that causes increased surface expression of this mutant receptor.
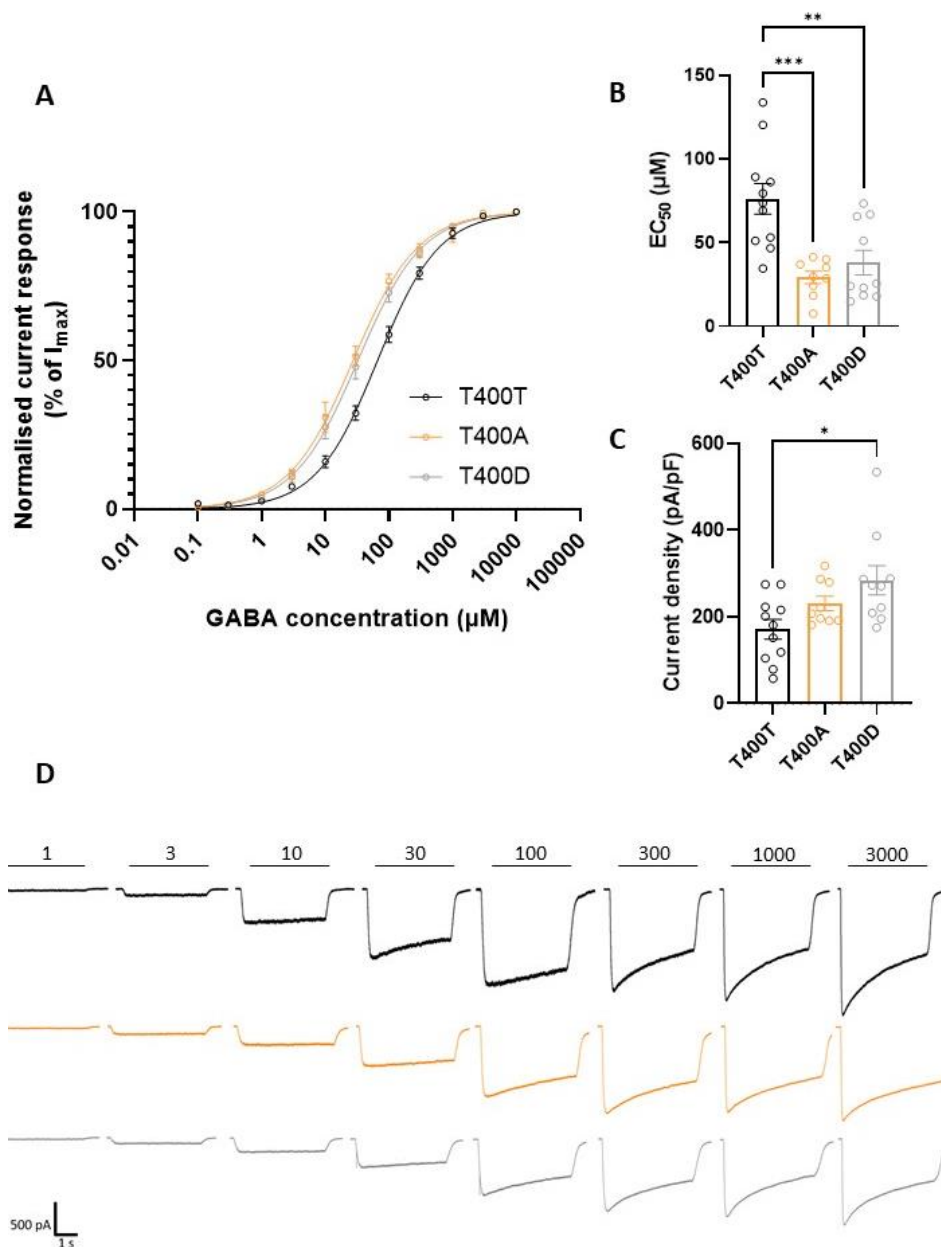
FIGURE 3.4. Alanine and aspartate substitutions of residue T400 in the gephyrin binding domain of the α3-GABA$_A$R increase receptor GABA sensitivity. **(A)** GABA CRC fitted to all data points of wildtype α3β3γ2L receptors (n=11; n_H=0.896; black), phospho-null α3^{T400A}β3γ2L (n=9; n_H=0.857; orange) and phospho-mimetic α3^{T400D}β3γ2L (n=10; n_H=0.860; grey) receptors. The CRCs of both the phospho-null and the phospho-mimetic receptors are shifted left compared to wildtype. **(B)** The mean GABA EC$_{50}$ value for wildtype receptors (76.1 $\pm$ 9.2 μM; n=11) was significantly higher than the mean values for α3^{T400A}β3γ2L (29.1 $\pm$ 3.7 μM; n=9) and α3^{T400D}β3γ2L receptors (38.1 $\pm$ 7.4 μM; n=10; one-way ANOVA and Tukey's multiple comparisons tests). The EC$_{50}$ values represent the means of those derived from curves fitted for each cell. **(C)** Maximum current density values for the α3^{T400D}β3γ2L receptors (270.7 $\pm$ 40.3 pA/pF; n=10) were significantly higher than those for the wildtype α3β3γ2L receptors (170.9 $\pm$ 22.6 pA/pF; n=11), while the current density values for the α3^{T400A}β3γ2L receptors (230.4 $\pm$ 16.9 pA/pF; n=9) were not (Kruskal-Wallis and Dunn's multiple comparisons tests). **(D)** Representative membrane currents resulting from 4 s applications of the indicated GABA concentrations (μM) to α3β3γ2L (black), α3^{T400A}β3γ2L (orange) and α3^{T400D}β3γ2L (grey) receptors. Circles, bars and error bars represent individual cells, population means and SEMs respectively. p values $\leq$ 0.05 *; $\leq$ 0.01 **; $\leq$ 0.001 ***.

Investigating the next residue, T401, revealed a leftward shift in the GABA CRC of the $\alpha3^{T401A}\beta3\gamma2L$ receptors compared to wildtype, while the CRC of the $\alpha3^{T401D}\beta3\gamma2L$ receptors remained the same as wildtype (Fig. 3.5A). Consistent with this finding, the EC_{50} of the phospho-null receptors, but not the phospho-mimetic receptors, was significantly lower than that of the wildtype receptor (Fig. 3.5B). This could suggest that the native state of this residue is phosphorylated and that preventing its phosphorylation with the alanine substitution causes the leftward CRC shift, demonstrating increased sensitivity to GABA.

The current density of the $\alpha3^{T401A}\beta3\gamma2L$ receptors, but not the $\alpha3^{T401D}\beta3\gamma2L$ receptors, was significantly higher than that of the wildtype receptors (Fig. 3.5C), mirroring the EC_{50} results. This suggests that preventing phosphorylation at residue T401 increases receptor cell surface expression.

The final residue to be investigated was Y402. The GABA CRC of the $\alpha3^{Y402D}\beta3\gamma2L$ receptors shifted left compared to that of the wildtype $\alpha3\beta3\gamma2L$ receptors, while the CRC of the $\alpha3^{Y402F}\beta3\gamma2L$ receptors remained the same as wildtype (Fig. 3.6A). This is reflected in the EC_{50} values: the EC_{50} of the $\alpha3^{Y402D}\beta3\gamma2L$ receptors, but not the $\alpha3^{Y402F}\beta3\gamma2L$ receptors, was significantly lower than that of the wildtype $\alpha3\beta3\gamma2L$ receptors (Fig. 3.6B). This could suggest that the basal state of residue Y402 is non-phosphorylated and mimicking phosphorylation causes the leftward shift in the GABA CRC and increased sensitivity to GABA.

In contrast to the previous two residues investigated, neither the phospho-null nor the phospho-mimetic receptor current density values differed from wildtype (Fig. 3.6C), indicating that neither mutation of Y402 affects the cell surface expression of the receptor.
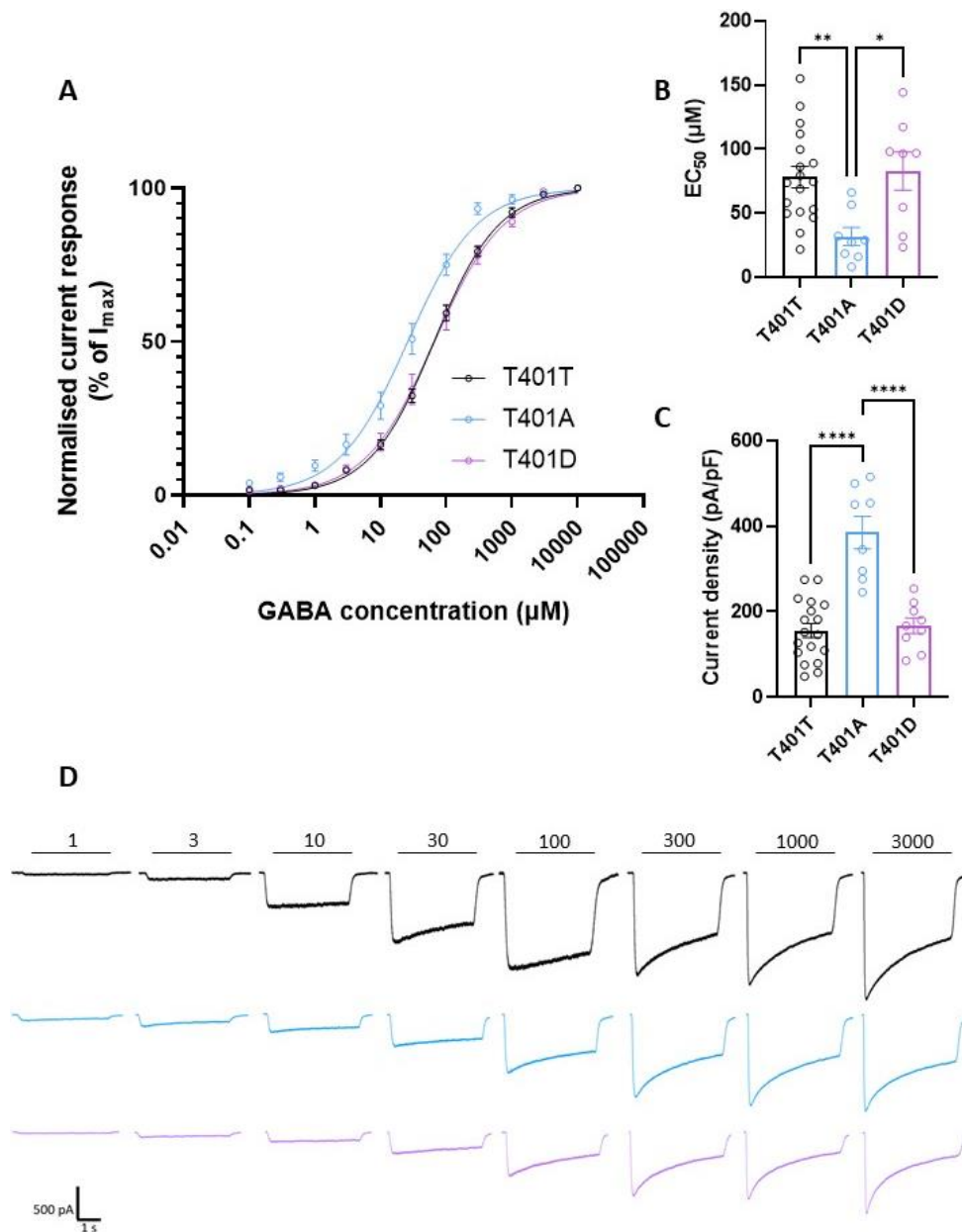
FIGURE 3.5. Preventing phosphorylation via alanine substitution at residue T401 in the gephyrin binding domain of the $\alpha3$-GABA$_A$R increases receptor GABA sensitivity and cell surface expression. **(A)** GABA CRC fitted to all data points of wildtype $\alpha3\beta3\gamma2L$ receptors (n=18; n_H=0.879; black), phospho-null $\alpha3^{T401A}\beta3\gamma2L$ (n=8; n_H=0.826; blue) and phospho-mimetic $\alpha3^{T401D}\beta3\gamma2L$ (n=8; n_H=0.822; purple) receptors. The CRC of the phospho-null receptors is shifted left compared to the CRCs of both the wildtype and $\alpha3^{T401D}\beta3\gamma2L$ receptors. **(B)** The mean GABA EC$_{50}$ value for the $\alpha3^{T401A}\beta3\gamma2L$ receptors (31.8 ± 7.1 µM; n=8) was significantly lower than that of the wildtype $\alpha3\beta3\gamma2L$ (78.3 µM ± 8.3; n=18) and phospho-mimetic $\alpha3^{T401D}\beta3\gamma2L$ receptors (82.8 ± 14.9 µM; n=8; one-way ANOVA and Tukey's multiple comparisons tests). The EC$_{50}$ values represent the means of those derived from curves fitted for each cell. **(C)** Maximum current density values for the $\alpha3^{T401A}\beta3\gamma2L$ receptors (385.3 ± 37.9 pA/pF; n=8) were significantly higher than those for wildtype $\alpha3\beta3\gamma2L$ (155.4 ± 16.8 pA/pF; n=18) and $\alpha3^{T401D}\beta3\gamma2L$ receptors (166.8 ± 18.3 pA/pF; n=8; one-way ANOVA and Tukey's multiple comparisons tests). **(D)** Representative membrane currents resulting from 4 s applications of the indicated GABA concentrations (µM) to $\alpha3\beta3\gamma2L$ (black), $\alpha3^{T401A}\beta3\gamma2L$ (blue) and $\alpha3^{T401D}\beta3\gamma2L$ (purple) receptors. Circles, bars and error bars represent individual cells, population means and SEMs respectively. *p* values ≤ 0.05 *; ≤ 0.01 **; ≤ 0.0001 ****.

75
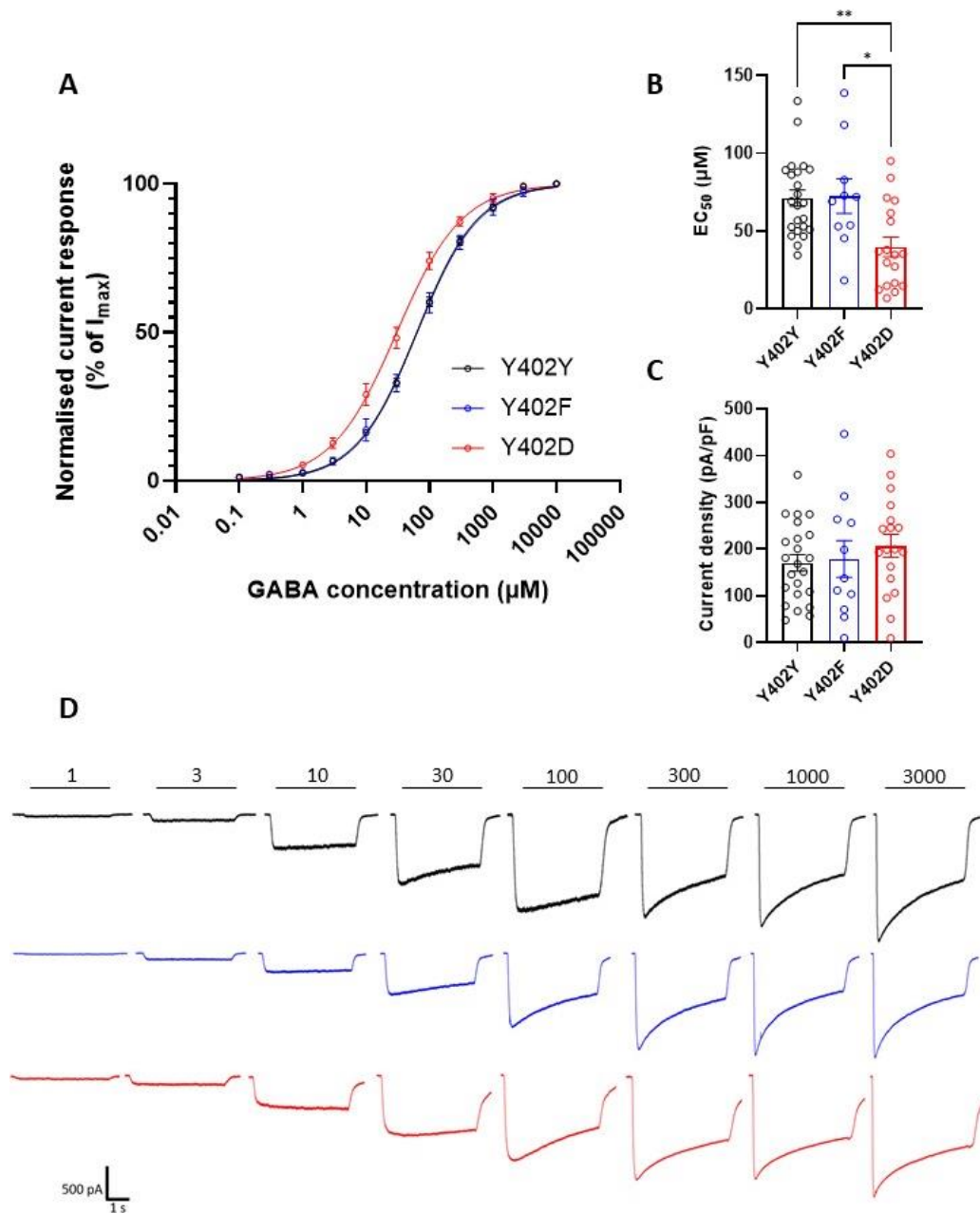
FIGURE 3.6. Mimicking phosphorylation via aspartate substitution at residue Y402 in the gephyrin binding domain of the α3-GABA$_A$R increases receptor GABA sensitivity. **(A)** GABA CRC fitted to all data points of wildtype α3β3γ2L receptors (n=23; n_H=0.910; black), phospho-null α3^{Y402F}β3γ2L (n=10; n_H=0.889; blue) and phospho-mimetic α3^{Y402D}β3γ2L (n=18; n_H=0.846; red) receptors. The CRC of the phospho-mimetic receptors is shifted left compared to the CRCs of both the wildtype and phospho-null receptors. **(B)** The mean GABA EC$_{50}$ value for the α3^{Y402D}β3γ2L receptors (39.8 ± 6.4 µM; n=18) was significantly lower than that of the wildtype α3β3γ2L (71.3 ± 5.2 µM; n=23) and α3^{Y402F}β3γ2L receptors (72.4 ± 11.1 µM; n=10; one-way ANOVA and Tukey's multiple comparisons tests). The EC$_{50}$ values represent the means of those derived from curves fitted for each cell. **(C)** Maximum current density values did not differ significantly between the wildtype α3β3γ2L receptors (179.8 ± 17.5 pA/pF; n=23), the α3^{Y402F}β3γ2L receptors (179 ± 39.4 pA/pF; n=10) and the α3^{Y402D}β3γ2L receptors (207.4 ± 24.6 pA/pF; n=18; one-way ANOVA test). **(D)** Representative membrane currents resulting from 4 s applications of the indicated GABA concentrations (µM) to α3β3γ2L (black), α3^{Y402F}β3γ2L (blue) and α3^{Y402D}β3γ2L (red) receptors. Circles, bars and error bars represent individual cells, population means and SEMs respectively. *p* values ≤ 0.05 *; ≤ 0.01 **.

3.2.3. The effects of aspartate substitution at residue Y402 appear to result from successful mimicry of phosphorylation

A criticism of phospho-mimetic mutations is that the functional effects they may elicit are not necessarily due to the successful mimicry of phosphorylation at a specific residue, but rather result from the mutations themselves allosterically affecting receptor activity – as appears to be the case with T400. While phenylalanine, which is structurally very similar to tyrosine (see Fig. 3.7D, E) was used for the phospho-null substitution of Y402, aspartate (Fig. 3.7C) was used to mimic phosphorylation. As substituting tyrosine with aspartate is a non-conservative structural change compared to substituting threonine with aspartate, it was deemed appropriate to investigate whether replacing tyrosine with another structurally different amino acid would elicit the same effects as the phospho-mimetic aspartate mutation on receptor GABA sensitivity.

To this end, a further mutation of residue Y402, $\alpha 3^{Y402A}$, was created by substituting tyrosine with alanine (Fig. 3.7B), which has a smaller side chain volume. As with the previous mutants, this subunit was expressed in HEK-293 cells along with equimolar ratios of $\beta 3$, $\gamma 2L$ and eGFP. Whole-cell electrophysiological concentration-response data for the $\alpha 3^{Y402A}\beta 3\gamma 2L$ receptors were gathered at the same time as the data for the $\alpha 3\beta 3\gamma 2L$, $\alpha 3^{Y402F}\beta 3\gamma 2L$ and $\alpha 3^{Y402D}\beta 3\gamma 2L$ recombinant receptors, which have already been presented. As such, the data for the wildtype, phospho-null and phospho-mimetic receptors presented in Fig. 3.7 is the same as that used in Fig. 3.6 to show the effects of $\alpha 3^{Y402A}$ on the receptor.
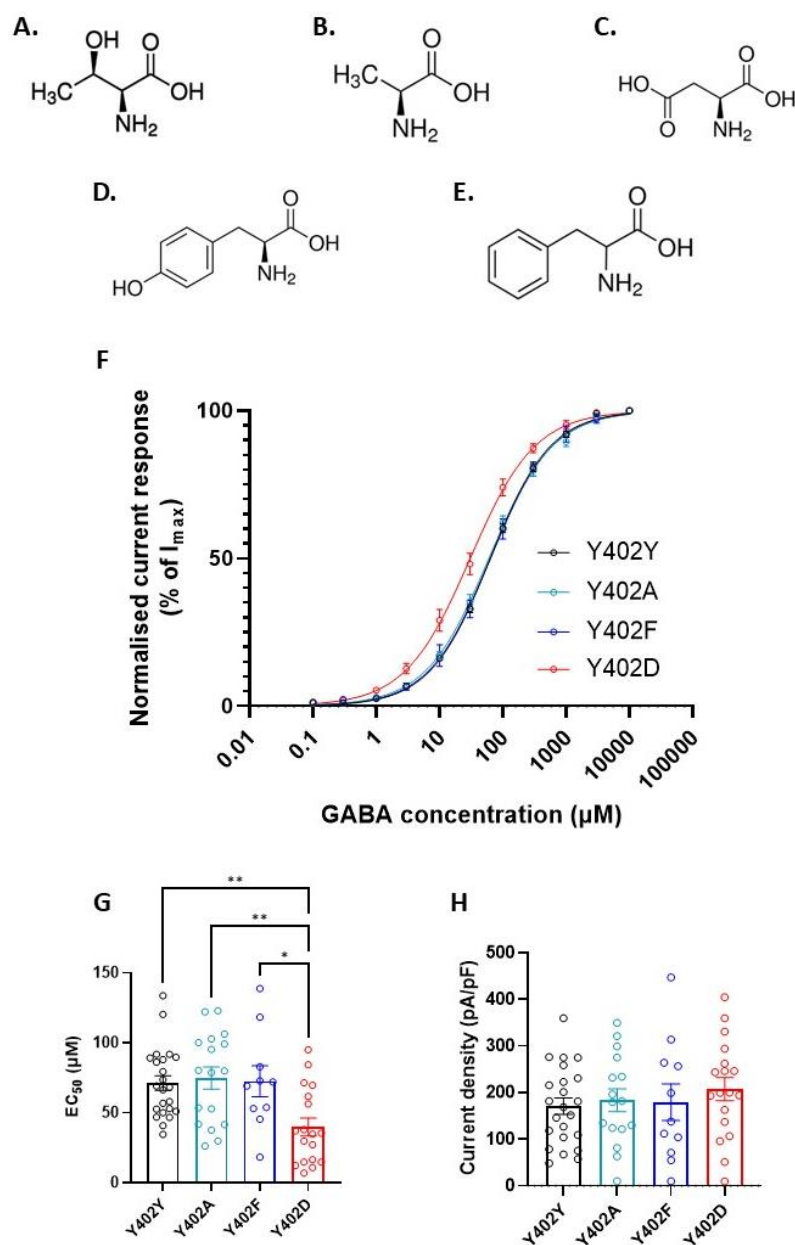
FIGURE 3.7. Substituting residue Y402 with alanine, a structurally dissimilar amino acid, does not elicit the same effects on α3-GABA$_A$R GABA sensitivity as caused by the structurally dissimilar phospho-mimetic substitution α3^{Y402D}. **(A)** Structural representation of the amino acid threonine / T. **(B)** Alanine / A. **(C)** Aspartate / D. **(D)** Tyrosine / Y. **(E)** Phenylalanine / F. **(F)** GABA CRC fitted to all data points of α3β3γ2L receptors (n=23; n_H=0.910; black), α3^{Y402A}β3γ2L receptors (n=17; n_H=0.865; light blue), α3^{Y402F}β3γ2L (n=10; n_H=0.889; dark blue) and α3^{Y402D}β3γ2L (n=18; n_H=0.846; red) receptors. The CRC of the phospho-mimetic receptors is shifted left compared to the CRCs of all the other receptors. **(G)** GABA EC$_{50}$ values for the α3^{Y402D}β3γ2L receptors (39.8 ± 6.4 µM; n=18) were significantly lower than those for the α3β3γ2L (71.3 ± 5.2 µM; n=23), the α3^{Y402A}β3γ2L receptors (74.8 ± 7.9 µM; n=17) and α3^{Y402F}β3γ2L receptors (72.4 ± 11.1 µM; n=10; one-way ANOVA and Tukey's multiple comparisons tests). The EC$_{50}$ values represent the means of those derived from curves fitted for each cell. **(H)** Maximum current density values did not differ significantly between the α3β3γ2L receptors (179.8 ± 17.5 pA/pF; n=23), the α3^{Y402A}β3γ2L receptors (183.2 ± 24.3 pA/pF; n=17), the α3^{Y402F}β3γ2L receptors (179.0 ± 39.4 pA/pF; n=10) or the α3^{Y402D}β3γ2L receptors (207.4 ± 24.6 pA/pF; n=18; one-way ANOVA test). Circles, bars and error bars represent individual cells, population means and SEMs respectively. p values ≤ 0.05 *; ≤ 0.01 **.

The GABA CRC of the $\alpha3^{Y402A}\beta3\gamma2L$ receptors did not shift relative to that of the wildtype $\alpha3\beta3\gamma2L$ receptors or the $\alpha3^{Y402F}\beta3\gamma2L$ receptors (Fig. 3.7F). This is mirrored by the EC_{50} values of the $\alpha3^{Y402A}\beta3\gamma2L$ receptors compared to the wildtype and phospho-null receptors, none of which are significantly different from one another (Fig. 3.7G). Furthermore, as with the phospho-null and phospho-mimetic receptors, the $\alpha3^{Y402A}\beta3\gamma2L$ receptor current density values do not differ compared to that of the wildtype receptors (Fig. 3.7H), suggesting that this mutation also has no effect on receptor cell surface expression.

It is plausible, therefore, is that the effect of the phospho-mimetic Y402D mutation on $\alpha3$-GABA$_A$R agonist sensitivity could be due to the successful mimicry of phosphorylation at this residue, as the mutation of Y402 to another structurally dissimilar amino acid did not elicit the same effects.

3.2.4. *Phospho-mimetic aspartate substitution at residue T401 increases both sIPSC rise time and decay tau in hippocampal neurons in cell culture*

Following the results produced by the investigation of the phospho-null and phospho-mimetic mutations in the $\alpha3$ gephyrin binding domain in HEK-293 cells, these mutants were further studied in hippocampal neurons in cell culture in order to assess their effects on inhibitory synaptic transmission. Of the three residues investigated in HEK-293 cells – T400, T401, and Y402 – only T400 was not investigated further using neurons in cell culture. This was because the similar effects on the concentration-response curves of $\alpha3^{T400A}$ and $\alpha3^{T400D}$ in HEK-293 cells indicated that the mutations had allosteric effects on the receptor, rather than effects resulting from phosphorylation (see Fig. 3.4).

The effects of the phospho-null and phospho-mimetic mutations in residues T401 and Y402 on neuronal inhibition were examined. In order to investigate T401 further, constructs expressing either the wildtype $\alpha3$, $\alpha3^{T401A}$ or $\alpha3^{T401D}$ subunits were co-transfected with eGFP into hippocampal neurons in cell culture prepared from an E18 rat (see section 2.3.1). Neurons transfected with eGFP only were used as a control, to

ensure any effects were not due to eGFP expression or transfection per se. In contrast to the HEK-293 cell transfections, only the α subunit (mutated or wildtype) and eGFP were transfected into the neurons; the β3 and γ2L subunits were not. This is because, unlike in HEK-293 cells, neurons endogenously express GABA$_A$Rs: by only transfecting in the α3 subunit, the amount of complete α3-containing receptors at the cell surface is limited by the availability of the endogenous β and γ subunits. This therefore helps to prevent overexpression of the receptor.

Whole-cell voltage-clamp electrophysiology was performed on the transfected neurons. Membrane currents were recorded and sIPSCs were detected and analysed as detailed in section 2.3.3. No significant differences in sIPSC peak amplitude (Fig. 3.8A) or mean sIPSC frequency (Fig. 3.8B) were observed between the eGFP control, wildtype α3, α3^{T401A} and α3^{T401D} transfections. However, while not statistically significant, there was a trend for the sIPSC peak amplitude of α3^{T401D} (-274.8 ± 78.0 pA) to be larger than that of wildtype α3 (-94.1 ± 10.4 pA; Fig. 3.8A). There was a similar trend for the mean sIPSC frequency of α3^{T401D} (1.9 ± 0.4 Hz) to be higher than that of α3 (0.9 ± 0.2 Hz; Fig. 3.8B).

Interestingly, both the sIPSC rise time (measured as the 10-90% rise time; Fig. 3.8C) and the sIPSC decay tau (Fig. 3.8D) of α3^{T401D} were significantly slower than those of eGFP, α3 and α3^{T401A}. The slower decay phase of the α3^{T401D} sIPSCs relative to those of the eGFP control and both the wildtype and α3^{T401A} receptors can be clearly seen in the representative peak-scaled mean sIPSC waveforms presented in Fig. 3.8F.

In addition to their synaptic localisation, α3-GABA$_A$Rs have been identified in extrasynaptic locations, where they mediate tonic inhibition (Devor et al., 2001; Marowsky et al., 2012). The effects of the α3^{T401A} and the α3^{T401D} receptors on tonic currents were investigated by blocking all GABA$_A$Rs with bicuculline (Fig. 3.9B), which acts as a competitive antagonist at the GABA binding site (Andrews & Johnston, 1979; Masiulis et al., 2019) (see section 1.3.2). No significant differences in tonic currents were observed between the eGFP control, wildtype α3, α3^{T401A} or α3^{T401D}. However, as with the sIPSC peak amplitude and mean frequency, there was a trend for the tonic current of α3^{T401D} (-70.2 ± 19.8 pA) to be larger than that of α3 (-42.4 ± 10.8 pA; Fig. 3.9A).

FIGURE 3.8. Aspartate substitution at residue T401 in the α3 gephyrin binding domain affects sIPSC kinetics in hippocampal neurons in cell culture. **(A)** sIPSC peak amplitude did not significantly differ between the eGFP control (-104.7 ± 19.3 pA; n=6), α3 (-94.11 ± 10.4 pA; n=6), α3^{T401A} (-177.2 ± 51.2 pA; n=6) or α3^{T401D} (-274.8 ± 78.0 pA; n=6; one-way ANOVA test). **(B)** Mean sIPSC frequency did not significantly differ between eGFP (1.1 ± 0.4 Hz; n=6), α3 (0.9 ± 0.2 Hz; n=5), α3^{T401A} (1.2 ± 0.2 Hz; n=6) or α3^{T401D} (1.9 ± 0.4 Hz; n=6; one-way ANOVA test). **(C)** The sIPSC 10-90 % rise time of α3^{T401D} (1.2 ± 0.1 ms; n=6) was significantly slower than that of the eGFP control (0.7 ± 0.07 ms; n=6), wildtype α3 (0.6 ± 0.05 ms; n=6) and α3^{T401A} (0.7 ± 0.1 ms; n=6; one-way ANOVA and Tukey's multiple comparisons tests). **(D)** The sIPSC decay tau of α3^{T401D} (56.8 ± 10.0 ms; n=6) was significantly slower than that of eGFP (29.8 ± 3.9 ms; n=6), α3 (31.3 ± 4.1 ms; n=6) and α3^{T401A} (27.1 ± 2.2 ms; n=6; one-way ANOVA and Tukey's multiple comparisons tests). **(E)** Representative sIPSC traces recorded from neurons transfected with eGFP only (green), α3 (black), α3^{T401A} (blue) and α3^{T401D} (purple) and voltage-clamped at -60 mV. **(F)** Representative peak-scaled mean sIPSC waveforms for the eGFP control (green; n=72 sIPSCs), wildtype α3 (black; n=97 sIPSCs), α3^{T401A} (blue; n=78 sIPSCs) and α3^{T401D} (purple; n=159 sIPSCs). Circles, bars and error bars represent individual cells, population means and SEMs respectively. *p* values ≤ 0.05 *; ≤ 0.01 **; ≤ 0.001 ***.

FIGURE 3.9. Alanine and aspartate substitutions at residue T401 in the α3 gephyrin binding domain do not affect tonic currents in hippocampal neurons in cell culture. **(A)** Tonic currents did not significantly differ between eGFP (-36.0 ± 6.4 pA; n=6), α3 (-42.4 ± 10.8 pA; n=6), α3^{T401A} (-30.0 ± 11.0 pA; n=6) and α3^{T401D} (-70.2 ± 19.8 pA; n=6; Kruskal-Wallis test). **(B)** Representative membrane currents recorded from neurons expressing eGFP only (green), α3 (black), α3^{T401A} (blue) and α3^{T401D} (purple). The competitive antagonist bicuculline (20 μM) reveals tonic inhibition by reducing the holding current, as indicated by the dashed red lines. Circles, bars and error bars represent individual cells, population means and SEMs respectively.

3.2.5. Phospho-mimetic aspartate substitution at residue Y402 increases both sIPSC rise time and decay tau in hippocampal neurons in cell culture

Following on from the HEK-293 concentration-response results for the phospho-null and phospho-mimetic substitutions for residue Y402, these mutations were also investigated further in hippocampal neurons in cell culture. As with T401, constructs expressing either the wildtype α3, α3^{Y402F} or the α3^{Y402D} subunit were co-expressed with eGFP in hippocampal neurons in cell culture. As before, neurons transfected with eGFP cDNA only were used as a control.

Unexpectedly, analysis of the recordings obtained from neurons expressing these constructs showed the sIPSC peak amplitude of the eGFP control to be significantly

higher than that of wildtype α3, while no significant differences were observed for α3^{Y402F} or α3^{Y402D} (Fig. 3.10A). This difference is difficult to explain, as eGFP was not expected to have any significant effect on sIPSC amplitude and kinetics. Some outliers may have skewed the data and this effect is unlikely to influence the results with the Y402 constructs since eGFP was always included in the transfection.

There were no significant differences between the mean sIPSC frequencies generated by the eGFP, α3, α3^{Y402F} or α3^{Y402D} receptors (Fig. 3.10B). However, there was a trend for the mean sIPSC frequency of α3^{Y402F} (1.8 ± 0.3 Hz) to be higher than that of wildtype α3 (1.1 ± 0.3 Hz; Fig. 3.10B).

α3^{Y402D} sIPSCs showed a significantly slower rise time than those of wildtype α3 (Fig. 3.10C), as was seen with the sIPSC rise time of α3^{T401D} at the T401 residue (Fig. 3.8C). Unlike α3^{T401D}, however, the α3^{Y402D} sIPSCs did not have a significantly slower rise time than those of eGFP or α3^{Y402F} (Fig. 3.10C). The sIPSC decay tau of 3^{Y402D} was significantly slower than that of eGFP, α3 and α3^{Y402F} (Fig. 3.10D), mirroring the sIPSC decay tau of α3^{T401D} (Fig. 3.8D). The slower decay phase of the α3^{Y402D} sIPSCs relative to those of the eGFP control and both the wildtype and α3^{Y402F} receptors can be clearly seen in the representative peak-scaled mean sIPSC waveforms presented in Fig. 3.10F.

As with residue T401, the effects of the α3^{Y402F} and α3^{Y402D} receptors on tonic currents were investigated by blocking all GABA$_A$Rs with bicuculline (Fig. 3.11B). No significant differences in tonic currents were observed between the eGFP control, wildtype α3, α3^{Y402F} or α3^{Y402D}. However, there was a trend for the tonic current of α3^{Y402F} (-14.7 pA ± 3.9) to be smaller than those of eGFP (-43.1 ± 13.0 pA), α3 (-32.7 pA ± 6.4) and α3^{Y402D} (-44.8 ± 12.1 pA; Fig. 3.11A).

Overall, these results clearly demonstrate that substitution of the residues T401 and Y402 with aspartate increases both the rise time and decay tau of α3-containing GABA$_A$Rs in hippocampal neurons in cell culture. As α3 subunit-containing GABA$_A$Rs display slower kinetics than other α subunit-containing receptors (Picton & Fisher, 2007; Syed et al., 2020) (see section 1.4.1), these results could indicate that these mutations increase the number of α3-GABA$_A$Rs at the synapse.
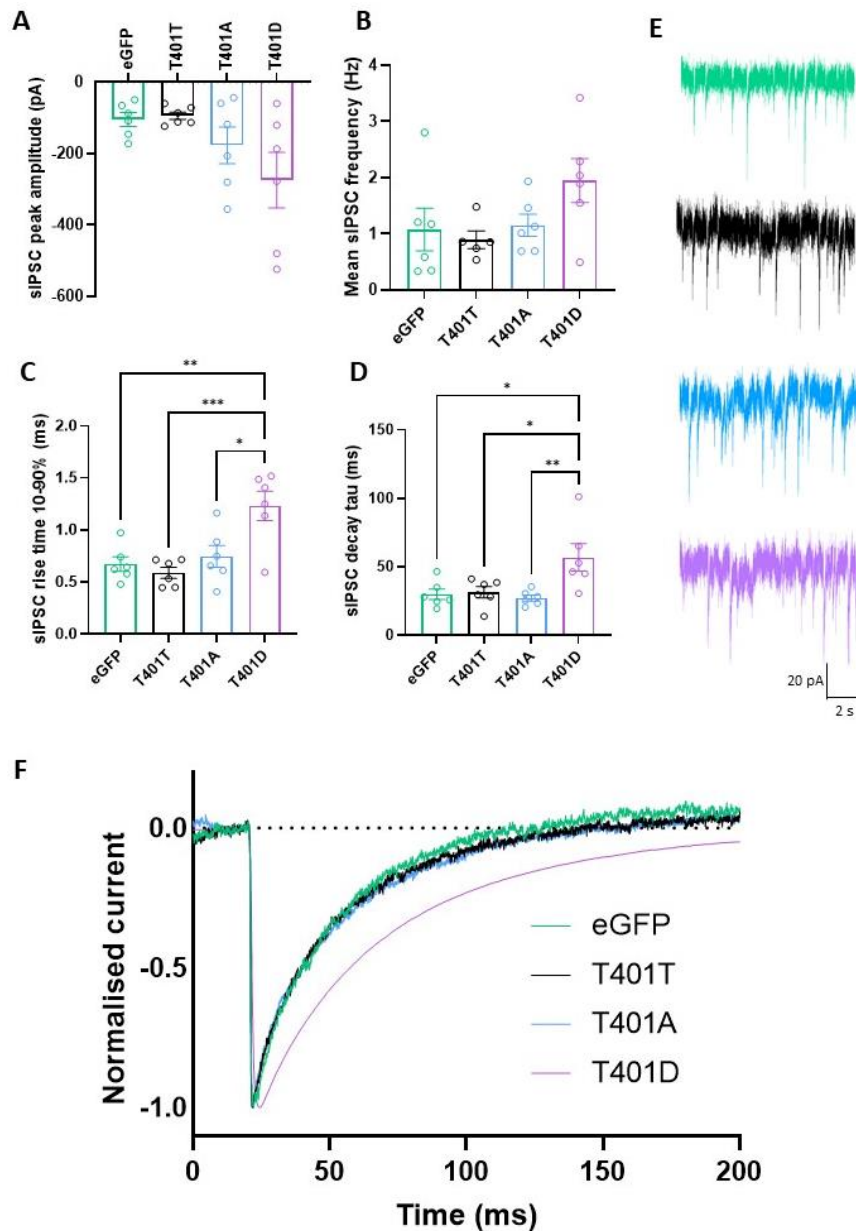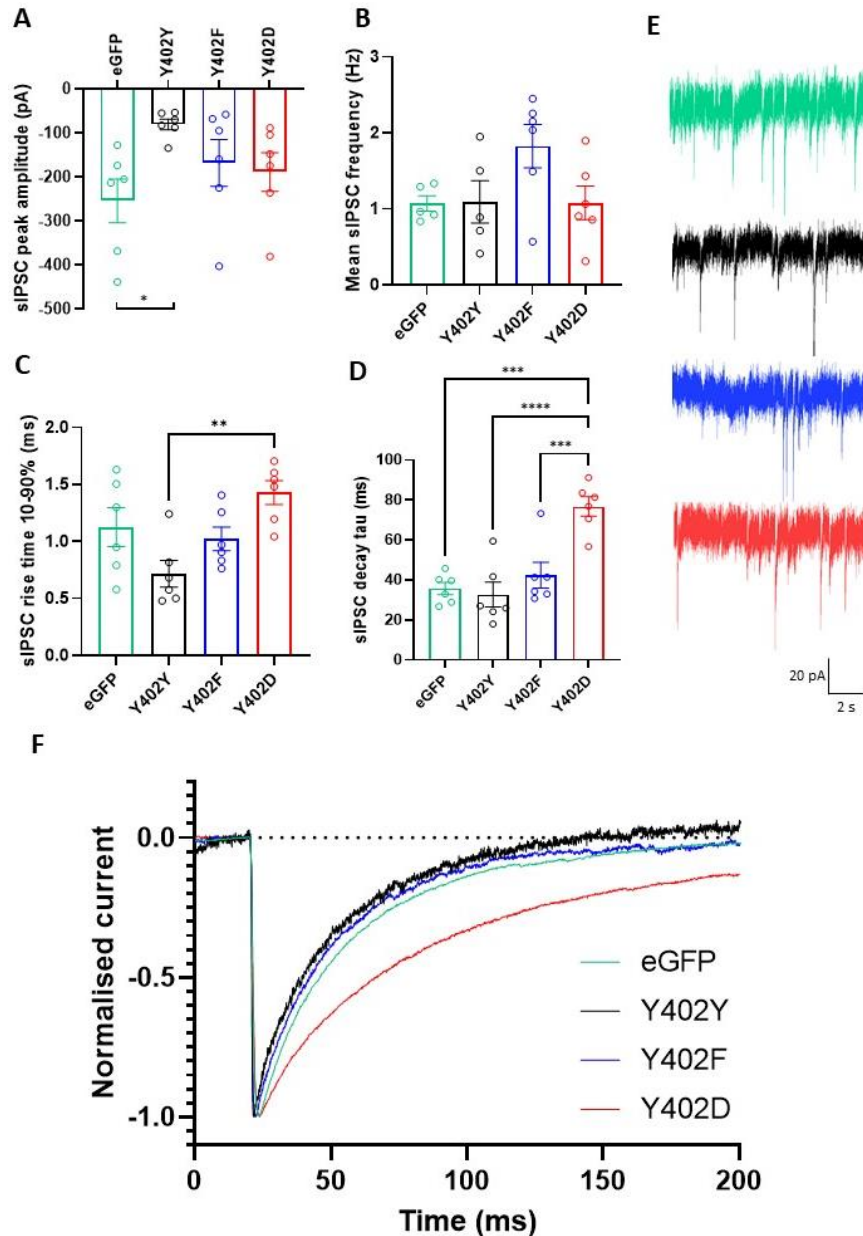
FIGURE 3.10. Aspartate substitution at residue Y402 in the α3 gephyrin binding domain affects sIPSC kinetics in hippocampal neurons in cell culture. **(A)** The sIPSC peak amplitude of the eGFP control (-254.4 ± 49.5 pA; n=6) was significantly higher than that of wildtype α3 (-80.6 ± 12.2 pA; n=6), but not than those of α3^{Y402F} (-168.1 ± 53.5 pA; n=6) or α3^{Y402D} (-188.7 ± 44.0 pA; n=6; one-way ANOVA and Tukey's multiple comparisons tests). **(B)** Mean sIPSC frequency did not significantly differ between eGFP (1.1 ± 0.1 Hz; n=5), α3 (1.1 ± 0.3 Hz; n=5), α3^{Y402F} (1.8 ± 0.3 Hz; n=6) or α3^{Y402D} (1.1 ± 0.2 Hz; n=6; one-way ANOVA test). **(C)** The sIPSC 10-90% rise time of α3^{Y402D} (1.4 ± 0.1 ms; n=6) was significantly slower than that of α3 (0.7 ± 0.1 ms), but not when compared to those of eGFP (1.1 ± 0.2 ms; n=6) or α3^{Y402F} (1.0 ± 0.1 ms; n=6; one-way ANOVA and Tukey's multiple comparisons tests). **(D)** The sIPSC decay tau of α3^{Y402D} (76.7 ± 4.9 ms; n=6) was significantly slower than that of eGFP (35.8 ± 3.0 ms; n=6), α3 (32.7 ± 6.2 ms; n=6) and α3^{Y402F} (42.4 ± 6.4 ms; n=6; one-way ANOVA and Tukey's multiple comparisons tests). **(E)** Representative sIPSC traces recorded from neurons transfected with eGFP only (green), α3 (black), α3^{Y402F} (blue) and α3^{Y402D} (red) and voltage-clamped at -60 mV. **(F)** Representative peak-scaled mean sIPSC waveforms for the eGFP control (green; n=53 sIPSCs), wildtype α3 (black; n=96 sIPSCs), α3^{Y402F} (blue; n=69 sIPSCs) and α3^{Y402D} (red; n=50 sIPSCs). Circles, bars and error bars represent individual cells, population means and SEMs respectively. *p* values ≤ 0.01 **; ≤ 0.001 ***; ≤ 0.0001 ****.
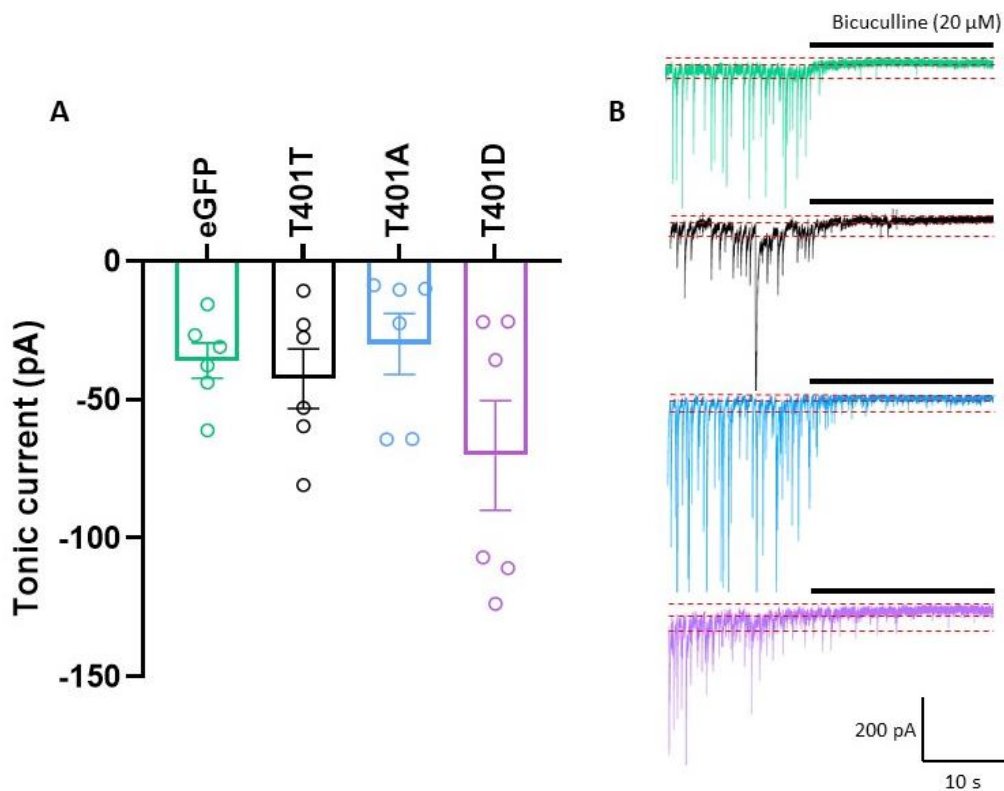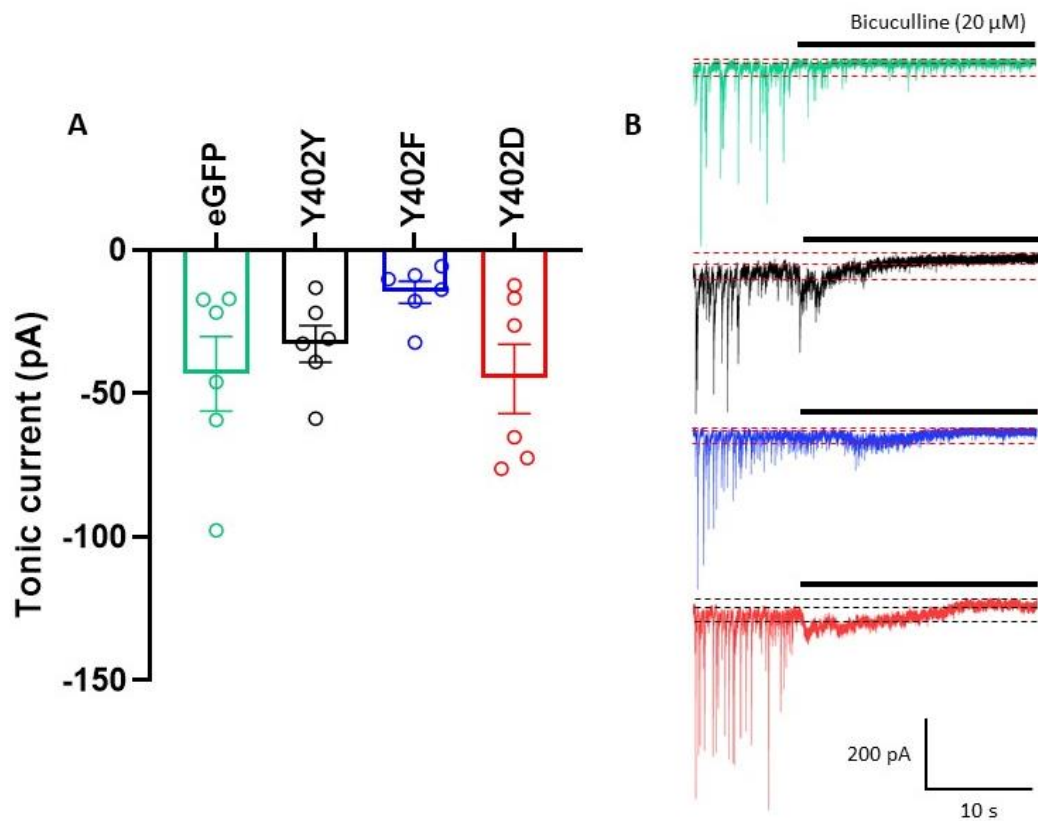
FIGURE 3.11. Alanine and aspartate substitutions at residue Y402 in the α3 gephyrin binding domain do not affect tonic currents in hippocampal neurons in cell culture. **(A)** Tonic currents did not significantly differ between eGFP (-43.1 ± 13.0 pA; n=6), α3 (-32.7 ± 6.4 pA; n=6), $α3^{Y402F}$ (-14.7 ± 3.9 pA; n=6) or $α3^{Y402D}$ (-44.8 ± 12.1 pA; n=6; one-way ANOVA test). **(B)** Representative tonic current traces recorded from neurons transfected with eGFP only (green), α3 (black), $α3^{Y402F}$ (blue) and $α3^{Y402D}$ (red). The competitive antagonist bicuculline (20 μM) reveals tonic inhibition by reducing the holding current, as indicated by the dashed red (or black, in the case of $α3^{Y402D}$) lines. Circles, bars and error bars represent individual cells, population means and SEMs respectively.

3.2.6. *Phospho-null and phospho-mimetic mutations affect whole-cell GABA current kinetics at Y402, but not T401*

In HEK-293 cells, phospho-null alanine substitution at residue T401 significantly increased the sensitivity of the $α3$-GABA$_A$R for GABA, compared to wildtype receptors and receptors containing the phospho-mimetic aspartate substitution (Fig. 3.5A, B). In contrast, at residue Y402, aspartate substitution significantly increased the sensitivity of the $α3$-GABA$_A$R for GABA compared to wildtype receptors and receptors containing the phenylalanine substitution (Fig. 3.6A, B). However, when these mutations were introduced into hippocampal neurons in cell culture, both the phospho-mimetic

$\alpha3^{T401D}$ and $\alpha3^{Y402D}$ mutations caused the same effects: increasing both sIPSC rise and decay time compared to eGFP, wildtype and phospho-null receptor sIPSCs (Figs. 3.8C, D & 3.10C, D).

At the end of the last section, the possibility that the changes in sIPSC rise and decay times observed with the aspartate mutations were due to altered numbers of $\alpha3$ at inhibitory synapses was raised (see section 3.2.5). An alternative possibility is that the mutations themselves cause a change in receptor kinetics and that this change is responsible for the slower sIPSC rise and decay times. This prompted a re-investigation of the original HEK-293 cell data, to discern whether these mutations had any effect on receptor kinetics in this heterologous expression system.

The desensitisation and deactivation kinetics of the recombinant receptors were characterised by measuring desensitisation and deactivation time constants for maximal whole-cell GABA-activated currents, as detailed in section 2.2.5. At residue T401, neither the alanine nor the aspartate substitution had any significant effect on receptor desensitisation (Fig. 3.12A) or receptor deactivation (Fig. 3.12B) compared to the wildtype $\alpha3\beta3\gamma2L$ receptors. At residue Y402, neither $\alpha3^{Y402F}$ nor $\alpha3^{Y402D}$ significantly affected receptor deactivation compared to wildtype (Fig. 3.12D). However, both mutations at Y402 affected the desensitisation of the receptor: the $\alpha3^{Y402F}\beta3\gamma2L$ receptors desensitised significantly more quickly than the $\alpha3\beta3\gamma2L$ receptors, while the $\alpha3^{Y402D}\beta3\gamma2L$ receptors desensitised significantly more slowly (Fig. 3.12C). Furthermore, the $\alpha3^{Y402D}\beta3\gamma2L$ receptors desensitised significantly more slowly than the $\alpha3^{Y402F}\beta3\gamma2L$ receptors (Fig. 3.12C).

Therefore, alanine and aspartate substitutions at residue T401 appear not to affect $\alpha3$-GABA$_A$R kinetics, in so far as can be assessed from whole-cell current data (Fig. 3.12A, B). However, phenylalanine and aspartate mutations at residue Y402 do alter $\alpha3$-GABA$_A$R whole-cell desensitisation kinetics in HEK-293 cells (Fig. 3.12C).
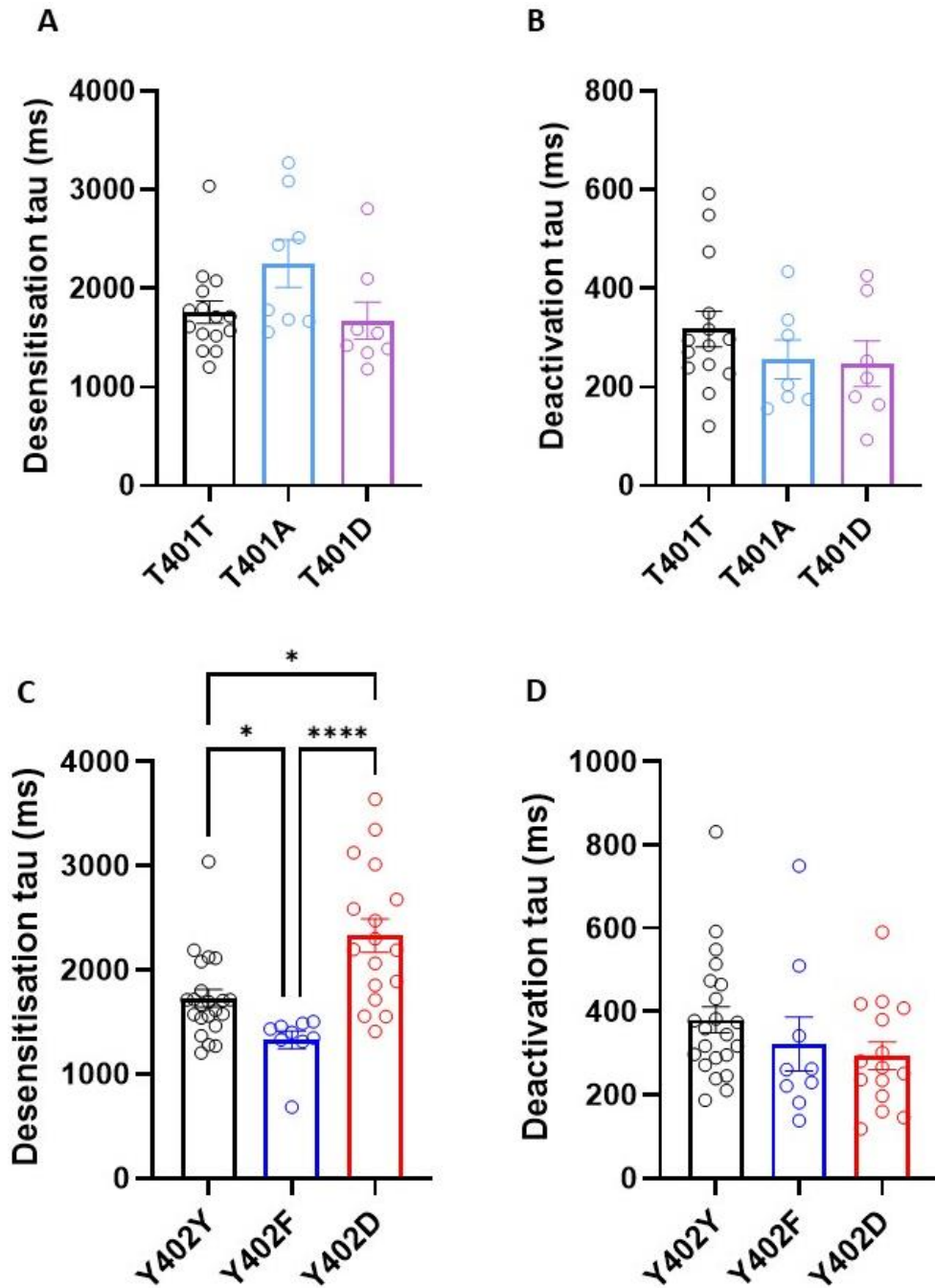
FIGURE 3.12. Phospho-null and phospho-mimetic substitutions at Y402, but not at T401, affect α3-GABA$_A$R desensitisation kinetics. **(A)** The desensitisation tau did not differ significantly between wildtype α3β3γ2L receptors (1759 ± 113.5 ms; n=15; black), α3^{T401A}β3γ2L receptors (2252 ± 239.8 ms; n=8; blue) or α3^{T401D}β3γ2L receptors (1673 ± 188.5 ms; n=8; purple; Kruskal-Wallis test). **(B)** The deactivation tau did not differ significantly between α3β3γ2L (317.8 ± 35.9 ms; n=15), α3^{T401A}β3γ2L (255.9 ± 39.5 ms; n=8) or α3^{T401D}β3γ2L receptors (247.3 ± 46.3 ms; n=8; Kruskal-Wallis test). **(C)** The desensitisation tau of the α3^{Y402D}β3γ2L receptors (2327 ± 160.6 ms; n=17; red) was significantly larger than those of both the α3β3γ2L (1726 ± 85.5 ms; n=22; black) and α3^{Y402F}β3γ2L (1327 ± 83.9 ms; n=9; blue) receptors. The desensitisation tau of the wildtype receptors was significantly larger than that of the α3^{Y402F}β3γ2L receptors (Kruskal-Wallis and Dunn's multiple comparisons tests). **(D)** The deactivation tau did not differ significantly between α3β3γ2L (380 ± 31.6 ms; n=22), α3^{Y402F}β3γ2L (321.5 ± 64.3 ms; n=9) or α3^{Y402D}β3γ2L receptors (293.9 ± 33.2 ms; n=17; Kruskal-Wallis test). Circles, bars and error bars represent individual cells, population means and SEMs respectively. *p* values ≤ 0.05 *; ≤ 0.0001 ****.

3.3. Discussion

3.3.1. Residues S426, T427 & S433 in the ICD of the α3 subunit are unlikely to be phosphorylated in HEK-293 cells

Phosphorylation is a post-translational modification capable of regulating many aspects of $GABA_AR$ subcellular localisation and function (Nakamura et al., 2015), as discussed in detail in section 1.1.4. This is especially true for the phosphorylation of residues in the ICD of a given $GABA_AR$ subunit. Phosphorylation of residues in the ICD of the α subunit, for example, regulates receptor modulation by neurosteroids (Abramian et al., 2014; Adams et al., 2015) and the binding of allosteric modulators such as benzodiazepines (Churn et al., 2004). Therefore, the three putative phosphorylation sites – S426, T427 and S433 – identified by Huttlin et al. (2010) in the ICD of the α3 subunit seemed likely candidates for the facilitation of phosphorylation-induced regulation of α3-$GABA_AR$ function. This hypothesis was strengthened by the fact these residues are located in a region of the α3 ICD that is not present in the α1, α2 or α5 subunits (Fig. 3.1).

However, preventing phosphorylation at these residues via their substitution with alanine had no significant effect on either GABA potency or receptor cell surface expression assessed using electrophysiological methods (Fig. 3.3). It could well be that these residues cannot actually be phosphorylated – they were highlighted only as putative phosphorylation sites, after all (Huttlin et al., 2010). Alternatively, these residues may be true phosphorylation sites, but their phosphorylation status has no discernible effect on the sensitivity of the receptor for GABA activation, or on receptor trafficking. Or perhaps, these residues are phosphorylation sites but are not basally phosphorylated in HEK-293 cells. Under these circumstances, mutation to alanine would show no difference in GABA sensitivity or trafficking compared to wildtype; a comparative phospho-mimetic aspartate mutation would be necessary to discern these effects.

It is worth reiterating here the contradictory reports on the affinity of α3-$GABA_AR$s for agonist: some studies have reported low GABA affinity (Verdoorn, 1994; Gingrich et al., 1995; Mortensen et al., 2011), others high (Keramidas & Harrison, 2010). While

conducting recombinant GABA$_A$R experiments in HEK-293 cells in the present study, a high amount of variability in the EC$_{50}$ of wildtype α3-GABA$_A$Rs was observed – much more so than from receptors containing other α subunits, including α1. To quantify this, the coefficients of variation (CV) were calculated, by dividing the standard deviation by the mean, from the EC$_{50}$ CRC HEK-293 cell data for α3β3γ2L and α1β3γ2L recombinant receptors. The CV of the α3β3γ2L receptors was 35.1%, compared to 20.1% for the α1β3γ2L receptors. This α3-specific increase in variability could potentially be attributed to varying phosphorylation levels. As such, it could be that no effects on receptor agonist sensitivity were observed with these mutations because the residues of the wildtype receptors were not phosphorylated in these cells.

3.3.2. Phospho-null and phospho-mimetic substitutions of three key residues in the gephyrin binding domain of the α3 subunit affect receptor function

Residues T400, T401 and Y402, located within the gephyrin binding domain of the α3 subunit, have been identified as being of critical importance for gephyrin binding, due to the hydrophobic interactions of their side chains with gephyrin (Maric et al., 2014). It is highly likely that the binding of α subunits to gephyrin is regulated by post-translational modifications such as phosphorylation: the subunits α1-3 and α5 each bind gephyrin with unique binding domains (Tretter et al., 2008; Mukherjee et al., 2011; Tretter et al., 2011; Brady & Jacob, 2015), yet the interaction is tight and highly specific for each of these subunits (Maric et al., 2014).

Preventing and mimicking phosphorylation at each of these three residues had differential effects on receptor function. At residue T400, both the α3^{T400A}β3γ2L and the α3^{T400D}β3γ2L receptors caused the GABA CRC to shift to the left, and the EC$_{50}$ to significantly reduce, compared to those of the wildtype α3β3γ2L receptors (Fig. 3.4A, B). These results indicate that both the alanine and the aspartate mutations increase the sensitivity of the receptor for GABA. As discussed in section 3.2.2, phospho-null mutations are not expected to give the same outcome as phospho-mimetic mutations. These results thus most likely suggest that substituting T400 with either alanine or

aspartate influences receptor activation through allosteric effects, which are unrelated to the prevention or mimicry of phosphorylation at this residue. Indeed, it may well be the case that the increased GABA potency observed with these mutant receptors would also arise if T400 was substituted with any other amino acid, although this experiment has not been performed here.

For the $\alpha 1$ subunit, putative phosphorylation at residue T375 has been shown to modulate receptor function in HEK-293 cells (Bell-Horner et al., 2006; Mukherjee et al., 2011). The results for T400 are therefore surprising, as T375 in the $\alpha 1$ subunit corresponds to T400 in the $\alpha 3$ subunit and is conserved in the gephyrin binding domains of $\alpha 1$-3 (Bell-Horner et al., 2006). However, the current density, which is an indirect measure of receptor cell surface expression, of the $\alpha 3^{T400D}\beta 3\gamma 2L$ receptor is higher than that of the wildtype receptor (Fig. 3.4C). This indicates that the $\alpha 3^{T400D}$ substitution may alter receptor trafficking in such a way that increases receptor surface expression, although this could well be a further manifestation of the allosteric effects of mutating this residue observed with the concentration-response data.

In contrast to T400, the phospho-null and phospho-mimetic mutations of residues T401 and Y402 did display differential effects. At T401, the $\alpha 3^{T401A}\beta 3\gamma 2L$ receptors caused a leftward shift of the GABA CRC, along with a corresponding reduction in the GABA EC_{50}, compared to the wildtype and $\alpha 3^{T401D}\beta 3\gamma 2L$ receptors (Fig. 3.5A, B). As with T400, the possibility that these results were caused by allosteric effects of the T401A mutation on the receptor cannot be excluded. However, in contrast to T400, this is less likely to be the case for T401, as the T401D mutation did not affect the receptor's GABA sensitivity. Furthermore, there was no difference in macroscopic current desensitisation or deactivation kinetics between the wildtype, alanine or aspartate mutant receptors (Fig. 3.12A, B). A possible interpretation of these data, therefore, is that T401 is basally phosphorylated in HEK-293 cells, and that by preventing phosphorylation at this residue via alanine substitution, the $\alpha 3$-GABA$_A$R's sensitivity for GABA is increased.

Interestingly, the current density of the $\alpha 3^{T401A}\beta 3\gamma 2L$ receptors, but not the $\alpha 3^{T401D}\beta 3\gamma 2L$ receptors, was significantly higher than that of the wildtype receptors (Fig. 3.5C). This may suggest that preventing phosphorylation at residue T401 affects

the trafficking of the receptor to the cell surface. This could arise in two ways: (1) preventing phosphorylation may affect the ability of the $\alpha3^{T401A}\beta3\gamma2L$ receptors to reach the surface; or (2) the $\alpha3^{T401A}\beta3\gamma2L$ receptors are trafficked to the surface as normal but are subsequently removed from the surface at a slower rate than the wildtype and $\alpha3^{T401D}\beta3\gamma2L$ receptors because they cannot be phosphorylated. Either way, the role of phosphorylation at this residue appears significant for both receptor GABA sensitivity and cell surface expression.

At residue Y402, the $\alpha3^{Y402D}\beta3\gamma2L$ receptors caused a leftward shift in the GABA CRC and a significantly lower EC_{50} compared to both the wildtype and the $\alpha3^{Y402F}\beta3\gamma2L$ receptors (Fig. 3.6A, B). As with T401, it cannot be ruled out that the aspartate substitution, which is structurally very dissimilar to tyrosine (see Fig. 3.7C, D) itself affects the kinetics of the receptor, causing the observed increase in GABA sensitivity. However, in contrast to the Y402D mutation, substituting Y402 with alanine, the structure of which is also very different from that of tyrosine (see Fig. 3.7B, D), does not affect the receptor GABA CRC or EC_{50} compared to wildtype (Fig. 3.7F, G). This suggests that the increase in GABA sensitivity observed for the $\alpha3^{Y402D}\beta3\gamma2L$ receptors is due to mimicking phosphorylation at this residue. It is therefore plausible that the native state of this residue is non-phosphorylated and that mimicking its phosphorylation increases the receptor's sensitivity to GABA.

Mutating Y402 does affect receptor desensitisation kinetics, as seen in Fig. 3.12C. However, the phenylalanine and aspartate mutations have divergent effects on the desensitisation time constant – decreasing and increasing it respectively – as is expected from opposing phosphorylation mutations. Furthermore, the corresponding residues to T401 in α1 (Munton et al., 2007), and Y402 in both the α1 and α2 subunits (Ballif et al., 2008), have already been shown to be phosphorylated *in vivo.* This, combined with the phospho-null and phospho-mimetic data at these residues, suggests that both T401 and Y402 could be phosphorylated *in vivo*.

3.3.3. *Aspartate substitutions at T401 & Y402 slow down α3-GABA$_A$R sIPSC kinetics*

Interestingly, while the aspartate substitutions at T401 and Y402 had different effects on recombinant α3-GABA$_A$R agonist sensitivity in HEK-293 cells (causing no effect relative to wildtype versus causing a leftward shift in the GABA CRC respectively; see Figs. 3.5A & 3.6A), these mutations induced the same effects on sIPSCs when investigated in hippocampal neurons in cell culture (Figs. 3.8 & 3.10). These mutations and their effects are summarised in Table 3.1. Given that the effects of these mutations on GABA sensitivity do not mirror the effects on sIPSC kinetics, it may be that the overall effect of these mutations on synaptic inhibition are caused by something else, such as affecting α3-GABA$_A$R subcellular localisation.

TABLE 3.1. Summary of the effects of mutations made within the α3 subunit of the GABA$_A$R. N/A indicates where a given mutation was not investigated in a particular system. WT indicates the wildtype genotype.

Mutation	Effect (HEK-293 cells)	Effect (hippocampal neurons in cell culture)
S426A	➤ None relative to WT	N/A
T427A	➤ None relative to WT	N/A
S433A	➤ None relative to WT	N/A
T400A	➤ CRC shifts left relative to WT ➤ Lower EC$_{50}$ than WT	N/A
T400D	➤ CRC shifts left relative to WT ➤ Lower EC$_{50}$ than WT ➤ Higher maximum current density than WT	N/A
T401A	➤ CRC shifts left relative to WT & T401D	➤ None relative to WT

T401A	➢ Lower EC$_{50}$ than WT & T401D ➢ Higher maximum current density than WT & T401D	
T401D	➢ None relative to WT	➢ Slower 10-90% rise time than eGFP, WT & T401A ➢ Slower decay tau than eGFP, WT & T401A
Y402A	➢ None relative to WT	N/A
Y402F	➢ Smaller desensitisation tau than WT & Y402D	➢ None relative to WT
Y402D	➢ CRC shifts left relative to WT, Y402A & Y402F ➢ Lower EC$_{50}$ than WT, Y402A & Y402F ➢ Larger desensitisation tau than WT & Y402F	➢ Slower 10-90% rise time than eGFP, WT & Y402F ➢ Slower decay tau than eGFP, WT & Y402F

The kinetic properties of the α3-GABA$_A$R are distinct: almost all of its measurable kinetic parameters are slower than those of other α subunit-containing receptors (Picton & Fisher, 2007) (see section 1.4.1). α3-GABA$_A$Rs have one of the slowest deactivation rates, comparable only to α6 subunit-containing receptors, and display the slowest rates of desensitisation and activation of all the α subunits (Picton & Fisher, 2007). Furthermore, the decay rate of the α3-GABA$_A$R is one of the slowest of all GABA$_A$R subtypes (Picton & Fisher, 2007), with recent data showing the decay time constant of α3β3γ2 receptors to be significantly slower than that of their α1β3γ2 counterparts (Syed et al., 2020). The sIPSCs recorded from transfected neurons represent a mixed GABA$_A$R population, with both endogenous receptors and receptors incorporating the introduced wildtype or mutant α3 subunits. Therefore, a possible interpretation of the slower sIPSC rise and decay times displayed by the α3^{T401D} and α3^{Y402D} mutants is that these mutations cause more α3-containing

GABA$_A$Rs to localise post-synaptically. This provides a potential explanation for the slower sIPSC kinetics observed with these phospho-mimetic receptors, as a greater proportion of the synaptic receptors may have been α3-GABA$_A$Rs when compared to the neurons transfected with the wildtype α3 subunit.

As with the HEK-293 cell data, it cannot be ruled out that the slower sIPSC rise and decay times observed with the α3^{T401D} and α3^{Y402D} mutant subunits are a result of the aspartate substitutions directly affecting receptor kinetics. In the case of residue T401, however, neither the alanine nor the aspartate mutations caused a discernible effect on receptor kinetics (Fig. 3.12A, B), although it should be noted here that these results are from whole-cell current recordings, the GABA applications for which are too slow to allow detection of receptors that may deactivate or desensitise very quickly. Rapid GABA applications onto membrane patches would have provided a more sensitive measurement. However, given the apparent lack of effect of α3^{T401D} on receptor kinetics in HEK-293 cells, it is unlikely that the effects seen on sIPSC α3^{T401D} kinetics result from the aspartate mutation affecting receptor kinetics in neurons in cell culture.

In contrast, aspartate substitution at Y402 caused the α3^{Y402D}β3γ2L receptors to desensitise more slowly than the wildtype α3β3γ2L receptors, while phenylalanine substitution caused the α3^{Y402F}β3γ2L receptors to desensitise more quickly (Fig. 3.12C). It is therefore possible that the slower sIPSC rise and decay times observed for α3^{Y402D} (Fig. 3.10C, D) are due to kinetics effects of the aspartate mutation on the receptor.

A further interpretation of these data relates to the interaction of the α3 subunit with the scaffold protein gephyrin. Both T401 and Y402 are located within the gephyrin binding domain of α3 (Tretter et al., 2011). The study by Maric et al. (2014) suggests that these residues are (1) of critical importance to gephyrin binding and (2) are strong candidates for mediating the regulation of such binding via post-translational modifications such as phosphorylation. Therefore, these results raise the possibility that mimicking phosphorylation at these residues affects interaction with gephyrin in such a way that the proportion of synaptic α3-GABA$_A$Rs is increased. This hypothesis will be investigated further in the following chapters.

3.4. Conclusions

1. Preventing phosphorylation using phospho-null alanine substitutions at the putative phosphorylation sites S426, T427 and S433 within the ICD of the α3 subunit does not affect α3-GABA$_A$R agonist sensitivity or cell surface expression.

2. Alanine and aspartate mutations of residue T400 within the gephyrin binding domain of the α3 subunit, intended to prevent and mimic phosphorylation respectively, both increase receptor GABA sensitivity, consistent with allosteric effects on receptor function.

3. Phospho-null alanine substitution at residue T401 within the gephyrin binding domain of the α3 subunit increases both receptor sensitivity to GABA and cell surface expression.

4. Phospho-mimetic aspartate substitution at residue Y402, also within the gephyrin binding domain of the α3 subunit, increases receptor sensitivity to GABA and slows macroscopic receptor desensitisation.

5. Mimicking phosphorylation via aspartate substitution at both T401 and Y402 significantly slows down the rise and decay times of sIPSCs in hippocampal neurons in cell culture. This may be due to these mutations causing an increase in the proportion of α3-GABA$_A$Rs located at inhibitory postsynaptic sites. Alternatively, for Y402, these effects on sIPSC kinetics may be related to the changes in receptor desensitisation observed in HEK-293 cells.

Chapter 4: exploring the role of Y402 in regulating α3 subunit-gephyrin binding and subcellular localisation

4.1. Introduction

In the previous chapter, phospho-mimetic aspartate substitutions at residues T401 and Y402 in the gephyrin binding domain of the α3 subunit were shown to slow down both the 10-90% rise time and the decay tau of neuronal sIPSCs. These slow kinetics are consistent with an increase in α3-GABA$_A$Rs being present at inhibitory synapses, compared to neurons expressing the wildtype or phospho-null phenylalanine- or alanine-substituted subunits. To investigate this hypothesis further, experiments to examine the subcellular localisation – synaptic or extrasynaptic – of these mutant receptors, as well as their interactions with the scaffold protein gephyrin, were performed.

Due to the technically difficult and time-consuming nature of these experiments, only residue Y402 was subjected to the further investigations detailed in this chapter. This was prioritised because, alongside the interesting electrophysiological results that the phospho-mimetic α3^{Y402D} substitution produced in HEK-293 cells and hippocampal neurons in cell culture (discussed in Chapter 3), Y402 has been previously highlighted as the residue that is most critical for mediating the binding of the α3 subunit to gephyrin, as its side chain is proposed to engage in key hydrophobic interactions with gephyrin (Maric et al., 2014).

Gephyrin is a principal scaffold protein that plays a key role in the recruitment and anchoring of GABA$_A$Rs at GABAergic synapses (Tyagarajan & Fritschy, 2014). In 2011, Mukherjee et al. demonstrated that residue T375 of the α1 subunit, a putative phosphorylation site in the gephyrin binding domain, modulates the binding affinity between α1 and gephyrin. Mimicking phosphorylation at this residue diminished the binding between α1 and gephyrin, consequentially reducing α1-GABA$_A$R accumulation at synapses and illustrating the importance of post-translational modifications in receptor regulation and localisation. It therefore follows that mimicking phosphorylation at Y402, located within the gephyrin binding domain of the α3 subunit, may also similarly affect binding between α3 and gephyrin.

Structured illumination microscopy (SIM) is a type of super-resolution imaging that allows the resolution limit of conventional fluorescence microscopy to be overcome (see Heintzmann & Huser (2017) for review). Multiple studies have employed SIM imaging to investigate the structure and organisation of postsynaptic densities (e.g., Crosby et al., 2019; Schmerl et al., 2020). For instance, Davenport et al. (2017) used SIM to demonstrate a loss of synaptic GABA$_A$R localisation in LFHPL4 knockout mice, therefore establishing an essential role for LFHPL4 in the functioning of inhibitory synapses. LFHPL4 is also known as GARHL and is proposed to bind directly to receptor γ2 subunits in the cell membrane (Yamasaki et al., 2017). SIM therefore provides an effective technique for examining the subcellular localisation of different proteins and protein complexes.

To investigate further whether mimicking phosphorylation affects GABA$_A$R subcellular localisation, immunocytochemistry and SIM imaging were performed on hippocampal neurons in cell culture transfected with myc-tagged α3, phospho-null α3^{Y402F} or phospho-mimetic α3^{Y402D} subunits. Co-immunoprecipitation experiments between wildtype and mutated α3-GABA$_A$Rs were subsequently performed to investigate whether these residue substitutions affect the binding between α3 and gephyrin.

4.2. Results

4.2.1. Phospho-mimetic aspartate substitution at Y402 increases synaptic α3 localisation but likely independently of gephyrin

To assess the effects of mimicking phosphorylation at residue Y402 on α3-GABA$_A$R subcellular localisation, myc tags were inserted into the N-termini, between residues 33 and 34 of the mature α3 subunit protein, of constructs expressing the wildtype α3, α3^{Y402F} and α3^{Y402D} subunits. These constructs were co-transfected, with eGFP, into hippocampal neurons in cell culture. The neurons were fixed with PFA, following which gephyrin, VIAAT (vesicular inhibitory amino acid transporter) and the transfected myc-tagged α3 proteins were labelled with selective antibodies (see section 2.4). In brief, cell surface α3 proteins were labelled with rabbit anti-myc (ab32, Abcam) at a 1:700 dilution. The neurons were subsequently permeabilised and the intracellular gephyrin

and VIAAT proteins labelled with mouse anti-gephyrin (147111, Synaptic Systems; 1:200) and guinea pig anti-VIAAT (AGP129, Alomone; 1:500) antibodies, respectively. These primary antibodies were then labelled with the fluorescent secondary antibodies goat anti-rabbit IgG H&L Alexa Fluor® 555 (A21424, ThermoFisher), goat anti-mouse IgG H&L Alexa Fluor® 488 (A11001, ThermoFisher) and goat anti-guinea pig IgG H&L Alexa Fluor® 647 (A21450, ThermoFisher), all at a dilution of 1:500.

SIM imaging was performed, and the resulting images processed, as described in section 2.5.1. Representative images of proximal dendrites of the labelled neurons expressing either myc-α3, myc-α3^{Y402F} or myc-α3^{Y402D} are shown in Fig. 4.1.

The open-source ImageJ distribution package FIJI (v1.53c) was used to analyse the processed SIM images, using the plugin DiAna (Gilles et al., 2017) (see section 2.5.2). DiAna was chosen as it offers accurate 3D segmentation for object identification and performs a thorough analysis of object-based co-localisation (Gilles et al., 2017). Volumes, mean grey values and co-localisation of the α3, gephyrin and VIAAT fluorescent puncta were assessed. VIAAT is a synaptic vesicle-located transporter protein that packages GABA into vesicles for release across the synaptic cleft (Juge et al., 2009); as such, it serves as a presynaptic marker for GABA-containing axon terminals. Therefore, with the assumption that VIAAT marks all and only GABAergic synapses, in this analysis α3 puncta that co-localised with VIAAT puncta were classed as synaptic, while α3 puncta that did not co-localise with VIAAT puncta were classed as extrasynaptic.
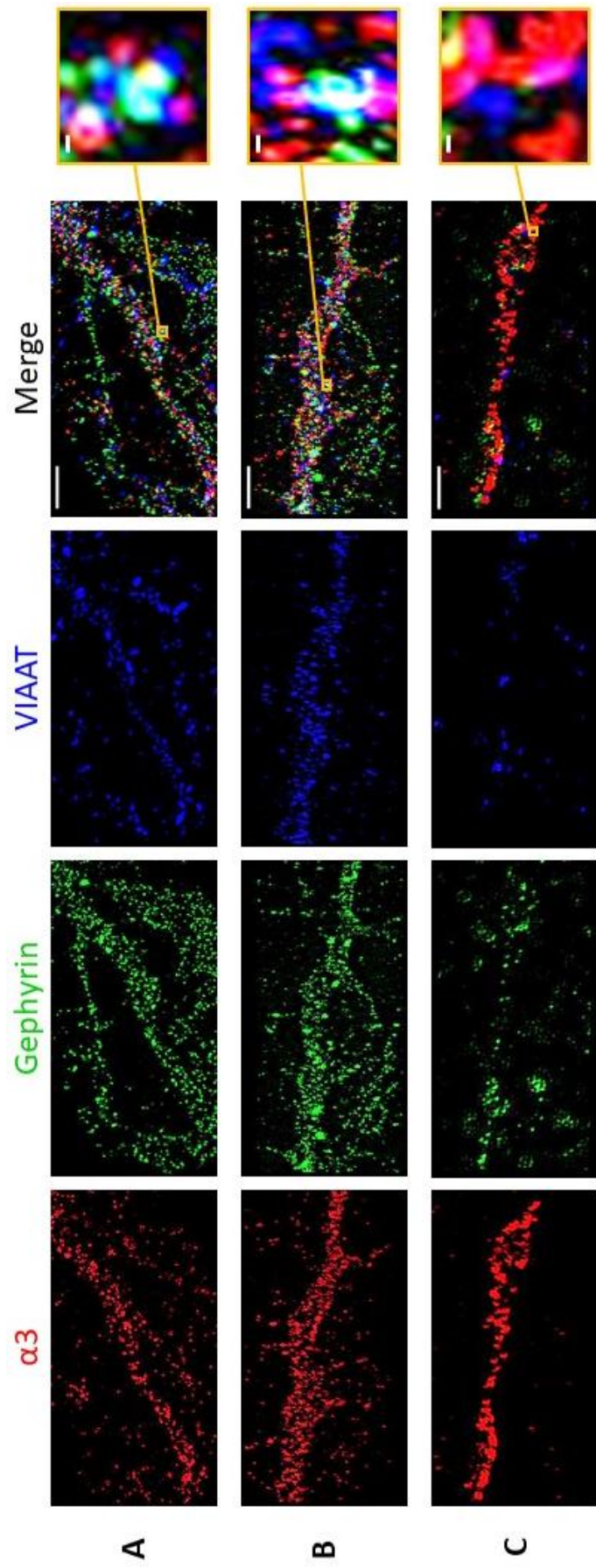
FIGURE 4.1. Representative SIM images of proximal dendrites of hippocampal neurons in cell culture expressing **(A)** myc-α3, **(B)** myc-α3^{Y402F} and **(C)** myc-α3^{Y402D} subunits. All neurons were antibody-labelled to indicate α3 (red), gephyrin (green) and VIAAT (blue). The white in the merge panels (see far right panel for higher resolution) indicates where all three proteins are co-localising. The scale bars on the merge panels represent 5 μm. The scale bars on the higher resolution panels represent 0.1 μm.

One interpretation of the sIPSC kinetic data discussed in the previous chapter, which showed that phospho-mimetic aspartate mutations at residue Y402 decreases both sIPSC 10-90% rise time and decay tau (Fig. 3.10), is that mimicking phosphorylation at Y402 increases the number of α3-GABA$_A$Rs localised at GABAergic synapses (see section 3.2.5). The volumes of the α3 puncta were therefore investigated, as increased volume would be expected if inhibitory synapses accrued increased amounts of GABA$_A$R protein.

No significant differences in total α3 puncta volumes were observed between wildtype α3, α3^{Y402F} or α3^{Y402D} (Fig. 4.2A). This held true for the volumes of both synaptic (Fig. 4.2B) and extrasynaptic (Fig. 4.2C) α3 puncta. Additionally, no significant differences were observed between α3, α3^{Y402F} or α3^{Y402D} for the puncta volumes of either gephyrin (Fig. 4.2D) or VIAAT (Fig. 4.2E).

Mean grey value is a measure of signal intensity: the higher the mean grey value, the greater the intensity of the fluorescent signal. Therefore, as with volume measurements, a higher mean grey value might indicate higher protein levels.

The mean grey values of the α3 puncta were investigated for potential differences between the three genotypes. No significant differences were observed between α3, α3^{Y402F} or α3^{Y402D} for the mean grey values of either total α3 (Fig. 4.3A) or extrasynaptic α3 (Fig. 4.3C). However, for synaptic α3, the mean grey value of α3^{Y402D} was significantly higher than that of both wildtype α3 and α3^{Y402F} (Fig. 4.3B). As with the sIPSC data (see section 3.2.5), this could suggest that α3^{Y402D} increases the number of synaptically-localised α3-GABA$_A$Rs.

Interestingly, this α3^{Y402D}-specific increase in mean grey value only holds true for synaptic puncta that do not co-localise with gephyrin (Fig. 4.3H). This may suggest that the increased synaptic clustering observed for α3^{Y402D}-GABA$_A$Rs is mediated by a gephyrin-independent clustering mechanism(s).
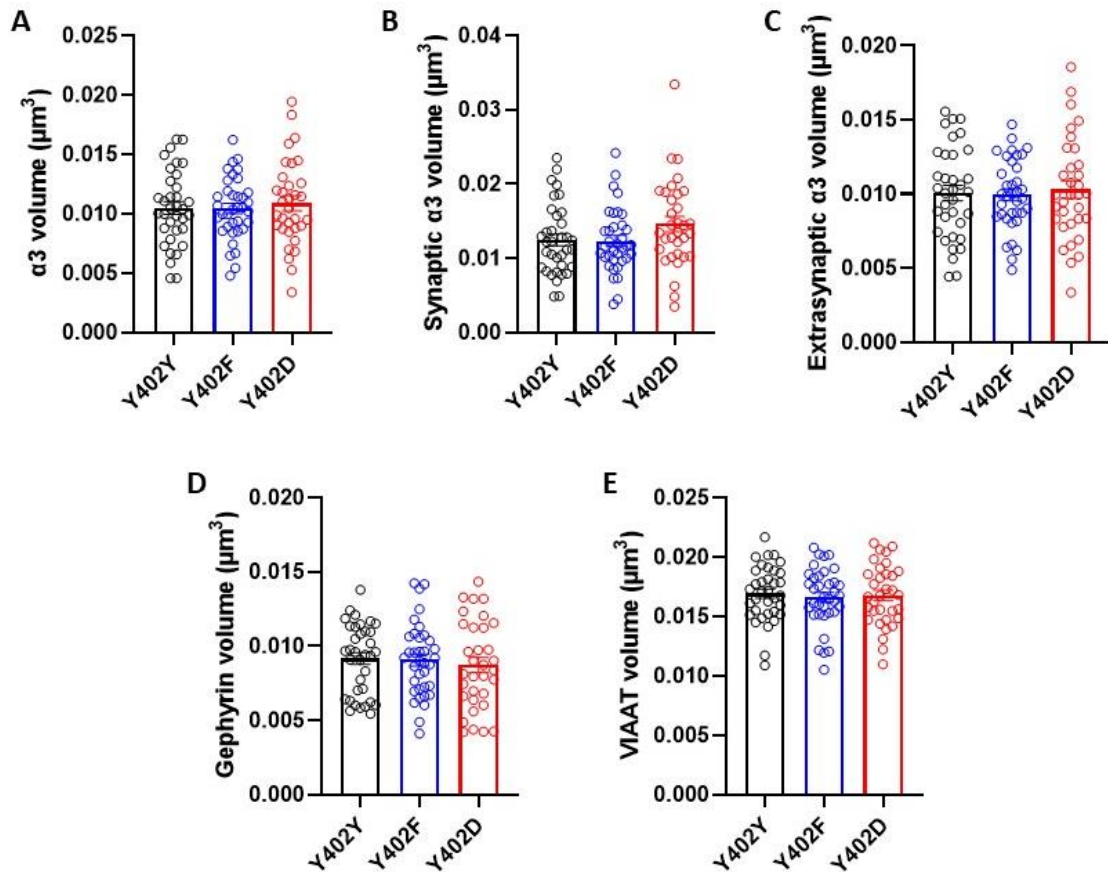
FIGURE 4.2. Neither phenylalanine nor aspartate substitutions at residue Y402 within the α3 subunit affect puncta volumes. **(A)** No significant differences in total α3 puncta volumes were observed between wildtype α3 (0.010 ± 0.0005 μm^3; n=35), α3^{Y402F} (0.010 ± 0.0004 μm^3; n=36) or α3^{Y402D} (0.010 ± 0.0006 μm^3; n=33; one-way ANOVA test). **(B)** No significant differences in synaptic α3 puncta volumes were observed between wildtype α3 (0.010 ± 0.0008 μm^3; n=35), α3^{Y402F} (0.010 ± 0.0007 μm^3; n=36) or α3^{Y402D} (0.010 ± 0.0010 μm^3; n=33; Kruskal-Wallis test). **(C)** No significant differences in extrasynaptic α3 puncta volumes were observed between wildtype α3 (0.010 ± 0.0005 μm^3; n=35), α3^{Y402F} (0.010 ± 0.0004 μm^3; n=36) or α3^{Y402D} (0.010 ± 0.0006 μm^3; n=33; one-way ANOVA test). **(D)** No significant differences in gephyrin puncta volumes were observed between wildtype α3 (0.009 ± 0.0004 μm^3; n=35), α3^{Y402F} (0.009 ± 0.0004 μm^3; n=36) or α3^{Y402D} (0.009 ± 0.0005 μm^3; n=33; Kruskal-Wallis test). **(E)** No significant differences in VIAAT puncta volumes were observed between wildtype α3 (0.020 ± 0.0004 μm^3; n=35), α3^{Y402F} (0.020 ± 0.0004 μm^3; n=36) or α3^{Y402D} (0.020 ± 0.0004 μm^3; n=33; one-way ANOVA test). Cells from three different hippocampal cultures were analysed, with 10-12 cells analysed from each culture. Circles, bars and error bars represent individual cells, population means and SEMs respectively.
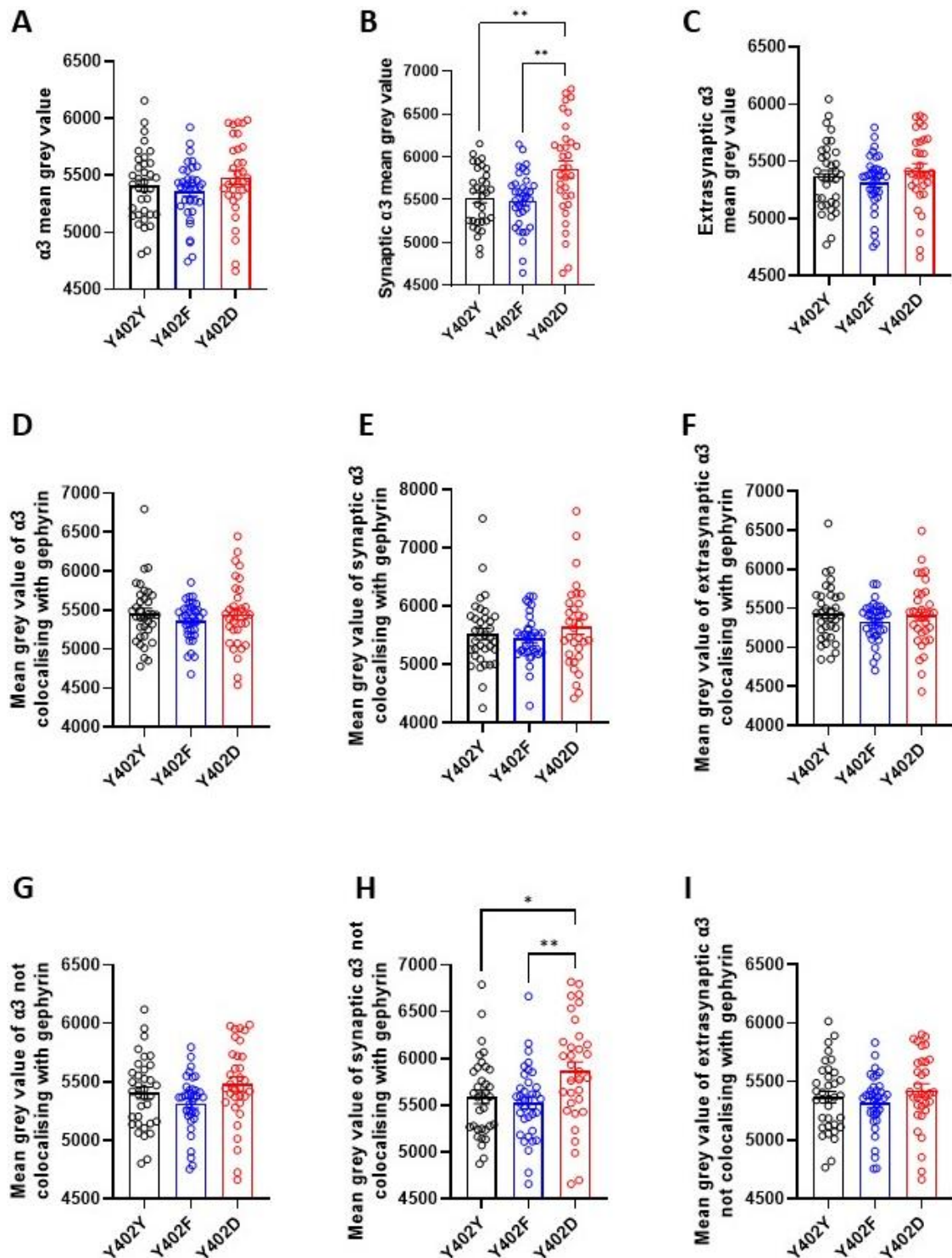
FIGURE 4.3. Phospho-mimetic aspartate substitution at residue Y402 within the α3 subunit increases the mean grey values of synaptic puncta that do not co-localise with gephyrin. **(A)** No significant differences in total α3 mean grey values were observed between wildtype α3 (5410 ± 52.1; n=35), α3^{Y402F} (5360 ± 43.1; n=36) or α3^{Y402D} (5483 ± 60.0; n=33; one-way ANOVA test). **(B)** Synaptic α3 mean grey values for α3^{Y402D} (5856 ± 98.7; n=33) were significantly higher than those for wildtype α3 (5524 ± 59.4; n=35) and α3^{Y402F} (5492 ± 57.3; n=35; one-way ANOVA and Tukey's multiple comparisons tests). **(C)** No significant differences in extrasynaptic α3 mean grey values were observed between wildtype α3 (5372 ± 50.0; n=35), α3^{Y402F} (5317 ± 40.0; n=36) or α3^{Y402D} (5425 ± 55.8; n=33; one-way ANOVA test). **(D)** No significant differences in the mean grey values of total α3 that co-localises with gephyrin were

observed between wildtype α3 (5456 ± 66.2; n=35), α3^{Y402F} (5360 ± 41.8; n=36) or α3^{Y402D} (5448 ± 75.5; n=33; Kruskal-Wallis test). **(E)** No significant differences in the mean grey values of synaptic α3 that co-localises with gephyrin were observed between wildtype α3 (5524 ± 99.0; n=35), α3^{Y402F} (5445 ± 65.9; n=36) or α3^{Y402D} (5649 ± 127.8; n=33; Kruskal-Wallis test). **(F)** No significant differences in the mean grey values of extrasynaptic α3 that co-localises with gephyrin were observed between wildtype α3 (5434 ± 61.4; n=35), α3^{Y402F} (5331 ± 41.0; n=36) or α3^{Y402D} (5416 ± 74.7; n=33; Kruskal-Wallis test). **(G)** No significant differences in the mean grey values of total α3 that does not co-localise with gephyrin were observed between wildtype α3 (5406 ± 51.6; n=35), α3^{Y402F} (5317 ± 40.0; n=36) or α3^{Y402D} (5482 ± 60.0; n=33; one-way ANOVA test). **(H)** The mean grey values of synaptic α3 that does not co-localise with gephyrin were significantly higher for α3^{Y402D} (5865 ± 99.3; n=33) than they were for wildtype α3 (5590 ± 72.0; n=35) or α3^{Y402F} (5529 ± 65.0; n=36; one-way ANOVA and Tukey's multiple comparisons tests). **(I)** No significant differences in the mean grey values of extrasynaptic α3 that does not co-localise with gephyrin were observed between wildtype α3 (5367 ± 49.8; n=35), α3^{Y402F} (5316 ± 40.7; n=36) or α3^{Y402D} (5424 ± 55.8; n=33; one-way ANOVA test). Cells from three different hippocampal cultures were analysed, with 10-12 cells analysed from each culture. Circles, bars and error bars represent individual cells, population means and SEMs respectively. *p* values ≤ 0.05 *; ≤ 0.01 **.

4.2.2. Aspartate substitution at residue Y402 reduces the number of inhibitory synapses containing α3^{Y402D}-GABA$_A$Rs, but these receptors are more concentrated in the synapses where they are retained

Co-localisation between proteins observed using super-resolution microscopy can provide an indication that said proteins interact with each another. As α3^{Y402D} only increased the mean grey value of synaptic α3 puncta that do not co-localise with gephyrin, the co-localisation between α3 and gephyrin puncta was investigated in order to assess whether it was impacted by α3^{Y402D}.

The proportion of α3^{Y402D} puncta that co-localised with gephyrin puncta was significantly lower than the proportion of either wildtype α3 or α3^{Y402F} puncta that co-localised with gephyrin puncta (Fig. 4.4A). This held true when co-localisation was assessed between synaptic α3 and gephyrin puncta (Fig. 4.4C), as well as extrasynaptic α3 and gephyrin puncta (Fig. 4.4D). Furthermore, the proportion of gephyrin puncta that co-localised with α3^{Y402D} puncta was also significantly lower than the proportion that co-localised with either α3 or α3^{Y402F} puncta (Fig. 4.4B). These data may therefore suggest that aspartate substitution at residue Y402 reduces the interaction between α3^{Y402D} and gephyrin.
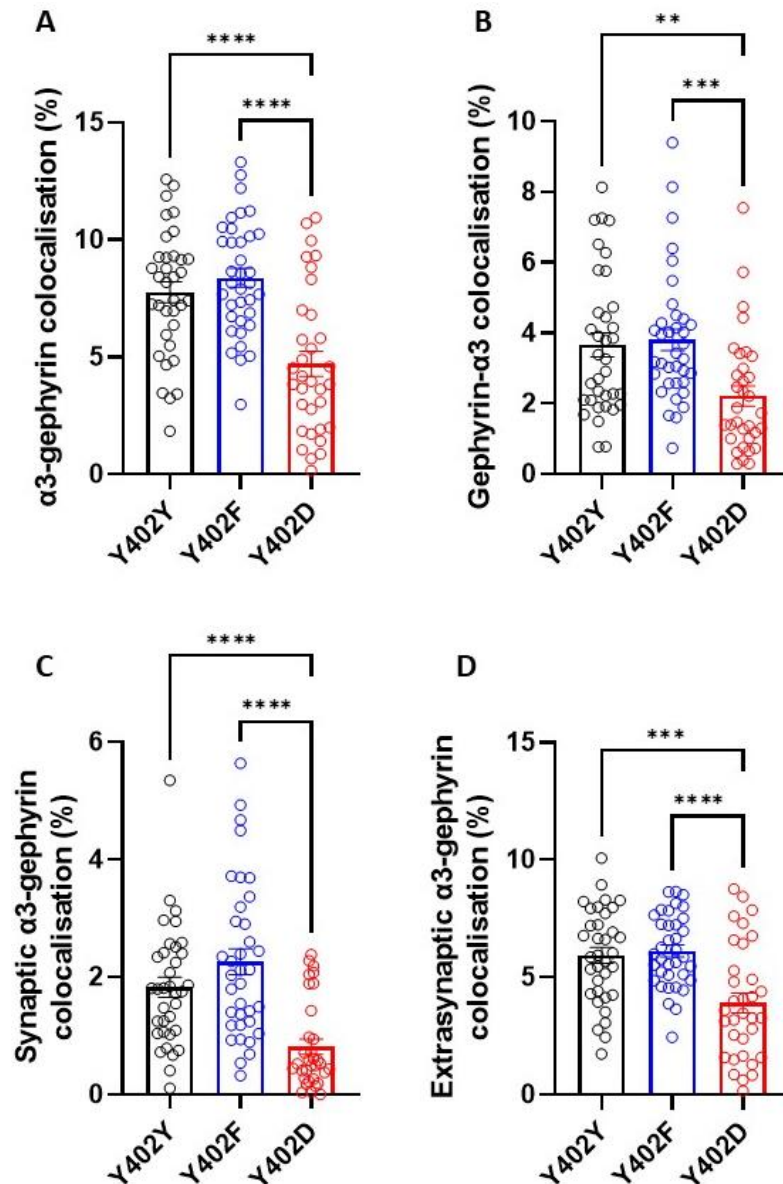
FIGURE 4.4. Aspartate substitution at residue Y402 within the α3 subunit decreases co-localisation between α3 and gephyrin puncta. **(A)** The proportion of α3^{Y402D} puncta that co-localised with gephyrin puncta (4.7 ± 0.5%; n=33) was significantly lower than the proportion of either wildtype α3 (7.8 ± 0.5%; n=35) or α3^{Y402F} (8.4 ± 0.4%; n=36) puncta that co-localised with gephyrin puncta (one-way ANOVA and Tukey's multiple comparisons tests). **(B)** The proportion of gephyrin puncta that co-localised with α3^{Y402D} puncta (2.2 ± 0.3%; n=33) was significantly lower than the proportion of gephyrin puncta that co-localised with either α3 (3.7 ± 0.3%; n=35) or α3^{Y402F} puncta (3.8 ± 0.3%; n=36; Kruskal-Wallis and Dunn's multiple comparisons tests). **(C)** The proportion of synaptic α3^{Y402D} puncta that co-localised with gephyrin puncta (0.8 ± 0.1%; n=33) was significantly lower than the proportion of either synaptic α3 (1.8 ± 0.2%; n=35) or synaptic α3^{Y402F} (2.3 ± 0.2%; n=36) puncta that co-localised with gephyrin puncta (Kruskal-Wallis and Dunn's multiple comparisons tests). **(D)** The proportion of extrasynaptic α3^{Y402D} puncta that co-localised with gephyrin puncta (3.9 ± 0.4%; n=33) was significantly lower than the proportion of either extrasynaptic α3 (5.9 ± 0.3%; n=35) or extrasynaptic α3^{Y402F} (6.1 ± 0.3%; n=36) puncta that co-localised with gephyrin puncta (one-way ANOVA and Tukey's multiple comparisons tests). Cells from three different hippocampal cultures were analysed, with 10-12 cells analysed from each culture. Circles, bars and error bars represent individual cells, population means and SEMs respectively. *p* values ≤ 0.01 **; ≤ 0.001 ***; ≤ 0.0001 ****.

A striking feature of the α3-gephyrin co-localisation data set is just how low the percentages of co-localisation are between these protein clusters. Only ~8% of wildtype α3 co-localised with gephyrin (Fig. 4.4A), of which ~2% was synaptic (Fig. 4.4C) and ~6% was extrasynaptic (Fig. 4.4D). These figures were approximately the same for the phospho-null mutant: ~8% of α3^{Y402F} co-localised with gephyrin (Fig. 4.4A), of which ~2% was synaptic (Fig. 4.4C) and ~6% was extrasynaptic (Fig. 4.4D). The numbers were slightly, yet statistically significantly, lower for the phospho-mimetic mutant: ~5% of α3^{Y402D} co-localised with gephyrin (Fig. 4.4A), of which ~1% was synaptic (Fig. 4.4C) and ~4% was extrasynaptic (Fig. 4.4D). This pattern remained when investigating the proportion of co-localisation between gephyrin and α3: approximately 4% of gephyrin clusters co-localised with each of wildtype α3 and α3^{Y402F}, while only ~2% co-localised with α3^{Y402D} (Fig. 4.4B). These data further support a likely reduction in the interaction between α3^{Y402D} and gephyrin. They also indicate that gephyrin is not as important for the clustering of GABA$_A$Rs (or at least those containing the α3 subunit) as the literature may imply (Essrich et al., 1998; Kneussel et al., 1999; Jacob et al., 2005; Mukherjee et al., 2011), further suggesting that gephyrin-independent mechanisms are likely to be involved in the clustering of these receptors.

As already mentioned, gephyrin is a scaffold protein that is proposed to play a role in the anchoring of GABA$_A$Rs at GABAergic synapses. However, the SIM imaging data so far suggests that aspartate substitution at Y402 increases the amount of α3^{Y402D}-GABA$_A$Rs localised at GABAergic synapses via a gephyrin-independent mechanism. To further assess the effect of α3^{Y402D} on the subcellular localisation of α3-GABA$_A$Rs, the co-localisation between the puncta of α3 and the inhibitory presynaptic marker VIAAT was analysed.
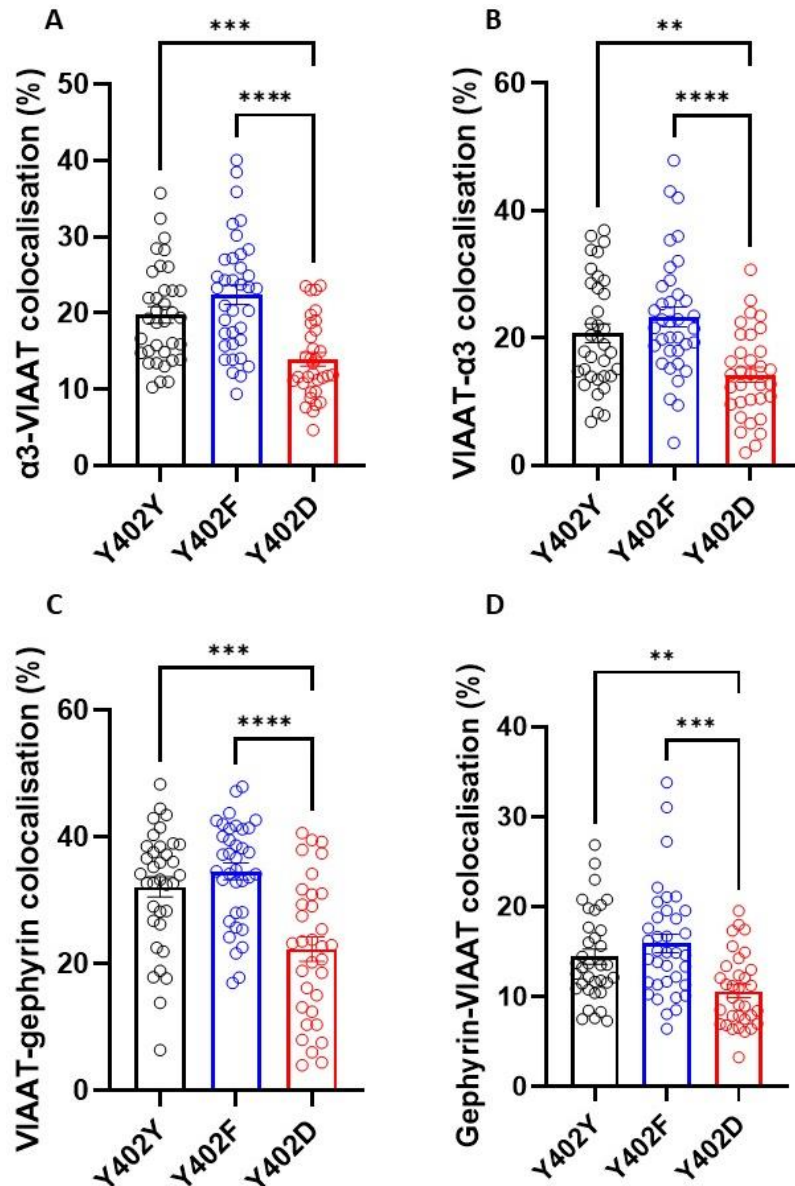
FIGURE 4.5. Phospho-mimetic aspartate substitution at residue Y402 within the α3 subunit decreases co-localisation between the puncta of α3 and VIAAT, a synaptic marker. **(A)** The proportion of α3[Y402D] puncta that co-localised with VIAAT puncta (13.9 ± 0.9%; n=33) was significantly lower than the proportion of either wildtype α3 (19.8 ± 1.1%; n=35) or α3[Y402F] (22.4 ± 1.3%; n=36) puncta that co-localised with VIAAT puncta (one-way ANOVA and Tukey's multiple comparisons tests). **(B)** The proportion of VIAAT puncta that co-localised with α3[Y402D] puncta (14.2 ± 1.2%; n=33) was significantly lower than the proportion of VIAAT puncta that co-localised with either wildtype α3 (20.7 ± 1.5%; n=35) or α3[Y402F] puncta (23.3 ± 1.6%; n=36; one-way ANOVA and Tukey's multiple comparisons tests). **(C)** The proportion of VIAAT puncta that co-localised with gephyrin puncta was significantly lower in cells transfected with α3[Y402D] (22.3 ± 1.9; n=33) than it was in cells transfected with either wildtype α3 (32.1 ± 1.6%; n=35) or α3[Y402F] (34.6 ± 1.3%; n=36; one-way ANOVA and Tukey's multiple comparisons tests). **(D)** The proportion of gephyrin puncta that co-localised with VIAAT puncta was significantly lower in cells transfected with α3[Y402D] (10.6 ± 0.7; n=33) than it was in cells transfected with either wildtype α3 (14.5 ± 0.8%; n=35) or α3[Y402F] (15.9 ± 1.0%; n=36; Kruskal-Wallis and Dunn's multiple comparisons tests). Cells from three different hippocampal cultures were analysed, with 10-12 cells analysed from each culture. Circles, bars and error bars represent individual cells, population means and SEMs respectively. *p* values ≤ 0.01 **; ≤ 0.001 ***; ≤ 0.0001 ****.

Unexpectedly, the proportion of $\alpha3^{Y402D}$ puncta that co-localised with VIAAT puncta was significantly lower than the proportion of either wildtype $\alpha3$ or $\alpha3^{Y402F}$ puncta that co-localised with VIAAT puncta (Fig. 4.5A). This suggests that the proportion of $\alpha3^{Y402D}$-GABA$_A$Rs localised at synaptic sites is reduced. Furthermore, the proportion of VIAAT puncta that co-localised with $\alpha3^{Y402D}$ puncta was significantly lower than the proportion of VIAAT puncta that co-localised with wildtype $\alpha3$ or $\alpha3^{Y402F}$ puncta (Fig. 4.5B). This suggests that the proportion of synapses that contain $\alpha3^{Y402D}$-GABA$_A$Rs is reduced. These results therefore contradict the previous SIM imaging data and the sIPSC kinetic data from chapter 3, instead indicating that phospho-mimetic aspartate substitution at residue Y402 causes a reduction in the proportion of synaptically-localised $\alpha3^{Y402D}$-GABA$_A$Rs.

Interestingly, as with the $\alpha3$-gephyrin co-localisation data, low levels of co-localisation were observed between $\alpha3$ and VIAAT. Only ~20% of wildtype $\alpha3$ puncta co-localised with VIAAT (Fig. 4.5A), while only ~21% of VIAAT puncta co-localised with wildtype $\alpha3$ (Fig. 4.5B). These results indicate that, in hippocampal neurons in cell culture, the majority of wildtype $\alpha3$-GABA$_A$Rs are not localised at synapses and that the majority of inhibitory synapses do not contain $\alpha3$-GABA$_A$Rs.

Given these results, the co-localisation between VIAAT and gephyrin was also analysed. As gephyrin is thought to be key for the synaptic anchoring of GABA$_A$Rs, it would be expected that a high proportion of synapses, defined by the presence of VIAAT, would contain gephyrin. Unexpectedly, however, in wildtype cells only ~32% of VIAAT puncta co-localised with gephyrin (Fig. 4.5C). This was approximately the same for cells transfected with $\alpha3^{Y402F}$ (~35% VIAAT-gephyrin co-localisation) but was significantly lower for cells transfected with $\alpha3^{Y402D}$ (~22% VIAAT-gephyrin co-localisation; Fig. 4.5C). Similarly, the proportion of gephyrin puncta that co-localised with VIAAT puncta was significantly lower in cells transfected with $\alpha3^{Y402D}$ (~11%) when compared to cells transfected with wildtype $\alpha3$ (~15%) or $\alpha3^{Y402F}$ (16%; Fig. 4.5D). These data suggest that aspartate substitution at Y402 reduces the proportion of synapses that contain gephyrin. Furthermore, as only a third of the synapses in cells transfected with wildtype $\alpha3$ actually co-localised with gephyrin, and indeed only

~15% of gephyrin puncta co-localised with VIAAT, these data further raise questions over the importance of gephyrin in tethering α3-GABA$_A$Rs at inhibitory synapses.

4.2.3. Investigating the effect of aspartate substitution at Y402 on the level of interaction between α3-GABA$_A$Rs and gephyrin using co-immunoprecipitation

Interaction between the α3 subunit and gephyrin has been reported in the literature (Tretter et al., 2011; Maric et al., 2014) and has been established using co-immunoprecipitation (co-IP) experiments to demonstrate that the two proteins bind to one another (Larson et al., 2020). Co-IPs use specialised beads that are conjugated to an antibody. The antibody specifically targets a protein of interest. The antibody-conjugated beads are incubated with a cell lysate that contains the target protein. The target protein binds to the antibody on the beads, while the target protein is also bound to any proteins that may interact with it, which can then be probed using specific antibodies. In this way, co-IPs enable the isolation of protein complexes.

To confirm that the reported binding between α3 subunits and gephyrin does indeed occur, co-IPs between wildtype α3β3γ2L receptors and gephyrin were performed. Semi-confluent HEK-293 cells were co-transfected with equimolar ratios of myc-GABA$_A$R-α3, GABA$_A$R-β3, GABA$_A$R-γ2L and GFP-gephyrin, as described in section 2.6. In brief, cell lysates were incubated with GFP-Trap agarose beads (ChromoTek) and the proteins eluted in SDS sample buffer. Proteins were separated via gel electrophoresis and analysed by western blotting, using an anti-myc antibody (ab32, Abcam; 1:500) to detect myc-α3 subunits.

α3 was successfully immunoprecipitated with GFP-tagged gephyrin (Fig. 4.6C), confirming the interaction between the proteins. Control western blots were performed on cell lysates to confirm that the cells were expressing both GFP-gephyrin (Fig. 4.6A) and myc-GABA$_A$R-α3 (Fig. 4.6B).

To assess whether mutating residue Y402 to aspartate affects the interaction between α3 subunits and gephyrin, further co-IP experiments were performed using HEK-293

cells transfected with either myc-GABA$_A$R-α3, myc-GABA$_A$R-α3^{Y402F} or myc-GABA$_A$R-α3^{Y402D}, along with equimolar amounts of GABA$_A$R-β3, GABA$_A$R-γ2L and GFP-gephyrin.

Unfortunately, when these experiments were performed, a band appeared in the negative control transfected with myc-GABA$_A$R-α3, GABA$_A$R-β3, GABA$_A$R-γ2L only (see Fig. 4.7C). As this sample did not contain GFP-gephyrin, α3 should not have been isolated by the GFP-Trap beads. These experiments were repeated multiple times (n=5); each time, the band in this negative control was present. It is unclear why this band did not appear in the initial co-IP experiments, between wildtype α3β3γ2L receptors and gephyrin, but did appear in the subsequent experiments between the mutant receptors and gephyrin.

The presence of this band likely indicates that the myc-tagged α3 protein binds non-specifically to the beads. Alternatively, one of the β3 or γ2 subunits may bind non-specifically to the beads, which is then detected with the anti-myc antibody as these proteins form a pentamer with the myc-tagged α3. Regardless, no interpretations could be made on whether aspartate substitution at Y402 affects the binding between α3 and gephyrin, as there is no way to determine which results are due to genuine interactions (or lack thereof) and which are due to non-specific binding to the beads.

Many different iterations of these co-IP experiments were performed in an attempt to overcome this problem, none of which were successful. Multiple different types of beads were tested: Protein G Dynabeads (ThermoFisher Scientific), Protein A Dynabeads (ThermoFisher Scientific) and Protein G Sepharose beads (Abcam). The beads were blocked at 4°C with a range of bovine serum albumin concentrations (from 0.1-5%) over a range of different incubation times (1 h to overnight). Not blocking the beads was also attempted. The cell lysates were pre-cleared (incubated with non-conjugated beads for 1 h at 4°C), with the aim of removing 'sticky' proteins, that may bind non-specifically to the beads, from the cell lysates before their incubation with the antibody-conjugated beads. The lysis buffer was changed from that described in section 2.6 to ComplexioLyte-48 (Logopharm), the buffer used in the co-IP experiments performed by Larson et al. (2020). The antibodies conjugated to the beads, used to pull down the protein complexes, were changed: rabbit anti-GFP (ab290, Abcam) and mouse anti-gephyrin (ab32206; 1:1000) were used to target

gephyrin-α3 complexes, while mouse anti-Myc (ab32, Abcam) and rabbit anti-α3 (AGA-003, Alomone Labs) were used to target α3-gephyrin complexes. Bizarrely, the same issue occurred when targeting α3 to isolate the protein complexes, although the offending band appeared in the GFP-gephyrin only negative control in this case.
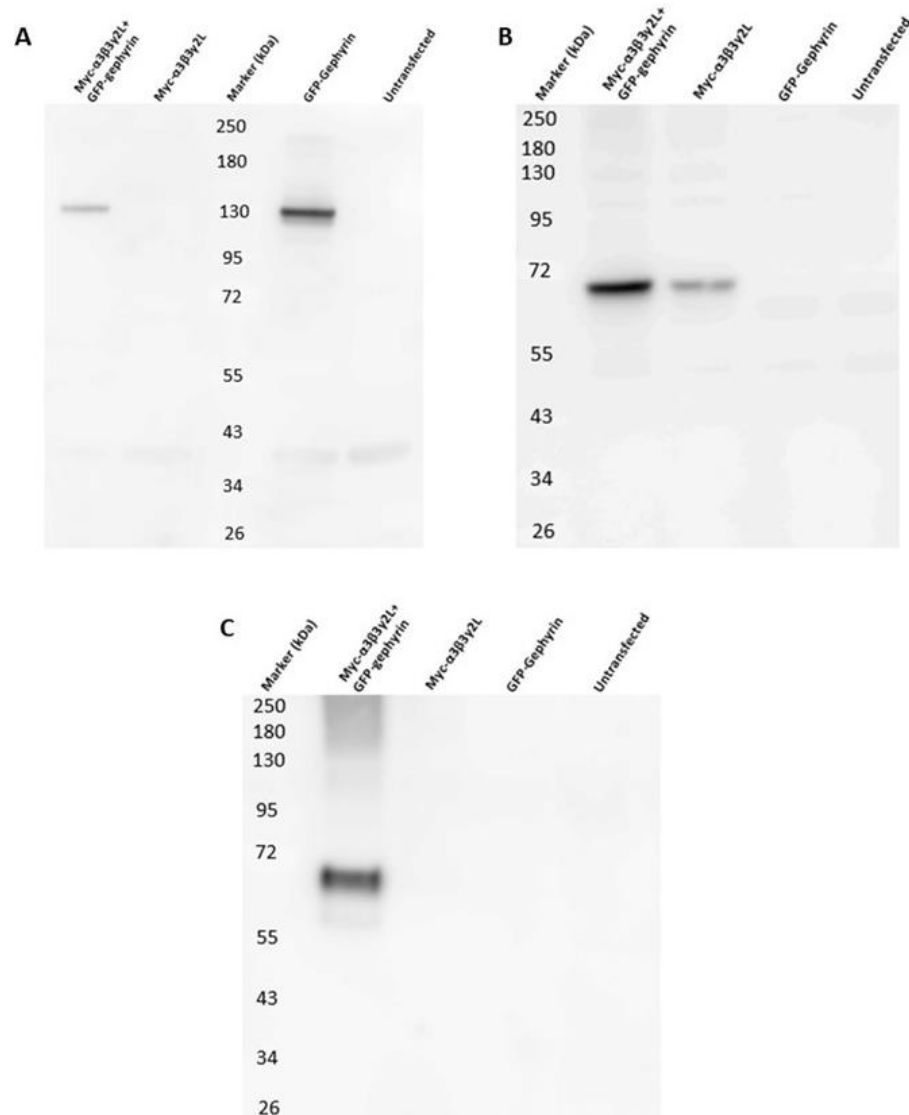
FIGURE 4.6. The α3 subunit of the GABA$_A$R interacts with, and binds to, gephyrin. **(A)** Western blot of lysates of HEK-293 cells transfected with myc-GABA$_A$R-α3, GABA$_A$R-β3 and GABA$_A$R-γ2L to form α3β3γ2L GABA$_A$R channels that have been co-expressed with GFP-gephyrin. Cells transfected with: myc-GABA$_A$R-α3, GABA$_A$R-β3 and GABA$_A$R-γ2L only; GFP-gephyrin only; and the CaCl$_2$-phosphate transfection buffer without any DNA all served as negative controls. Immunoblotting was performed with a rabbit anti-GFP antibody (ab290, Abcam; 1:1000). **(B)** Western blot of lysates of HEK-293 cells with the same transfections as described in (A). Immunoblotting was performed with a mouse anti-myc antibody (ab32, Abcam; 1:500). **(C)** Western blot of eluates of cell lysates with the same transfections as described in (A), immunoprecipitated using GFP-Trap agarose beads (ChromoTek) and analysed by immunoblotting with a mouse anti-myc antibody (ab32, Abcam; 1:500).

FIGURE 4.7. It was not possible to assess the effects of either phospho-null phenylalanine nor phospho-mimetic aspartate substitutions at residue Y402 of the α3 subunit of the GABA$_A$R on the interaction of the α3-GABA$_A$R with gephyrin, due to non-specific binding of α3 to the GFP-Trap agarose beads (ChromoTek). **(A)** Western blot of lysates of HEK-293 cells transfected with either myc-GABA$_A$R-α3, myc-GABA$_A$R-α3^{Y402F} or myc-GABA$_A$R-α3^{Y402D}. Cells were co-transfected with GABA$_A$R-β3 and GABA$_A$R-γ2L to form α3β3γ2L GABA$_A$R channels, as well as with GFP-gephyrin. Cells transfected with: myc-GABA$_A$R-α3, GABA$_A$R-β3 and GABA$_A$R-γ2L only; GFP-gephyrin only; and the CaCl$_2$-phosphate transfection buffer without any DNA all served as negative controls. Immunoblotting was performed with a rabbit anti-GFP antibody (ab290, Abcam; 1:1000). **(B)** Western blot of lysates of HEK-293 cells with the same transfections as described in (A). Immunoblotting was performed with a mouse anti-myc antibody (ab32, Abcam; 1:500). **(C)** Western blot of eluates of cell lysates with the same transfections as described in (A), immunoprecipitated using GFP-Trap agarose beads (ChromoTek) and analysed by immunoblotting with a mouse anti-myc antibody (ab32, Abcam; 1:500). The presence of a band in the myc-α3β3γ2L lane indicates that α3 binds non-specifically to the beads.

After the many different iterations of the co-IPs detailed above were unsuccessful, these experiments were regrettably abandoned. Consequently, it was not possible to

assess the potential effect(s) that either aspartate or phenylalanine substitution at residue Y402 may have on the level of binding between the α3 subunit and gephyrin.

4.3. Discussion

In the previous chapter, it was shown that mimicking phosphorylation via aspartate substitution at residue Y402 within the gephyrin binding site of the α3 subunit slowed down both the 10-90% rise time and the decay tau of sIPSC kinetics (see section 3.2.5). These effects may be caused by the aspartate substitution directly affecting receptor kinetics. However, an alternative – or indeed additional – explanation for the slower kinetics is that the aspartate substitution causes more $\alpha3^{Y402D}$-GABA$_A$Rs to localise at GABAergic synapses. This effect on trafficking is plausible since receptors containing the α3 subunit do exhibit slower kinetics (Picton & Fisher, 2007; Syed et al., 2020) and thus if more α3 receptors resided at inhibitory synapses they would be expected to impact on, and possibly dominate, the kinetic profiles of the sIPSCs. Further discussion in chapter 3 highlighted the possibility that this potential increase in synaptically-localised $\alpha3^{Y402D}$-GABA$_A$Rs is due to the aspartate substitution affecting the interaction of the receptor with the key scaffold protein gephyrin, as the substituted residue is located within the gephyrin binding domain residing in the large intracellular loop of α3 subunits.

The present chapter therefore focussed on assessing how $\alpha3^{Y402D}$ affects both the subcellular localisation of the α3-GABA$_A$R, as well as the interaction of this receptor with gephyrin. This was primarily done using SIM imaging, along with co-immunoprecipitation experiments.

The subcellular localisation of the α3-GABA$_A$Rs – whether they were synaptic or extrasynaptic – was determined based on their co-localisation with the presynaptic marker VIAAT, as captured in images taken using structured illumination microscopy. Object segmentation and co-localisation analyses were performed using the ImageJ plugin DiAna (Gilles et al., 2017) (see section 2.5.2). α3 puncta that co-localised with VIAAT puncta were classed as synaptic, while α3 puncta that did not co-localise with VIAAT puncta were classed as extrasynaptic.

In addition, using SIM, puncta volume measurements can provide an insight into the relative amounts of a particular protein at a given location, with a higher volume indicating an increased amount of protein. Neither the phospho-null phenylalanine substitution, nor the phospho-mimetic aspartate substitution, affected α3 puncta volumes (Fig. 4.2). In the case of $\alpha3^{Y402D}$ this was a little unexpected, given the hypothesis of this mutation causing an increase in the number of α3-GABA$_A$Rs at synapses. However, given the resolution of SIM is ~120 nm laterally and ~300 nm axially, this may reflect a limit on the detection of puncta volumes.

Although the volume data did not reveal any differences between the respective puncta representing the α3 phosphorylation variants, there was found to be a difference between the mean grey values for wildtype α3, $\alpha3^{Y402F}$ and $\alpha3^{Y402D}$ puncta. Notably, the mean grey value of synaptic $\alpha3^{Y402D}$ puncta was higher than that of α3 or $\alpha3^{Y402F}$ (Fig. 4.3B). In conjunction with the sIPSC kinetic data from chapter 3, these data support the hypothesis that mimicking phosphorylation within the gephyrin binding domain of α3 subunits by expressing $\alpha3^{Y402D}$ increases the number of cell surface α3-GABA$_A$Rs at inhibitory synapses.

Upon further interrogation of the data, it was found that this increase in the mean grey value of synaptic $\alpha3^{Y402D}$ only holds true for puncta that do not co-localise with gephyrin (Fig. 4.3H). This may potentially suggest that the increased synaptic clustering observed for $\alpha3^{Y402D}$-GABA$_A$Rs is mediated by a gephyrin-independent clustering mechanism(s). This was unexpected: given the key role that gephyrin is purported to play in anchoring GABA$_A$Rs at GABAergic synapses (Essrich et al., 1998; Kneussel et al., 1999; Jacob et al., 2005; Mukherjee et al., 2011), it may be expected that the observed increase in synaptic clustering of $\alpha3^{Y402D}$-GABA$_A$Rs is mediated by gephyrin, particularly considering that the substituted residue is located within the gephyrin binding site of α3.

Given these data, it may be expected that $\alpha3^{Y402D}$ does not affect α3-GABA$_A$R interaction with gephyrin. However, the imaging data revealed that there was significantly less co-localisation between $\alpha3^{Y402D}$-GABA$_A$R and gephyrin clusters, compared to wildtype or $\alpha3^{Y402F}$-GABA$_A$Rs (Fig. 4.4). While co-localisation between two proteins, ascertained using imaging methods, cannot confirm their interaction, it

can provide an indication of their potential interaction. Furthermore, interaction between the α3 subunit and gephyrin has been demonstrated biochemically using co-IP experiments as shown in Fig. 4.6C, as well as in the literature (Larson et al., 2020). This does not discount binding of the α3-GABA$_A$Rs to other interactors at inhibitory synapses, such as collybistin (Chiou et al., 2011; George et al., 2021). Indeed, gephyrin-independent GABA$_A$R clustering has been reported before: the clustering of α1 and α5 subunits is unaffected in gephyrin knockout mice (Kneussel et al., 2001), while cell surface labelling experiments have indicated that gephyrin does not contribute to the insertion or stabilisation of α2- and γ2-GABA$_A$Rs in the plasma membrane of hippocampal inhibitory synapses (Lévi et al., 2004). Furthermore, Niwa et al. (2012) used quantitative immunochemistry and single-particle tracking of quantum dot labelled GABA$_A$Rs to show that NMDA-induced excitatory activity, which enhances GABA$_A$R lateral motility, causes GABA$_A$R clusters to disperse from inhibitory synapses prior to the dispersal of gephyrin clusters in hippocampal neurons in cell culture. Niwa and colleagues further showed that synaptic GABA$_A$R mobility and clustering following sustained excitatory activity are independent of the amount of synaptic gephyrin present. Therefore together, the observed reduction in co-localisation, and hence likely in interaction, between α3^{Y402D}-GABA$_A$Rs and gephyrin further supports the hypothesis that the α3^{Y402D} receptors, which mimic phosphorylation of native α3 receptors, are clustered at synapses via a gephyrin-independent mechanism.

Additionally, the α3-gephyrin co-localisation data revealed a very low proportion of co-localisation between these two proteins. Only ~8% of wildtype α3 clusters co-localised with gephyrin (Fig. 4.4A), while only ~4% of gephyrin clusters co-localised with α3 (Fig. 4.4B). These numbers were approximately the same for the phospho-null receptor, but fell significantly for the phospho-mimetic receptor, with ~5% of α3^{Y402D} clusters co-localising with gephyrin (Fig. 4.4A) and ~2% of gephyrin clusters co-localising with α3^{Y402D} (Fig. 4.4B). These data further support the existence of a gephyrin-independent clustering mechanism.

Interestingly, a similar study performed by Crosby et al. (2019), which examined co-localisation between γ2-GABA$_A$Rs, gephyrin and VIAAT in hippocampal neurons in cell culture, reported a much higher level of co-localisation between γ2-GABA$_A$Rs and

gephyrin, and between gephyrin and γ2-GABA$_A$Rs, of 82% and 93% respectively. These numbers are strikingly different to those reported in the present investigation and may reflect the ubiquitous and high expression levels of the γ2 subunit compared to the α3 subunit in the rat brain (Fritschy & Mohler, 1995; Pirker et al., 2000). The putative importance of gephyrin in clustering GABA$_A$Rs has been suggested many times in the literature (see Tyagarajan & Fritschy (2014) for review). However, the disparity in the GABA$_A$R-gephyrin co-localisation data between the present study and Crosby et al. (2019) suggests that, while gephyrin may play an important role in synaptic clustering for certain GABA$_A$R subtypes, including those containing γ2, it may not be as critical for the synaptic localisation of GABA$_A$Rs containing the α3 subunit. Instead, α3-GABA$_A$R subcellular localisation may be mediated by other clustering proteins, such as collybistin (Chiou et al., 2011; George et al., 2021), neurobeachin (Nair et al., 2012), GARLH (Davenport et al., 2017; Yamasaki et al., 2017) or NL2 (Poulopoulos et al., 2009).

Low levels of co-localisation were also observed between α3 and VIAAT clusters (~20%; Fig. 4.5A). These results again contrast with the co-localisation levels of ~60% reported between γ2-GABA$_A$Rs and VIAAT by Crosby et al. (2019), indicating that in hippocampal neurons in cell culture, there are fewer α3-GABA$_A$Rs than there are γ2-GABA$_A$Rs located at GABAergic synapses. Additionally, in neurons transfected with wildtype α3, ~32% of VIAAT clusters co-localised with gephyrin (Fig. 4.5C), indicating that approximately a third of inhibitory synapses contain gephyrin. This percentage is lower, although not as strikingly so as the previous data, than the VIAAT-gephyrin co-localisation level of ~42% reported by Crosby and colleagues. Both figures suggest that over a half of synapses do not contain gephyrin, again calling into question the importance of gephyrin as a synaptic scaffold protein.

Unexpectedly, the α3-VIAAT co-localisation data also revealed there to be significantly less co-localisation between α3^{Y402D}-GABA$_A$R and VIAAT clusters compared to α3- or α3^{Y402F}-GABA$_A$Rs (Fig. 4.5). In contrast to the previous sIPSC kinetic data and the mean

grey value imaging data, this likely suggests a reduction in the proportion of $\alpha3^{Y402D}$ receptors localised at synaptic sites.

To summarise the data thus far: $\alpha3^{Y402D}$ slows down sIPSC kinetics (see section 3.2.5). As $\alpha3$-GABA$_A$Rs display some of the slowest activation, desensitisation and deactivation kinetic properties of all GABA$_A$R subtypes (Picton & Fisher, 2007; Syed et al., 2020), a potential (albeit not the only) interpretation of such data is that $\alpha3^{Y402D}$ increases the amount of $\alpha3$-GABA$_A$Rs located at synapses. Furthermore, the mean grey value of synaptic $\alpha3^{Y402D}$-GABA$_A$R clusters is significantly higher than that of wildtype or $\alpha3^{Y402F}$-GABA$_A$Rs (Fig. 4.3B), again suggesting that $\alpha3^{Y402D}$ increases the synaptic clustering of $\alpha3$-containing receptors. However, this increased mean grey value only holds true for synaptic $\alpha3^{Y402D}$-GABA$_A$Rs that do not co-localise with gephyrin (Fig. 4.3H). Additionally, there is significantly less co-localisation between $\alpha3^{Y402D}$-GABA$_A$Rs and gephyrin (Fig. 4.4). Both of these results suggest that the synaptic clustering of $\alpha3^{Y402D}$-GABA$_A$Rs may be mediated by a gephyrin-independent mechanism. Finally, there is significantly less co-localisation between $\alpha3^{Y402D}$ receptors and VIAAT (Fig. 4.5) which, in contrast to the previous data, suggests a reduction in the proportion of synaptically-localised $\alpha3^{Y402D}$-GABA$_A$Rs.

There are a couple of possible explanations that account for all of these results. The first is that aspartate substitution at Y402 reduces $\alpha3$ subunit interaction with the scaffold protein gephyrin, which in turn reduces the accumulation of $\alpha3$-GABA$_A$Rs at inhibitory synapses. This is supported by a previous study which reported that mimicking phosphorylation at T375, a residue within the gephyrin binding site of the $\alpha1$ subunit, diminished the binding between $\alpha1$ and gephyrin and consequentially reduced $\alpha1$-GABA$_A$R accumulation at synapses (Mukherjee et al., 2011). However, while there is a reduction in the proportion of GABAergic synapses containing $\alpha3^{Y402D}$-GABA$_A$Rs, these receptors are more concentrated in the synapses that retain them. These synapses may also lack gephyrin, given that the increased mean grey value observed for $\alpha3^{Y402D}$-GABA$_A$Rs only holds true for synaptic receptors that do not co-localise with gephyrin (Fig. 4.3H) and that the proportion of VIAAT clusters that co-localise with gephyrin significantly decreases in cells transfected with the phospho-

mimetic receptor (Fig. 4.5C). This increased concentration of the $\alpha3^{Y402D}$-GABA$_A$Rs at such synapses is likely mediated by a gephyrin-independent clustering mechanism(s).

This interpretation of the data would have been given more credence had the co-IP experiments, to determine the effects of the phospho-null and phospho-mimetic mutations on the binding between the $\alpha3$-GABA$_A$R and gephyrin, been successful (see Fig. 4.7). The $\alpha3$-VIAAT co-localisation data, combined with the study by Mukherjee et al. (2011), suggests that there should be a reduction in binding between $\alpha3^{Y402D}$-GABA$_A$Rs and gephyrin compared to $\alpha3$- and $\alpha3^{Y402F}$ receptors if a gephyrin-independent binding mechanism is important for phosphorylated $\alpha3$ subunit receptors. However, due to difficulties encountered while performing the co-IPs (explained in section 4.2.3), this unfortunately could not be confirmed experimentally.

Perisynaptic δ subunit-containing GABA$_A$Rs that are activated by GABA spillover and that consequently significantly slow down the decay time constants of sIPSCs have been previously identified in the mouse dentate gyrus (Wei et al., 2003). Considering this, another explanation that may account for all of the observed results in this study is that aspartate substitution at Y402 causes $\alpha3^{Y402D}$ receptors to accumulate at perisynaptic sites. If this were the case, the receptors may be far enough removed from the centre of the synapse so as not to co-localise with VIAAT, thus being classed as 'extrasynaptic' in the SIM analysis, yet close enough to the synapse to be able to influence the sIPSC kinetic profile. Following the findings of Wei and colleagues, this would provide an explanation for the slower decay time constant observed for $\alpha3^{Y402D}$-receptors in hippocampal neurons in cell culture. While a speculative interpretation of the data, it nevertheless may be possible.

4.4. Conclusions

1. Phospho-mimetic aspartate substitution of residue Y402 within the gephyrin binding domain of the $\alpha3$ subunit increases the mean grey value of $\alpha3$-GABA$_A$R clusters localised at GABAergic synapses, as determined by their co-localisation

with the presynaptic marker VIAAT. This applied only to synaptic $\alpha3^{Y402D}$-GABA$_A$Rs that do not also co-localise with the scaffold protein gephyrin.

2. Aspartate substitution at residue Y402 significantly reduces the level of co-localisation between $\alpha3$-GABA$_A$Rs and gephyrin.

3. Only ~8% of wildtype $\alpha3$ clusters co-localise with gephyrin, suggesting other clustering proteins may be more important in the subcellular localisation of $\alpha3$-GABA$_A$Rs.

4. Aspartate substitution at residue Y402 significantly reduces the level of co-localisation between $\alpha3$-GABA$_A$R and VIAAT clusters, with potentially fewer inhibitory synapses containing $\alpha3$-GABA$_A$Rs.

5. Only ~20% of wildtype $\alpha3$ clusters co-localise with VIAAT, indicating that the majority of $\alpha3$-GABA$_A$Rs in hippocampal neurons in cell culture are extrasynaptic.

6. Gephyrin binds to $\alpha3$-GABA$_A$Rs, as demonstrated biochemically using co-immunoprecipitation experiments.

Chapter 5: investigating the functional profile of the α3-GABA$_A$R

5.1. Introduction

While in-depth studies have been made of most GABA$_A$R subtypes, relatively little is known about the α3-GABA$_A$R (see section 1.4). The subcellular localisation of the receptor contributes significantly to the physiological role it plays: the main example that has been used throughout this thesis is that synaptically-localised α3-GABA$_A$Rs in the nRT mediate phasic inhibition (Studer et al., 2006; Schofield & Huguenard, 2007), while extrasynaptically-localised α3-GABA$_A$Rs in the BLA mediate tonic inhibition (Marowsky et al., 2012). Therefore, depending on its localisation, the α3-GABA$_A$R likely functions in quite diverse roles for different areas of the brain.

This chapter focusses on elucidating some of the physiological roles that α3-GABA$_A$Rs may perform using a two-pronged approach:

(1) Isolation of sIPSCs specifically mediated through α3-GABA$_A$Rs to determine the kinetic properties conferred on phasic inhibition by the presence of synaptic α3 subunits; and

(2) knockdown of endogenous α3 subunit expression to observe the resulting effects on sIPSC kinetics.

The macroscopic kinetics of α3-GABA$_A$Rs have been investigated in heterologous expression systems with recombinant GABA$_A$Rs (Picton & Fisher, 2007), while a HEK-293 cell-neuron co-culture expression system has been used to identify, in relative isolation, the slower sIPSC decay rate of α3-GABA$_A$R-mediated sIPSCs (Syed et al., 2020). However, a study has never been performed wherein the α3-GABA$_A$R-mediated sIPSCs are isolated in a cultured neuron system and analysed to investigate the kinetic parameters of the native receptor effectively *in situ*.

Picrotoxin (PTX) is a non-competitive GABA$_A$R antagonist that binds within the channel pore of the receptor (Masiulis et al., 2019) (see section 1.3.2). Sun et al. (2018) introduced a point mutation into the δ subunit to confer PTX resistance, following which they pharmacologically isolated the δ subunit-containing receptors, most likely comprising αβδ subunits, with PTX application to demonstrate that, despite a

consensus view, these receptors can contribute to IPSCs in mouse dentate granule neurons.

It has been previously reported that substitution of the 6' threonine at residue 260 with phenylalanine in TM2 of the α1 subunit abolishes receptor PTX sensitivity (Sedelnikova et al., 2006). Furthermore, the mutation had only a minimal effect on receptor GABA sensitivity (Sedelnikova et al., 2006). Transfection of a PTX-insensitive α3 subunit into hippocampal neurons in cell culture would enable the sIPSCs mediated only through the PTX-insensitive α3-GABA$_A$Rs to be isolated following the application of PTX. Therefore, in order to address aim (1), residue T313 of the α3 subunit, which is the equivalent residue to T260 in α1, was mutated to phenylalanine in an attempt to confer PTX resistance.

The functions performed by a protein of interest can also be investigated through reducing the endogenous expression of the target protein and observing the resulting effects, in this case on sIPSCs. Short hairpin RNAs (shRNAs) have been demonstrated to effectively reduce target protein expression (Paddison et al., 2002; Li et al., 2005; Lambeth & Smith, 2013). Therefore, in order to address aim (2), α3-selective shRNAs were used in an attempt to knockdown α3 subunit expression in hippocampal neurons in cell culture. The results of experiments involving both PTX-insensitive α3 mutants and α3-specific shRNA knockdown are reported and discussed in the following sections.

5.2.   Results

5.2.1.   *Mutation of residue T313 to phenylalanine in the α3 subunit confers insensitivity to PTX but also affects other aspects of receptor function*

In order to create a PTX-insensitive α3 subunit, residue T313 was mutated to phenylalanine to create α3^{T313F}. This construct was transfected into HEK-293 cells, along with equimolar ratios of constructs expressing β3, γ2L and eGFP. Whole-cell voltage-clamp electrophysiology was performed on cells transfected with wildtype (α3β3γ2L) and mutant (α3^{T313F}β3γ2L) receptors.

To test whether $\alpha3^{T313F}$ abolishes PTX sensitivity, receptors were first activated with a 4 s application of 100 µM GABA, following which 100 µM GABA and 50 µM PTX were co-applied twice, for 4 s each time. The peak current responses of the receptors were measured for each application.

$\alpha3^{T313F}$ confers significant, although not complete, insensitivity to PTX: for wildtype $\alpha3\beta3\gamma2L$ receptors, the peak GABA current was 6.6 ± 1.1 % of the control at the second co-application with PTX. In contrast, the second co-application with PTX only reduced the peak GABA current of the $\alpha3^{T313F}\beta3\gamma2L$ receptors to 63.3 ± 2.4 % of the control (Fig. 5.1).

To assess whether mutation of threonine to phenylalanine at residue T313 of the $\alpha3$ subunit has an effect on receptor GABA sensitivity or cell surface expression, whole-cell concentration-response experiments were performed on HEK-293 cells transfected with $\alpha3\beta3\gamma2L$ or $\alpha3^{T313F}\beta3\gamma2L$ receptors, along with eGFP. Peak current responses of the receptors were measured in response to 4 s applications of eleven different GABA concentrations: 0.1 µM, 0.3 µM, 1 µM, 3 µM, 10 µM, 30 µM, 100 µM, 300 µM, 1 mM, 3 mM and 10 mM. These different GABA concentrations were applied to the cells in a random order, with normalising 300 µM applications interspersed throughout. GABA concentration-response data were collected for each cell and curve fitted with the Hill equation (Equation 1, section 2.2.3) to generate CRCs for each receptor. Maximum current density, an indirect measure of receptor cell surface expression, was calculated by normalising the maximum current, generated following a 10 mM GABA application, to the cell membrane capacitance (see section 2.2.4).
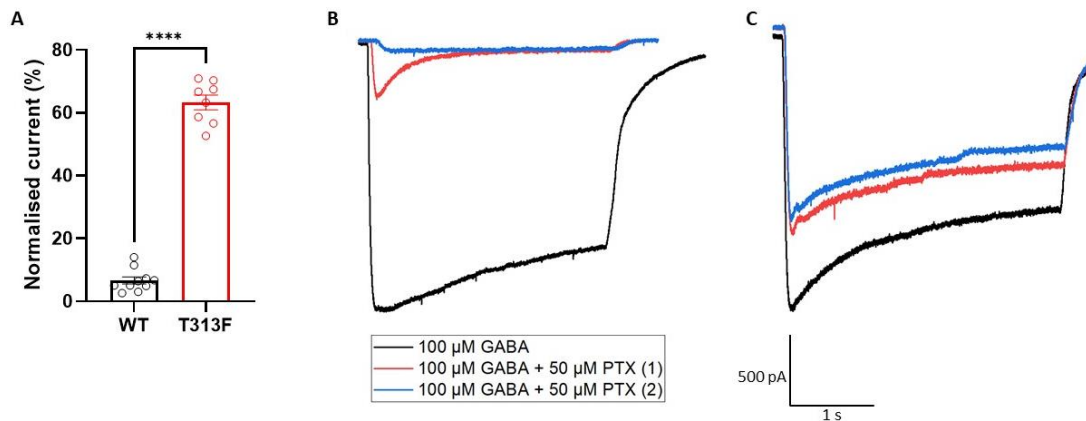
FIGURE 5.1. Mutation of residue T313 to phenylalanine within the α3 subunit confers reduced sensitivity to the GABA$_A$R antagonist PTX. **(A)** The normalised 100 μM GABA current following two co-applications of 50 μM PTX was significantly greater when mediated through α3^{T313F}β3γ2L receptors (63.3 ± 2.4 %; n=8) compared to wildtype α3β3γ2L receptors (6.6 ± 1.1 %; n=10; unpaired t test). **(B)** Representative membrane currents resulting from 4 s applications of 100 μM GABA (black) followed by two co-applications of 100 μM GABA and 50 μM PTX (red and blue respectively) to wildtype α3β3γ2L receptors. **(C)** Representative membrane currents resulting from 4 s applications of 100 μM GABA (black) followed by two co-applications of 100 μM GABA and 50 μM PTX (red and blue respectively) to α3^{T313F}β3γ2L receptors. Circles, bars and error bars represent individual cells, population means and SEMs respectively. p values ≤ 0.0001 ****.

The CRC for the PTX-insensitive α3^{T313F}β3γ2L receptors displayed an approximately 10-fold rightward shift compared to the CRC of the wildtype receptors (Fig. 5.2A). This is reflected in the GABA EC$_{50}$ values of the mutant receptors, which were significantly higher than those of the wildtype receptor (Fig. 5.2B), indicating that the α3^{T313F} substitution reduces the sensitivity of the receptor for GABA. Furthermore, the maximum current density values of the mutant receptors were significantly lower than those of the wildtype receptors (Fig. 5.2C). A possible explanation for this result is that the substitution causes an alteration in receptor trafficking that reduces the surface expression of the mutant α3^{T313F}β3γ2L receptors. Alternatively, as the T313F substitution is located within the channel pore, the change in current density may be due to changes in single channel kinetics or conductance. Regardless, these results were unexpected, given the equivalent PTX-insensitivity mutation in the α1 subunit caused only a minimal two-fold rightward shift in the GABA CRC compared to wildtype (Sedelnikova et al., 2006).
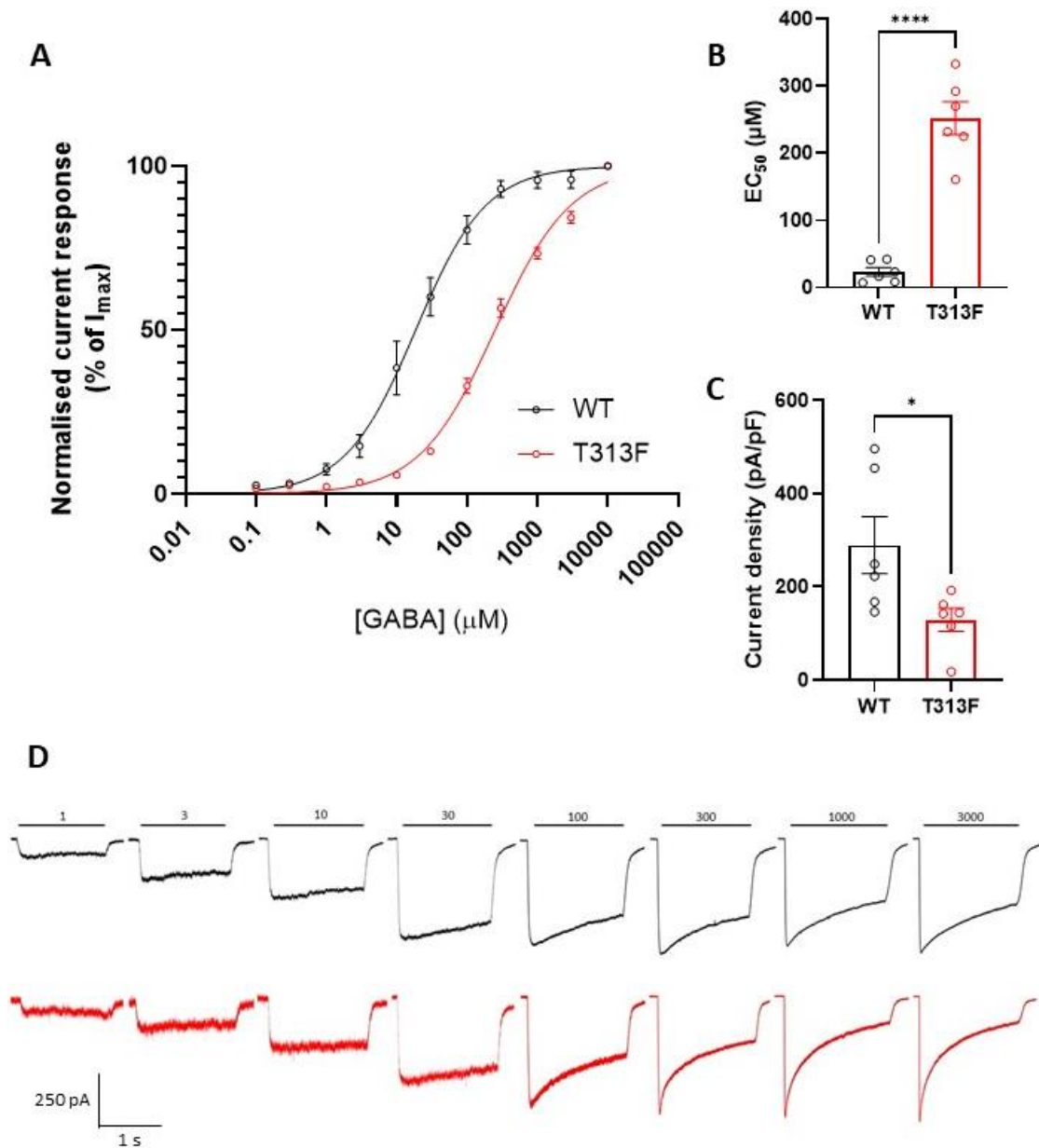
FIGURE 5.2. Mutation of residue T313 to phenylalanine in the α3 subunit of the $GABA_AR$ affects receptor GABA sensitivity and cell surface expression. **(A)** GABA CRC fitted to all data points of wildtype α3β3γ2L receptors (n=6; n_H=0.867; black) and mutant α3^{T313F}β3γ2L (n=6; n_H=0.805; red) receptors. The CRC of the mutant receptors is shifted right compared to the CRC of the wildtype receptors. **(B)** The mean GABA EC_{50} value for the α3^{T313F}β3γ2L receptors (252.3 ± 24.5 µM; n=6) was significantly higher than that of the wildtype α3β3γ2L receptors (23.2 µM ± 6.3; n=6; unpaired t test). The EC_{50} values represent the means of those derived from curves fitted for each cell. **(C)** Maximum current density values for the α3^{T313F}β3γ2L receptors (129.0 ± 24.5 pA/pF; n=6) were significantly lower than those for the wildtype α3β3γ2L receptors (289.4 ± 61.0 pA/pF; n=6; unpaired t test). **(D)** Representative membrane currents resulting from 4 s applications of the indicated GABA concentrations (µM) to α3β3γ2L (black) and α3^{T313F}β3γ2L (red) receptors. Circles, bars and error bars represent individual cells, population means and SEMs respectively. *p* values ≤ 0.05 *; ≤ 0.0001 ****.

Additionally, the membrane current traces recorded from the mutant receptors appeared to show a difference in desensitisation compared to the wildtype receptors (Fig. 5.2D). Therefore, the macroscopic desensitisation and deactivation kinetics of the recombinant receptors were characterised by measuring the desensitisation and deactivation time constants for maximal whole-cell GABA-activated currents (see section 2.2.5 for details of these measurements). The $\alpha3^{T313F}\beta3\gamma2L$ receptors both desensitised (Fig. 5.3A) and deactivated (Fig. 5.3B) significantly more quickly than the wildtype $\alpha3\beta3\gamma2L$ receptors. Therefore, in addition to receptor GABA sensitivity and possibly trafficking, the T313F substitution also affects whole-cell desensitisation and deactivation kinetics in HEK-293 cells.

Given these results, no further experiments were performed using the PTX-insensitive $\alpha3^{T313F}$ subunit since ideally, such a reporter mutation should have minimal effects on other aspects of receptor function.
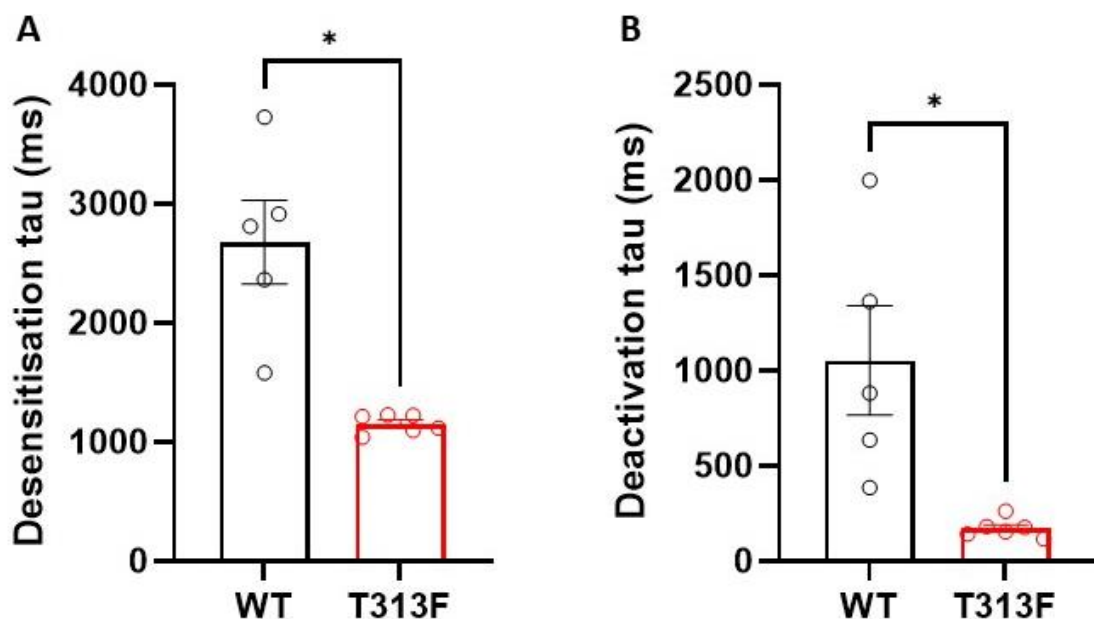
FIGURE 5.3. Mutation of residue T313 to phenylalanine affects macroscopic $\alpha3$-GABA$_A$R desensitisation and deactivation kinetics. **(A)** The desensitisation tau of the mutant $\alpha3^{T313F}\beta3\gamma2L$ receptors (1152 ± 78.4 ms; n=6) was significantly faster than that of the wildtype $\alpha3\beta3\gamma2L$ receptors (2677 ± 352.1 ms; n=5; Welch's t test). **(B)** The deactivation tau of the mutant $\alpha3^{T313F}\beta3\gamma2L$ receptors (171.1 ± 20.4 ms; n=6) was significantly faster than that of the wildtype $\alpha3\beta3\gamma2L$ receptors (1052.0 ± 286.3 ms; n=5; Welch's t test). Circles, bars and error bars represent individual cells, population means and SEMs respectively. *p* values ≤ 0.05 *.

5.2.2. Substitution of V309 of the α3-GABA$_A$R with either serine or cysteine does not confer insensitivity to PTX

A number of mutation studies have identified the 2' residue within TM2 of a GABA$_A$R subunit as being necessary for PTX block of the receptor channel pore. Ffrench-Constant et al. (1993) and Zhang et al. (1994) both found that mutation of the 2' alanine to serine within the *Drosophila* GABA receptor conferred resistance to PTX. Furthermore, it has been reported that mutation of the 2' residue V257 to cysteine in the α1 subunit confers PTX-insensitivity (Xu et al., 1995), as does mutation of the equivalent 2' residue – also V257 – to tryptophan in the α2 subunit (Ueno et al., 2000).

Valine 309 is the equivalent TM2 2' residue in the α3 subunit. To assess whether mutation of V309 abolishes PTX-sensitivity in the α3-GABA$_A$R, mutants were created wherein V309 was substituted with cysteine and serine to give α3^{V309C} and α3^{V309S} respectively. These constructs were transfected into HEK-293 cells, along with equimolar ratios of constructs expressing β3, γ2L and eGFP. Whole-cell voltage-clamp electrophysiology was performed on transfected cells. As with the previous α3^{T313F} experiments, the receptors were first activated with a 4 s application of 100 μM GABA, following which 100 μM GABA and 50 μM PTX were co-applied twice, for 4 s each time. The peak current responses of the receptors were measured for each application.

Neither mutation was found to confer effective receptor insensitivity to PTX: for wildtype α3β3γ2L receptors, the peak GABA current was 5.0 ± 1.9 % of the control at the second co-application with PTX. For comparison, the second co-application with PTX reduced the peak GABA current to 16.5 ± 2.7 % of the control for the α3^{V309C}β3γ2L receptors, and to 10.0 ± 1.7 % of the control for the α3^{V309S}β3γ2L receptors (Fig. 5.4). While the α3^{V309C}β3γ2L receptors caused a statistically significant increase in PTX resistance compared to wildtype (Fig. 5.4A), PTX still blocks the receptors to an extent of 83.5 %. This block is too substantial to be able to isolate sIPSCs mediated through these receptors. Therefore, following these results, no further attempts to create a PTX-insensitive α3-GABA$_A$R to enable the isolation of sIPSCs mediated specifically through α3-GABA$_A$Rs were made.
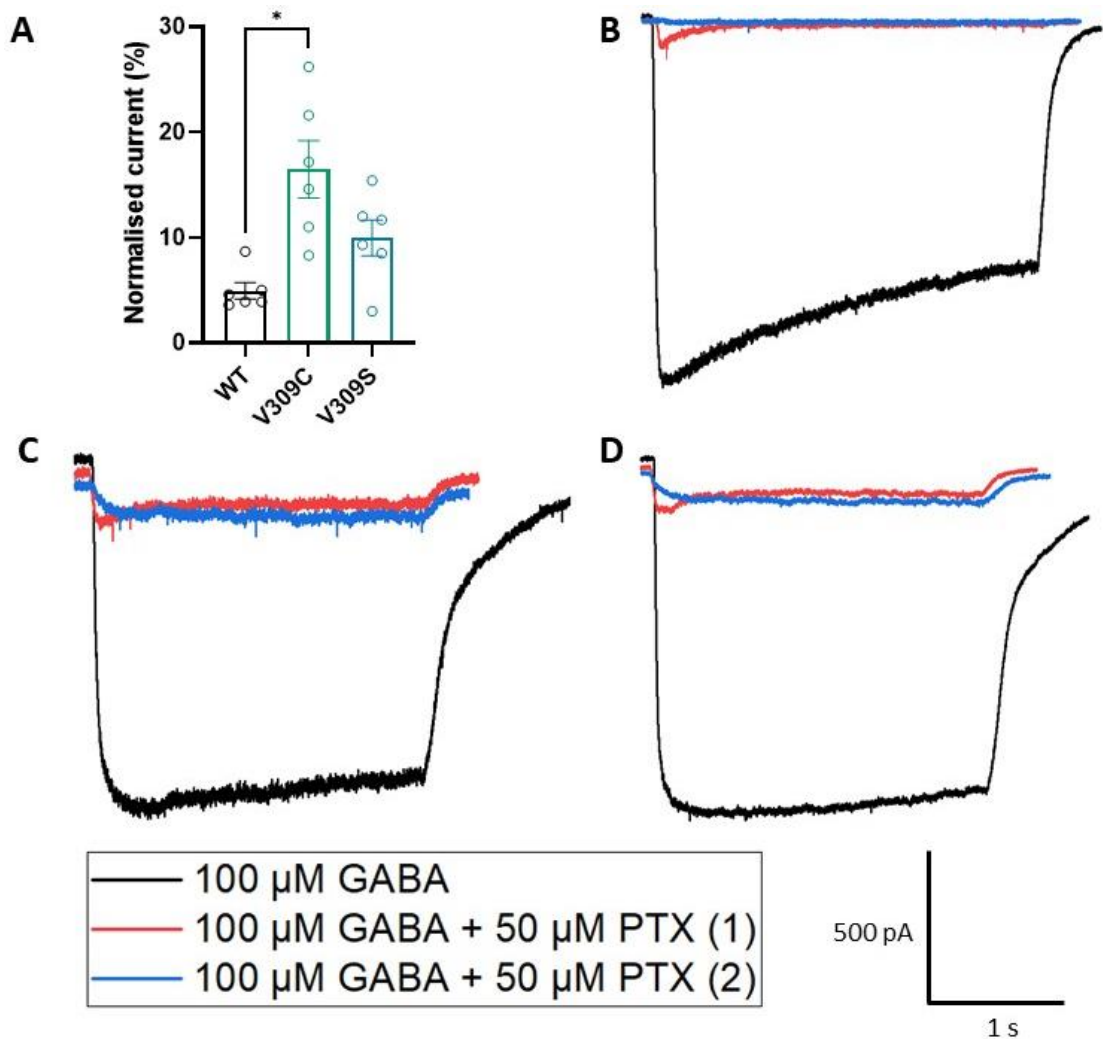
FIGURE 5.4. Mutation of residue V309 to either cysteine or serine does not confer insensitivity to the GABA$_A$R antagonist PTX. **(A)** The normalised 100 μM GABA current following two co-applications of 50 μM PTX was significantly higher when mediated through α3^{V309C}β3γ2L receptors (16.5 ± 2.7 %; n=6), but not when mediated through α3^{V309S}β3γ2L receptors (10.0 ± 1.7 %; n=6), when compared to wildtype α3β3γ2L receptors (5.0 ± 1.9 %; n=10; Kruskal-Wallis and Dunn's multiple comparisons tests). **(B)** Representative membrane currents resulting from 4 s applications of 100 μM GABA (black) followed by two co-applications of 100 μM GABA and 50 μM PTX (red and blue respectively) to wildtype α3β3γ2L receptors. **(C)** Representative membrane currents resulting from 4 s applications of 100 μM GABA (black) followed by two co-applications of 100 μM GABA and 50 μM PTX (red and blue respectively) to α3^{V309C}β3γ2L receptors. **(D)** Representative membrane currents resulting from 4 s applications of 100 μM GABA (black) followed by two co-applications of 100 μM GABA and 50 μM PTX (red and blue respectively) to α3^{V309S}β3γ2L receptors. Circles, bars and error bars represent individual cells, population means and SEMs respectively. *p* values ≤ 0.05 *.

5.2.3. Knockdown of α3-GABA$_A$R expression was not detectably achieved with multiple different α3-specific shRNAs provided by Horizon Discovery

Reducing the expression levels of a given gene can be an effective means of determining the function of the encoded protein. Therefore, knockdown of α3 subunit expression, and hence α3-GABA$_A$R expression, was attempted using shRNAs. Three different α3-specific shRNAs targeting different sequences within *Gabra3* were ordered from Horizon Discovery. For ease, these shRNAs are here referred to as shRNA A, shRNA B and shRNA C (see Table 2.2 for clone IDs and sequences). HEK-293 cells were transfected with equimolar ratios of constructs expressing α3, β3, γ2L and eGFP, as well as one of each of shRNA A, shRNA B, shRNA C, or an equimolar combination of all three. Control cells were transfected with α3, β3, γ2L, eGFP and a scrambled, non-specific shRNA. Whole-cell voltage-clamp electrophysiology was performed on transfected cells and the maximal peak responses of the shRNA-targeted receptors were measured in response to 4 s applications of 10 mM GABA. Maximum current density was then calculated by normalising the maximum current to the cell membrane capacitance (see section 2.2.4).

None of the shRNAs A, B or C, nor the combination of all three, significantly reduced the maximum current densities of α3β3γ2L receptors compared to the scrambled shRNA (Fig. 5.5). As maximum current density provides an indirect measure of receptor cell surface expression, these results indicate that, at least as can be measured through this experimental system, none of the shRNAs tested were effective at reducing α3 expression.

While the α3-specific shRNAs appeared to be ineffective when tested on α3β3γ2L receptors transfected into HEK-293 cells, previous shRNA knockdown experiments in the lab have found that reduced gene expression, mediated by shRNAs, can be identified when performed on endogenous proteins in hippocampal neurons in cell culture. To assess whether this was the case for the α3-specific shRNAs A, B and C, equimolar ratios of each shRNA, or an equimolar combination of all three, were co-transfected with eGFP into hippocampal neurons in cell culture.
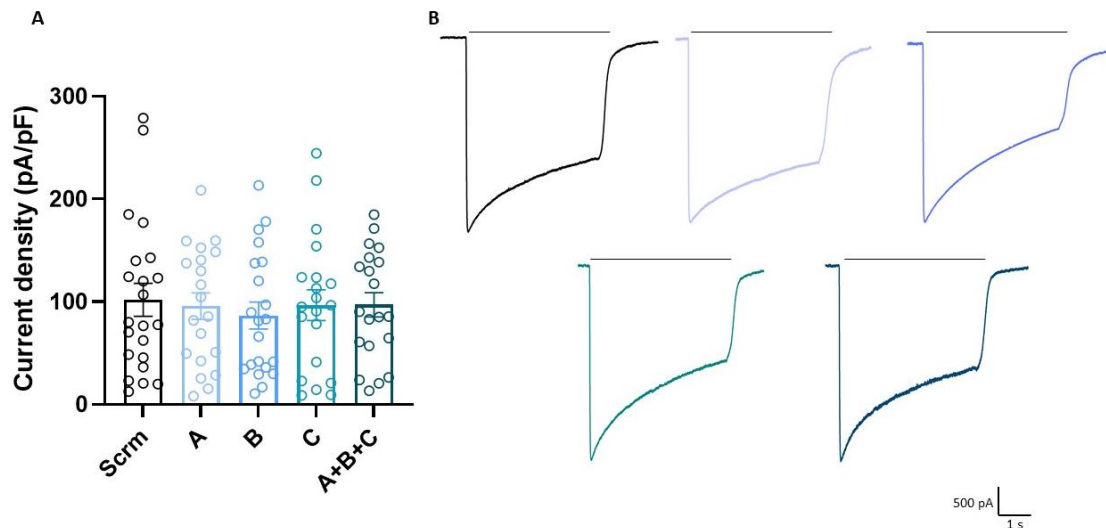
FIGURE 5.5. None of the three α3-specific shRNAs A, B or C individually, nor a combination of all three, reduced the maximum current density values, which serve as a measure of receptor cell surface expression, of α3-GABA$_A$Rs when compared to a scrambled (scrm) control. **(A)** Maximum current density values did not differ significantly between the wildtype α3β3γ2L receptors co-transfected with scrambled shRNA (101.8 ± 16.0 pA/pF; n=22), shRNA A (95.8 ± 13.0 pA/pF; n=20), shRNA B (86.4 ± 13.1 pA/pF; n=21), shRNA C (96.7 ± 14.9 pA/pF; n=20) or an equimolar combination of shRNAs A, B and C (97.0 ± 12.0 pA/pF; n=20; one-way ANOVA test). **(B)** Representative membrane currents resulting from 4 s applications of 10 mM GABA, indicated by the black lines, to α3β3γ2L receptors co-transfected with scrambled shRNA (black), shRNA A (light blue), shRNA B (blue), shRNA C (blue green) and an equimolar combination of shRNAs A, B and C (dark blue). Circles, bars and error bars represent individual cells, population means and SEMs respectively.

Whole-cell voltage-clamp electrophysiology was performed on the transfected neurons. Membrane currents were recorded and sIPSCs were detected and analysed as detailed in section 2.3.3. No significant differences in sIPSC peak amplitude were observed between the scrambled control and any of the shRNA transfections (Fig. 5.6A). However, there was a trend for the sIPSC peak amplitudes of the neurons transfected with the α3-specific shRNAs (ranging from -207.9 ± 121.1 pA for a combination of shRNAs A+B+C to -355.3 ± 142.1 pA for shRNA C) to be larger than those transfected with the scrambled shRNA (-74.0 ± 7.1 pA; Fig. 5.6A). Interestingly, the mean sIPSC frequency was significantly higher for shRNA B compared to the scrambled control or any of the other shRNA transfections (Fig. 5.6B). However, none of the other measured parameters of sIPSC kinetics differed between any of the shRNA transfections and the scrambled control: there were no significant differences in the values of the 10-90% rise time (Fig. 5.6C), nor sIPSC decay tau (Fig. 5.6D).

To investigate any potential effects the α3-specific shRNAs may have on tonic currents, all GABA$_A$Rs were blocked with bicuculline (Fig. 5.7B), which acts as a competitive antagonist at the GABA binding site (Andrews & Johnston, 1979; Masiulis et al., 2019) (see section 1.3.2.). No significant differences in tonic currents were observed between any of the shRNA transfections (Fig. 5.7A). However, there was a trend for the tonic current to be larger in neurons transfected with shRNA B (-47.1 ± 11.8 pA) and shRNA C (-38.5 ± 12.7 pA) compared to those transfected with the scrambled control (-20.4 ± 4.4 pA).

Overall, these data do not provide much indication of an effective shRNA-mediated reduction of *Gabra3* expression, at least in so far as can be detected through whole-cell electrophysiology in HEK-293 cells and hippocampal neurons in cell culture. However, there is a tendency towards larger synaptic and tonic currents, as well as an increased sIPSC frequency, with some shRNAs.
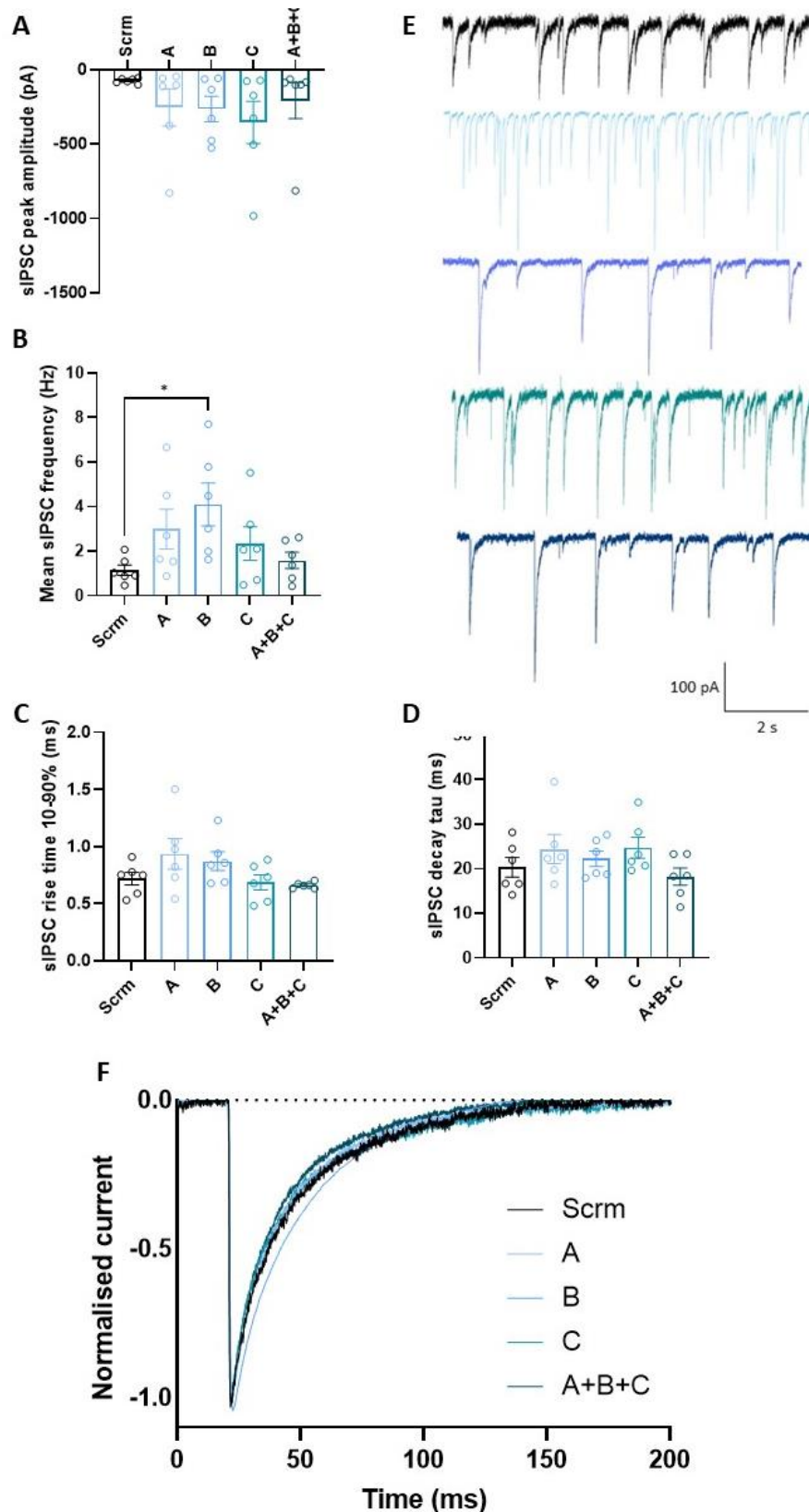
FIGURE 5.6. Three α3-specific shRNAs A, B and C, applied individually, as well as a combination of the three, had little effect on endogenous GABA$_A$R sIPSC kinetics in hippocampal neurons in cell culture when compared to a scrambled (scrm) control. **(A)** sIPSC peak amplitude did not significantly differ between neurons transfected with the scrambled control (-74.0 ± 7.1 pA; n=6), shRNA A (-253.7 ± 125.0 pA; n=6), shRNA B (-263.9 ± 85.3 pA; n=6), shRNA C (-355.3 ± 142.1 pA; n=6) or an equimolar

combination of shRNAs A+B+C (-207.9 ± 121.1 pA; n=6; Kruskal-Wallis test). **(B)** The mean sIPSC frequency was significantly higher for neurons transfected with shRNA B (4.1 ± 1.0 Hz; n=6) compared to those transfected with the scrambled control (1.1 ± 0.2 Hz; n=6), shRNA A (3.0 ± 0.9 Hz; n=6), shRNA C (2.3 ± 0.8 Hz, n=6) or an equimolar combination of shRNAs A+B+C (1.6 ± 0.4 Hz; n=6; one-way ANOVA and Tukey's multiple comparisons tests). **(C)** sIPSC 10-90% rise time did not significantly differ between neurons transfected with the scrambled control (0.7 ± 0.06 ms; n=6), shRNA A (0.9 ± 0.1 ms; n=6), shRNA B (0.9 ± 0.08 ms; n-6), shRNA C (0.7 ± 0.07 ms; n=6) or an equimolar combination of shRNAs A+B+C (0.7 ± 0.01 ms; n=6; one-way ANOVA test). **(D)** sIPSC decay tau did not differ significantly between neurons transfected with the scrambled control (20.4 ± 2.2 ms; n=6), shRNA A (24.4 ± 3.3 ms; n=6), shRNA B (22.3 ± 1.7 ms; n=6); shRNA C (24.7 ± 2.4 ms; n=6) or an equimolar combination of shRNAs A+B+C (18.2 ± 1.9 ms; n=6; one-way ANOVA test). **(E)** Representative sIPSC traces recorded from neurons transfected with scrambled shRNA (black), shRNA A (light blue), shRNA B (blue), shRNA C (blue green) or an equimolar combination of shRNAs A, B and C (dark blue) and voltage-clamped at -60 mV. **(F)** Representative peak-scaled mean sIPSC waveforms from neurons transfected with the scrambled control (black; n=51 sIPSCs), shRNA A (light blue; n=55 sIPSCs), shRNA B (blue; n=75 sIPSCs), shRNA C (blue green; n=59 sIPSCs) or an equimolar combination of shRNAs A, B and C (dark blue; n=74 sIPSCs). Circles, bars and error bars represent individual cells, population means and SEMs respectively. *p* values ≤ 0.05 *; ≤ 0.01 **; ≤ 0.001 ***; ≤ 0.0001 ****.
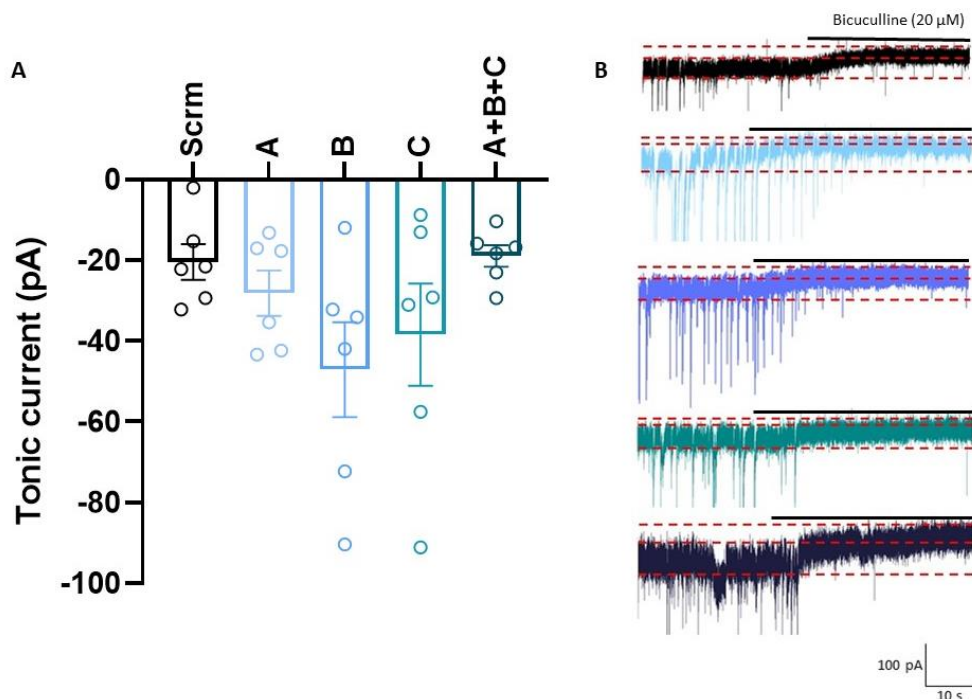
FIGURE 5.7. Transfection of hippocampal neurons in cell culture with shRNAs targeting the α3 subunit of the GABA$_A$R does not affect tonic currents. **(A)** Tonic currents did not significantly differ between neurons transfected with the scrambled control (-20.4 ± 4.4 pA; n=6), shRNA A (-28.2 ± 5.6 pA; n=6), shRNA B (-47.1 ± 11.8 pA; n=6), shRNA C (-38.5 ± 12.7 pA; n=6) or an equimolar combination of shRNAs A+B+C (-19.0 ± 2.7 pA; n=6; one-way ANOVA test). **(B)** Representative tonic current traces recorded from neurons transfected with the scrambled control (black), shRNA A (light blue), shRNA B (blue), shRNA C (blue green) and an equimolar combination of shRNAs A, B and C (dark blue). The antagonist bicuculline (20 μM) reveals tonic inhibition by reducing the holding current, as indicated by the dashed red lines. Circles, bars and error bars represent individual cells, population means and SEMs respectively.

5.2.4. Knockdown of α3-GABA$_A$R expression was not detectably achieved with multiple different α3-specific shRNAs from Merck

Following on from the largely ineffective knockdown experiments using α3-specific shRNAs from Horizon Discovery, three more shRNAs that specifically target sequences in *Gabra3* were identified and ordered from Merck. For ease, these shRNAs are here referred to as shRNA D, shRNA E and shRNA F (see Table 2.2 for clone IDs and sequences).

As with the previous shRNA experiments, HEK-293 cells were transfected with equimolar ratios of constructs expressing α3, β3, γ2L and eGFP, as well as one of each of shRNA D, shRNA E, shRNA F, or an equimolar combination of all three. Control cells were transfected with α3, β3, γ2L, eGFP and a scrambled, non-specific shRNA. Whole-cell voltage-clamp electrophysiology was performed on transfected cells and the maximal peak responses of the shRNA-targeted receptors were measured in response to 4 s applications of 10 mM GABA. As before, maximum current density was then calculated by normalising the maximum current to the cell membrane capacitance.

None of the shRNAs D, E or F, nor the combination of all three, significantly reduced the maximum current densities of α3β3γ2L receptors compared to the scrambled shRNA (Fig. 5.8). As with the previous experiment, these results suggest that these other shRNAs are also ineffective at reducing *Gabra3* expression, insofar as can be measured with whole-cell electrophysiology in this recombinant expression system. Given the minimal results obtained from transfecting the A, B and C shRNAs into hippocampal neurons in cell culture when they had provided no indication of effective knockdown in HEK-293 cells, it was not deemed worthwhile to attempt to reduce knockdown of endogenous α3 expression in neurons in cell culture with the D, E and F shRNAs from Merck.
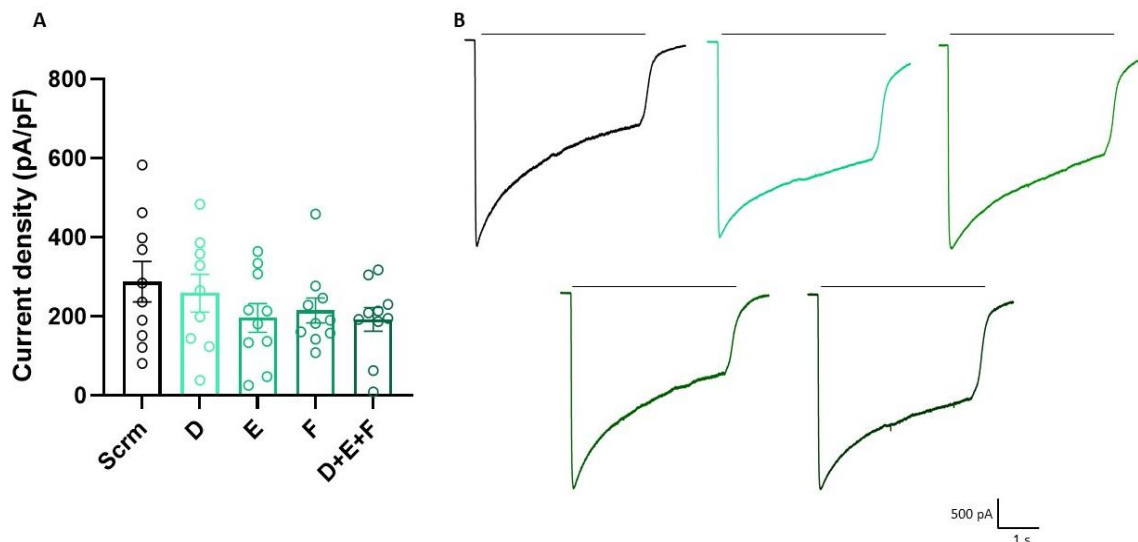
FIGURE 5.8. None of the three α3-specific shRNAs D, E or F individually, nor a combination of all three, reduced the maximum current density values, which serve as a measure of receptor cell surface expression, of α3-GABA$_A$Rs when compared to a scrambled (scrm) control. **(A)** Maximum current density values did not differ significantly between the wildtype α3β3γ2L receptors co-transfected with scrambled shRNA (287.9 ± 51.4 pA/pF; n=10), shRNA D (258.7 ± 47.9 pA/pF; n=9), shRNA E (196.1 ± 36.4 pA/pF; n=10), shRNA F (215.2 ± 31.5 pA/pF; n=20) or an equimolar combination of shRNAs D, E and F (192.1 ± 30.0 pA/pF; n=20; one-way ANOVA test). **(B)** Representative membrane currents resulting from 4 s applications of 10 mM GABA, indicated by the black lines, to α3β3γ2L receptors co-transfected with scrambled shRNA (black), shRNA D (light green), shRNA E (green), shRNA F (olive green) or an equimolar combination of shRNAs D, E and F (dark green). Circles, bars and error bars represent individual cells, population means and SEMs respectively.

5.3.   Discussion

5.3.1.   Resistance to PTX could not be conferred without affecting other aspects of receptor function

As the α3 subunit of the GABA$_A$R is relatively understudied, the aim of this chapter was to elucidate some of the functions that the α3-GABA$_A$R may perform physiologically. Isolation of the sIPSCs mediated solely through α3-GABA$_A$Rs would allow for the kinetic properties of these receptors to be investigated. Therefore, attempts were made to create a PTX-insensitive α3 subunit: application of PTX to neurons transfected with this subunit would block GABAergic transmission mediated through all GABA$_A$Rs except those containing the PTX-insensitive α3 subunit. This kind of pharmacological isolation has been previously performed with δ subunit-containing GABA$_A$Rs (Sun et al., 2018).

It has been previously reported that mutation of the 6' threonine in TM2 of α1 to phenylalanine confers resistance to PTX while having a very minimal effect on receptor GABA sensitivity (Sedelnikova et al., 2006). Based on this study, the equivalent 6' residue in TM2 of α3 – T313 – was substituted with phenylalanine. However, while α3^{T313F}β3γ2L receptors were largely insensitive to PTX (Fig. 5.1), the concentration-response curve of these receptors was at least 10-fold right-shifted, and the GABA EC$_{50}$ values were significantly higher, than those of wildtype α3β3γ2L receptors, indicating a significantly reduced sensitivity to GABA (Fig. 5.2A, B). It is therefore clear that α3^{T313F} affects receptor GABA sensitivity more than the equivalent mutation in α1 (Sedelnikova et al., 2006).

Furthermore, the maximum current density values of the mutant receptors were significantly lower than those of the wildtype receptors (Fig. 5.2C), which may suggest that the substitution causes an alteration in receptor trafficking and/or disrupts the efficiency of receptor assembly, which may reduce the surface expression of the mutant α3^{T313F}β3γ2L receptors. In addition, the α3^{T313F}β3γ2L receptors both desensitised and deactivated significantly more quickly than the wildtype α3β3γ2L receptors (Fig. 5.3), suggesting that phenylalanine substitution at residue T313 affects the macroscopic kinetics of the receptor. Given these results, α3^{T313F} was not introduced into hippocampal neurons in cell culture as a means of isolating α3-GABA$_A$R-specific sIPSCs with PTX application, as it is very unlikely that the kinetics of sIPSCs resulting from the activation of these mutant receptors would be at all representative of wildtype α3-GABA$_A$Rs.

The 2' residue of TM2 in a number of different GABA$_A$R subunits has also been identified as being necessary for mediating PTX block of the receptor channel pore: several studies have reported that mutation of this residue abolishes PTX sensitivity (Ffrench-Constant et al., 1993; Zhang et al., 1994; Xu et al., 1995; Ueno et al., 2000). Therefore, V257, the 2' TM2 residue in the α3 subunit, was substituted with both cysteine (the same exchange as used by Xu et al. (1995)) and serine (utilised in the *Drosophila* GABA receptor by both Ffrench-Constant et al. (1993) and Zhang et al. (1994)). Unfortunately, neither α3^{V257C} nor α3^{V257S} conferred complete insensitivity to PTX (Fig. 5.4). Following these unsuccessful attempts to create an α3 subunit that was

insensitive to PTX but retained similar GABA sensitivity and kinetic properties to wildtype α3, no further attempts were made. Attention was subsequently shifted to reducing the expression of endogenous α3 with shRNA knockdown experiments.

5.3.2. *Knockdown of α3-GABA$_A$R expression was not clearly detected with whole-cell electrophysiology when attempted with different α3-specific shRNAs*

Gene knockdown experiments have long been performed as a means of investigating gene function. They work by reducing the expression levels of a target gene (and thus the levels of the encoded protein) and observing the resulting effects. shRNAs have been demonstrated to provide an effective means of reducing target gene expression (Paddison et al., 2002; Li et al., 2005; Lambeth & Smith, 2013). α3-selective shRNAs were therefore used in an attempt to knockdown endogenous α3 subunit expression.

The efficacy of these shRNAs was first tested by assessing their ability to reduce maximum current density values in HEK-293 cells expressing wildtype α3β3γ2L receptors, where a reduction in maximum current density would indicate reduced surface α3 subunit expression. The current density values were unchanged between the scrambled control and any of the α3-selective shRNAs obtained from two different companies (Figs. 5.5 & 5.8). However, in an attempt to knockdown endogenous α3 expression, transfection of hippocampal neurons in cell culture with the set of shRNAs from one company (A, B and C from Horizon Discovery) still proceeded following these results, as previous shRNA knockdown experiments in the lab had found shRNAs to be efficacious in hippocampal neurons in cell culture when they were not in HEK-293 cells. This could perhaps be due to the inability of the shRNAs to knockdown recombinant α3 subunit expression in HEK-293 cells that is being driven by the strong human cytomegalovirus (CMV) major immediate-early (MIE) promoter used.

The results of the neuronal shRNA experiments do not provide any clear indication that knockdown of endogenous α3 expression was successful (Figs. 5.6 & 5.7). The only statistically significant result was that the mean frequency of sIPSCs recorded in neurons transfected with shRNA B was higher than those transfected with the scrambled control (Fig. 5.6B), although there was a trend for all of the shRNAs to

increase the mean sIPSC frequency compared to the scrambled control (Fig. 5.6B). This could suggest that the mean sIPSC frequency of α3-GABA$_A$Rs is normally slower, and that reducing *Gabra3* expression results in the increased frequency seen with shRNA B. However, in the absence of any other statistically significant effects of shRNA on sIPSC kinetics, this is a tenuous conclusion to draw. Furthermore, there is no published data to suggest that the presence of the α3 subunit within a GABA$_A$R affects sIPSC frequency.

Perhaps a more likely interpretation of the observed increase in mean sIPSC frequency involves the knockdown of α3-GABA$_A$Rs expressed on presynaptic interneurons. sIPSC frequency is normally seen as a measure of presynaptic activity, as it reflects the release of GABA from presynaptic interneurons. Therefore, the simplest explanation of this effect on frequency is that there are α3-GABA$_A$Rs expressed on the soma and dendrites of presynaptic interneurons that normally act to reduce excitability; by knocking down the expression of these receptors with shRNA B, excitability increases. Hence, there is an increase in synaptic GABA release onto the cell being recorded. Alternatively, the shRNA may be knocking down α3-GABA$_A$Rs expressed on the axons of presynaptic interneurons, which normally act to reduce presynaptic GABA release (Wang et al., 2019; earlier work reviewed by Kullmann et al., 2005), thus resulting in the observed increase in presynaptic GABA release. These possible interpretations of the data would therefore provide evidence for presynaptic α3-GABA$_A$Rs on interneurons that are involved in regulating the release of GABA. However, more experiments would need to be done to test this hypothesis further. For example, tetrodotoxin (TTX) could be used to isolate miniature IPSCS (mIPSCs). TTX selectively blocks voltage-gated sodium channels in neuronal membranes, thus preventing the firing of action potentials (Narahashi et al., 1964). If the increase in frequency observed with shRNA B was still apparent with mIPSCs in the presence of TTX, this would indicate the presence of axon terminal α3-GABA$_A$Rs that affect presynaptic GABA release. If the increase in mean frequency disappeared with TTX, this may indicate that the α3-GABA$_A$Rs are expressed on the soma and/or dendrites of upstream interneurons, where they act to reduce excitability.

There are two additional trends in the data which, while not statistically significant, may indicate an effect of the shRNAs. First, the mean peak sIPSC amplitudes recorded from neurons transfected with any of the three shRNAs individually, or a combination of all three, were higher than those of scrambled control transfected-neurons by up to 5-fold (Fig. 5.6A). This could indicate that the peak sIPSC amplitudes resulting from activation of synapses containing α3-GABA$_A$Rs are normally smaller and that by knocking down endogenous α3 expression, higher peak amplitudes occur due to GABAergic transmission instead being mediated through other GABA$_A$R subtypes. Alternatively, as larger peak amplitudes suggest increased numbers of synaptic receptors (Nusser et al., 1997), this trend could imply that α3-GABA$_A$R knockdown results in their replacement with a greater number of other synaptic receptor subtypes. A further possibility for this trend for larger sIPSCs in cells transfected with α3-selective shRNAs is related to the presynaptic effects described in the above paragraph. It has already been noted that for shRNAs A, B and C, there is a trend for increased mean sIPSC frequency (Fig. 5.6B). Therefore, it could be the case that the putative increase in presynaptic GABA release (possibly multivesicular release) increases the likelihood of two or more synapses being active at the same time and generating much larger synchronous sIPSCs by summation.

The final trend in the data is that the tonic currents of neurons transfected with shRNAs B or C were higher than those of neurons transfected with the scrambled control (Fig. 5.7). This may indicate that reducing α3 subunit expression increases the tonic current, perhaps due to an increase in the expression of traditional extrasynaptic receptor subtypes that have a higher GABA sensitivity (e.g., α4βδ-GABA$_A$Rs – see Farrant & Nusser, 2005). This trend can also be linked with the potential effects of knocking down α3 subunit expression on presynaptic GABA release. An increase in sIPSC frequency means there is more GABA release; therefore, there may be higher ambient GABA levels, resulting in a larger tonic current.

Of course, given the very minimal effects of these shRNAs on sIPSC kinetics, it is still possible that the shRNAs are simply not effective at silencing *Gabra3* expression, as suggested by the lack of impact on currents mediated by recombinant receptors in HEK-293 cells. While this may well be true, there is an alternative explanation as to

why the shRNAs appeared to be (mostly) ineffective in hippocampal neurons in cell culture.

It could be that, in these neurons in cell culture, α3-GABA$_A$Rs comprise only a small proportion of the GABA$_A$Rs located at inhibitory synapses. If this is the case, then these endogenous α3-GABA$_A$Rs likely only contribute minimally to the sIPSCs mediated at these synapses; shRNA-induced reduction in α3 subunit expression would therefore be unlikely to be detected through changes in sIPSC kinetics. There is potential evidence to support this theory: in chapter 4, wildtype, phospho-null and phospho-mimetic α3 subunits were transfected into hippocampal neurons in cell culture and their subcellular localisation assessed using SIM imaging (see sections 4.2.1 and 4.2.2). The imaging results demonstrated that only a limited subset (~21%) of inhibitory synapses contain α3-GABA$_A$Rs (Fig. 4.5B). Moreover, all immunostaining reported in chapter 4 was performed against GABA$_A$Rs expressed on cells transfected with the α3 subunit; therefore, endogenous α3-GABA$_A$R expression at synapses may be even lower.

If the lack of effect of these shRNAs on sIPSC kinetics is indeed due to minimal expression of α3-GABA$_A$Rs at endogenous synapses, a more effective means of determining the efficacy of the shRNAs would have been through immunostaining: lower α3 protein levels can be detected through smaller α3 puncta volumes, or reduced α3 mean grey values, for example. While there was not time to conduct these experiments in the present study, it may prove valuable for the shRNA efficacy to be assessed in this way in the future.

5.4.   Conclusions

1. Mutation of the 6' threonine, T313, of TM2 of the α3 subunit to phenylalanine confers substantial insensitivity to the non-competitive GABA$_A$R antagonist picrotoxin, but also affects other aspects of receptor function, including reducing α3^{T313F}β3γ2L receptor sensitivity to GABA.

2. Mutation of the 2' valine, V309, of TM2 of the α3 subunit to either cysteine or serine does not confer substantial insensitivity to picrotoxin.

3. Six different α3-specific shRNAs from two different companies, A, B and C (from Horizon Discovery) and D, E and F (from Merck), were not effective at reducing the maximum current densities – a measure of cell surface expression – of recombinant α3β3γ2L receptors in HEK-293 cells.

4. The α3-specific shRNA B increased the mean sIPSC frequency compared to a non-specific scrambled control shRNA in hippocampal neurons in cell culture. There was a trend for the α3-specific shRNAs A and C to also increase mean sIPSC frequency.

5. There were trends for the α3-specific shRNAs A, B and C to increase sIPSC peak amplitude, and for shRNAs B and C to increase tonic currents, compared to a non-specific scrambled control shRNA.

6. The number of α3 subunits expressed in hippocampal neurons in cell culture may be minimal.

Chapter 6: General Discussion

6.1. Summary: literature review and project aims

The subunit composition of the $GABA_AR$ principally determines its biophysical and pharmacological properties, as well as its subcellular localisation. α3 subunit expression is targeted to specific regions of the adult brain, occurring primarily at inhibitory synapses of the nRT (Studer et al., 2006; Liu et al., 2007) and reelin-positive cells in the medial entorhinal cortex (Berggaard et al., 2018). α3 is also expressed extrasynaptically in the BLA (Marowsky et al., 2012) and the inferior olivary nucleus (Devor et al., 2001).

The subcellular localisation of the α3-$GABA_AR$ determines the physiological function it performs. Two examples have been used to illustrate this point throughout this thesis: the synaptic localisation of the α3-$GABA_AR$ in the nRT, where it mediates phasic inhibition (Studer et al., 2006; Schofield & Huguenard, 2007); and the extrasynaptic localisation of the α3-$GABA_AR$ in the BLA, where it mediates tonic inhibition (Marowsky et al., 2012). Both regions are associated with pathological disease states (Sajdyk & Shekhar, 1997; Christian et al., 2013; Lüthi & Lüscher, 2014; Terlau et al., 2020).

The principal inhibitory scaffold protein gephyrin plays a key role in the recruitment and anchoring of $GABA_ARs$ at GABAergic synapses (Tyagarajan & Fritschy, 2014). The gephyrin binding site in the α3 subunit has been identified within the ICD (Tretter et al., 2011); analogous gephyrin binding sites have also been identified in the ICDs of the α1 (Mukherjee et al., 2011), α2 (Tretter et al., 2008) and α5 subunits (Brady & Jacob, 2015). Phosphorylation of residues in the ICD of α subunits is known to play an important role in regulating dynamic processes, including receptor accumulation (trafficking) at inhibitory synapses (Abramian et al., 2010; Mukherjee et al., 2011), modulation by endogenously occurring neurosteroids (Abramian et al., 2014; Adams et al., 2015) and the binding of allosteric modulators such as benzodiazepines (Churn et al., 2004) (see section 1.1.4).

Maric et al. (2014) used a combination of chemical, biophysical and structural investigations to identify three residues within the α3 gephyrin binding motif – T400, T401 and Y402 – as being of major importance in mediating the binding of the α3 subunit to gephyrin, due to the thermodynamic interactions of their side chains with gephyrin. While the different α subunits mediate gephyrin binding through unique binding motifs, they all engage in robust and specific direct interactions with gephyrin, indicating that these interactions may be regulated through subunit-specific post-translational modifications. In their 2014 study, Maric and colleagues suggest that functional investigations of the phosphorylation states of the residues T400, T401 and Y402 of the α3 subunit are likely to reveal an important role for the regulation of gephyrin binding via this post-translational modification. Given the importance of gephyrin for tethering GABA$_A$Rs to inhibitory synapses, phosphorylation of these residues may also, by extension, regulate the subcellular localisation of the α3-GABA$_A$R.

Given the above, the primary aim of the present study was to investigate the molecular mechanism(s) that control the differential subcellular localisation of α3-GABA$_A$Rs in distinct brain regions, with a particular focus on the role of phosphorylation in this process. This aim was addressed in chapters 3 and 4. The secondary aim was to investigate the functional profile of the α3-GABA$_A$R, as it is a relatively understudied GABA$_A$R subtype. This aim was addressed in chapter 5.

6.2. Major findings

6.2.1. Phospho-mutants of T400, T401 and Y402 in the gephyrin binding domain affect receptor GABA sensitivity

To investigate the potential effects of phosphorylation of the three residues T400, T401 and Y402 identified by Maric et al. (2014), phospho-null and phospho-mimetic mutants were created of each residue via substitution with alanine (phenylalanine in the case of Y402) or aspartate respectively. The phospho-null mutants mimic unphosphorylated residues, as the (phenyl)alanine lacks the hydroxyl group required for residue phosphorylation. The phospho-mimetic mutants are considered to mimic

phosphorylated residues, as the negative charge of the aspartate residue mimics that conferred by a phosphate group.

The receptor GABA sensitivity was affected by the phospho-mutants for all three residues, but in different ways. At residue T400, both the $\alpha3^{T400A}\beta3\gamma2L$ and the $\alpha3^{T400D}\beta3\gamma2L$ receptors caused the GABA CRC to shift to the left, and the EC_{50} to significantly reduce, compared to that of the wildtype $\alpha3\beta3\gamma2L$ receptors (Fig. 3.4A, B). Thus, both mutations increase the sensitivity of the receptor for GABA. As phospho-null mutations are not expected to give the same outcome as phospho-mimetic mutations, these results likely suggest that substituting T400 with either alanine or aspartate influences receptor activation through allosteric effects, which are unrelated to the prevention or mimicry of phosphorylation at this residue.

The phospho-null and phospho-mimetic mutations of residues T401 and Y402, however, did display differential effects. At T401, the phospho-null $\alpha3^{T401A}\beta3\gamma2L$ receptors caused a leftward shift in the GABA CRC, along with a corresponding reduction in the GABA EC_{50}, compared to the wildtype and $\alpha3^{T401D}\beta3\gamma2L$ receptors (Fig. 3.5A, B). In contrast, at Y402, the phospho-mimetic $\alpha3^{Y402D}\beta3\gamma2L$ receptors caused a leftward shift in the GABA CRC and a significantly lower EC_{50} compared to both the wildtype and the $\alpha3^{Y402F}\beta3\gamma2L$ receptors (Fig. 3.6A, B). As with T400, the possibility that these results were caused by allosteric effects of the respective T401A and Y402D mutations on the receptor cannot be excluded. However, this is less likely to be the case for these residues, as the opposing T401D and Y402F mutations did not affect receptor sensitivity to GABA. A more plausible interpretation of these data, therefore, is that T401 is basally phosphorylated in HEK-293 cells, while the native state of Y402 is non-phosphorylated; by preventing and mimicking phosphorylation at these respective residues, the sensitivity of the $\alpha3$-GABA$_A$R for GABA is increased. These differential effects of phosphorylation at T401 and Y402 would also involve different kinase signalling pathways: serine/threonine kinase(s) for T401 and tyrosine kinase(s) for Y402.

6.2.2. *Mimicking phosphorylation at T401 and Y402 slows down sIPSC kinetics*

The further investigation of the phospho-mutants in hippocampal neurons in cell culture revealed that aspartate substitution at both T401 and Y402 significantly slowed both sIPSC 10-90% rise time (Fig. 3.8C; Fig. 3.10C) and decay tau (Fig. 3.8D, F; Fig. 3.10D, F) compared to wildtype, eGFP control and phospho-null receptors.

As has been previously discussed, the kinetic properties of the $\alpha 3$-GABA$_A$R are distinct, with most of its kinetic parameters being slower than those of other α subunit-containing receptors (Picton & Fisher, 2007) (see section 1.4.1). Of particular note is the decay – both desensitisation and deactivation – rate of $\alpha 3$-GABA$_A$Rs: Picton & Fisher (2007) describe it as one of the slowest of all GABA$_A$R subtypes, while Syed et al. (2020) found the decay time constant of sIPSCs mediated by $\alpha 3 \beta 3 \gamma 2$ receptors to be significantly slower than that of their $\alpha 1 \beta 3 \gamma 2$ counterparts.

As the sIPSCs recorded from transfected neurons represent a mixed GABA$_A$R population of both endogenous receptors and receptors containing either the introduced wildtype or mutant $\alpha 3$ subunits, a potential interpretation of the slower sIPSC decay rates displayed by the $\alpha 3^{T401D}$ and $\alpha 3^{Y402D}$ mutants is that these substitutions cause more $\alpha 3$-containing GABA$_A$Rs to localise at inhibitory synapses. This interpretation provides an explanation for these slower sIPSC kinetics: a greater proportion of the synaptic receptors may have been $\alpha 3$-GABA$_A$Rs when compared to the neurons transfected with the wildtype $\alpha 3$ subunit.

It cannot be ruled out that the observed effects on the sIPSC rise and decay times are caused by the aspartate substitutions directly affecting receptor kinetics. This pertains to residue Y402 in particular, given both phenylalanine and aspartate substitutions at this residue affect macroscopic receptor desensitisation kinetics (Fig. 3.12C). However, substituting Y402 with the structurally non-conservative amino acid alanine does not affect receptor GABA sensitivity or cell surface expression, while the (also structurally non-conservative) Y402D substitution does (Fig. 3.7), suggesting that this effect arises from successful mimicry of phosphorylation at this residue. Furthermore, the corresponding residues of T401 in $\alpha 1$ (Munton et al., 2007), and of Y402 in both the $\alpha 1$ and $\alpha 2$ subunits (Ballif et al., 2008), have already been shown to be

phosphorylated *in vivo* which, combined with the HEK-293 cell GABA CRC and neuronal sIPSC data, support the hypothesis that the observed effects are caused by successful mimicry of phosphorylation at these residues.

6.2.3. A potential role for gephyrin-independent mechanisms in the clustering of α3-GABA$_A$Rs at inhibitory synapses

Structured illumination microscopy is a type of super-resolution imaging that has been used by multiple studies to investigate the structure and organisation of postsynaptic densities (Davenport et al., 2017; Crosby et al., 2019; Schmerl et al., 2020). In the present study, SIM imaging was used on hippocampal neurons in cell culture transfected with wildtype α3, α3^{Y402F} or α3^{Y402D} subunits to assess the impact of mimicking phosphorylation at residue Y402 on α3-GABA$_A$R subcellular clustering and localisation.

The hypothesis that aspartate substitution at Y402 increases the synaptic localisation of α3-GABA$_A$Rs is supported by the results of these SIM experiments. The mean grey value of synaptically-localised α3^{Y402D} puncta was significantly higher than that of synaptic wildtype α3 and α3^{Y402F} puncta (Fig. 4.3B). This indicates an increase in the number of α3^{Y402D}-GABA$_A$Rs localised at inhibitory synapses, as suggested by the sIPSC data (Fig. 3.10). Unexpectedly however, further interrogation of the data revealed that this increase in the mean grey value of synaptic α3^{Y402D} only holds true for puncta that do not co-localise with gephyrin (Fig. 4.3H), potentially indicating that the increased synaptic clustering observed for α3^{Y402D}-GABA$_A$Rs is mediated by a gephyrin-independent clustering mechanism(s).

The imaging data also revealed that there was significantly less co-localisation between α3^{Y402D}-GABA$_A$R and gephyrin clusters, compared to wildtype or α3^{Y402F}-GABA$_A$Rs (Fig. 4.4), suggesting that aspartate substitution at Y402 may reduce the interaction of the α3 subunit with gephyrin. Maric et al. (2014) suggested that Y402 is critically important for gephyrin binding and is a strong candidate for mediating the regulation of such binding via post-translational modifications such as phosphorylation. Therefore, it is unsurprising that mimicking phosphorylation at this

residue affects the co-localisation, and hence likely the interaction, between the α3 subunit and gephyrin. While the phospho-mimetic-induced reduction in α3 subunit-gephyrin binding could not be confirmed biochemically due to difficulties with the co-IP experiments (Fig. 4.7), Mukherjee et al. (2011) reported that mimicking phosphorylation at T375, a residue within the gephyrin binding site of the α1 subunit, diminished the binding between α1 and gephyrin. Therefore, similar studies on other α subunits support the idea that mimicking phosphorylation at residue Y402 may lessen the binding between the α3-GABA$_A$R and gephyrin.

The hypothesised reduction in binding between α3 and gephyrin would explain the observed reduction in co-localisation between α3^{Y402D}-GABA$_A$R and VIAAT clusters: fewer α3-GABA$_A$Rs bind to the scaffold protein gephyrin, which in turn reduces the number of receptors that gephyrin can anchor at GABAergic synapses. The aforementioned study by Mukherjee et al. (2011) reported exactly this for α1: mimicking phosphorylation at T375 diminished the binding between α1 and gephyrin and consequentially reduced α1-GABA$_A$R accumulation at synapses.

However, the α3-gephyrin co-localisation data also showed there to be a very low proportion of co-localisation between wildtype α3 and gephyrin: only ~8% of α3 clusters co-localised with gephyrin (Fig. 4.4A), while only ~4% of gephyrin clusters co-localised with α3 (Fig. 4.4B). While these numbers did fall significantly for α3^{Y402D} (~5% of α3^{Y402D} clusters co-localised with gephyrin (Fig. 4.4A) and ~2% of gephyrin clusters co-localised with α3^{Y402D} (Fig. 4.4B)), they are extremely low even for the wildtype α3-GABA$_A$Rs, suggesting that gephyrin may not be important for the synaptic clustering of α3-GABA$_A$Rs. Furthermore, in neurons transfected with wildtype α3, ~32% of VIAAT clusters co-localised with gephyrin, indicating that only a third of inhibitory synapses contain gephyrin (Fig. 4.5C). Given gephyrin's supposedly critical role in the anchoring of GABA$_A$Rs at GABAergic synapses (Essrich et al., 1998; Kneussel et al., 1999; Jacob et al., 2005; Mukherjee et al., 2011), the minimal co-localisation observed between α3 and gephyrin, as well as between VIAAT and gephyrin, is surprising and highlights the strong likelihood of the existence of gephyrin-independent clustering mechanisms. Indeed, gephyrin-independent GABA$_A$R clustering has been reported before (Kneusssel et al., 2001; Lévi et al., 2004; Niwa et al., 2012) (see section 4.3).

Furthermore, a variety of other clustering proteins have been identified which may be involved in the localisation of α3-GABA$_A$Rs at inhibitory synapses in place of gephyrin, including collybistin (Chiou et al., 2011; George et al., 2021), neurobeachin (Nair et al., 2012), GARLH (Davenport et al., 2017; Yamasaki et al., 2017) and NL2 (Poulopoulos et al., 2009). Therefore, as a scaffold protein, gephyrin may not play a particularly important role in the subcellular localisation of these receptors.

Worthy of note are the low levels of co-localisation that were observed between wildtype α3 and the presynaptic marker VIAAT: ~20% of α3 clusters co-localised with VIAAT (Fig. 4.5A), while ~21% of VIAAT clusters co-localised with α3 (Fig. 4.5B). These data indicate that the majority of α3-GABA$_A$Rs in hippocampal neurons are extrasynaptic. However, in the nRT, α3-GABA$_A$Rs are localised synaptically (Pirker et al., 2000; Studer et al., 2006; Liu et al., 2007; Hörtnagl et al., 2013). Consequently, in this brain region, gephyrin and/or other interacting proteins may be much more critical for α3 subunit-containing receptor clustering at GABAergic synapses.

6.2.4. Mimicking phosphorylation at Y402 affects α3-GABA$_A$R subcellular localisation

α3^{Y402D} slows down sIPSC kinetics (see section 3.2.5). As α3-GABA$_A$Rs display some of the slowest kinetic properties of all GABA$_A$R subtypes (Picton & Fisher, 2007; Syed et al., 2020), a possible interpretation of such data is that α3^{Y402D} increases the amount of α3-GABA$_A$Rs located at synapses. Furthermore, the mean grey value of synaptic α3^{Y402D}-GABA$_A$R clusters is significantly higher than that of wildtype or α3^{Y402F}-GABA$_A$Rs (Fig. 4.3B), again suggesting that α3^{Y402D} increases the synaptic clustering of α3-containing receptors. However, this increased mean grey value only reflects synaptic α3^{Y402D}-GABA$_A$Rs that do not co-localise with gephyrin (Fig. 4.3H). Additionally, while already quite minimal for wildtype α3 under basal conditions, there is significantly less co-localisation between α3^{Y402D}-GABA$_A$Rs and gephyrin (Fig. 4.4).

Unexpectedly, the α3-VIAAT co-localisation data revealed significantly less co-localisation between α3^{Y402D}-GABA$_A$R and VIAAT clusters compared to α3- or α3^{Y402F}-GABA$_A$Rs (Fig. 4.5). In contrast to the previous sIPSC kinetic data and the mean grey

value imaging data, this may suggest a reduction in the proportion of $\alpha 3^{Y402D}$ receptors localised at synaptic sites.

At face value, these apparently contradictory results are confusing. One could assume that the slower sIPSC rise and decay rates observed with the $\alpha 3^{Y402D}$ receptors are due to kinetic effects of the mutation on the receptor – an entirely plausible interpretation of the data. However, this still does not explain why the mean grey value data show an increase in $\alpha 3^{Y402D}$ puncta at postsynaptic sites.

There are a couple of alternative interpretations of the data that take into account all of the observed results. The first is based on the findings of a study by Wei et al. (2003), which identified a population of perisynaptic δ subunit-containing GABA$_A$Rs in the mouse dentate gyrus that are activated by GABA spillover and that significantly slow down the decay time constants of sIPSCs. Applying these findings to the present study, it is possible that $\alpha 3^{Y402D}$ receptors accumulate at perisynaptic sites, where the receptors may be far enough removed from the centre of the synapse to not co-localise with VIAAT and so be categorised as 'extrasynaptic' in the SIM analysis, yet close enough to the synapse to be able to influence and slow down the sIPSC kinetic profile. However, given that there is no evidence from earlier studies suggesting a perisynaptic location of $\alpha 3$ GABA$_A$Rs, this is a speculative interpretation of the data.

This thesis has largely focussed on how phosphorylation of specific residues located within the gephyrin binding domain of the $\alpha 3$ subunit may affect gephyrin binding, and consequently the subcellular localisation, of $\alpha 3$-GABA$_A$Rs. While the SIM imaging data indicates a less significant role for gephyrin in the clustering of $\alpha 3$-GABA$_A$Rs than has been suggested for other α subunit-containing receptor isoforms (Essrich et al., 1998; Kneussel et al., 1999; Jacob et al., 2005; Mukherjee et al., 2011), another possible interpretation of the collective data does involve gephyrin.

It may be that aspartate substitution at Y402 reduces $\alpha 3$ subunit interaction with the scaffold protein gephyrin, which in turn reduces the accumulation of $\alpha 3$-GABA$_A$Rs at inhibitory synapses. This is supported by the study by Mukherjee et al. (2011), described in the previous section, which reported that mimicking phosphorylation at T375, a residue within the gephyrin binding site of the $\alpha 1$ subunit, diminished the

binding between α1 and gephyrin and consequentially reduced α1-GABA$_A$R accumulation at synapses. However, while there is a reduction in the proportion of GABAergic synapses containing α3^{Y402D}-GABA$_A$Rs, these receptors are more concentrated in the synapses that retain them. These synapses may also lack gephyrin, given that the increased mean grey value observed for α3^{Y402D}-GABA$_A$Rs only holds true for synaptic receptors that do not co-localise with gephyrin (Fig. 4.3H) and that the proportion of VIAAT clusters that co-localise with gephyrin significantly decreases in cells transfected with the phospho-mimetic receptor (Fig. 4.5C). This increased concentration of the α3^{Y402D}-GABA$_A$Rs at such synapses is likely mediated by a gephyrin-independent clustering mechanism(s). Perhaps there are even separate 'types' of inhibitory synapse – gephyrin-dependent and gephyrin-independent – with α3^{Y402D} receptors being directed towards the latter. Regardless, it is clear that mimicking phosphorylation via aspartate substitution at Y402 in the gephyrin binding site of the α3 subunit affects the subcellular localisation of α3-GABA$_A$Rs at or near inhibitory synapses, and largely independently of gephyrin.

6.3. Project limitations

The theory proposed to explain the results of the various experiments conducted throughout this project would have been stronger had various other attempted experiments been successful. These experiments are discussed in the following sections.

6.3.1. Co-immunoprecipitation experiments

The aim of the co-IP experiments was to determine whether the phospho-null phenylalanine and/or the phospho-mimetic aspartate substitutions at residue Y402 affected the binding between the α3 subunit and gephyrin. The SIM imaging data indicated that the binding is weakened between α3^{Y402D} and gephyrin, but without the definitive biochemical evidence that would have been supplied by a successful co-IP experiment, this cannot be confirmed.

As described in section 4.2.3, many different iterations of the co-IP experiments were performed in an attempt to make them function effectively. The ultimate failure to do so was particularly frustrating given the success of the initial co-IP experiments (Fig. 4.6), performed to confirm the biochemical interaction between α3 and gephyrin that has been reported in the literature (Tretter et al., 2011; Maric et al., 2014; Larson et al., 2020).

Given so many different variations of this experiment were performed, all of which were unsuccessful, it is unlikely that the effects of $\alpha3^{Y402F}$ and $\alpha3^{Y402D}$ on the binding between the α3 subunit and gephyrin can be determined in this manner. However, affinity capillary electrophoresis, which can be used to estimate binding constants between molecules (Chu et al., 1992) may provide an alternative experimental approach for the quantitative interrogation of the α3-gephyrin binding interaction.

6.3.2. Picrotoxin-insensitive α3-GABA$_A$Rs

As previously stated, the α3-GABA$_A$R is a lesser studied GABA$_A$R isoform, with relatively little known about certain properties of the receptor. This thesis relied on the results of two studies – Picton & Fisher (2007) and Syed et al. (2020) – for the kinetic properties of α3-GABA$_A$Rs. Picton & Fisher (2007) used rapid ligand application recordings from excised macropatches to investigate the activation, deactivation, desensitisation and recovery kinetics for each of the six α subunit isoforms, including α3. Syed et al. (2020) employed a HEK-293 cell-neuron co-culture expression system, which enabled the recording of IPSCs mediated by a pure population of GABA$_A$Rs with a defined subunit composition. While both approaches have their merits, one of the aims of this project was to further investigate how α3-GABA$_A$Rs influence the kinetic properties of sIPSCs by recording in the native and more physiological setting of hippocampal neurons in cell culture.

PTX has previously been successfully used to pharmacologically isolate engineered PTX-resistant δ subunit-containing receptors (Sun et al., 2018). To this end, attempts were made to create an α3 subunit equivalent that was insensitive to this mixed non-competitive GABA$_A$R antagonist, based on literature highlighting residues that induce

PTX resistance when mutated in other GABA$_A$R subunits (Ffrench-Constant et al., 1993; Zhang et al., 1994; Xu et al., 1995; Ueno et al., 2000; Sedelnikova et al., 2006). Transfection of a normally PTX-insensitive subunit into hippocampal neurons in cell culture would then enable the sIPSCs mediated only through PTX-insensitive α3-GABA$_A$Rs to be isolated following application of PTX, consequently allowing the study of α3-GABA$_A$R-mediated sIPSCs in effective isolation.

Mutation of residue T313 in TM2 of the α3 subunit to phenylalanine (based on an equivalent study in α1 by Sedelnikova et al. (2006)) conferred substantial, although not total, resistance to PTX (Fig. 5.1). However, this same mutation significantly reduced the sensitivity of the receptor for GABA, causing a ten-fold rightward shift in the GABA CRC (Fig. 5.2A). This was unexpected, given the equivalent mutation in α1 caused only a minimal, two-fold rightward shift (Sedelnikova et al., 2006). The mutant α3^{T313F}β3γ2L receptors also had significantly lower maximum current density values (Fig. 5.2C), and they deactivated and desensitised significantly more quicky (Fig. 5.3), compared to the wildtype α3β3γ2L receptors. Given the extent of the effect of α3^{T313F} on receptor function, it was deemed inappropriate to use the modified subunit to isolate α3-GABA$_A$R-specific sIPSCs as ideally, such a reporter mutation should have minimal effects on other aspects of receptor function.

Two further attempts were made to create a PTX-insensitive α3 subunit, by substituting residue V309 with cysteine and serine respectively. While these substitutions have imparted PTX resistance in other receptor subtypes (Ffrench-Constant et al., 1993; Zhang et al., 1994; Xu et al., 1995; Ueno et al., 2000), neither did so for the α3 subunit (Fig. 5.4), highlighting important differences between subunits.

While a mutation could not be made to the α3 subunit that abolishes receptor PTX sensitivity without affecting other receptor properties, these experiments represent a creative idea for isolating sIPSCs mediated through specific GABA$_A$R subtypes without having to use complicated and less physiological HEK-293 cell-neuron co-culture systems. Perhaps they will be more successful for other GABA$_A$R subunits, or other α3 subunit residues may yield usable receptor variants.

6.3.3. shRNA knockdown experiments

In a further attempt to investigate the contribution of α3-GABA$_A$Rs to inhibitory neurotransmission, shRNAs that specifically target sequences within *Gabra3* mRNA were assessed as a means of knocking down native α3 subunit expression. As shRNAs are a standard means of silencing gene expression (Lambeth & Smith, 2013), and have been shown to be effective against other GABA$_A$R subunits (e.g., Li et al., 2005), it was surprising that none of the six α3-specific shRNAs tested in this study appeared effective at knocking down expression of α3 (Figs. 5.5-5.8), with the exception of a mild effect on sIPSC frequency (the potential implications of which are discussed in section 5.3.2). Indeed, other studies have successfully used shRNAs – albeit targeting sequences within human, rather than rat or mouse, *GABRA3* – to silence α3 expression (Liu et al., 2008; Liu et al., 2016).

This raises the question of whether these shRNAs were truly all ineffective at reducing α3 subunit expression. Gene knockdown is most often assessed biochemically (e.g., using western blots, as was the case in Liu et al. (2008) and Liu et al. (2016)) or via immunocytochemistry. In this study, knockdown was assessed using electrophysiological techniques. It could be the case that whole-cell electrophysiological experiments cannot detect shRNA-mediated reductions in gene expression, particularly if such reductions are only partial and not complete. However, the aim of these experiments was to assess the impact of knocking down the expression of endogenous α3 on neuronal sIPSC kinetics, which can only be assessed using electrophysiology. Therefore, while it may well be the case that the shRNAs used here silence *Gabra3* expression, and this may well be detected using another experimental system, such other systems would not have provided the information desired from these experiments.

6.4. Remaining questions and future work

6.4.1. Are residues T401 and Y402 in the gephyrin binding domain of the α3 subunit phosphorylation sites?

This project was built on the basis that phosphorylation of the investigated consensus residues could regulate the binding of the α3-GABA$_A$R to gephyrin and consequently, the subcellular localisation of this receptor isoform. While a number of studies indicate that these residues are potential phosphorylation sites (Bell-Horner et al., 2006; Munton et al., 2007; Ballif et al., 2008; Mukherjee et al., 2011; Maric et al., 2014), there as yet exists no definitive evidence to demonstrate that the residues actually are phosphorylated *in vivo.* Experiments to determine whether residues T401 and Y402 in the gephyrin binding domain of the α3 subunit are phosphorylation sites would therefore be desirable. Phos-tag SDS PAGE electrophoresis could potentially provide a simple means of doing this; however, previous experiments conducted by other lab members have found that these Phos-tag gels can be compromised as a means of assessing phosphorylation for GABA$_A$Rs due to receptor aggregation. An alternative method of determining whether these residues are phosphorylated (or indeed, subject to any other form of post-translational modification) could instead be provided through mass spectrometry, which can detect post-translational modifications either as a mass increment or as a mass deficit relative to the unmodified protein (Larsen et al., 2006).

6.4.2. Does phosphorylation of Y402 diminish the interaction between the α3 subunit and gephyrin?

As already discussed, mimicking phosphorylation via aspartate substitution at Y402 seems to disrupt the interaction between α3 and gephyrin; however, this could not be confirmed using co-IP experiments (see section 4.2.3). Nevertheless, this is still important for understanding the role that Y402 plays in regulating gephyrin binding and subsequent α3-GABA$_A$R subcellular localisation. α3^{Y402D} receptors displayed significantly less co-localisation with gephyrin compared to their wildtype and phospho-null counterparts (Fig. 4.4). Therefore, establishing whether this mutation

diminishes the binding between α3 and gephyrin would confirm whether this observed reduction in co-localisation is due to the reduced or weakened binding of gephyrin to the α3-GABA$_A$R, or whether it is due to some other, as yet to be determined, mechanism. As mentioned in section 6.3.1, a potential experimental approach to quantitatively investigate the α3-gephyrin binding interaction may be found in affinity capillary electrophoresis (Chu et al., 1992).

6.4.3. What other proteins are involved in the subcellular localisation of the α3-GABA$_A$R?

A key interpretation of the SIM imaging data presented in this thesis is that α3^{Y402D}-GABA$_A$Rs are clustered at GABAergic synapses that retain them via a gephyrin-independent mechanism (see chapter 4). Multiple different proteins are involved in GABA$_A$R clustering, with the principal scaffold protein gephyrin having long been purported to play a key role in the recruitment and anchoring of GABA$_A$Rs at GABAergic synapses (Essrich et al., 1998; Kneussel et al., 1999; Jacob et al., 2005; Mukherjee et al., 2011). However, as discussed in previous sections, gephyrin-independent clustering mechanisms clearly also exist (Kneusssel et al., 2001; Lévi et al., 2004; Niwa et al., 2012). Therefore, experiments to determine what the potential gephyrin-independent mechanism(s) responsible for the synaptic clustering of α3^{Y402D}-GABA$_A$Rs may be, as well as the proteins involved, would further illuminate how α3-GABA$_A$R subcellular localisation is regulated. Potential candidates already exist in the clustering proteins collybistin (Chiou et al., 2011; George et al., 2021), neurobeachin (Nair et al., 2012), GARLH (Davenport et al., 2017; Yamasaki et al., 2017) and NL2 (Poulopoulos et al., 2009).

Additionally, α3-GABA$_A$Rs are one of the few receptor subtypes that localise at both synaptic and extrasynaptic sites (Studer et al., 2006; Liu et al., 2007; Marowsky et al., 2013). Indeed, the α3-VIAAT co-localisation data indicates that the majority (~80%) of α3-GABA$_A$Rs in hippocampal neurons in cell culture are extrasynaptic (Fig. 4.5A). α5-GABA$_A$Rs also exhibit this differential localisation (Serwanski et al., 2006). It has been shown that the actin-binding protein radixin specifically localises α5-GABA$_A$Rs at

extrasynaptic sites (Loebrich et al., 2006); it would not be unreasonable to assume the existence of an analogous protein (or proteins) that mediates the extrasynaptic clustering of α3-GABA$_A$Rs. Experiments to identify such proteins would thus also be of benefit.

6.4.4. *Which kinases and phosphatases regulate the putative phosphorylation of Y402?*

If Y402 is shown to be a true phosphorylation site, experiments could be conducted to identify the kinase(s) and phosphatase(s) involved in regulating phosphorylation at this residue. This could be done by performing whole-cell electrophysiology on HEK-293 cells transfected with wildtype and mutant α3-GABA$_A$Rs in the presence of a broad-spectrum kinase inhibitor, such as staurosporine. Gradually, the specificity of the inhibitor could be narrowed down (to genistein or the tyrphostins, for example) (Dunne et al., 1998) in order to identify the putative kinases responsible for phosphorylating Y402. The same process can be performed with phosphatase inhibitors.

Identification of the kinases and phosphatases responsible for regulating Y402 phosphorylation would subsequently enable the expansion of research into means of manipulating the phosphorylation state of the residue in order to influence the subcellular localisation of α3-GABA$_A$Rs. Given the disease states α3-GABA$_A$Rs have been implicated in (see section 1.4), such manipulation may prove to be of significant therapeutic benefit.

6.5. Concluding remarks

Prior to this study, our understanding of the molecular mechanisms that control the subcellular localisation of the α3-GABA$_A$ receptor, including its interactions with the synaptic scaffold protein gephyrin, was limited. In the present study, phospho-null (phenyl)alanine and phospho-mimetic aspartate substitutions of three key residues, T400, T401 and Y402, located within the gephyrin binding domain of the α3 subunit,

were used to investigate the role that phosphorylation plays in the regulation of α3-GABA$_A$R subcellular localisation.

Here, we demonstrated that preventing and/or mimicking phosphorylation at all three of these residues affects receptor GABA sensitivity when assessed using whole-cell electrophysiology on transfected HEK-293 cells. Electrophysiological interrogation of the T401 and Y402 phospho-mimetic mutants in hippocampal neurons in cell culture further demonstrated alterations in receptor kinetics consistent with changes in subcellular localisation. Subsequent protein localisation analysis using structured illumination microscopy revealed a reduction in the proportion of inhibitory synapses containing α3^{Y402D}-GABA$_A$Rs. However, these receptors were more concentrated in those synapses where they were retained. As the SIM imaging data also revealed less co-localisation between the α3^{Y402D}-GABA$_A$Rs receptors and gephyrin compared to wildtype and α3^{Y402F}-GABA$_A$ receptors, it is highly likely that this concentration is mediated through gephyrin-independent clustering mechanisms.

References

Abramian, A.M., Comenencia-Ortiz, E., Modgil, A., Vien, T.N., et al. (2014) Neurosteroids promote phosphorylation and membrane insertion of extrasynaptic GABA$_A$ receptors. Proceedings of the National Academy of Sciences of the United States of America. 111 (19), 7132–7137.

Abramian, A.M., Comenencia-Ortiz, E., Vithlani, M., Tretter, E.V., et al. (2010) Protein kinase C phosphorylation regulates membrane insertion of GABA$_A$ receptor subtypes that mediate tonic inhibition. The Journal of Biological Chemistry. 285 (53), 41795–41805.

Adams, J.M., Thomas, P. & Smart, T.G. (2015) Modulation of neurosteroid potentiation by protein kinases at synaptic- and extrasynaptic-type GABA$_A$ receptors. Neuropharmacology. 88, 63–73.

Alam, S., Laughton, D.L., Walding, A. & Wolstenholme, A.J. (2006) Human peripheral blood mononuclear cells express GABA$_A$ receptor subunits. Molecular Immunology. 43 (9), 1432–1442.

Alldred, M.J., Mulder-Rosi, J., Lingenfelter, S.E., Chen, G., et al. (2005) Distinct γ2 subunit domains mediate clustering and synaptic function of postsynaptic GABA$_A$ receptors and gephyrin. The Journal of Neuroscience. 25 (3), 594–603.

Allen, K., Fuchs, E.C., Jaschonek, H., Bannerman, D.M., et al. (2011) Gap junctions between interneurons are required for normal spatial coding in the hippocampus and short-term spatial memory. The Journal of Neuroscience. 31 (17), 6542–6552.

Amin, J. & Weiss, D.S. (1993) GABA$_A$ receptor needs two homologous domains of the β-subunit for activation by GABA but not by pentobarbital. Nature. 366 (6455), 565–569.

Andrews, P.R. & Johnston, G.A. (1979) GABA agonists and antagonists. Biochemical Pharmacology. 28 (18), 2697–2702.

Ardito, F., Giuliani, M., Perrone, D., Troiano, G., et al. (2017) The crucial role of protein phosphorylation in cell signaling and its use as targeted therapy. International Journal of Molecular Medicine.   40 (2), 271–280.

Atack, J.R., Hutson, P.H., Collinson, N., Marshall, G., et al. (2005) Anxiogenic properties of an inverse agonist selective for α3 subunit-containing GABA$_A$ receptors. British Journal of Pharmacology. 144 (3), 357–366.

Ballif, B.A., Carey, G.R., Sunyaev, S.R. & Gygi, S.P. (2008) Large-scale identification and evolution indexing of tyrosine phosphorylation sites from murine brain. Journal of Proteome Research. 7 (1), 311–318.

Baulieu, E.E. (1997) Neurosteroids: of the nervous system, by the nervous system, for the nervous system. Recent progress in hormone research. 52, 1–32.

Baumann, S.W., Baur, R. & Sigel, E. (2002) Forced subunit assembly in α1β2γ2 GABA$_A$ receptors. Insight into the absolute arrangement. The Journal of Biological Chemistry. 277 (48), 46020–46025.

Belelli, D., Casula, A., Ling, A. & Lambert, J.J. (2002) The influence of subunit composition on the interaction of neurosteroids with GABA$_A$ receptors. Neuropharmacology. 43 (4), 651–661.

Bell-Horner, C.L., Dohi, A., Nguyen, Q., Dillon, G.H., et al. (2006) ERK/MAPK pathway regulates GABA$_A$ receptors. Journal of Neurobiology. 66 (13), 1467–1474.

Ben-Ari, Y. (2002) Excitatory actions of GABA during development: the nature of the nurture. Nature Reviews. Neuroscience. 3 (9), 728–739.

Benjamin, P.R., Staras, K. & Kemenes, G. (2010) What roles do tonic inhibition and disinhibition play in the control of motor programs? Frontiers in Behavioral Neuroscience. 4, 30.

Berggaard, N., Seifi, M., van der Want, J.J.L. & Swinny, J.D. (2018) Spatiotemporal distribution of GABA$_A$ receptor subunits within layer II of mouse medial entorhinal cortex: implications for grid cell excitability. Frontiers in Neuroanatomy. 12, 46.

Bianchi, M.T., Haas, K.F. & Macdonald, R.L. (2002) α1 and α6 subunits specify distinct desensitization, deactivation and neurosteroid modulation of GABA$_A$ receptors containing the δ subunit. Neuropharmacology. 43 (4), 492–502.

Bianchi, M.T. & Macdonald, R.L. (2003) Neurosteroids shift partial agonist activation of GABA$_A$ receptor channels from low- to high-efficacy gating patterns. The Journal of Neuroscience. 23 (34), 10934–10943.

Bjurstöm, H., Wang, J., Ericsson, I., Bengtsson, M., et al. (2008) GABA, a natural immunomodulator of T lymphocytes. Journal of Neuroimmunology. 205 (1–2), 44–50.

Bogdanov, Y., Michels, G., Armstrong-Gold, C., Haydon, P.G., et al. (2006) Synaptic GABA$_A$ receptors are directly recruited from their extrasynaptic counterparts. The EMBO Journal. 25 (18), 4381–4389.

Böhme, I., Rabe, H. & Lüddens, H. (2004) Four amino acids in the α subunits determine the γ-aminobutyric acid sensitivities of GABA$_A$ receptor subtypes. The Journal of Biological Chemistry. 279 (34), 35193–35200.

Bowery, N.G. & Smart, T.G. (2006) GABA and glycine as neurotransmitters: a brief history. British Journal of Pharmacology. 147 Suppl 1, S109-19.

Brady, M.L. & Jacob, T.C. (2015) Synaptic localization of α5-GABA$_A$ receptors via gephyrin interaction regulates dendritic outgrowth and spine maturation. Developmental Neurobiology. 75 (11), 1241–1251.

Brickley, S.G., Cull-Candy, S.G. & Farrant, M. (1996) Development of a tonic form of synaptic inhibition in rat cerebellar granule cells resulting from persistent activation of GABA$_A$ receptors. The Journal of Physiology. 497 (Pt 3), 753–759.

Brickley, S.G. & Mody, I. (2012) Extrasynaptic GABA$_A$ receptors: their function in the CNS and implications for disease. Neuron. 73 (1), 23–34.

Bright, D.P., Aller, M.I. & Brickley, S.G. (2007) Synaptic release generates a tonic GABA$_A$ receptor-mediated conductance that modulates burst precision in thalamic relay neurons. The Journal of Neuroscience. 27 (10), 2560–2569.

Bright, D.P., Renzi, M., Bartram, J., McGee, T.P., et al. (2011) Profound desensitization by ambient GABA limits activation of δ-containing GABA$_A$ receptors during spillover. The Journal of Neuroscience. 31 (2), 753–763.

Brown, N., Kerby, J., Bonnert, T.P., Whiting, P.J., et al. (2002) Pharmacological characterization of a novel cell line expressing human α(4)β(3)δ GABA$_A$ receptors. British Journal of Pharmacology. 136 (7), 965–974.

Brünig, I., Scotti, E., Sidler, C. & Fritschy, J.-M. (2002) Intact sorting, targeting, and clustering of γ-aminobutyric acid A receptor subtypes in hippocampal neurons in vitro. The Journal of Comparative Neurology. 443 (1), 43–55.

Callachan, H., Cottrell, G.A., Hather, N.Y., Lambert, J.J., et al. (1987) Modulation of the GABA$_A$ receptor by progesterone metabolites. Proceedings of the Royal Society of London. Series B, Containing Papers of a Biological Character. Royal Society (Great Britain). 231 (1264), 359–369.

Caraiscos, V.B., Elliott, E.M., You-Ten, K.E., Cheng, V.Y., et al. (2004) Tonic inhibition in mouse hippocampal CA1 pyramidal neurons is mediated by α5 subunit-containing γ-aminobutyric acid type A receptors. Proceedings of the National Academy of Sciences of the United States of America. 101 (10), 3662–3667.

Charych, E.I., Yu, W., Miralles, C.P., Serwanski, D.R., et al. (2004) The brefeldin A-inhibited GDP/GTP exchange factor 2, a protein involved in vesicular trafficking, interacts with the β subunits of the GABA receptors. Journal of Neurochemistry. 90 (1), 173–189.

Chen, Z.-W., Bracamontes, J.R., Budelier, M.M., Germann, A.L., et al. (2019) Multiple functional neurosteroid binding sites on GABA$_A$ receptors. PLoS Biology. 17 (3), e3000157.

Cheng, V.Y., Martin, L.J., Elliott, E.M., Kim, J.H., et al. (2006) α5-GABA$_A$ receptors mediate the amnestic but not sedative-hypnotic effects of the general anesthetic etomidate. The Journal of Neuroscience. 26 (14), 3713–3720.

Chiou, T.-T., Bonhomme, B., Jin, H., Miralles, C.P., et al. (2011) Differential regulation of the postsynaptic clustering of γ-aminobutyric acid type A (GABA$_A$) receptors by collybistin isoforms. The Journal of Biological Chemistry. 286 (25), 22456–22468.

Cho, Y.S., Song, W.S., Yoon, S.H., Park, K.-Y., et al. (2018) Syringaresinol suppresses excitatory synaptic transmission and picrotoxin-induced epileptic activity in the hippocampus through presynaptic mechanisms. Neuropharmacology. 131, 68–82.

Christian, C.A., Herbert, A.G., Holt, R.L., Peng, K., et al. (2013) Endogenous positive allosteric modulation of GABA$_A$ receptors by diazepam binding inhibitor. Neuron. 78 (6), 1063–1074.

Christian, C.A. & Huguenard, J.R. (2013) Astrocytes potentiate GABAergic transmission in the thalamic reticular nucleus via endozepine signaling. Proceedings of the National Academy of Sciences of the United States of America. 110 (50), 20278–20283.

Christian, E.P., Snyder, D.H., Song, W., Gurley, D.A., et al. (2015) EEG-β/γ spectral power elevation in rat: a translatable biomarker elicited by $GABA_A(\alpha2/3)$-positive allosteric modulators at nonsedating anxiolytic doses. Journal of Neurophysiology. 113 (1), 116–131.

Chu, Y.H., Avila, L.Z., Biebuyck, H.A. & Whitesides, G.M. (1992) Use of affinity capillary electrophoresis to measure binding constants of ligands to proteins. Journal of Medicinal Chemistry. 35 (15), 2915–2917.

Churn, S.B., Rana, A., Lee, K., Parsons, J.T., et al. (2004) Calcium/calmodulin-dependent kinase II phosphorylation of the $GABA_A$ receptor α1 subunit modulates benzodiazepine binding. Journal of Neurochemistry. 82 (5), 1065–1076.

Cobb, S.R., Buhl, E.H., Halasy, K., Paulsen, O., et al. (1995) Synchronization of neuronal activity in hippocampus by individual GABAergic interneurons. Nature. 378 (6552), 75–78.

Collinson, N., Kuenzi, F.M., Jarolimek, W., Maubach, K.A., et al. (2002) Enhanced learning and memory and altered GABAergic synaptic transmission in mice lacking the α5 subunit of the $GABA_A$ receptor. The Journal of Neuroscience. 22 (13), 5572–5580.

Colombi, I., Mahajani, S., Frega, M., Gasparini, L., et al. (2013) Effects of antiepileptic drugs on hippocampal neurons coupled to micro-electrode arrays. Frontiers in Neuroengineering. 6, 10.

Colquhoun, D. (1998) Binding, gating, affinity and efficacy: the interpretation of structure-activity relationships for agonists and of the effects of mutating receptors. British Journal of Pharmacology. 125 (5), 924–947.

Crosby, K.C., Gookin, S.E., Garcia, J.D., Hahm, K.M., et al. (2019) Nanoscale subsynaptic domains underlie the organization of the inhibitory synapse. Cell reports. 26 (12), 3284-3297.e3.

Daniel, C. & Ohman, M. (2009) RNA editing and its impact on GABA$_A$ receptor function. Biochemical Society Transactions. 37 (Pt 6), 1399–1403.

Daniel, C., Wahlstedt, H., Ohlson, J., Björk, P., et al. (2011) Adenosine-to-inosine RNA editing affects trafficking of the γ-aminobutyric acid type A (GABA$_A$) receptor. The Journal of Biological Chemistry. 286 (3), 2031–2040.

Davenport, E.C., Pendolino, V., Kontou, G., McGee, T.P., et al. (2017) An Essential Role for the Tetraspanin LHFPL4 in the Cell-Type-Specific Targeting and Clustering of Synaptic GABA$_A$ Receptors. Cell reports. 21 (1), 70–83.

Dawson, G.R., Maubach, K.A., Collinson, N., Cobain, M., et al. (2006) An inverse agonist selective for α5 subunit-containing GABA$_A$ receptors enhances cognition. The Journal of Pharmacology and Experimental Therapeutics. 316 (3), 1335–1345.

Devor, A., Fritschy, J.M. & Yarom, Y. (2001) Spatial distribution and subunit composition of GABA$_A$ receptors in the inferior olivary nucleus. Journal of Neurophysiology. 85 (4), 1686–1696.

Dias, R., Sheppard, W.F.A., Fradley, R.L., Garrett, E.M., et al. (2005) Evidence for a significant role of α3-containing GABA$_A$ receptors in mediating the anxiolytic effects of benzodiazepines. The Journal of Neuroscience. 25 (46), 10682–10688.

Duggan, M.J., Pollard, S. & Stephenson, F.A. (1991) Immunoaffinity purification of GABA$_A$ receptor α-subunit iso-oligomers. Demonstration of receptor populations containing α1 α2, α1 α3, and α2 α3 subunit pairs. The Journal of Biological Chemistry. 266 (36), 24778–24784.

Dunne, E.L., Moss, S.J. & Smart, T.G. (1998) Inhibition of GABA$_A$ receptor function by tyrosine kinase inhibitors and their inactive analogues. Molecular and Cellular Neurosciences. 12 (4–5), 300–310.

Eickhoff, M., Kovac, S., Shahabi, P., Ghadiri, M.K., et al. (2014) Spreading depression triggers ictaform activity in partially disinhibited neuronal tissues. Experimental Neurology. 253, 1–15.

Essrich, C., Lorez, M., Benson, J.A., Fritschy, J.M., et al. (1998) Postsynaptic clustering of major GABA$_A$ receptor subtypes requires the γ2 subunit and gephyrin. Nature Neuroscience. 1 (7), 563–571.

Everington, E.A., Gibbard, A.G., Swinny, J.D. & Seifi, M. (2018) Molecular Characterization of GABA$_A$ Receptor Subunit Diversity within Major Peripheral Organs and Their Plasticity in Response to Early Life Psychosocial Stress. Frontiers in Molecular Neuroscience. 11, 18.

Farrant, M. & Nusser, Z. (2005) Variations on an inhibitory theme: phasic and tonic activation of GABA$_A$ receptors. Nature Reviews. Neuroscience. 6 (3), 215–229.

Ferrante, M., Migliore, M. & Ascoli, G.A. (2009) Feed-forward inhibition as a buffer of the neuronal input-output relation. Proceedings of the National Academy of Sciences of the United States of America. 106 (42), 18004–18009.

Ffrench-Constant, R.H., Rocheleau, T.A., Steichen, J.C. & Chalmers, A.E. (1993) A point mutation in a Drosophila GABA receptor confers insecticide resistance. Nature. 363 (6428), 449–451.

Field, M., Dorovykh, V., Thomas, P. & Smart, T.G. (2021) Physiological role for GABA$_A$ receptor desensitization in the induction of long-term potentiation at inhibitory synapses. Nature Communications. 12 (1), 2112.

Fischer, B.D., Atack, J.R., Platt, D.M., Reynolds, D.S., et al. (2011) Contribution of GABA$_A$ receptors containing α3 subunits to the therapeutic-related and side effects of benzodiazepine-type drugs in monkeys. Psychopharmacology. 215 (2), 311–319.

Fritschy, J.M., Benke, D., Mertens, S., Oertel, W.H., et al. (1992) Five subtypes of type A γ-aminobutyric acid receptors identified in neurons by double and triple immunofluorescence staining with subunit-specific antibodies. Proceedings of the National Academy of Sciences of the United States of America. 89 (15), 6726–6730.

Fritschy, J.M. & Brünig, I. (2003) Formation and plasticity of GABAergic synapses: physiological mechanisms and pathophysiological implications. Pharmacology & Therapeutics. 98 (3), 299–323.

Fritschy, J.M., Harvey, R.J. & Schwarz, G. (2008) Gephyrin: where do we stand, where do we go? Trends in Neurosciences. 31 (5), 257–264.

Fritschy, J.M. & Mohler, H. (1995) GABA$_A$-receptor heterogeneity in the adult rat brain: differential regional and cellular distribution of seven major subunits. The Journal of Comparative Neurology. 359 (1), 154–194.

Fritschy, J.M. & Panzanelli, P. (2014) GABA$_A$ receptors and plasticity of inhibitory neurotransmission in the central nervous system. The European Journal of Neuroscience. 39 (11), 1845–1865.

Gaspary, H.L., Wang, W. & Richerson, G.B. (1998) Carrier-mediated GABA release activates GABA receptors on hippocampal neurons. Journal of Neurophysiology. 80 (1), 270–281.

George, S., Bear, J., Taylor, M.J., Kanamalla, K., et al. (2021) Collybistin SH3-protein isoforms are expressed in the rat brain promoting gephyrin and GABA$_A$ receptor clustering at GABAergic synapses. Journal of Neurochemistry. 157 (4), 1032–1051.

Gilles, J.F., Dos Santos, M., Boudier, T., Bolte, S., et al. (2017) DiAna, an ImageJ tool for object-based 3D co-localization and distance analysis. Methods. 115, 55–64.

Gingrich, K.J., Roberts, W.A. & Kass, R.S. (1995) Dependence of the $GABA_A$ receptor gating kinetics on the α-subunit isoform: implications for structure-function relations and synaptic transmission. The Journal of Physiology. 489 (Pt 2), 529–543.

Glykys, J. & Mody, I. (2007) The main source of ambient GABA responsible for tonic inhibition in the mouse hippocampus. The Journal of Physiology. 582 (Pt 3), 1163–1178.

Gonzalez-Burgos, G., Hashimoto, T. & Lewis, D.A. (2010) Alterations of cortical GABA neurons and network oscillations in schizophrenia. Current Psychiatry Reports. 12 (4), 335–344.

Groen, M.R., Paulsen, O., Pérez-Garci, E., Nevian, T., et al. (2014) Development of dendritic tonic GABAergic inhibition regulates excitability and plasticity in CA1 pyramidal neurons. Journal of Neurophysiology. 112 (2), 287–299.

Gu, Y., Chiu, S.-L., Liu, B., Wu, P.-H., et al. (2016) Differential vesicular sorting of AMPA and $GABA_A$ receptors. Proceedings of the National Academy of Sciences of the United States of America. 113 (7), E922-31.

Gumireddy, K., Li, A., Kossenkov, A.V., Sakurai, M., et al. (2016) The mRNA-edited form of GABRA3 suppresses GABRA3-mediated Akt activation and breast cancer metastasis. Nature Communications. 7, 10715.

Günther, U., Benson, J., Benke, D., Fritschy, J.M., et al. (1995) Benzodiazepine-insensitive mice generated by targeted disruption of the γ2 subunit gene of γ-aminobutyric acid type A receptors. Proceedings of the National Academy of Sciences of the United States of America. 92 (17), 7749–7753.

Haas, K.F. & Macdonald, R.L. (1999) GABA$_A$ receptor subunit γ2 and δ subtypes confer unique kinetic properties on recombinant GABA$_A$ receptor currents in mouse fibroblasts. The Journal of Physiology. 514 (1), 27–45.

Hedblom, E. & Kirkness, E.F. (1997) A novel class of GABA$_A$ receptor subunit in tissues of the reproductive system. The Journal of Biological Chemistry. 272 (24), 15346–15350.

Heintzmann, R. & Huser, T. (2017) Super-Resolution Structured Illumination Microscopy. Chemical Reviews. 117 (23), 13890–13908.

Hörtnagl, H., Tasan, R.O., Wieselthaler, A., Kirchmair, E., et al. (2013) Patterns of mRNA and protein expression for 12 GABA$_A$ receptor subunits in the mouse brain. Neuroscience. 236, 345–372.

Hosie, A.M., Clarke, L., da Silva, H. & Smart, T.G. (2009) Conserved site for neurosteroid modulation of GABA$_A$ receptors. Neuropharmacology. 56 (1), 149–154.

Hosie, A.M., Wilkins, M.E., da Silva, H.M.A. & Smart, T.G. (2006) Endogenous neurosteroids regulate GABA$_A$ receptors through two discrete transmembrane sites. Nature. 444 (7118), 486–489.

Hosie, A.M., Wilkins, M.E. & Smart, T.G. (2007) Neurosteroid binding sites on GABA$_A$ receptors. Pharmacology & Therapeutics. 116 (1), 7–19.

Houston, C.M., Lee, H.H.C., Hosie, A.M., Moss, S.J., et al. (2007) Identification of the sites for CaMK-II-dependent phosphorylation of GABA$_A$ receptors. The Journal of Biological Chemistry. 282 (24), 17855–17865.

Houston, C.M. & Smart, T.G. (2006) CaMK-II modulation of GABA$_A$ receptors expressed in HEK293, NG108-15 and rat cerebellar granule neurons. The European Journal of Neuroscience. 24 (9), 2504–2514.

Hübner, C.A. & Holthoff, K. (2013) Anion transport and GABA signaling. Frontiers in Cellular Neuroscience. 7, 177.

Huguenard, J.R. & McCormick, D.A. (2007) Thalamic synchrony and dynamic regulation of global forebrain oscillations. Trends in Neurosciences. 30 (7), 350–356.

Huttlin, E.L., Jedrychowski, M.P., Elias, J.E., Goswami, T., et al. (2010) A tissue-specific atlas of mouse protein phosphorylation and expression. Cell. 143 (7), 1174–1189.

Jacob, T.C., Bogdanov, Y.D., Magnus, C., Saliba, R.S., et al. (2005) Gephyrin regulates the cell surface dynamics of synaptic GABA$_A$ receptors. The Journal of Neuroscience. 25 (45), 10469–10478.

Jacob, T.C., Moss, S.J. & Jurd, R. (2008) GABA$_A$ receptor trafficking and its role in the dynamic modulation of neuronal inhibition. Nature Reviews. Neuroscience. 9 (5), 331–343.

Jensen, M.L., Wafford, K.A., Brown, A.R., Belelli, D., et al. (2013) A study of subunit selectivity, mechanism and site of action of the delta selective compound 2 (DS2) at human recombinant and rodent native GABA$_A$ receptors. British Journal of Pharmacology. 168 (5), 1118–1132.

Johnston, G.A.R. (2013) Advantages of an antagonist: bicuculline and other GABA antagonists. British Journal of Pharmacology. 169 (2), 328–336.

Juge, N., Muroyama, A., Hiasa, M., Omote, H., et al. (2009) Vesicular inhibitory amino acid transporter is a Cl$^-$/γ-aminobutyrate Co-transporter. The Journal of Biological Chemistry. 284 (50), 35073–35078.

Kalitin, K.Y., Grechko, O.Y., Spasov, A.A., Sukhov, A.G., et al. (2018) GABAergic Mechanism of Anticonvulsive Effect of Chemical Agent RU-1205. Bulletin of Experimental Biology and Medicine. 164 (5), 629–635.

Kang, S.U., Heo, S. & Lubec, G. (2011) Mass spectrometric analysis of GABA$_A$ receptor subtypes and phosphorylations from mouse hippocampus. Proteomics. 11 (11), 2171–2181.

Kellenberger, S., Malherbe, P. & Sigel, E. (1992) Function of the α1β2γ12S γ-aminobutyric acid type A receptor is modulated by protein kinase C via multiple phosphorylation sites. The Journal of Biological Chemistry. 267 (36), 25660–25663.

Keller, C.A., Yuan, X., Panzanelli, P., Martin, M.L., et al. (2004) The γ2 subunit of GABA$_A$ receptors is a substrate for palmitoylation by GODZ. The Journal of Neuroscience. 24 (26), 5881–5891.

Kelly, L., Seifi, M., Ma, R., Mitchell, S.J., et al. (2020) Identification of intraneuronal amyloid β oligomers in locus coeruleus neurons of Alzheimer's patients and their potential impact on inhibitory neurotransmitter receptors and neuronal excitability. Neuropathology and Applied Neurobiology.

Keramidas, A. & Harrison, N.L. (2010) The activation mechanism of α1β2γ2S and α3β3γ2S GABA$_A$ receptors. The Journal of General Physiology. 135 (1), 59–75.

Kim, Y.S. & Yoon, B.E. (2017) Altered GABAergic signaling in brain disease at various stages of life. Experimental neurobiology. 26 (3), 122–131.

Kins, S., Betz, H. & Kirsch, J. (2000) Collybistin, a newly identified brain-specific GEF, induces submembrane clustering of gephyrin. Nature Neuroscience. 3 (1), 22–29.

Kittler, J.T., Chen, G., Honing, S., Bogdanov, Y., et al. (2005) Phospho-dependent binding of the clathrin AP2 adaptor complex to GABA$_A$ receptors regulates the efficacy of inhibitory synaptic transmission. Proceedings of the National Academy of Sciences of the United States of America. 102 (41), 14871–14876.

Kittler, J.T., Delmas, P., Jovanovic, J.N., Brown, D.A., et al. (2000) Constitutive endocytosis of GABA$_A$ receptors by an association with the adaptin AP2 complex modulates inhibitory synaptic currents in hippocampal neurons. The Journal of Neuroscience. 20 (21), 7972–7977.

Kittler, J.T., Thomas, P., Tretter, V., Bogdanov, Y.D., et al. (2004) Huntingtin-associated protein 1 regulates inhibitory synaptic transmission by modulating γ-aminobutyric acid type A receptor membrane trafficking. Proceedings of the National Academy of Sciences of the United States of America. 101 (34), 12736–12741.

Klausberger, T. & Somogyi, P. (2008) Neuronal diversity and temporal dynamics: the unity of hippocampal circuit operations. Science. 321 (5885), 53–57.

Kneussel, M., Brandstätter, J.H., Gasnier, B., Feng, G., et al. (2001) Gephyrin-independent clustering of postsynaptic GABA$_A$ receptor subtypes. Molecular and Cellular Neurosciences. 17 (6), 973–982.

Kneussel, M., Brandstätter, J.H., Laube, B., Stahl, S., et al. (1999) Loss of postsynaptic GABA$_A$ receptor clustering in gephyrin-deficient mice. The Journal of Neuroscience. 19 (21), 9289–9297.

Koester, C., Rudolph, U., Haenggi, T., Papilloud, A., et al. (2013) Dissecting the role of diazepam-sensitive γ-aminobutyric acid type A receptors in defensive behavioral reactivity to mild threat. Pharmacology, Biochemistry, and Behavior. 103 (3), 541–549.

Korpi, E.R., Gründer, G. & Lüddens, H. (2002) Drug interactions at GABA$_A$ receptors. Progress in Neurobiology. 67 (2), 113–159.

Korshoej, A.R., Holm, M.M., Jensen, K. & Lambert, J.D.C. (2010) Kinetic analysis of evoked IPSCs discloses mechanism of antagonism of synaptic GABA$_A$ receptors by picrotoxin. British Journal of Pharmacology. 159 (3), 636–649.

Kowalczyk, S., Winkelmann, A., Smolinsky, B., Förstera, B., et al. (2013) Direct binding of GABA$_A$ receptor β2 and β3 subunits to gephyrin. The European Journal of Neuroscience. 37 (4), 544–554.

Krabbe, S., Gründemann, J. & Lüthi, A. (2018) Amygdala inhibitory circuits regulate associative fear conditioning. Biological Psychiatry. 83 (10), 800–809.

Kralic, J.E., Sidler, C., Parpan, F., Homanics, G.E., et al. (2006) Compensatory alteration of inhibitory synaptic circuits in cerebellum and thalamus of γ-aminobutyric acid type A receptor α1 subunit knockout mice. The Journal of Comparative Neurology. 495 (4), 408–421.

Krishek, B.J., Xie, X., Blackstone, C., Huganir, R.L., et al. (1994) Regulation of GABA$_A$ receptor function by protein kinase C phosphorylation. Neuron. 12 (5), 1081–1095.

Krogsgaard-Larsen, P., Frølund, B., Liljefors, T. & Ebert, B. (2004) GABA$_A$ agonists and partial agonists: THIP (Gaboxadol) as a non-opioid analgesic and a novel type of hypnotic. Biochemical Pharmacology. 68 (8), 1573–1580.

von Krosigk, M., Bal, T. & McCormick, D.A. (1993) Cellular mechanisms of a synchronized oscillation in the thalamus. Science. 261 (5119), 361–364.

Kullmann, D.M., Ruiz, A., Rusakov, D.M., Scott, R., et al. (2005) Presynaptic, extrasynaptic and axonal GABA$_A$ receptors in the CNS: where and why? Progress in Biophysics and Molecular Biology. 87 (1), 33–46.

Kuriyama, K., Hirouchi, M. & Nakayasu, H. (1993) Structure and function of cerebral GABA$_A$ and GABA$_B$ receptors. Neuroscience Research. 17 (2), 91–99.

Lambeth, L.S. & Smith, C.A. (2013) Short hairpin RNA-mediated gene silencing. Methods in Molecular Biology. 942, 205–232.

Larsen, M.R., Trelle, M.B., Thingholm, T.E. & Jensen, O.N. (2006) Analysis of posttranslational modifications of proteins by tandem mass spectrometry. Biotechniques. 40 (6), 790–798.

Larson, E.A., Accardi, M.V., Wang, Y., D'Antoni, M., et al. (2020) Nitric Oxide Signaling Strengthens Inhibitory Synapses of Cerebellar Molecular Layer Interneurons through a GABARAP-Dependent Mechanism. The Journal of Neuroscience. 40 (17), 3348–3359.

Laurie, D.J., Wisden, W. & Seeburg, P.H. (1992) The distribution of thirteen $GABA_A$ receptor subunit mRNAs in the rat brain. III. Embryonic and postnatal development. The Journal of Neuroscience. 12 (11), 4151–4172.

Laverty, D., Thomas, P., Field, M., Andersen, O.J., et al. (2017) Crystal structures of a $GABA_A$-receptor chimera reveal new endogenous neurosteroid-binding sites. Nature Structural & Molecular Biology. 24 (11), 977–985.

Lavoie, A.M., Tingey, J.J., Harrison, N.L., Pritchett, D.B., et al. (1997) Activation and deactivation rates of recombinant $GABA_A$ receptor channels are dependent on α-subunit isoform. Biophysical Journal. 73 (5), 2518–2526.

Lee, H.J., Absalom, N.L., Hanrahan, J.R., van Nieuwenhuijzen, P., et al. (2016) A pharmacological characterization of GABA, THIP and DS2 at binary α4β3 and β3δ receptors: GABA activates β3δ receptors via the β3(+)δ(-) interface. Brain Research. 1644, 222–230.

Lee, S., Yoon, B.E., Berglund, K., Oh, S.J., et al. (2010) Channel-mediated tonic GABA release from glia. Science. 330 (6005), 790–796.

Leil, T.A., Chen, Z.W., Chang, C.S.S. & Olsen, R.W. (2004) $GABA_A$ receptor-associated protein traffics $GABA_A$ receptors to the plasma membrane in neurons. The Journal of Neuroscience. 24 (50), 11429–11438.

Lévi, S., Logan, S.M., Tovar, K.R. & Craig, A.M. (2004) Gephyrin is critical for glycine receptor clustering but not for the formation of functional GABAergic synapses in hippocampal neurons. The Journal of Neuroscience. 24 (1), 207–217.

Li, R.W., Yu, W., Christie, S., Miralles, C.P., et al. (2005) Disruption of postsynaptic GABA receptor clusters leads to decreased GABAergic innervation of pyramidal neurons. Journal of Neurochemistry. 95 (3), 756–770.

Lisman, J.E. & Jensen, O. (2013) The θ-γ neural code. Neuron. 77 (6), 1002–1016.

Liu, L., Yang, C., Shen, J., Huang, L., et al. (2016) GABRA3 promotes lymphatic metastasis in lung adenocarcinoma by mediating upregulation of matrix metalloproteinases. Oncotarget. 7 (22), 32341–32350.

Liu, X.-B., Coble, J., van Luijtelaar, G. & Jones, E.G. (2007) Reticular nucleus-specific changes in α3 subunit protein at GABA synapses in genetically epilepsy-prone rats. Proceedings of the National Academy of Sciences of the United States of America. 104 (30), 12512–12517.

Liu, Y., Li, Y.H., Guo, F.J., Wang, J.J., et al. (2008) γ-aminobutyric acid promotes human hepatocellular carcinoma growth through overexpressed γ-aminobutyric acid A receptor α3 subunit. World Journal of Gastroenterology. 14 (47), 7175–7182.

Loebrich, S., Bähring, R., Katsuno, T., Tsukita, S., et al. (2006) Activated radixin is essential for GABA$_A$ receptor α5 subunit anchoring at the actin cytoskeleton. The EMBO Journal. 25 (5), 987–999.

Long, M., Zhan, M., Xu, S., Yang, R., et al. (2017) miR-92b-3p acts as a tumor suppressor by targeting Gabra3 in pancreatic cancer. Molecular Cancer. 16 (1), 167.

Lorenz-Guertin, J.M. & Jacob, T.C. (2018) GABA type A receptor trafficking and the architecture of synaptic inhibition. Developmental Neurobiology. 78 (3), 238–270.

Loup, F., Picard, F., André, V.M., Kehrli, P., et al. (2006) Altered expression of α3-containing GABA$_A$ receptors in the neocortex of patients with focal epilepsy. Brain: A Journal of Neurology. 129 (Pt 12), 3277–3289.

Löw, K., Crestani, F., Keist, R., Benke, D., et al. (2000) Molecular and neuronal substrate for the selective attenuation of anxiety. Science. 290 (5489), 131–134.

de Lucas, A.G., Ahring, P.K., Larsen, J.S., Rivera-Arconada, I., et al. (2015) GABA$_A$ α5 subunit-containing receptors do not contribute to reversal of inflammatory-induced spinal sensitization as indicated by the unique selectivity profile of the GABA$_A$ receptor allosteric modulator NS16085. Biochemical Pharmacology. 93 (3), 370–379.

Ludvig, N., Baptiste, S.L., Tang, H.M., Medveczky, G., et al. (2009) Localized transmeningeal muscimol prevents neocortical seizures in rats and nonhuman primates: therapeutic implications. Epilepsia. 50 (4), 678–693.

Luscher, B., Fuchs, T. & Kilpatrick, C.L. (2011) GABA$_A$ receptor trafficking-mediated plasticity of inhibitory synapses. Neuron. 70 (3), 385–409.

Lüthi, A. & Lüscher, C. (2014) Pathological circuit function underlying addiction and anxiety disorders. Nature Neuroscience. 17 (12), 1635–1643.

Macdonald, R.L., Rogers, C.J. & Twyman, R.E. (1989) Kinetic properties of the GABA$_A$ receptor main conductance state of mouse spinal cord neurones in culture. The Journal of Physiology. 410, 479–499.

Magnin, E., Francavilla, R., Amalyan, S., Gervais, E., et al. (2019) Input-Specific Synaptic Location and Function of the α5 GABA$_A$ Receptor Subunit in the Mouse CA1 Hippocampal Neurons. The Journal of Neuroscience. 39 (5), 788–801.

Majewska, M.D., Harrison, N.L., Schwartz, R.D., Barker, J.L., et al. (1986) Steroid hormone metabolites are barbiturate-like modulators of the GABA receptor. Science. 232 (4753), 1004–1007.

Mangan, P.S., Sun, C., Carpenter, M., Goodkin, H.P., et al. (2005) Cultured hippocampal pyramidal neurons express two kinds of GABA$_A$ receptors. Molecular Pharmacology. 67 (3), 775–788.

Mann, E.O. & Mody, I. (2010) Control of hippocampal gamma oscillation frequency by tonic inhibition and excitation of interneurons. Nature Neuroscience. 13 (2), 205–212.

Maric, H.M., Kasaragod, V.B., Hausrat, T.J., Kneussel, M., et al. (2014) Molecular basis of the alternative recruitment of GABA$_A$ versus glycine receptors through gephyrin. Nature Communications. 5, 5767.

Marowsky, A., Rudolph, U., Fritschy, J.M. & Arand, M. (2012) Tonic inhibition in principal cells of the amygdala: a central role for α3 subunit-containing GABA$_A$ receptors. The Journal of Neuroscience. 32 (25), 8611–8619.

Masiulis, S., Desai, R., Uchański, T., Serna Martin, I., et al. (2019) GABA$_A$ receptor signalling mechanisms revealed by structural pharmacology. Nature. 565 (7740), 454–459.

McCartney, M.R., Deeb, T.Z., Henderson, T.N. & Hales, T.G. (2007) Tonically active GABAA receptors in hippocampal pyramidal neurons exhibit constitutive GABA-independent gating. Molecular Pharmacology. 71 (2), 539–548.

McClellan, A.M. & Twyman, R.E. (1999) Receptor system response kinetics reveal functional subtypes of native murine and recombinant human GABA$_A$ receptors. The Journal of Physiology. 515 (Pt 3), 711–727.

McCormick, D.A. & Bal, T. (1997) Sleep and arousal: thalamocortical mechanisms. Annual Review of Neuroscience. 20, 185–215.

McDonald, B.J., Amato, A., Connolly, C.N., Benke, D., et al. (1998) Adjacent phosphorylation sites on GABA$_A$ receptor β subunits determine regulation by cAMP-dependent protein kinase. Nature Neuroscience. 1 (1), 23–28.

McDonald, B.J. & Moss, S.J. (1997) Conserved phosphorylation of the intracellular domains of GABA$_A$ receptor β2 and β3 subunits by cAMP-dependent protein kinase, cGMP-dependent protein kinase, protein kinase C and Ca^{2+}/calmodulin type II-dependent protein kinase. Neuropharmacology. 36 (10), 1377–1385.

McDonald, B.J. & Moss, S.J. (1994) Differential phosphorylation of intracellular domains of γ-aminobutyric acid type A receptor subunits by calcium/calmodulin type 2-dependent protein kinase and cGMP-dependent protein kinase. The Journal of Biological Chemistry. 269 (27), 18111–18117.

McKernan, R.M., Quirk, K., Prince, R., Cox, P.A., et al. (1991) GABA$_A$ receptor subtypes immunopurified from rat brain with α subunit-specific antibodies have unique pharmacological properties. Neuron. 7 (4), 667–676.

McKernan, R.M., Wafford, K., Quirk, K., Hadingham, K.L., et al. (1995) The pharmacology of the benzodiazepine site of the GABA$_A$ receptor is dependent on the type of γ-subunit present. Journal of Receptor and Signal Transduction Research. 15 (1–4), 173–183.

McKernan, R.M. & Whiting, P.J. (1996) Which GABA$_A$-receptor subtypes really occur in the brain? Trends in Neurosciences. 19 (4), 139–143.

Miller, P.S. & Aricescu, A.R. (2014) Crystal structure of a human GABA$_A$ receptor. Nature. 512 (7514), 270–275.

Mitchell, S.J. & Silver, R.A. (2003) Shunting inhibition modulates neuronal gain during synaptic excitation. Neuron. 38 (3), 433–445.

Mody, I. (2001) Distinguishing between GABA$_A$ receptors responsible for tonic and phasic conductances. Neurochemical Research. 26 (8–9), 907–913.

Möhler, H. (2006) GABA$_A$ receptor diversity and pharmacology. Cell and Tissue Research. 326 (2), 505–516.

Morris, H.V., Dawson, G.R., Reynolds, D.S., Atack, J.R., et al. (2006) Both α2 and α3 GABA$_A$ receptor subtypes mediate the anxiolytic properties of benzodiazepine site ligands in the conditioned emotional response paradigm. The European Journal of Neuroscience. 23 (9), 2495–2504.

Mortensen, M., Ebert, B., Wafford, K. & Smart, T.G. (2010) Distinct activities of GABA agonists at synaptic- and extrasynaptic-type GABA$_A$ receptors. The Journal of Physiology. 588 (Pt 8), 1251–1268.

Mortensen, M., Frølund, B., Jørgensen, A.T., Liljefors, T., et al. (2002) Activity of novel 4-PIOL analogues at human α1β2γ2S GABA$_A$ receptors--correlation with hydrophobicity. European Journal of Pharmacology. 451 (2), 125–132.

Mortensen, M., Patel, B. & Smart, T.G. (2011) GABA Potency at GABA$_A$ Receptors Found in Synaptic and Extrasynaptic Zones. Frontiers in Cellular Neuroscience. 6, 1.

Mortensen, M. & Smart, T.G. (2006) Extrasynaptic αβ subunit GABA$_A$ receptors on rat hippocampal pyramidal neurons. The Journal of Physiology. 577 (Pt 3), 841–856.

Moss, S.J., Doherty, C.A. & Huganir, R.L. (1992a) Identification of the cAMP-dependent protein kinase and protein kinase C phosphorylation sites within the major intracellular domains of the β1, γ2S, and γ2L subunits of the γ-aminobutyric acid type A receptor. The Journal of Biological Chemistry. 267 (20), 14470–14476.

Moss, S.J., Gorrie, G.H., Amato, A. & Smart, T.G. (1995) Modulation of GABA$_A$ receptors by tyrosine phosphorylation. Nature. 377 (6547), 344–348.

Moss, S.J. & Smart, T.G. (2001) Constructing inhibitory synapses. Nature Reviews. Neuroscience. 2 (4), 240–250.

Moss, S.J. & Smart, T.G. (1996) Modulation Of Amino Acid-Gated Ion Channels By Protein Phosphorylation. International review of neurobiology volume 39. Elsevier. pp. 1–52.

Moss, S.J., Smart, T.G., Blackstone, C.D. & Huganir, R.L. (1992b) Functional modulation of GABA$_A$ receptors by cAMP-dependent protein phosphorylation. Science. 257 (5070), 661–665.

Mozrzymas, J.W., Zarnowska, E.D., Pytel, M. & Mercik, K. (2003) Modulation of GABA$_A$ receptors by hydrogen ions reveals synaptic GABA transient and a crucial role of the desensitization process. The Journal of Neuroscience. 23 (22), 7981–7992.

Mukherjee, J., Kretschmannova, K., Gouzer, G., Maric, H.-M., et al. (2011) The residence time of GABA$_A$Rs at inhibitory synapses is determined by direct binding of the receptor α1 subunit to gephyrin. The Journal of Neuroscience. 31 (41), 14677–14687.

Munton, R.P., Tweedie-Cullen, R., Livingstone-Zatchej, M., Weinandy, F., et al. (2007) Qualitative and quantitative analyses of protein phosphorylation in naive and stimulated mouse synaptosomal preparations. Molecular & Cellular Proteomics. 6 (2), 283–293.

Nair, R., Lauks, J., Jung, S., Cooke, N.E., et al. (2013) Neurobeachin regulates neurotransmitter receptor trafficking to synapses. The Journal of Cell Biology. 200 (1), 61–80.

Nakamura, Y., Darnieder, L.M., Deeb, T.Z. & Moss, S.J. (2015) Regulation of GABA$_A$Rs by phosphorylation. Advances in Pharmacology. 72, 97–146.

Narahashi, T., Moore, J.W. & Scott, W.R. (1964) Tetrodotoxin blockage of sodium conductance increase in lobster giant axons. The Journal of General Physiology. 47, 965–974.

Neumann, E., Ralvenius, W.T., Acuña, M.A., Rudolph, U., et al. (2018) TP003 is a non-selective benzodiazepine site agonist that induces anxiolysis via α2GABA$_A$ receptors. Neuropharmacology. 143, 71–78.

Newland, C.F. & Cull-Candy, S.G. (1992) On the mechanism of action of picrotoxin on GABA receptor channels in dissociated sympathetic neurones of the rat. The Journal of Physiology. 447, 191–213.

Niturad, C.E., Lev, D., Kalscheuer, V.M., Charzewska, A., et al. (2017) Rare GABRA3 variants are associated with epileptic seizures, encephalopathy and dysmorphic features. Brain: A Journal of Neurology. 140 (11), 2879–2894.

Niwa, F., Bannai, H., Arizono, M., Fukatsu, K., et al. (2012) Gephyrin-independent GABA$_A$R mobility and clustering during plasticity. Plos One. 7 (4), e36148.

Nuss, P. (2015) Anxiety disorders and GABA neurotransmission: a disturbance of modulation. Neuropsychiatric Disease and Treatment. 11, 165–175.

Nusser, Z., Cull-Candy, S. & Farrant, M. (1997) Differences in Synaptic GABA$_A$ Receptor Number Underlie Variation in GABA Mini Amplitude. Neuron. 19 (3), 697–709.

Ohlson, J., Pedersen, J.S., Haussler, D. & Ohman, M. (2007) Editing modifies the GABA$_A$ receptor subunit α3. RNA (New York). 13 (5), 698–703.

Olsen, R.W. (2018) GABA$_A$ receptor: Positive and negative allosteric modulators. Neuropharmacology. 136 (Pt A), 10–22.

Olsen, R.W. & Sieghart, W. (2009) GABA$_A$ receptors: subtypes provide diversity of function and pharmacology. Neuropharmacology. 56 (1), 141–148.

Overstreet, L.S., Westbrook, G.L. & Jones, M.V. (2002) Transmembrane Transporters. M W Quick (ed.). Hoboken, New Jersey, Wiley Liss Inc.

Paddison, P.J., Caudy, A.A., Bernstein, E., Hannon, G.J., et al. (2002) Short hairpin RNAs (shRNAs) induce sequence-specific silencing in mammalian cells. Genes & Development. 16 (8), 948–958.

Palma, E., Ruffolo, G., Cifelli, P., Roseti, C., et al. (2017) Modulation of GABA$_A$ receptors in the treatment of epilepsy. Current Pharmaceutical Design. 23 (37), 5563–5568.

Panzanelli, P., Gunn, B.G., Schlatter, M.C., Benke, D., et al. (2011) Distinct mechanisms regulate GABA$_A$ receptor and gephyrin clustering at perisomatic and axo-axonic synapses on CA1 pyramidal cells. The Journal of Physiology. 589 (Pt 20), 4959–4980.

Papke, D., Gonzalez-Gutierrez, G. & Grosman, C. (2011) Desensitization of neurotransmitter-gated ion channels during high-frequency stimulation: a comparative study of Cys-loop, AMPA and purinergic receptors. The Journal of Physiology. 589 (Pt 7), 1571–1585.

Patel, B., Bright, D.P., Mortensen, M., Frølund, B., et al. (2016) Context-Dependent Modulation of GABA$_A$R-Mediated Tonic Currents. The Journal of Neuroscience. 36 (2), 607–621.

Pavlov, I., Savtchenko, L.P., Kullmann, D.M., Semyanov, A., et al. (2009) Outwardly rectifying tonically active GABA$_A$ receptors in pyramidal cells modulate neuronal offset, not gain. The Journal of Neuroscience. 29 (48), 15341–15350.

Pavlov, I., Savtchenko, L.P., Song, I., Koo, J., et al. (2014) Tonic GABA$_A$ conductance bidirectionally controls interneuron firing pattern and synchronization in the CA3 hippocampal network. Proceedings of the National Academy of Sciences of the United States of America. 111 (1), 504–509.

Picton, A.J. & Fisher, J.L. (2007) Effect of the α subunit subtype on the macroscopic kinetic properties of recombinant GABA$_A$ receptors. Brain Research. 1165, 40–49.

Pillai, G.V., Smith, A.J., Hunt, P.A. & Simpson, P.B. (2004) Multiple structural features of steroids mediate subtype-selective effects on human α4β3δ GABA$_A$ receptors. Biochemical Pharmacology. 68 (5), 819–831.

Pinault, D. (2004) The thalamic reticular nucleus: structure, function and concept. Brain Research. Brain Research Reviews. 46 (1), 1–31.

Pirker, S., Schwarzer, C., Wieselthaler, A., Sieghart, W., et al. (2000) GABA$_A$ receptors: immunocytochemical distribution of 13 subunits in the adult rat brain. Neuroscience. 101 (4), 815–850.

Pouille, F. & Scanziani, M. (2001) Enforcement of temporal fidelity in pyramidal cells by somatic feed-forward inhibition. Science. 293 (5532), 1159–1163.

Poulopoulos, A., Aramuni, G., Meyer, G., Soykan, T., et al. (2009) Neuroligin 2 drives postsynaptic assembly at perisomatic inhibitory synapses through gephyrin and collybistin. Neuron. 63 (5), 628–642.

Reddy, D.S. (2010) Neurosteroids: endogenous role in the human brain and therapeutic potentials. Progress in Brain Research. 186, 113–137.

Richerson, G.B. & Wu, Y. (2003) Dynamic equilibrium of neurotransmitter transporters: not just for reuptake anymore. Journal of Neurophysiology. 90 (3), 1363–1374.

Robertson, C.E., Ratai, E.-M. & Kanwisher, N. (2016) Reduced GABAergic action in the autistic brain. Current Biology. 26 (1), 80–85.

Rogers, C.J., Twyman, R.E. & Macdonald, R.L. (1994) Benzodiazepine and β-carboline regulation of single GABA$_A$ receptor channels of mouse spinal neurones in culture. The Journal of Physiology. 475 (1), 69–82.

Roth, T., Lines, C., Vandormael, K., Ceesay, P., et al. (2010) Effect of gaboxadol on patient-reported measures of sleep and waking function in patients with Primary Insomnia: results from two randomized, controlled, 3-month studies. Journal of clinical sleep medicine: official publication of the American Academy of Sleep Medicine. 6 (1), 30–39.

Rudolph, U., Crestani, F., Benke, D., Brünig, I., et al. (1999) Benzodiazepine actions mediated by specific γ-aminobutyric acid(A) receptor subtypes. Nature. 401 (6755), 796–800.

Rula, E.Y., Lagrange, A.H., Jacobs, M.M., Hu, N., et al. (2008) Developmental modulation of GABA$_A$ receptor function by RNA editing. The Journal of Neuroscience. 28 (24), 6196–6201.

Sajdyk, T.J. & Shekhar, A. (1997) Excitatory amino acid receptors in the basolateral amygdala regulate anxiety responses in the social interaction test. Brain Research. 764 (1–2), 262–264.

Saliba, R.S., Kretschmannova, K. & Moss, S.J. (2012) Activity-dependent phosphorylation of GABA$_A$ receptors regulates receptor insertion and tonic current. The EMBO Journal. 31 (13), 2937–2951.

Schmerl, B., Gimber, N., Kuropka, B., Rentsch, J., et al. (2020) The postsynaptic MAGUK scaffold protein MPP2 organises a distinct interactome that incorporates GABA$_A$ receptors at the periphery of excitatory synapses. BioRxiv.

Schofield, C.M. & Huguenard, J.R. (2007) GABA affinity shapes IPSCs in thalamic nuclei. The Journal of Neuroscience. 27 (30), 7954–7962.

Schofield, C.M., Kleiman-Weiner, M., Rudolph, U. & Huguenard, J.R. (2009) A gain in GABA$_A$ receptor synaptic strength in thalamus reduces oscillatory activity and absence seizures. Proceedings of the National Academy of Sciences of the United States of America. 106 (18), 7630–7635.

Schweizer, C. (2003) The γ2 subunit of GABA$_A$ receptors is required for maintenance of receptors at mature synapses. Molecular and Cellular Neuroscience. 24 (2), 442–450.

Scimemi, A. (2014) Structure, function, and plasticity of GABA transporters. Frontiers in Cellular Neuroscience. 8, 161.

Scimemi, A. & Beato, M. (2009) Determining the neurotransmitter concentration profile at active synapses. Molecular Neurobiology. 40 (3), 289–306. doi:10.1007/s12035-009-8087-7.

Sedelnikova, A., Erkkila, B.E., Harris, H., Zakharkin, S.O., et al. (2006) Stoichiometry of a pore mutation that abolishes picrotoxin-mediated antagonism of the GABA$_A$ receptor. The Journal of Physiology. 577 (Pt 2), 569–577.

Seifi, M., Rodaway, S., Rudolph, U. & Swinny, J.D. (2018) GABA$_A$ Receptor Subtypes Regulate Stress-Induced Colon Inflammation in Mice. Gastroenterology. 155 (3), 852-864.e3.

Serwanski, D.R., Miralles, C.P., Christie, S.B., Mehta, A.K., et al. (2006) Synaptic and non-synaptic localization of GABA$_A$ receptors containing the α5 subunit in the rat brain. The Journal of Comparative Neurology. 499 (3), 458–470.

Sexton, C.A., Penzinger, R., Mortensen, M., Bright, D.P., et al. (2021) Structural determinants and regulation of spontaneous activity in GABA$_A$ receptors. Nature Communications. 12 (1), 5457.

Shen, H., Gong, Q.H., Yuan, M. & Smith, S.S. (2005) Short-term steroid treatment increases δ GABA$_A$ receptor subunit expression in rat CA1 hippocampus: pharmacological and behavioral effects. Neuropharmacology. 49 (5), 573–586.

Sieghart, W. & Sperk, G. (2002) Subunit composition, distribution and function of GABA$_A$ receptor subtypes. Current Topics in Medicinal Chemistry. 2 (8), 795–816.

Sigel, E., Baur, R., Kellenberger, S. & Malherbe, P. (1992) Point mutations affecting antagonist affinity and agonist dependent gating of GABA$_A$ receptor channels. The EMBO Journal. 11 (6), 2017–2023.

Sigel, E. & Lüscher, B.P. (2011) A closer look at the high affinity benzodiazepine binding site on GABA$_A$ receptors. Current Topics in Medicinal Chemistry. 11 (2), 241–246.

Sigel, E. & Steinmann, M.E. (2012) Structure, function, and modulation of GABA$_A$ receptors. The Journal of Biological Chemistry. 287 (48), 40224–40231.

Simon, J., Wakimoto, H., Fujita, N., Lalande, M., et al. (2004) Analysis of the set of GABA(A) receptor genes in the human genome. The Journal of Biological Chemistry. 279 (40), 41422–41435.

Smart, T.G. & Constanti, A. (1986) Studies on the mechanism of action of picrotoxinin and other convulsants at the crustacean muscle GABA receptor. Proceedings of the Royal Society of London. Series B, Containing Papers of a Biological Character. Royal Society (Great Britain). 227 (1247), 191–216.

Somogyi, P. & Klausberger, T. (2005) Defined types of cortical interneurone structure space and spike timing in the hippocampus. The Journal of Physiology. 562 (Pt 1), 9–26.

Song, I., Volynski, K., Brenner, T., Ushkaryov, Y., et al. (2013) Different transporter systems regulate extracellular GABA from vesicular and non-vesicular sources. Frontiers in Cellular Neuroscience. 7, 23.

Stafstrom, C.E. & Rho, J.M. (2017) Neurophysiology of seizures and epilepsy. Swaiman's Pediatric Neurology. Elsevier. pp. 506–512.

Stórustovu, S.I. & Ebert, B. (2006) Pharmacological characterization of agonists at δ-containing GABA$_A$ receptors: Functional selectivity for extrasynaptic receptors is dependent on the absence of γ2. The Journal of Pharmacology and Experimental Therapeutics. 316 (3), 1351–1359.

Studer, R., von Boehmer, L., Haenggi, T., Schweizer, C., et al. (2006) Alteration of GABAergic synapses and gephyrin clusters in the thalamic reticular nucleus of GABA$_A$ receptor α3 subunit-null mice. The European Journal of Neuroscience. 24 (5), 1307–1315.

Sun, M.Y., Shu, H.J., Benz, A., Bracamontes, J., et al. (2018) Chemogenetic isolation reveals synaptic contribution of δ GABA$_A$ receptors in mouse dentate granule neurons. The Journal of Neuroscience. 38 (38), 8128–8145.

Syed, P., Durisic, N., Harvey, R.J., Sah, P., et al. (2020) Effects of GABA$_A$ receptor α3 subunit epilepsy mutations on inhibitory synaptic signaling. Frontiers in Molecular Neuroscience. 13, 602559.

Terlau, J., Yang, J.W., Khastkhodaei, Z., Seidenbecher, T., et al. (2020) Spike-wave discharges in absence epilepsy: segregation of electrographic components reveals distinct pathways of seizure activity. The Journal of Physiology. 598 (12), 2397–2414.

Thomas, P., Mortensen, M., Hosie, A.M. & Smart, T.G. (2005) Dynamic mobility of functional GABA$_A$ receptors at inhibitory synapses. Nature Neuroscience. 8 (7), 889–897.

Tia, S., Kotchabhakdi, N., Wang, J.F. & Vicini, S. (1996) Distinct deactivation and desensitization kinetics of recombinant GABA$_A$ receptors. Neuropharmacology. 35 (9–10), 1375–1382.

Tretter, V., Jacob, T.C., Mukherjee, J., Fritschy, J.M., et al. (2008) The clustering of GABA$_A$ receptor subtypes at inhibitory synapses is facilitated via the direct binding of receptor α2 subunits to gephyrin. The Journal of Neuroscience. 28 (6), 1356–1365.

Tretter, V., Kerschner, B., Milenkovic, I., Ramsden, S.L., et al. (2011) Molecular basis of the γ-aminobutyric acid A receptor α3 subunit interaction with the clustering protein gephyrin. The Journal of Biological Chemistry. 286 (43), 37702–37711.

Tretter, V., Mukherjee, J., Maric, H.M., Schindelin, H., et al. (2012) Gephyrin, the enigmatic organizer at GABAergic synapses. Frontiers in Cellular Neuroscience. 6, 23.

Twyman, R.E. & Macdonald, R.L. (1992) Neurosteroid regulation of GABA$_A$ receptor single-channel kinetic properties of mouse spinal cord neurons in culture. The Journal of Physiology. 456, 215–245.

Tyagarajan, S.K. & Fritschy, J.M. (2014) Gephyrin: a master regulator of neuronal function? Nature Reviews. Neuroscience. 15 (3), 141–156.

Ueno, S., Bracamontes, J., Zorumski, C., Weiss, D.S., et al. (1997) Bicuculline and gabazine are allosteric inhibitors of channel opening of the GABAA receptor. The Journal of Neuroscience. 17 (2), 625–634.

Ueno, S., Lin, A., Nikolaeva, N., Trudell, J.R., et al. (2000) Tryptophan scanning mutagenesis in TM2 of the $GABA_A$ receptor α subunit: effects on channel gating and regulation by ethanol. British Journal of Pharmacology. 131 (2), 296–302.

Verdoorn, T.A. (1994) Formation of heteromeric γ-aminobutyric acid type A receptors containing two different α subunits. Molecular Pharmacology. 45 (3), 475–480.

Vetiska, S.M., Ahmadian, G., Ju, W., Liu, L., et al. (2007) $GABA_A$ receptor-associated phosphoinositide 3-kinase is required for insulin-induced recruitment of postsynaptic $GABA_A$ receptors. Neuropharmacology. 52 (1), 146–155.

Wafford, K.A., van Niel, M.B., Ma, Q.P., Horridge, E., et al. (2009) Novel compounds selectively enhance δ subunit containing $GABA_A$ receptors and increase tonic currents in thalamus. Neuropharmacology. 56 (1), 182–189.

Wafford, K.A., Thompson, S.A., Thomas, D., Sikela, J., et al. (1996) Functional characterization of human γ-aminobutyric acid A receptors containing the α4 subunit. Molecular Pharmacology. 50 (3), 670–678.

Wang, L., Kloc, M., Maher, E., Erisir, A., et al. (2019) Presynaptic $GABA_A$ receptors modulate thalamocortical inputs in layer 4 of rat V1. Cerebral Cortex. 29 (3), 921–936.

Wei, W., Zhang, N., Peng, Z., Houser, C.R., et al. (2003) Perisynaptic localization of δ subunit-containing $GABA_A$ receptors and their activation by GABA spillover in the mouse dentate gyrus. The Journal of Neuroscience. 23 (33), 10650–10661.

Whiting, P., McKernan, R.M. & Iversen, L.L. (1990) Another mechanism for creating diversity in γ-aminobutyrate type A receptors: RNA splicing directs expression of two forms of γ2 phosphorylation site. Proceedings of the National Academy of Sciences of the United States of America. 87 (24), 9966–9970.

Wieland, H.A., Lüddens, H. & Seeburg, P.H. (1992) A single histidine in GABA$_A$ receptors is essential for benzodiazepine agonist binding. The Journal of Biological Chemistry. 267 (3), 1426–1429.

Wisden, W., Laurie, D.J., Monyer, H. & Seeburg, P.H. (1992) The distribution of 13 GABA$_A$ receptor subunit mRNAs in the rat brain. I. Telencephalon, diencephalon, mesencephalon. The Journal of Neuroscience. 12 (3), 1040–1062.

Wongsamitkul, N., Maldifassi, M.C., Simeone, X., Baur, R., et al. (2017) α subunits in GABA$_A$ receptors are dispensable for GABA and diazepam action. Scientific Reports. 7 (1), 15498.

Wooltorton, J.R.A., Moss, S.J. & Smart, T.G. (1997) Pharmacological and physiological characterization of murine homomeric β3 GABA$_A$ receptors. European Journal of Neuroscience. 9 (11), 2225–2235.

Wu, X., Wu, Z., Ning, G., Guo, Y., et al. (2012) γ-Aminobutyric acid type A (GABA$_A$) receptor α subunits play a direct role in synaptic versus extrasynaptic targeting. The Journal of Biological Chemistry. 287 (33), 27417–27430.

Xu, M., Covey, D.F. & Akabas, M.H. (1995) Interaction of picrotoxin with GABA$_A$ receptor channel-lining residues probed in cysteine mutants. Biophysical Journal. 69 (5), 1858–1867.

Yamasaki, T., Hoyos-Ramirez, E., Martenson, J.S., Morimoto-Tomita, M., et al. (2017) GARLH family proteins stabilize GABA$_A$ receptors at synapses. Neuron. 93 (5), 1138-1152.e6.

Yee, B.K., Keist, R., von Boehmer, L., Studer, R., et al. (2005) A schizophrenia-related sensorimotor deficit links α3-containing GABA$_A$ receptors to a dopamine hyperfunction. Proceedings of the National Academy of Sciences of the United States of America. 102 (47), 17154–17159.

Yoon, B.-E., Jo, S., Woo, J., Lee, J.-H., et al. (2011) The amount of astrocytic GABA positively correlates with the degree of tonic inhibition in hippocampal CA1 and cerebellum. Molecular Brain. 4, 42.

Zhang, H.G., Ffrench-Constant, R.H. & Jackson, M.B. (1994) A unique amino acid of the Drosophila GABA receptor with influence on drug sensitivity by two mechanisms. The Journal of Physiology. 479 (Pt 1), 65–75.